DEPARTMENT OF GEOLOGY AND PALEONTOLOGY, FACULTY OF SCIENCE, CHARLES UNIVERSITY, PRAGUE

JAROSLAVA HAJNÁ

TECTONIC EVOLUTION OF THE CENTRAL PART OF THE TEPLÁ–BARRANDIAN UNIT

Ph.D. thesis

Principal Advisor: Jiří Žák

Co-advisor: Václav Kachlík

Prague 2012

I certify herewith that I have worked on this Ph.D. thesis by myself and that I have properly cited all the relevant literature and other sources of information. I also certify that the thesis, or any substantial part of the thesis, has not been submitted elsewhere to get any other comparable degree. I also accept that this Ph.D. thesis is subject to Law no. 121/2000 of the statute book, and especially the fact that the Charles University is entitled to make a licence agreement to use this Ph.D. thesis as a scholastic work according to § 60, article 1 of this law.

Jaroslava Hajná

Prague, May 15th, 2012

Abstract

The principal goal of the thesis is to examine the tectonic evolution of the Teplá–Barrandian unit (TBU) of the central Bohemian Massif from Cadomian subduction and active margin processes, through Cambro–Ordovician extension to Variscan terrane collisions. The thesis is based on extensive field research, detailed structural mapping, and structural analysis, combined with other analytical methods such as the anisotropy of magnetic susceptibility (AMS) coupled with an analysis of magnetic mineralogy, analysis of deformational microstructures, and U, Th and Pb isotope analyses carried out by laser ablation – inductively coupled plasma–mass spectrometry (LA–ICP–MS).

The most important conclusions of the thesis are as follows. (1) The Neoproterozoic (Cadomian) basement of the Teplá–Barrandian unit reveals a complex structure and mostly unclear stratigraphic relations of its components. It was proposed that this unit exposes perhaps the best preserved fragment of an accretionary wedge of the whole Avalonian–Cadomian belt, represented by the newly defined Blovice Complex. In the central part of the TBU, this complex consists of three lithotectonic belts differing in style and intensity of deformation, magnetic fabric, and degree of Cadomian regional metamorphism. In addition, the central Radnice–Kralupy belt is interpreted as a complex of Franciscan-type mélanges of dual, sedimentary and tectonic origin. (2) The Cambro–Ordovician rifting following the cessation of the Cadomian subduction and causing the break-up of the northern margin of Gondwana was also recorded in the Barrandian area of the TBU. Directions of the principal crustal extension during the Cambro–Ordovician rifting was reconstructed from orientations of dikes, interpreted as being feeders to the associated extrusive rocks of the Křivoklát–Rokycany Volcanic Complex, and by the depocenters and facies distribution in the Lower Ordovician of the Prague Basin which developed on eroded Cadomian accretionary wedge. The Upper Cambrian dikes and Lower Ordovician rocks of the Prague Basin record a major kinematic change in the amount and directions of regional extension. Dikes supplying the volcanic complex indicate minor E–W crustal extension in the late Cambrian whereas the linear array of depocentres suggests opening of this Rheic Ocean rift-related basin during the NW–SE pure shear-dominated extension. This kinematic change was accompanied by the onset of basic submarine volcanism, presumably resulting from decompression mantle melting as the amount of extension increased. The triggering mechanism of this extension may have been the onset of subduction of the Iapetus Ocean at around 510 Ma. Unequal extension resulted in the break-up and drift of some terranes while other portions of the belt remained adjacent to Gondwana. (3) According to studies in areas to the NW from the Kralovice–Rakovník belt, the Variscan orogenic processes in the TBU resulting from the Saxothuringian/Teplá–Barrandian convergence was strongly partitioned. Newly mapped and analyzed NE–SW-trending dextral transpressional Krakovec Shear Zone (KSZ) represents a principal orogen-scale tectonic feature that separates two crustal segments with contrasting Cadomian and Variscan deformation and metamorphic histories and delimits the northwestern front of Variscan ductile reworking in the TBU. Finally, a synthetic model for the deformation partitioning in the Teplá–Barrandian upper crust in response to the Late Devonian to early Carboniferous subduction and underthrusting of the Saxothuringan lithosphere was proposed. In this model, the TBU is interpreted as consisting of pure shear-dominated domains alternating with narrow, orogen-parallel, high-strain zones.

CONTENTS

Acknowledgements 2

Preface 3

Introduction 4

Chapter 1 – Subduction-driven shortening and differential exhumation in a Cadomian accretionary wedge: The Teplá–Barrandian unit, Bohemian Massif 9

Chapter 2 – Structure and stratigraphy of the Teplá–Barrandian Neoproterozoic, Bohemian Massif: a new plate-tectonic reinterpretation 52

Chapter 3 – Neoproterozoic to early Cambrian Franciscan-type mélanges in the Teplá–Barrandian unit, Bohemian Massif: evidence of modern-style accretionary processes along the Cadomian active margin of Gondwana? 90

Chapter 4 – Timing, styles, and kinematics of Cambro-Ordovician extension in the Teplá–Barrandian Unit, Bohemian Massif, and its bearing on the opening of the Rheic Ocean 127

Chapter 5 – Deciphering the Variscan tectonothermal overprint and deformation partitioning in the Cadomian basement of the Teplá–Barrandian unit, Bohemian Massif 157

Summary 193

Appendices 198

ACKNOWLEDGEMENTS

I would like to gratefully acknowledge my advisor Jiří Žák and my co-advisor Václav Kachlík for all of their help. I also would like to thank my family for their support.

This study was supported by the Ministry of Education, Youth and Sports of the Czech Republic Research Plan No. MSM0021620855 and SVV261203. Part of the research was carried out under the framework of the Academic Research Plan AV0Z30130516 of Institute of Geology, Academy of Sciences of the Czech Republic, v.v.i. and Grant No. 134908 from the Grant Agency of Charles University in Prague (GAUK).

PREFACE

The goal of this Ph.D. thesis, which I started to work on at the Institute of Geology and Paleontology in October 2008 and finished in May 2012, is to reveal the tectonic evolution of the Teplá–Barrandian unit (TBU) of the central Bohemian Massif from Cadomian subduction and active margin processes, through Cambro–Ordovician extension to Variscan terrane collisions. The thesis presents new data collected from the (meta-)sedimentary, volcanic, and plutonic rocks from various parts of the TBU. These data are then integrated into several geological models for the Neoproterozoic (Cadomian) and early Paleozoic tectonic evolution of the TBU. I believe that these models have a great potential for unravelling geologic evolution of the Bohemian massif and for broader correlations with the tectonic development of other terranes originated in the Avalonian–Cadomian tectonostratigraphic belt.

This Ph.D. thesis is based on extensive field research, detailed structural mapping, and structural analysis, combined with other analytical methods such as the anisotropy of magnetic susceptibility (AMS) and analysis of magnetic mineralogy, analysis of deformational microstructures, and U, Th and Pb isotope analyses carried out by laser ablation – inductively coupled plasma–mass spectrometry (LA–ICP–MS).

The thesis is organized into seven sections: goals, motivation, and the state-of-the-art knowledge are outlined in the Introduction, the main topics are then presented in five separate manuscripts (three published, one in review, and one in preparation almost completed for submission) and, finally, the most significant results and outcomes of the research are highlighted in the Summary.

INTRODUCTION

The earliest geologic record in the Bohemian Massif, a mosaic of geologic units forming the easternmost inlier of the Variscan orogen in Central Europe, commences in the late Neoproterozoic (Ediacaran), with the exception of only a few isolated orthogneiss bodies that yielded Paleoproterozoic and Mesoproterozoic protolith ages. During the late Neoproterozoic, the individual tectonostratigraphic terranes, now welded together to form the Bohemian Massif, were separate components of the Avalonian−Cadomian orogenic belt. This belt developed along the northern active margin of Gondwana during *ca.* 750 to *ca.* 530 Ma as a collage of microcontinents, accretionary complexes, island arcs, and intervening sedimentary basins (Nance et al., 1991; Nance and Murphy, 1994; Wortman et al., 2000; Murphy et al., 2002, 2004, 2006; Linnemann and Romer, 2002; von Raumer et al., 2002; Linnemann et al., 2007, 2008a,b; Nance et al., 2010). The geodynamic processes in this belt were predominantly driven by subduction of an unnamed oceanic plate beneath Gondwana and are collectively referred to as the Cadomian Orogeny. Fragments of the Avalonian−Cadomian belt were then rifted off unknown distance from the mainland Gondwana and involved in huge collisional zone (the Ouachita–Variscan belt), closing the Rheic Ocean during late Paleozoic (Nance et al., 2010). Consequently, the original terranes are now found dispersed within younger Appalachian, Caledonian, Variscan, and Alpine orogens.

In the Bohemian Massif (and elsewhere), much of the Cadomian basement has been pervasively overprinted during the Devonian/Carboniferous Variscan Orogeny. The reworking has commonly obscured the pre-Variscan geologic history, leaving many uncertainties as to the deformation style, paleogeography, plate kinematics, or even polarity of the Cadomian subduction, that can be deduced only from small ribbon-like crustal

fragments. One of the best settings where the Cadomian basement is superbly exposed and not affected by the Variscan reworking and thus wherein the earliest history of the Bohemian Massif can be deciphered is the Teplá–Barrandian unit (TBU). This low-grade, upper-crustal block belongs to the easterly terranes in the original Avalonian–Cadomian belt (presumably adjacent to the West African craton) and has never been buried to great depths, escaping the Variscan pervasive metamorphism, magmatism, and deformation and largely preserving the Cadomian structures.

In short, the protracted tectonic history of the TBU commenced with subduction, accretion, and island arc formation on the northern margin of Gondwana at *ca.* 660–560 Ma (e.g., Zulauf, 1997; Zulauf et al., 1997, 1999; Cháb, 1993; Kříbek et al., 2000; Dörr et al., 2002; Drost et al., 2004, 2007, 2011; Sláma et al., 2008), followed by arc/continent collision and deposition of sedimentary flysch successions at *ca.* 560–530 Ma (Sláma et al., 2008). Convergence perhaps changed to dextral transtension (Zulauf et al., 1997; Dörr et al., 2002; Linnemann et al., 2007, 2008b) during the Middle Cambrian to Early Ordovician, as portions of the Avalonian−Cadomian belt began to break up and separate from the Gondwana margin during the Middle Cambrian to Early Ordovician (Linnemann et al., 2004, 2007; von Raumer and Stampfli, 2008). This process was associated with lithospheric thinning, extensive intra-plate magmatism, and deposition of Ordovician to Lower Devonian passive-margin successions (Zulauf et al., 1997; Dörr et al., 1998; Kachlík and Patočka, 1998; Dostal et al., 2001; Pin et al., 2007). After break-up and the formation of the Rheic Ocean, the TBU drifted northward during the Early Paleozoic (Krs et al., 2001; Cocks and Torsvik, 2002; Patočka et al., 2003; Torsvik and Cocks, 2004) and was incorporated into the Variscan orogen during the Late Devonian to Early Carboniferous.

Despite the long-lasting research into the Neoproterozoic and Lower Paleozoic of the

Bohemian Massif, the Cadomian Orogeny and its role in the subsequent geologic history remain poorly understood, especially in the case of the TBU. This was largely due to the lack of modern structural data (note that the last structural scheme of the Teplá–Barrandian Neoproterozoic was published by Holubec in late 1960s). The outstanding questions that are to be addressed are: (1) What was the the geotectonic significance and position of individual geologic units in the TBU? (2) What was the polarity of Cadomian subduction, that means, where was located the subduction zone, accretionary wedge, volcanic arc, back-arc, and the Gondwana mainland? (3) Is the northwesterly Mariánské Lázně Complex with protolith ages of *ca.* 540 Ma a relict of Neoproterozoic/Cambrian ocean floor? (4) What is the stratigraphic range of individual segments of the Barrandian Neoproterozoic basins and their space and time migration in relation to the subduction/collision processes? (5) What was the structural history of the TBU from the Cadomian subduction to Variscan collisions? (6) What was the exact timing of Cadomian accretion, subduction, magmatism, and deformation in the TBU? (7) What was the large-scale kinematics (oblique? frontal?) in the TBU during Cadomian orogeny and during subsequent rifting (extension? transtension? oblique?)? (8) What was the role of inherited Neoproterozoic (Cadomian) architecture of the TBU in the Cambro−Ordovician rifting, development of sedimentary basins, and in the separation of the new microcontinents from Gondwana during the Early Paleozoic? (9) How did the Cadomian structural inheritance contribute to the geometry and kinematics of the Late Devonian to early Carboniferous Variscan subductions and continental collisions? (10) What is the real extent of Variscan pervasive overprint and where can we observe unaffected Cadomian structures?

The ambition of this thesis is to address, at least in part, these questions.

References

Cháb, J., 1993. General problems of the TB (Teplá–Barrandian) Precambrian, Bohemian Massif, the Czech Republic. Bull. Geosci. 68, 1–6.

Cocks, L.R.M., Torsvik, T.H., 2002. Earth geography from 500 to 400 million years ago. A faunal and palaeomagnetic review. J. Geol. Soc. London 159, 631–644.

Dörr, W., Fiala, J., Vejnar, Z., Zulauf, G., 1998. U–Pb zircon ages and structural development of metagranitoids of the Teplá crystalline complex—evidence for pervasive Cambrian plutonism within the Bohemian Massif (Czech Republic). Geol. Rundsch. 87, 135–149.

Dörr, W., Zulauf, G., Fiala, J., Franke, W., Vejnar, Z., 2002. Neoproterozoic to Early Cambrian history of an active plate margin in the Teplá–Barrandian unit – a correlation of U–Pb isotopic-dilution-TIMS ages (Bohemia, Czech Republic). Tectonophysics 352, 65–85.

Dostal, J., Patočka, F., Pin, C., 2001. Middle/Late Cambrian intracontinental rifting in the central West Sudetes, NE Bohemian Massif (Czech Republic): geochemistry and petrogenesis of the bimodal metavolcanic rocks. Geol. J. 36, 1–17.

Drost, K., Linnemann, U., McNaughton, N., Fatka, O., Kraft, P., Gehmlich, M., Tonk, Ch., Marek, J., 2004. New data on the Neoproterozoic–Cambrian geotectonic setting of the Teplá–Barrandian volcano-sedimentary successions: geochemistry, U–Pb zircon ages, and provenance (Bohemian Massif, Czech Republic). Int. J. Earth Sci. 93, 742–757.

Drost, K., Romer, R.L., Linnemann, U., Fatka, O., Kraft, P., Marek, J., 2007. Nd–Sr–Pb isotopic signatures of Neoproterozoic—early Paleozoic siliciclastic rocks in response to changing geotectonic regimes: a case study from the Barrandian area (Bohemian Massif, Czech Republic). In: Linnemann, U., Nance, D., Kraft, P., Zulauf, G. (Eds.), The Evolution of the Rheic Ocean: From Avalonian–Cadomian Active Margin to Alleghenian–Variscan Collision. Geol. Soc. Am. Spec. Paper 423, pp. 191–208.

Drost, K., Gerdes, A., Jeffries, T., Linnemann, U., Storey, C., 2011. Provenance of Neoproterozoic and early Paleozoic siliciclastic rocks of the Teplá–Barrandian unit (Bohemian Massif): Evidence from U–Pb detrital zircon ages. Gondwana Res. 19, 213–231.

Kachlík, V., Patočka, F., 1998. Cambrian/Ordovician intracontinental rifting and Devonian closure of the rifting generated basins in the Bohemian Massif realms. Acta Univ. Carol., Geol. 42, 433–441.

Krs, M., Pruner, P., Man, O., 2001. Tectonic and paleogeographic interpretation of the paleomagnetism of Variscan and pre-Variscan formations of the Bohemian Massif, with special reference to the Barrandian terrane. Tectonophysics 332, 93–114.

Kříbek, B., Pouba, Z., Skoček, V., Waldhausrová, J., 2000. Neoproterozoic of the Teplá–Barrandian Unit as a part of the Cadomian orogenic belt: a review and correlation aspects. Bull. Czech Geol. Surv. 75, 175–196.

Linnemann, U., Romer, R.L., 2002. The Cadomian orogeny in Saxo-Thuringia, Germany: geochemical and Nd–Sr–Pb isotopic characterization of marginal basins with constraints to geotectonic setting and provenance. Tectonophysics 352, 33–64.

Linnemann, U., McNaughton, N.J., Romer, R.L., Gehmlich, M., Drost, K., Tonk, C., 2004. West African provenance for Saxo-Thuringia (Bohemian Massif): did Armorica ever leave pre-Pangean Gondwana? U/Pb-SHRIMP zircon evidence and the Ndisotopic record. Int. J. Earth Sci. 93, 683–705.

Linnemann, U., Gerdes, A., Drost, K., Buschmann, B., 2007. The continuum between Cadomian orogenesis and opening of the Rheic Ocean: constraints from LA-ICP-MS U–Pb zircon dating and analysis of plate-tectonic setting (Saxo-Thuringian zone, northeastern Bohemian Massif, Germany). In: Linnemann, U., Nance, D., Kraft, P., Zulauf, G. (Eds.), The Evolution of the Rheic Ocean: From Avalonian–Cadomian active margin to Alleghenian–Variscan Collision. Geol. Soc. Am. Spec. Paper 423, pp. 61–96.

Linnemann, U., Pereira, F., Jeffries, T.E., Drost, K., Gerdes, A., 2008a. The Cadomian orogeny and the opening of the Rheic Ocean: the diacrony of geotectonic processes constrained by LA-ICP-MS U–Pb zircon dating (Ossa-Morena and Saxo-Thuringian Zones, Iberian and Bohemian Massifs). Tectonophysics 461, 21–43.

Linnemann, U., D'Lemos, R.S., Drost, K., Jeffries, T., Gerdes, A., Romer, R.L., Samson, S.D., Strachan, R.A., 2008b. Cadomian tectonics. In: McCann, T. (Ed.), The Geology of Central Europe, vol. 1: Precambrian and Palaeozoic. Geological Society, London, pp. 103–154.

Murphy, J.B., Eguiluz, L., Zulauf, G., 2002. Cadomian orogens, peri-Gondwanan correlatives and Laurentia–Baltica connections. Tectonophysics 352, 1–9.

Murphy, J.B., Pisarevsky, S.A., Nance, R.D., Keppie, J.D., 2004. Neoproterozoic–Early Paleozoic evolution of peri-Gondwanan terranes: implications for Laurentia–Gondwana connections. Int. J. Earth Sci. 93, 659–682.

Murphy, J.B., Gutierrez-Alonso, G., Nance, R.D., Fernandez-Suarez, J., Keppie, J.D., Quesada, C., Strachan, R.A., Dostal, J., 2006. Origin of the Rheic Ocean: rifting along a Neoproterozoic suture? Geology 34, 325–328.

Nance, R.D., Murphy, J.B., Strachan, R.A., D'Lemos, R.S., Taylor, G.K., 1991. Late Proterozoic tectonostratigraphic evolution of the Avalonian and Cadomian terranes. Precambrian Res. 53, 41–78.
Nance, R.D., Murphy, J.B., 1994. Constraining basement isotopic signatures and the palinspastic restoration of peripheral orogens: example from the Neoproterozoic Avalonian–Cadomian belt. Geology 22, 617–620.
Nance, R.D., Gutierrez-Alonso, G., Keppie, J.D., Linnemann, U., Murphy, J.B., Quesada, C., Strachan, R.A., Woodcock, N.H., 2010. Evolution of the Rheic Ocean. Gondwana Res. 17, 194–222.
Patočka, F., Pruner, P., Štorch, P., 2003. Palaeomagnetism and geochemistry of Early Palaeozoic rocks of the Barrandian (Teplá–Barrandian Unit, Bohemian Massif): palaeotectonic implications. Phys. Chem. Earth 28, 735–749.
Pin, C., Kryza, R., Oberc-Dziedzic, T., Mazur, S., Turniak, K., Waldhausrová, J., 2007. The diversity and geodynamic significance of Late Cambrian (ca. 500 Ma) felsic anorogenic magmatism in the northern part of Bohemian Massif: a review based on Sm–Nd isotope and geochemical data. In: Linnemann, U., Nance, D., Kraft, P., Zulauf, G. (Eds.), The Evolution of the Rheic Ocean: From Avalonian–Cadomian Active Margin to Alleghenian–Variscan Collision. Geol. Soc. Am. Spec. Paper 423, pp. 209–229.
Sláma, J., Dunkley, D.J., Kachlík, V., Kusiak, M.A., 2008. Transition from island-arc to passive setting on the continental margin of Gondwana: U–Pb zircon dating of Neoproterozoic metaconglomerates from the SE margin of the Teplá–Barrandian Unit, Bohemian Massif. Tectonophysics 461, 44–59.
Torsvik, T.H., Cocks, L.R.M., 2004. Earth geography from 400 to 250 Ma: a palaeomagnetic, faunal and facies review. J. Geol. Soc. London 161, 555–572.
von Raumer, J.F., Stampfli, G.M., 2008. The birth of the Rheic Ocean—Early Palaeozoic subsidence patterns and subsequent tectonic plate scenarios. Tectonophysics 461, 9–20.
von Raumer, J.F., Stampfli, G.M., Borel, G., Bussy, F., 2002. Organization of pre-Variscan basement areas at the north-Gondwanan margin. Int. J. Earth. Sci. 91, 35–52.
Wortman, G.L., Samson, S.D., Hibbard, J.P., 2000. Precise U–Pb zircon constraints on the earliest magmatic history of the Carolina terrane. J. Geol. 108, 321–338.
Zulauf, G., 1997. From very low-grade to eclogite-facies metamorphism: tilted crustal sections as a consequence of Cadomian and Variscan orogeny in the Teplá–Barrandian unit (Bohemian Massif). Geotekt. Forsch. 89, 1–302.
Zulauf, G., Dörr, W., Fiala, J., Vejnar, Z., 1997. Late Cadomian crustal tilting and Cambrian transtension in the Teplá–Barrandian unit (Bohemian Massif, Central European Variscides). Geol. Rundsch. 86, 571–587.
Zulauf, G., Schritter, F., Riegler, G., Finger, F., Fiala, J., Vejnar, Z., 1999. Age constraints on the Cadomian evolution of the Teplá–Barrandian unit (Bohemian Massif) through electron microprobe dating of metamorphic monazite. Zt. Deutsch. Geol. Ges. 180, 627–639.

CHAPTER 1

Jaroslava Hajná, Jiří Žák, Václav Kachlík, Martin Chadima: Subduction-driven shortening and differential exhumation in a Cadomian accretionary wedge: The Teplá–Barrandian unit, Bohemian Massif.

Precambrian Research 176, 27–45, 2010

Subduction-driven shortening and differential exhumation in a Cadomian accretionary wedge: The Teplá–Barrandian unit, Bohemian Massif

Jaroslava Hajná[a], Jiří Žák [a,b], Václav Kachlík[a], Martin Chadima[c,d]

a Institute of Geology and Paleontology, Faculty of Science, Charles University, Albertov 6, Prague, 12843, Czech Republic

b Czech Geological Survey, Klárov 3, Prague, 11821, Czech Republic

c AGICO Inc., Ječná 29, Brno, 62100, Czech Republic

d Institute of Geology, Academy of Sciences of the Czech Republic, v.v.i., Rozvojová 269, Prague, 16500, Czech Republic

Abstract

The Teplá–Barrandian unit (TBU) of Central Europe's Bohemian Massif exposes perhaps the best preserved fragment of an accretionary wedge in the Avalonian–Cadomian belt, which developed along the northern active margin of Gondwana during Late Neoproterozoic. In the central TBU, three NE–SW-trending lithotectonic units (Domains 1–3) separated by antithetic brittle faults differ in lithology, style and intensity of deformation, magnetic fabric (AMS), and degree of Cadomian regional metamorphism. The flysch-like Domain 1 to the NW is the most outboard (trenchward) unit which has never been significantly buried and experienced only weak deformation and folding. The central, mélange-like Domain 2 is characterized by heterogenous intense deformation developed under lower greenschist facies conditions, and was thrust NW over Domain 1 along a SE-

dipping fault. To the SE, the most inboard (arcward) Domain 3 is lithologically monotonous (dominated by graywackes and slates), was buried to depths corresponding up to the lower greenschist facies conditions, where it was overprinted by a pervasive SE-dipping cleavage and then was exhumed along a major NW-dipping normal fault.

We interpret these domains to represent allochtonous tectonic slices that were differentially buried and then exhumed from various depths within the accretionary wedge during Cadomian subduction. The NW-directed thrusting of Domain 2 over Domain 1 may have been caused by accretion at the wedge front, whereas the SE-dipping cleavage and SE-side-up exhumation of Domain 3 may record inclined pervasive shortening during tectonic underplating and subsequent horizontal extension of the rear of the wedge. The boundary faults were later reactivated during Cambro–Ordovician extension and Variscan compression.

Compared to related terranes of the Cadomian belt, the TBU lacks exposed continental basement, evidence for regional strike-slip shearing, and extensive backarc magmatism and LP–HT metamorphism, which could be interpreted to reflect flat-slab Cadomian subduction. This, in turn, suggests that Cadomian accretionary wedges developed in a manner identical to those of modern settings, elevating the TBU to a key position for understanding the style, kinematics, and timing of accretionary processes along the Avalonian–Cadomian belt.

***Keywords**: Accretionary wedge, Anisotropy of magnetic susceptibility (AMS), Bohemian Massif, Cadomian orogeny, Teplá–Barrandian unit, Variscan orogeny*

1. Introduction

The Avalonian–Cadomian belt developed as a collage of microcontinents, accretionary complexes, island arcs, and intervening sedimentary basins along the northern active margin of Gondwana during Late Neoproterozoic (Nance et al., 1991; Nance and Murphy, 1994; Wortman et al., 2000; Murphy et al., 2002, 2004, 2006; Linnemann and Romer, 2002; von Raumer et al., 2002; Linnemann et al., 2007, 2008a,b). Fragments of this once continuous belt are now found as tectonostratigraphic terranes dispersed within younger Appalachian, Caledonian, Variscan, and Alpine orogens (Fig. I.1a and b; e.g., von Raumer et al., 2003). As a consequence of their involvement in younger orogens, the direct structural record of Cadomian tectonic processes in these terranes is commonly obscured leaving uncertainities as to the deformation style, kinematics, or even polarity of subduction (e.g., Kříbek et al., 2000; Drost et al., 2004; Sláma et al., 2008).

An excellent setting where the Cadomian basement is superbly exposed and where the Cadomian structures can be examined in detail and unequivocally separated from Variscan (Late Devonian to Early Carboniferous) overprint is the Teplá–Barrandian unit (TBU) of the Bohemian Massif in Central Europe (Fig. I.1). This upper-crustal unit represents one of the easterly terranes of the Avalonian–Cadomian belt (Fig. I.1a) and its central part has recently been interpreted to represent a fragment of Cadomian accretionary wedge (Dörr et al., 2002; Sláma et al., 2008) located between a paleo-subduction zone to the ~NW (present-day coordinates) and a volcanic arc to the ~SE (the Jílové Belt in Fig. I.1d; see also detailed discussion and Fig. 12 in Sláma et al., 2008). This polarity of subduction is supported by the following evidence: (1) a Cadomian ~540Ma ophiolite complex was accreted to the northwestern margin of the TBU before ~500Ma (MLC in Fig. I.2; Štědrá et al., 2002; Timmermann et al., 2004), (2) the proportion of detritic material derived from more evolved

continental crust increases significantly to the SE (towards a retroarc basin southeast of the Jílové Belt volcanic arc; Sláma et al., 2008), and (3) complex deformation patterns, juxtaposition of contrasting lithotectonic units, and the presence of "block-in-matrix" mélanges (described in this paper) are typical of an accretionary wedge setting (e.g., Osozawa et al., 2009; Braid et al., in press).

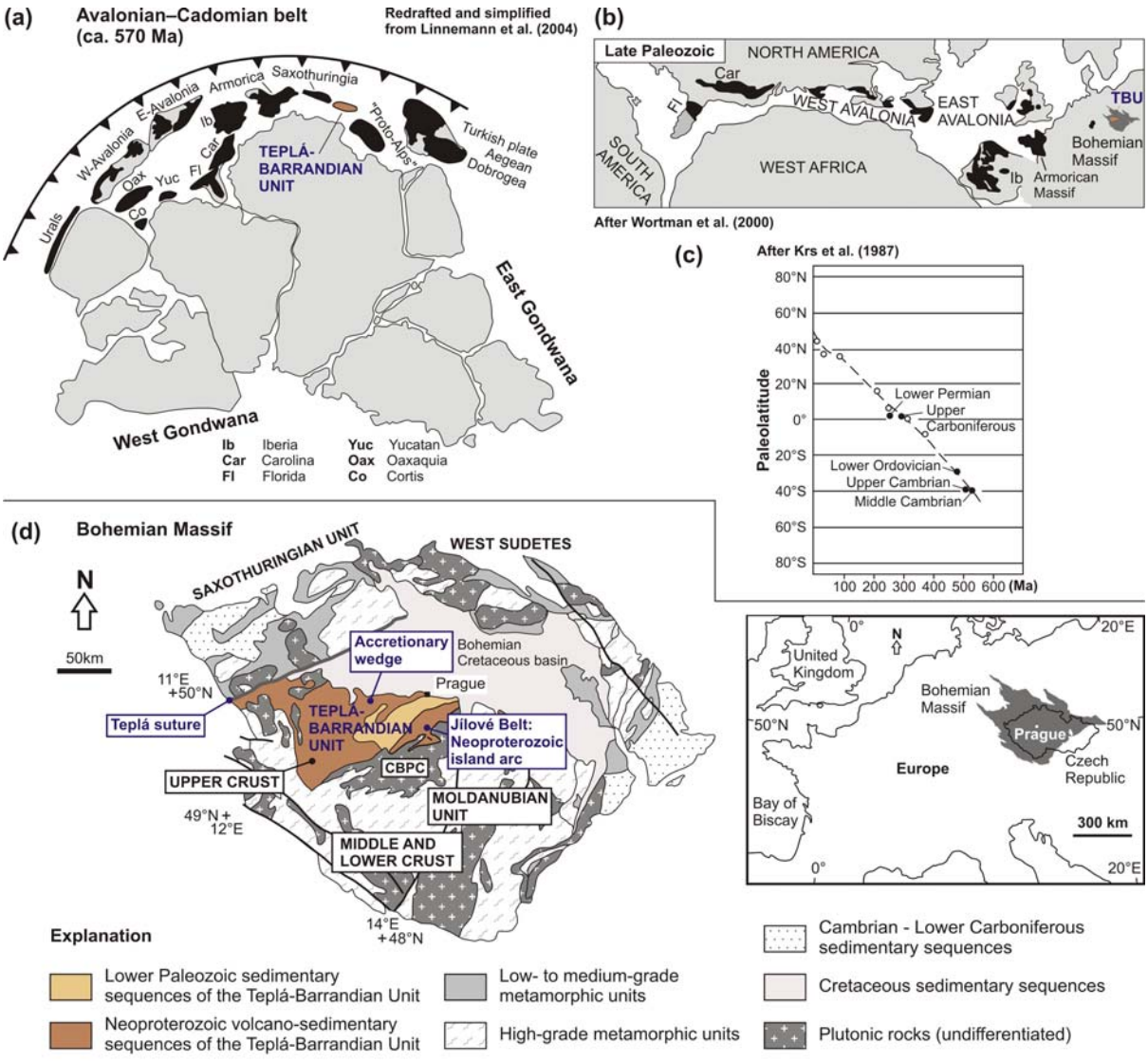

Fig. I.1. (a) Paleogeographic position of the Teplá–Barrandian unit (TBU) within the Avalonian–Cadomian belt on the active northern margin of Gondwana during the Late Neoproterozoic (after Linnemann et al., 2004). (b) Late Paleozoic reconstruction of the Avalonian–Cadomian terranes incorporated into younger orogens (Wortman et al., 2000). (c) Paleozoic drift of the TBU estimated from paleomagnetic data (Krs et al., 1987). (d) Present-day position of the TBU in the central part of the Bohemian Massif. The TBU is interpreted to represent a Cadomian accretionary wedge between a paleo-subduction zone to the NW (Teplá suture) and an island arc (Jílové Belt) to the SE. Inset shows location of the Bohemian Massif in central Europe.

In short, the protracted tectonic history of the TBU commenced with subduction, accretion, and island arc formation on the northern margin of Gondwana at ~660–560Ma (e.g., Zulauf, 1997; Zulauf et al., 1997, 1999; Cháb, 1993; Kříbek et al., 2000; Dörr et al., 2002; Drost et al., 2004, 2007; Sláma et al., 2008), followed by arc/continent collision and deposition of sedimentary flysch successions at ~560–530Ma (Sláma et al., 2008).

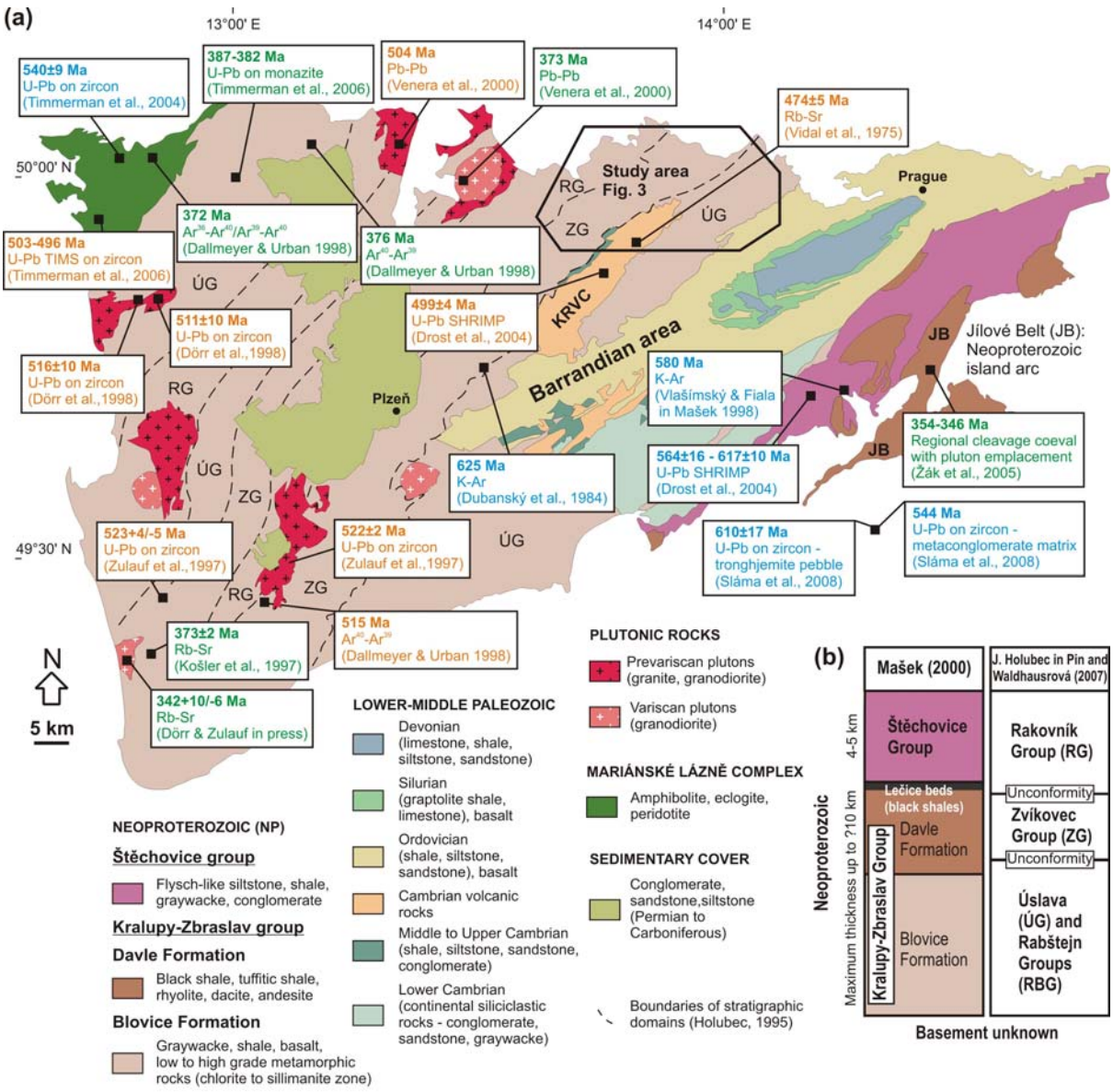

Fig. I.2. (a) Simplified geologic map of the Teplá–Barrandian unit with selected geochronologic data. Redrafted from Geologic map of the Czech Republic, scale 1:500,000, published by the Czech Geological Survey in 2007. Lithologic units in the legend are arranged in stratigraphic order following Mašek (2000), dashed lines in the map correspond to lithostratigraphic belts of Holubec (1995). KRVC – Křivoklát–Rokycany volcanic complex, JB – Jílové Belt. (b) Comparison of two main lithostratigraphic concepts proposed for the Barrandian Neoproterozoic.

Convergence changed to dextral transtension (Zulauf et al., 1997; Dörr et al., 2002; Linnemann et al., 2007, 2008b) during the Middle Cambrian to Early Ordovician, as portions of the Avalonian–Cadomian belt began to break-up and separate from the Gondwana margin (Linnemann et al., 2004, 2007; von Raumer and Stampfli, 2008). This process was associated with lithospheric thinning, extensive intra-plate magmatism, and deposition of Ordovician passive-margin successions (Zulauf et al., 1997; Dörr et al., 1998; Kachlík and Patočka, 1998; Dostal et al., 2001; Pin et al., 2007). After the break-up and formation of the Rheic Ocean, the TBU drifted northward during the Early Paleozoic (Fig. I.1c; Krs et al., 1987, 2001; Cocks and Torsvik, 2002; Patočka et al., 2003; Torsvik and Cocks, 2004) and was incorporated into the Variscan orogen during the Late Devonian to Early Carboniferous (Fig. I.1b).

This paper describes in detail the geology, structure, magnetic fabric, and deformational microstructures of the Neoproterozoic basement in the central part of the TBU, just northwest of the Lower Paleozoic overlap sedimentary successions (referred to as "the Barrandian area"; Fig. I.2a). On the basis of comparison of structures in the Neoproterozoic and Lower Paleozoic, we rigorously characterize and separate Cadomian deformation from subsequent Cambro–Ordovician transtension and Variscan shortening and propose a new kinematic model for the Teplá–Barrandian accretionary wedge during the Cadomian orogeny. Finally, we discuss plate-kinematic scenarios proposed for the TBU in comparison with those of the related Cadomian terranes (Saxothuringia, Armorica s.s.; Fig. I.1a).

2. Geologic overview of the central part of the Teplá–Barrandian unit

The TBU is an upper-crustal block in the center of the Bohemian Massif, occupying the hanging-wall position with respect to the neighboring Saxothuringian and Moldanubian

units (Figs. I.1d and I.2a; for review see, e.g., Vrána and Štědrá, 1997; McCann, 2008). The central part of the TBU consisting of low-grade Neoproterozoic to Lower Paleozoic volcanic and sedimentary rocks has never been buried to great depths, and escaped the Variscan (Late Devonian to Early Carboniferous) pervasive metamorphism and deformation.

2.1. Barrandian Neoproterozoic

The Neoproterozoic rocks of the TBU comprise volcanosedimentary complex (the Kralupy–Zbraslav Group) conformably overlain by a flysch succession of the Štěchovice Group (Dallmeyer and Urban, 1998; Dörr and Zulauf, in press; Dubanský , 1984; Košler et al., 1997; Timmermann et al., 2006; Venera et al., 2000; Fig. I.2b). For the sake of simplicity, we here use this widely adopted subdivision of Mašek (2000), however, in a companion paper we outline some new ideas on the TBU stratigraphy. In total, the thickness of both groupsmay exceed 10 km(a rough estimate by Chaloupský et al., 1995; Chlupáč et al., 1998); the real thickness is difficult to constrain due to unexposed basement, strong Cadomian and Variscan shortening, and crustal tilting.

The Kralupy–Zbraslav Group is composed of volcanic, volcaniclastic, and clastic sedimentary rocks and is further subdivided into the presumably older Blovice and younger Davle Formations (Mašek, 2000), which differ in their spatial distribution (Fig. I.2) and in the composition of volcanic rocks. Two compositional groups of basalts have been defined in the Blovice Formation. One group is similar to recent MORB and E-MORB and indicates formation from REE-depleted mantle sources in a suprasubduction zone environment (Pin and Waldhausrová, 2007). The other, probably younger group of basalts is transitional and more evolved (similarly to recent OIB), lacks features of suprasubduction mantle metasomatism, and was presumably derived from a REEenriched mantle source (Pin and Waldhausrová, 2007). In contrast, calc-alkaline basalts, andesites, dacites, rhyolites, and

associated volcaniclastic rocks are typical of the Davle Formation (exposed in antiformal structures along the SE flank of the TBU; Fig. I.2), including the Jílové Belt which may represent a fringing volcanic arc system (Fig. I.1d; Waldhausrová, 1984) developed on oceanic crust close to the continental margin (see Sláma et al., 2008 for details).

The clastic sedimentary rocks of the Kralupy–Zbraslav Group include rhythmically interbedded shales and siltstones alternating with graywackes, the former indicating sedimentation in a deep-water, less dynamic environment, while the latter has been interpreted as turbidite and gravity-flow sediments (Cháb and Pelc, 1968; Dörr et al., 2002). Slump structures and olistoliths are locally abundant in 10–100 m-wide zones within the graywacke–shale sequences. The graywackes contain significant amounts of island-arc-derived material (Jakeš et al., 1979; Lang, 2000); the contribution from the mainland continental crust is minor in the Blovice Formation but increases to the SE (in the overlying Štěechovice Group; Sláma et al., 2008). In addition, the clastic sedimentary rocks of the Blovice Formation locally contain 10–100 m-thick lenses of chert of diverse origin (Pouba and Kříbek, 1986; Fatka and Gabriel, 1991; Pouba et al., 2000) and rare limestone intercalations.

The uppermost part of the Kralupy–Zbraslav Group is capped by up to 150 m-thick horizon of silicified black shales (the Lečice beds), passing upwards into flysch-like, rythmically alternating shales, siltstones, graywackes, and polymictic conglomerates of the Štěchovice Group. Syn-sedimentary textures (e.g., graded bedding, slump structures, flute marks) and inferred depositional processes (various types of turbidites, debris flows and mudflows) are indicative of relatively deep-water flysch-like sedimentation. Volcanic rocks are absent except for thin tuff and tuffite beds and ~540–520Ma boninite dikes (Dörr et al., 2002; Sláma et al., 2008).

2.2. Barrandian Lower Paleozoic

The Neoproterozoic basement is unconformably overlain by unmetamorphosed Lower Cambrian to Middle Devonian sedimentary successions and associated volcanic complexes (e.g., Chlupáč et al., 1998; Štorch, 2006). In brief, the Lower Paleozoic rocks comprise (1) Lower Cambrian molasse-type continental siliciclastic deposits interpreted to have formed in intramontane basins within the Cadomian orogen (Patočka and Štorch, 2004), passing upwards into Middle Cambrian marine shales (overview in Geyer et al., 2008), (2) an Upper Cambrian to Lower Ordovician subaeric calc-alkaline volcanic suite ranging from minor basalts to andesites, dacites, and widespread rhyolites (Vidal et al., 1975; Waldhausrová, 1971; Pin et al., 2007), (3) a >2 km-thick sequence of Ordovician passive-margin siliciclastic and associated submarine within-plate rift-related basic volcanic rocks, (4) Silurian graptolite shales, basic volcanic and pyroclastic rocks, and limestone/shale interbeds in the upper part of the succession, and (5) Lower Devonian limestones and subordinate shales passing upward into Middle Devonian (Givetian) flysch-like siltstones and sandstones, the latter indicating the onset of the Variscan orogeny.

2.3. Existing geochronology

Radiometric ages from the TBU fall into three main groups (Fig. I.2a and references therein), reflecting the major episodes in its tectonic history: (1) the Cadomian orogeny from ~620 to 560 (a period of island arc growth and active subduction) to ~530Ma (flysch sedimentation and deformation of arc-derived siliciclastic rocks; Sláma et al., 2008); (2) a period of extensive magmatism at the end of Cambrian to the early Ordovician (~524–474 Ma) associated with intracontinental rifting during the break-up of the northern margin of Gondwana (Pin et al., 2007); and (3) Late Devonian (~382 and ~371 Ma) and early Carboniferous (~354–343 Ma) Variscan overprinting deformation and plutonism, localized

particularly along margins of the TBU (Fig. I.2a).

3. Geology of the northwestern margin of the Barrandian area

From NW to SE, the following key geologic units make up the northwestern margin of the Barrandian area (Fig. I.3): (1) The Barrandian Neoproterozoic consists here of three lithologically distinct ~NE–SW-trending belts. The northwestern belt (Figs. I.3 and I.4a; the Kralovice–Rakovník belt of Röhlich, 1965; or flysch facies of Cháb and Pelc, 1968) is a very low-grade flysch-like sequence of rhythmicaly alternating graywackes, slates, and siltstones devoid of volcanic rocks. The average thickness of graywacke beds ranges from 20cm to several meters, the thickness of slate interbeds varies from several centimeters to decimeters. The central belt (Figs. I.3 and I.4b and c; the Radnice–Kralupy belt of Röhlich, 1965 or volcanogenic facies of Cháb and Pelc, 1968) is more complex, consisting of graywackes, slates, and siltstones with abundant syn-sedimentary slump structures and olistoliths (Cháb and Pelc, 1968; Mašek, 2000), and up to km-scale lens-shaped to irregular bodies of tholeiitic (MORB-like and PMORB) to alkaline basalts (Fiala, 1977; Pin and Waldhausrová, 2007). This mélange-like unit contains structurally isolated graywacke blocks and fragments of ocean floor (both up to several hundreds meters in size) dispersed in host slates and presumably represents a broken formation (Hsü, 1968; or graywacke-argillite mélange of Cowan, 1974). By contrast, the southeasterly Zbiroh–Šárka belt (Figs. I.3 and I.4d; Röhlich, 1965; monotonous facies of Cháb and Pelc, 1968) is dominated by graywackes, siltstones and slates (Fig. I.4d) with abundant lenses of chert.

(2) In the south-central part of the area, unmetamorphosed Middle Cambrian marine conglomerates, sandstones, and shales (~200m total thickness) unconformably overlie the Neoproterozoic basement rocks (Fig. I.3). This spectacular angular unconformity was first described by Kettner (1923) and Kettner and Slavík (1929). Both the Neoproterozoic and

Middle Cambrian strata are capped by the Upper Cambrian to Lower Ordovician Křivoklát–Rokycany volcanic complex (KRVC in Fig. I.3; Waldhausrová, 1966, 1971; Vidal et al., 1975; Pin et al., 2007), a ~NE–SW-trending belt up to 1500m thick, consisting of multiple stacked subaerial lava flows of basaltic to rhyolitic composition, and subordinate explosive volcanic products (ignimbrites, coarse-grained agglomerates). To the N and NW of the complex, rhyolite dikes of unknown radiometric age cut across the host Neoproterozoic rocks. In spite of some differences in geochemistry and textures, the dikes closely resemble felsic rocks of the uppermost part of volcanic complex.

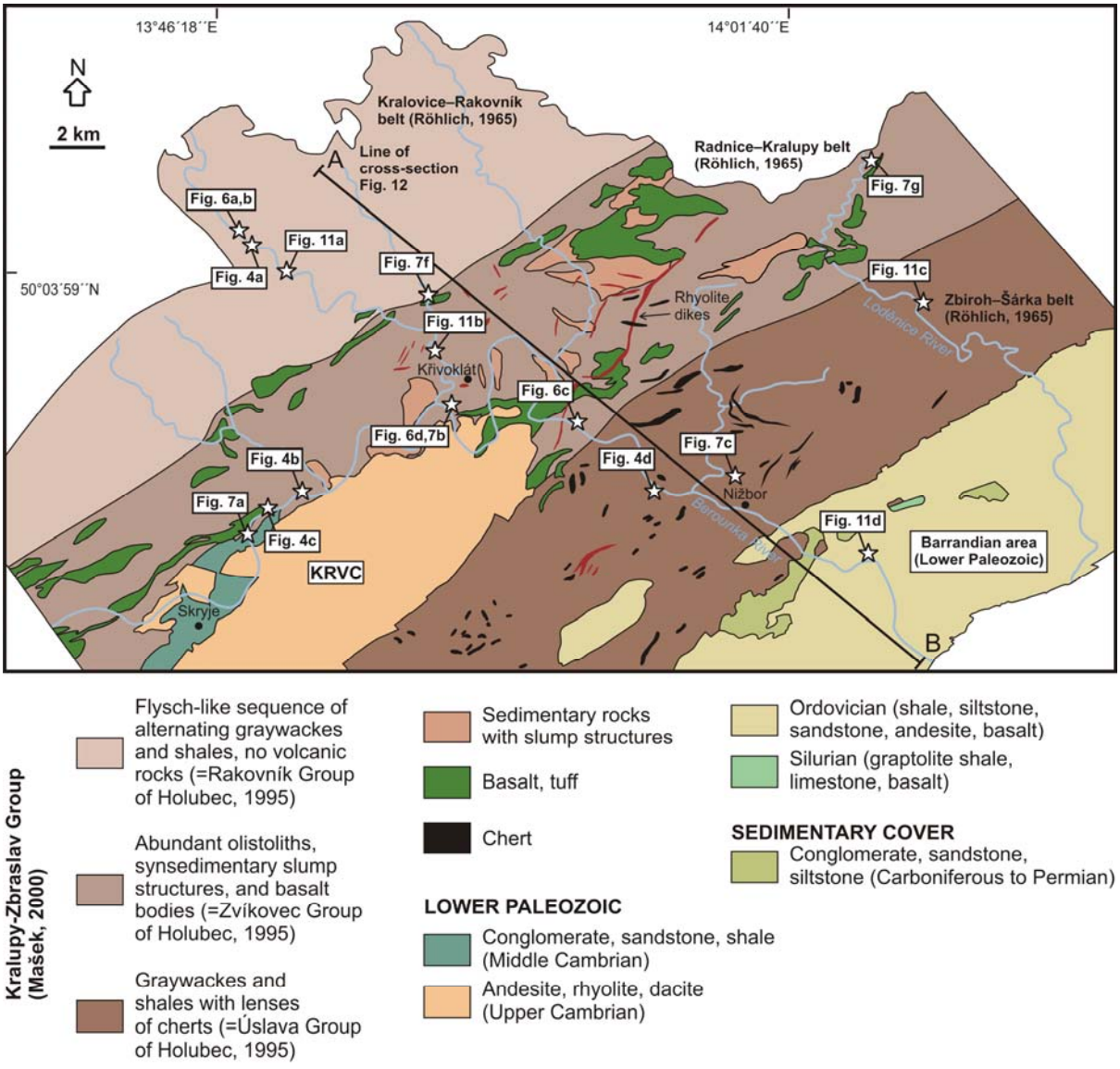

Fig. I.3. Simplified geologic map of the study area along the northwestern margin of the Barrandian area.

Geology and lithostratigraphic belts compiled from Geologic map of the Křivoklát area 1:50,000 published by the Czech Geological Survey in 1997, and Geologic map of the Czech Republic 1:50,000 sheets 12–41 Beroun and 12–23 Kladno. Stars indicate location of photographs, line A–B shows location of cross-section (see Fig. I.12c).

(3) To the southeast, Lower Paleozoic (Ordovician and Silurian) sedimentary rocks of the Prague Basin (Chlupáč et al., 1998) regionally overlap the Neoproterozoic basement (Fig. I.3). The basal Ordovician marine shallow-water conglomerates, sandstones, and graywackes contain clasts of Neoproterozoic chert and Upper Cambrian volcanic rocks. Younger formations comprise Lower to Middle Ordovician quartzites, shales and sandstones, accompanied by a thick complex of predominantly basic submarine lavas and volcaniclastic rocks (Chlupáč et al., 1998). Silurian rocks are represented by black graptolite shales, carbonatic shales, and limestones.

4. Structural pattern

In the Neoproterozoic rocks along the northwestern margin of the Barrandian area, we define three contrasting ~NE–Swtrending structural domains (Fig. I.5) on the basis of their lithology, mesoscopic structures, magnetic fabric, microstructural characteristics, and mineral associations as described below. These structural domains roughly correspond to the lithostratigraphic belts defined previously at much larger-scale by Röhlich (1965), Cháb and Pelc (1968), or in an unpublished report by J. Holubec (cited in Pin and Waldhausrová, 2007; Fig. I.3). In this study, we use descriptive terms (“Domains 1–3” - numbered consecutively from the NW to the SE; Fig. I.5) to avoid any stratigraphic implications.

4.1. Domain 1

Well-defined bedding typical of Domain 1 (thick graywacke beds with thin slate interbeds; Fig. I.4a) either strikes ~ENE–WSW and dips gently (~10–30°) to the ~NNW (in the southwestern part of the area), or strikes ~NE–SW and dips gently to the ~NW(Fig. I.5).

Bedding-parallel cleavage is localized preferentially in the incompenent slate interbeds, while the more rigid graywackes are either entirely devoid of macroscopically discernible cleavage or contain only a locally developed weak spaced cleavage. A lineation, interpreted as slip lineation, is developed on cleavage planes in slates and is parallel to the stretching lineation in graywackes along contacts with slates. The lineation plunges gently (~10–25°) west, oblique to the strike of the bedding (Fig. I.5).

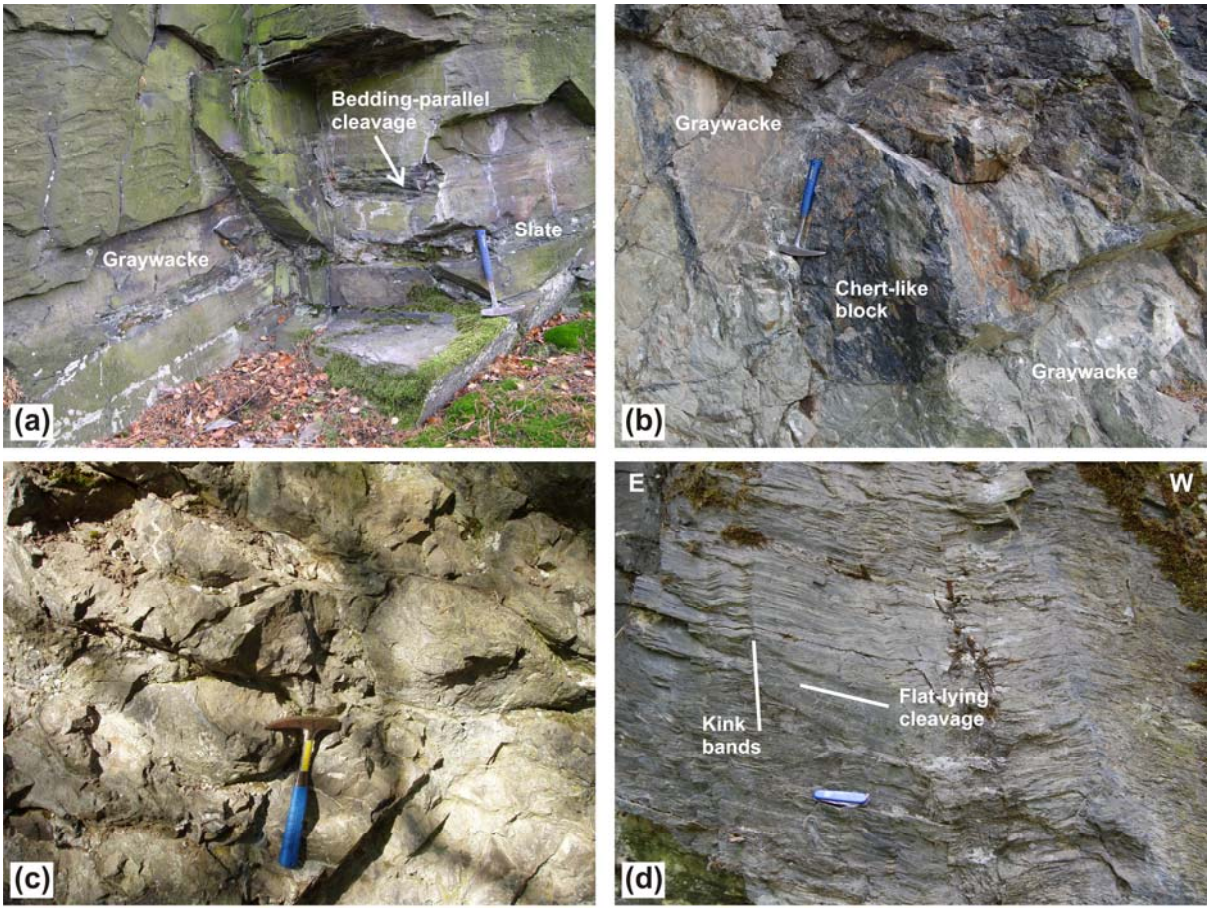

Fig. I.4. Characteristic lithologic features of the Neoproterozoic rocks along the northwestern margin of the Barrandian area. (a) Bedding in alternating graywackes and slates typical of Domain 1. Cleavage is localized in incompetent thin slate interbeds; Dolní Chlum. Hammer for scale. (b) Chert-like block (olistolith?) in tightly folded graywackes, Domain 2; Kněžská skála. Hammer for scale. (c) Deformed pillow lava, Domain 2; Čertova skála. Hammer for scale. (d) Pervasive cleavage in slates, Domain 3; Žloukovice. Swiss Army penknife (9 cm long) for scale. See Fig. I.3 for location of outcrops.

Domain 1 is characterized by a simple fold style, expressed both on outcrop- and map-scale by the monoclinal orientation of the bedding. Significant localization of

deformation into weak slates indicates that the dominant folding mechanism was flexural slip. Bedded sequences are locally cross-cut by meter-scale overthrusts and contractional duplexes (Fig. I.6a and b).

4.2. Domain 2

Unlike Domain 1, well-defined bedding is preserved only in larger lenses or boudins of graywackes that are embedded in intensely deformed finer-grained slates and graywackes. Bedding strike scatters widely but ~E–W bedding, dipping moderately to steeply ~N–NW dominates and is generally parallel to cleavage in the surrounding slates (Fig. I.6c). The slates are characterized by pervasive cleavage that transposes the original bedding or fine-scale lamination (Fig. I.6c) and is associated with weak or no lineation. The cleavage exhibits two main orientations. The dominant cleavage strikes ~ENE–WSW to ~ESE–WNW and dips moderately to steeply to the ~NNW–NNE or ~SSW (cleavage poles cluster around the maximum principal eigenvector 194°/37°; Fig. I.5). However, some cleavages are steep, dipping to the ~ENE or ~WSW (Fig. I.5). In outcrop, the steep pervasive cleavage in the Neoproterozoic slates is unconformably overlain by only moderately tilted (50–60° to the ~SE) and unstrained Middle Cambrian basal sandstones and conglomerates (Fig. I.7a).

To the N and NW of the Křivoklát–Rokycany volcanic complex, rhyolite dikes (Fig. I.7b) and irregularly shaped rhyolite intrusions choked with abundant host rock xenoliths (magmatic breccias) cut across the pervasive cleavage in the Neoproterozoic slates along knife-sharp discordant contacts. The cleavage is also contained in the host rock xenoliths and rafts within the dikes.

Two distinct types of folds were documented in Domain 2 depending on lithology: rare meter-scale tight to isoclinal upright folds occur in competent graywacke beds, and tight chevron folds and contractional monoclinal kink-bands occur in slates, with their axial planes

dipping steeply to the NW. While cleavage is axialplanar to the first type of folds, the kink-bands are superposed onto the pre-existing cleavage.

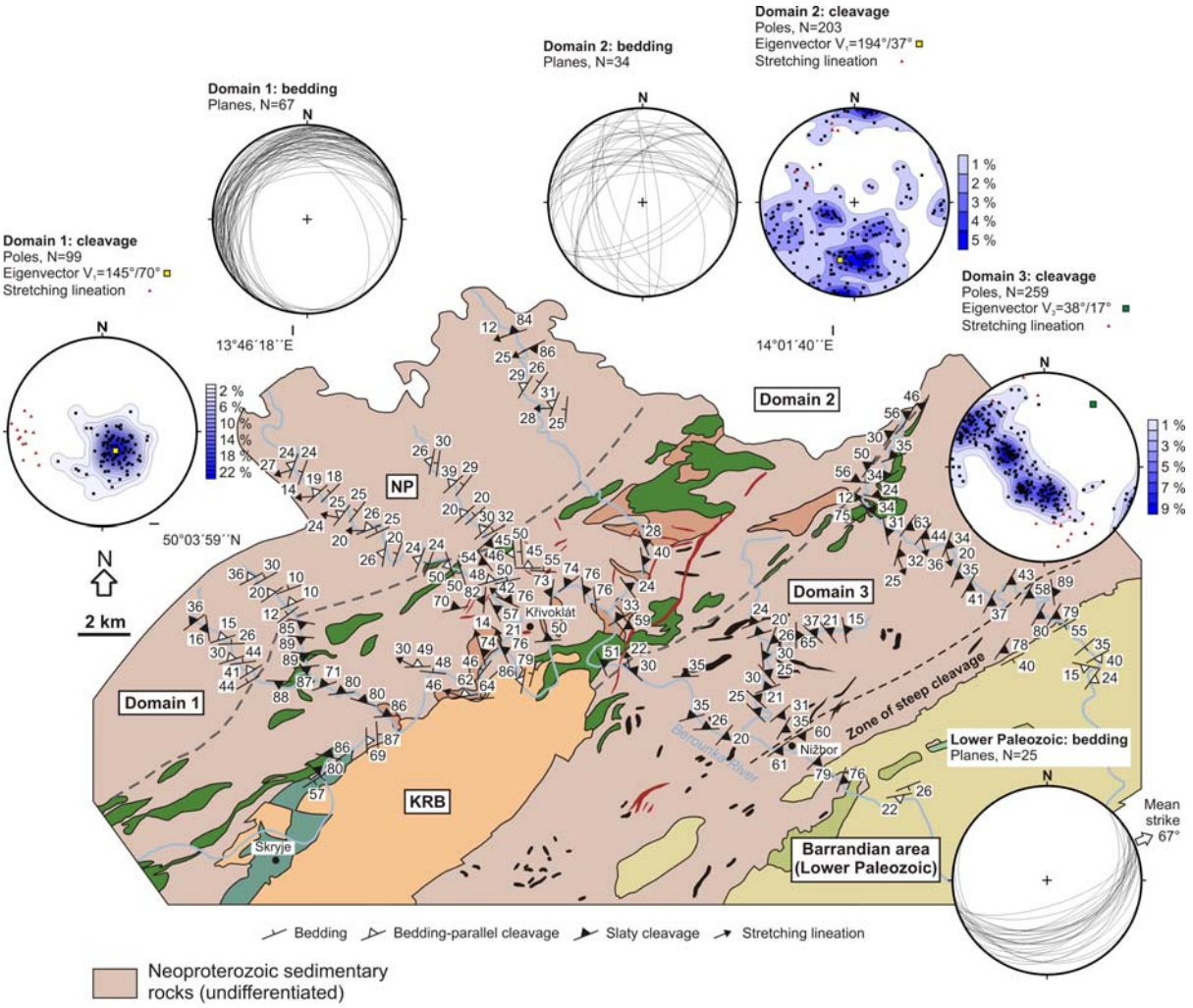

Fig. I.5. Structural map of the study area showing contrasting structural patterns in Domains 1–3 and overlying Lower Paleozoic rocks. Stereonets (equal area projection, lower hemisphere) show orientation of bedding, cleavage, and stretching lineation. Dashed lines represent inferred Domain boundaries (faults). Lithologic units coloured as in Fig. I.3, lithostratigraphic belts in the Neoproterozoic omitted for clarity. KRVC–Křivoklát–Rokycany volcanic complex, NP–Neoproterozoic.

4.3. Domain 3 and Barrandian Lower Paleozoic overlap sequence

Graywackes and slates in Domain 3 are characterized by intensely developed pervasive cleavage with only rarely discernible bedding or lamination (Figs. I.4d and I.6d). On a stereonet, cleavage poles define a girdle around a subhorizontal ~NE–SW axis (mean calculated as the minimum eigenvector of the orientation tensor is 038°/17°). The cleavage

shows bimodal orientation in much of the Domain, either striking ~NE–SW and dipping moderately to the ~SE, or striking ~NW–SE and dipping shallowly to moderately to the ~NNW–NE (Fig. I.5). Within a 2 km-wide zone along the contact with the overlying Barrandian Lower Paleozoic rocks, the cleavage progressively steepens while maintaining the ~NE–SW strike and ~SE dip (Fig. I.5).

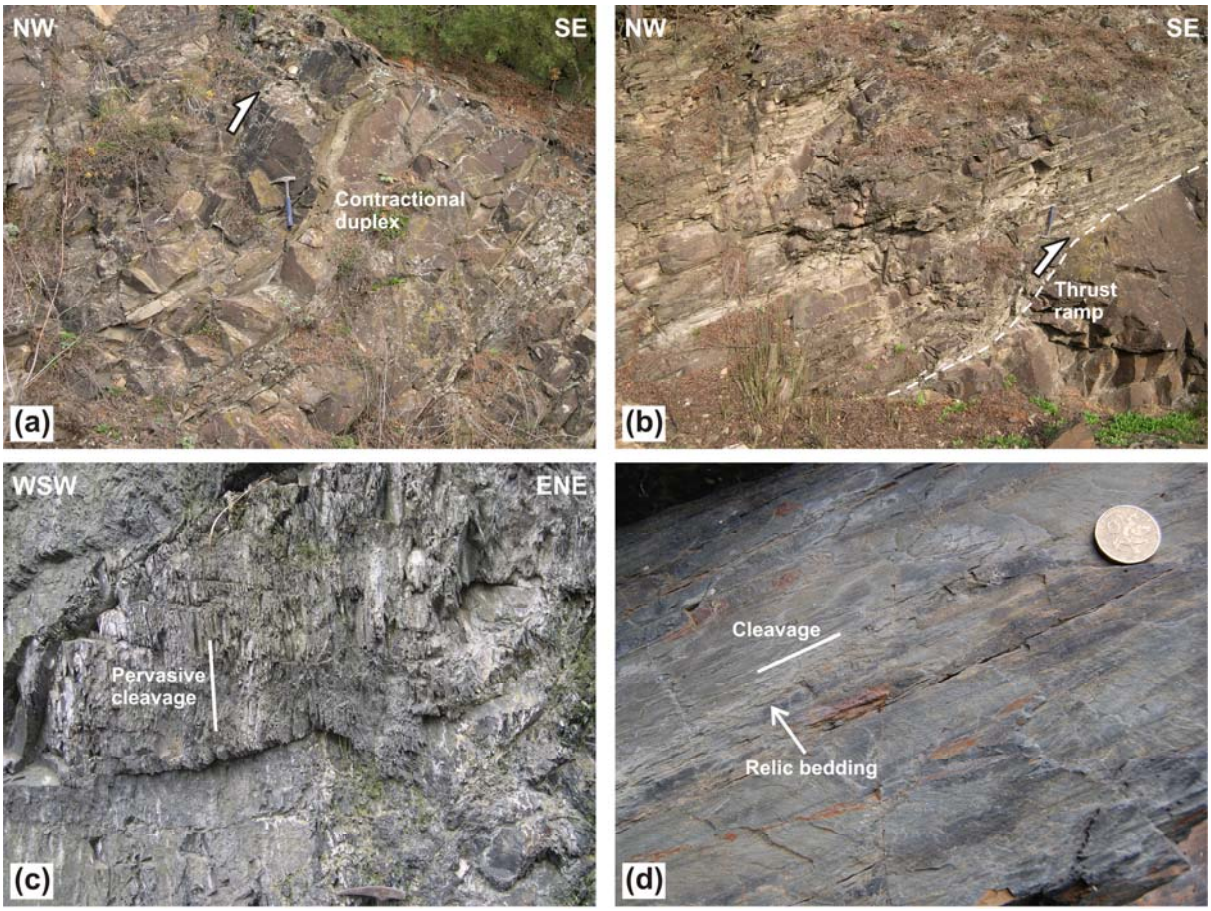

Fig. I.6. Mesoscopic deformational structures in the Neoproterozoic rocks. (a, b) Contractional duplexes and thrust faults in rhytmically interbedded graywacke–slate sequences of Domain 1; Chlum u Rakovníka. Hammer for scale. (c) Steep pervasive cleavage in slates, Domain 2; Roztoky u Křivoklátu. Hammer for scale. (d) Relic bedding parallel to intensely developed cleavage, Domain 3; Račice. Hammer for scale. See Fig. I.3 for location of outcrops.

As with Domain 2, the angular unconformity between the Neoproterozoic slates and overlying basal Ordovician beds is welldocumented both in outcrop and at map-scale in the southeastern part of the area (Fig. I.5). Here, cleavage in the Neoproterozoic slates dips steeply to the ~SE and is sharply truncated by the overlying basal Ordovician strata. Bedding

in both the basal conglomerates and overlying younger formations strikes ~ENE–WSW and dips moderately to the ~SSE (mean strike is 067°). The Lower Paleozoic strata are devoid of cleavage, except for bedding-parallel cleavage in shale interbeds between competent sandstones.

Fold style in the Neoproterozoic slates is identical to that of Domain 2: meter-scale chevron folds (Fig. I.7c) and contractional conjugate and monoclinal kink-bands are superposed on the pre-existing flat-lying and steep cleavage, respectively (Figs. I.4d and I.7d and e). Where the cleavage is steep along the contact with the Barrandian Lower Paleozoic (Fig. I.5), the kink-band axial planes dip shallowly to moderately ~NW(Fig. I.7e), whereas in flat-lying cleavage away from the contact zone they dip moderately to steeply ~NW and ~SE (Fig. I.7d).

4.4. The nature of domain boundaries

At map-scale, the boundaries between structural domains are expressed as ~NE–SW-trending sharp structural breaks, truncating bedding and cleavage on either side. Structures and lithology are remarkably discordant across the domain boundaries (Fig. I.5).

The boundary between Domains 1 and 2 (referred here to as the Městečko fault; MF in Fig. I.5) was documented on one outcrop as a more than ~10mwide zone of intensely deformed and mineralized fault breccia consisting of angular fragments of graywackes and slates set in a fine-grained crushed matrix. The fault zone strikes ~NE–SWand dips moderately (~45°) to the SE, i.e., beneath Domain 2 (Fig. I.7f). This orientation measured on the outcrop thus corresponds well with the general orientation of the boundary in the map (Fig. I.5). Kinematic indicators are rare in the breccia zone; a few asymmetric non-brecciated blocks indicate top-to-the-NW kinematics (Domain 2 over Domain 1; Fig. I.7f). In other places the boundary is not exposed, but can be well constrained to within a few tens of metres in

the field and mapped as a line separating neighboring outcrops assigned to Domains 1 and 2.

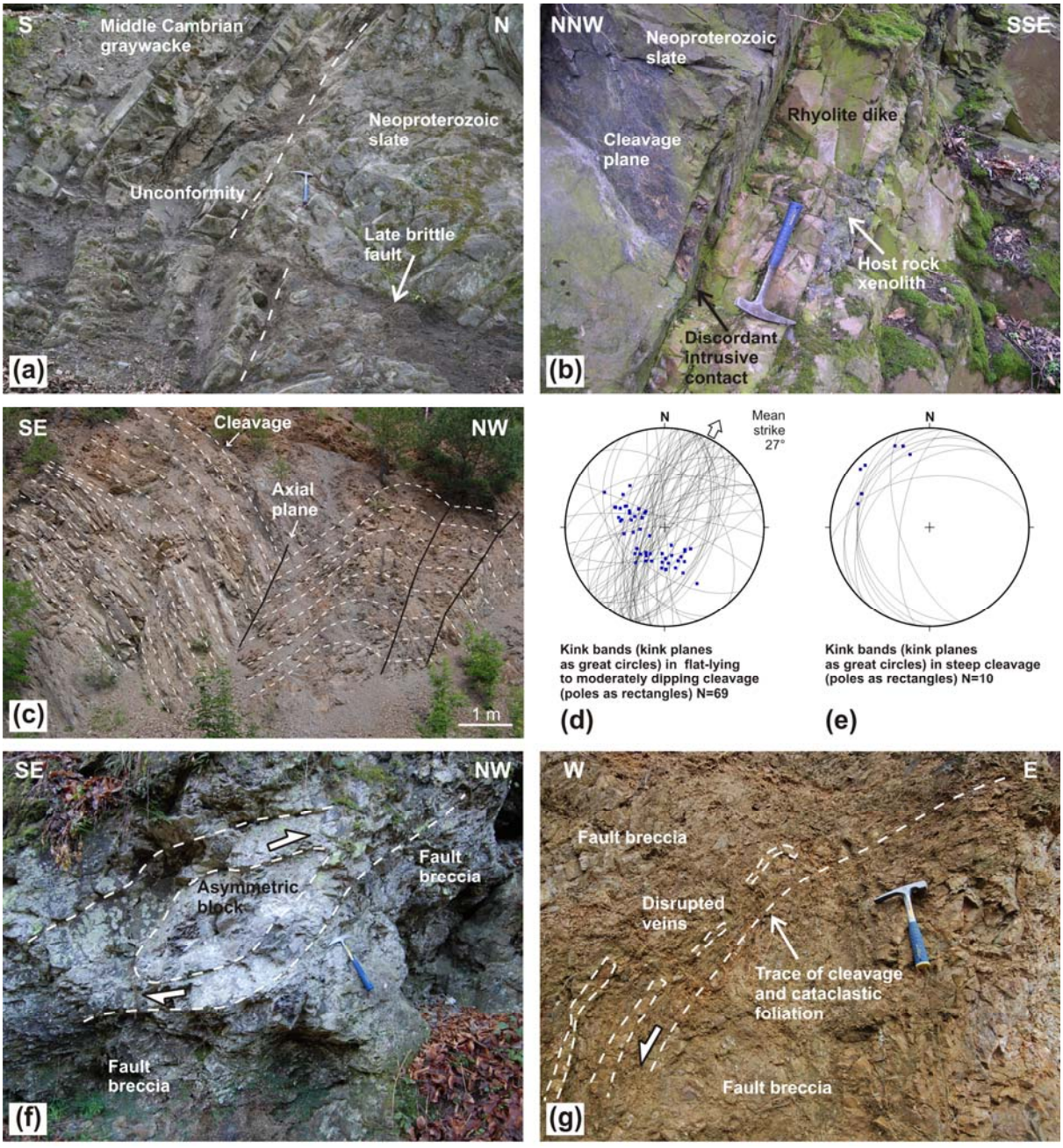

Fig. I.7. (a) Angular uncomformity between the Neoproterozoic slates and Middle Cambrian graywackes, Domain 2; Týřovice. Hammer for scale. (b) Rhyolite dike cutting across steep cleavage in slates, Domain 2; Roztoky u Křivoklátu. Hammer for scale. (c) Chevron fold superposed on cleavage in slates, Domain 3; roadcut near Nižbor. (d, e) Stereonets (equal area projection, lower hemisphere) showing orientation of kink axial planes superposed on flat-lying and steep cleavage, Domain 3. (f) Cataclastic fault zone separating Domain 1 and 2 and showing top-to-the-NW kinematics; near Městečko. Hammer for scale. (g) Cataclastic fault zone separating Domain 2 and 3, rotated flat-lying cleavage indicates SE-side-up kinematics; Družec. Hammer for scale. See Fig. I.3 for location of outcrops.

The boundary between Domains 2 and 3 (referred here to as the Družec fault; DF in Fig. I.5) is best exposed in its NE segment. Here, the flat-lying (25–35° dip) cleavage typical of Domain 3 is deflected into the boundary-parallel, ~NE–SW strike and steepens up to 60° dip to the NW (i.e., beneath the Domain 2). The rotated cleavage grades into meters to first tens of meters wide cataclastic zone (fault breccia in Fig. I.7g). Within the cataclastic zone, both the (rotated) cleavage and overprinting cataclastic foliation have the same orientation, striking ~NE–SW and moderately to steeply dipping to the NW. These structural relations indicate SE-side-up kinematics (Domain 2 down, Domain 3 up).

5. Anisotropy of magnetic susceptibility (AMS)

Magnetic fabric, as derived from anisotropy of magnetic susceptibility (AMS; for reviews and basic principles of the method see, e.g., Hrouda, 1982; Tarling and Hrouda, 1993) was used to corroborate the structural data and to describe the fabric parameters and fabric gradients across the three structural domains (Figs. I.8–I.10).

5.1. Methodology

Anisotropy of magnetic susceptibility is mathematically described as a symmetric second rank tensor which can be visualized as an ellipsoid; its semi-axis lengths, $k1 \geq k2 \geq k3$, are termed the principal susceptibilities and their orientations, K1, K2, K3, are denoted as the principal directions. Such an ellipsoid defines a magnetic fabric where the maximum direction (K1) is denoted as magnetic lineation and the plane perpendicular to the minimum direction (K3) and containing the maximum and intermediate directions (K1, K2) is denoted as magnetic foliation. Quantitatively, AMS data can be described by bulk susceptibility, degree of anisotropy, and anisotropy shape parameter. Bulk (mean) susceptibility is calculated as an arithmetical mean of the principal susceptibilities, $kb = (k1 + k2 + k3)/3$, and reflects the type and relative content of magnetic minerals in a rock. Degree of anisotropy,

expressed as P = k1/k3 (Nagata, 1961), reflects the intensity of magnetic fabric. Anisotropy shape parameter, calculated as T = 2 ln(k2/k3)/ln(k1/k3)−1 (Jelínek, 1981) quantitatively describes the shape of the anisotropy ellipsoid; it varies from −1 (perfectly prolate ellipsoid, i.e., linear fabric) through 0 (neutral or triaxial ellipsoid) to +1 (perfectly oblate ellipsoid, i.e., planar fabric).

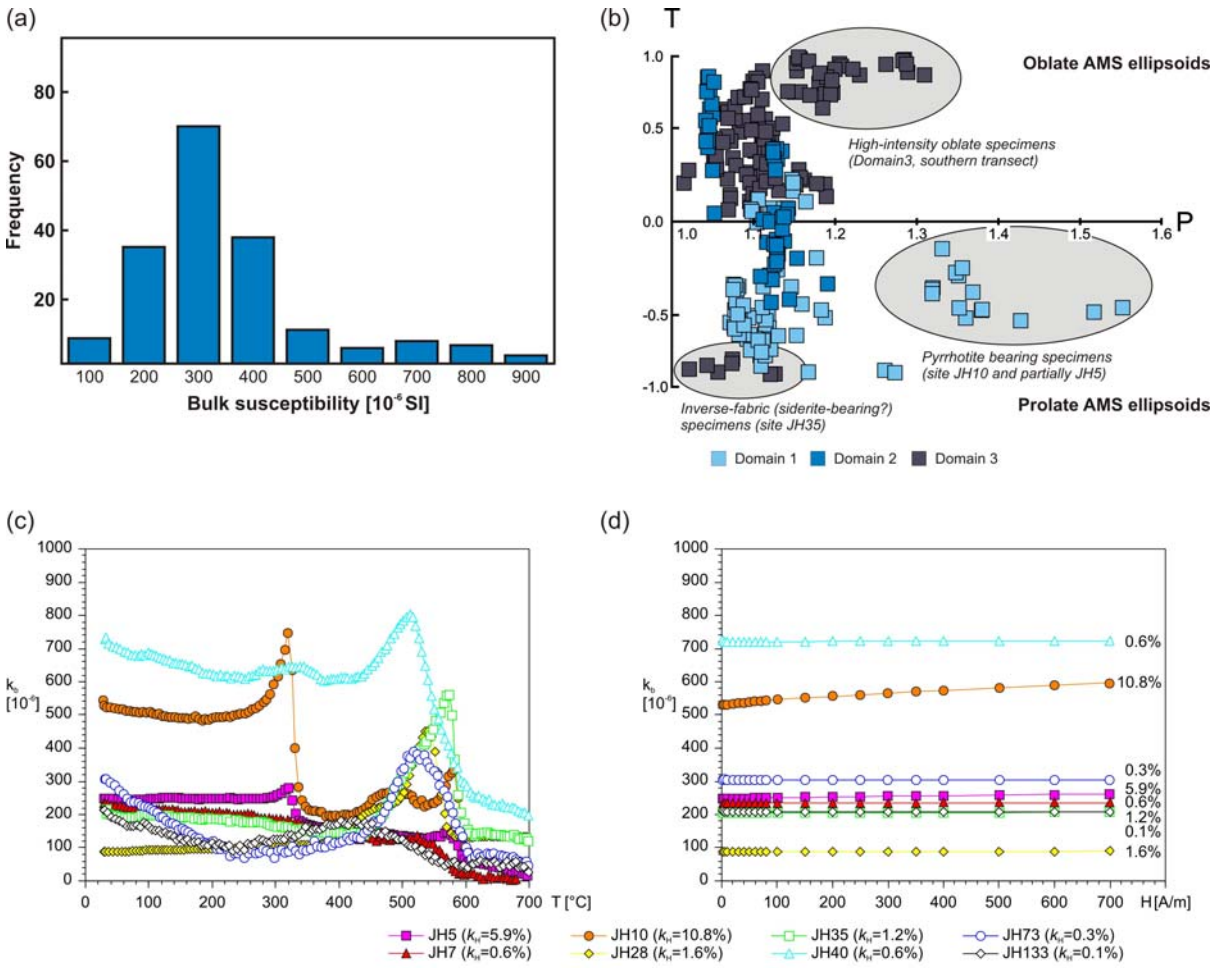

Fig. I.8. (a) Histogram of bulk susceptibility and (b) the plot of the AMS intensity (P) vs. ellipsoid shape (T) of all analyzed specimens. (c) Magnetic susceptibility as a function of temperature, heating in air atmosphere, heating rate ca. 10°C/min, and (d) magnetic susceptibility as a function of increasing AC field of eight representative samples. Field dependence is quantified as kH= 100 × (k700 – k10) / k700, where kx denotes a susceptibility measured in respective AC fields in A/m, peak values.

In total, 66 oriented samples (cores 2.5cm in diameter) were taken using a portable drill at 23 sampling sites in the Neoproterozoic rocks along two ~NW–SE oriented transects

(Fig. I.9). After laboratory cutting, these samples yielded 267 standard oriented specimens (ca. 2.2cm in height). AMS measurements and other rock magnetic experiments were performed using an Agico MFK1-FA Multi-function Kappabridge coupled with a temperature control unit CS-3 at AGICO Inc., Brno, Czech Republic. Statistical analysis ofthe AMS data was carried out using the ANISOFT 4.2 program (written by M. Chadima and V. Jelínek; www.agico.com).

5.2. Magnetic mineralogy

In all the investigated specimens bulk susceptibility does not exceed 1000×10−6 SI. The susceptibility distribution is slightly bimodal having one pronounced maximum at ca. 300×10−6 SI and the other indistinct maximum at ca. 700×10−6 SI (Fig. I.8a). Relatively low susceptibility values indicate that the carriers of magnetic susceptibility are predominantly paramagnetic minerals, presumably phyllosilicates (in our case most probably chlorite and clastic biotite). Few specimens with relatively higher susceptibility values, however, may indicate the presence of another magnetic mineral.

For the majority of specimens the degree of magnetic anisotropy ranges from 1.03 to 1.20 with AMS ellipsoids being moderately prolate, neutral, to moderately oblate in shape (Fig. I.8b). Such a distribution of magnetic fabric can be explained as being controlled by phyllosilicate grains with various types of preferred orientations provided that the magnetic anisotropy of a phyllosilicate grain is perfectly oblate having anisotropy degree P≅1.30 (Martín-Hernández and Hirt, 2003). In addition to the phyllosilicate-controlled fabric, some specimens display a highintensity oblate fabric (P≅1.15–1.3, T > 0.7), a low-intensity highly prolate fabric (P < 1.10, T <−0.8), and a high-intensity moderately prolate fabric (P≅1.30–1.60, T≅−0.5). Whereas the high-intensity oblate fabric can be carried by sub-parallel

orientation of phyllosilicates, there is no means for obtaining such high-intensity or highly prolate fabrics solely by the preferred orientation of (oblateanisotropy) phyllosilicate grains. These extreme cases of prolate fabric suggest that, at least in some specimens, the magnetic fabric is not exclusively dominated by the preferred orientation of paramagnetic phyllosilicates.

In order to analyze the carriers of magnetic fabric, magnetic susceptibility was measured as a function of temperature (from room temperature up to 700 °C, at a heating rate of ca. 10 °C/min) and amplitude of applied AC field (in the range of 2–700 A/m, peak values). For some analyzed specimens (Fig. I.8c, JH10, JH40, JH73, JH133), magnetic susceptibility hyperbolically decreases as a function of increasing temperature up to ca. 300 °C, being more or less constant for the other specimens (JH5, JH7, JH28, JH35). Gradual hyperbolic decrease is typical behavior of paramagnetic minerals where magnetic susceptibility is inversely proportional to the absolute temperature. In some specimens (JH10 and JH5) there is a pronounced peak in susceptibility at ca. 320 °C corresponding to the Curie temperature of pyrrhotite. Further increase in susceptibility above ca. 400 °C can be attributed to the growth of new magnetite as a result of phyllosilicate (and other iron minerals) decomposition and oxidation during increased temperature. Indeed, a sharp susceptibility decrease above ca. 550 °C corresponds to the Curie temperature of magnetite. The presence of pyrrhotite in some specimens (namely in JH10 and JH5) is further verified by increasing susceptibility as a function of applied field (Fig. I.8d); field dependence starting at relatively low field is a characteristic feature of pyrrhotite (e.g., Worm et al., 1993). The field dependence of the other representative specimens is insignificant (Fig. I.8d).

5.3. Magnetic fabric

Combining magnetic mineralogy analyses (Fig. I.8c and d) and magnetic fabric data

(Fig. I.8a and b), the high-intensity, moderately prolate fabric cluster of specimens (P≅1.30–1.60, T≅−0.5) is seen to correspond to sites JH10 and JH5 where the presence of pyrrhotite was demonstrated (Fig. I.8c and d). The low-intensity highly prolate fabric (P < 1.10, T <−0.8) corresponds to site JH35, which exhibits an inverse magnetic fabric where both magnetic lineation and foliation are in inverse orientation with respect to the mesoscopic lineation and foliation (Fig. I.9, JH35). Such a behavior in sedimentary rocks can be attributed to the magnetic fabric being controlled by siderite (e.g., Winkler et al., 1996; Chadima et al., 2006). Since any regional fabric pattern can be studied only by comparing the magnetic fabrics in sites not significantly different in magnetic mineralogy, the pyrrhotite- and siderite (?)-bearing specimens are excluded from further interpretation. In their absence, a gradual spatial development of magnetic fabric can be observed going through the structural domains (Fig. I.9). In Domain 1, the degree of anisotropy ranges from 1.07 to 1.20 with an average value of 1.16. The AMS ellipsoids are mostly prolate to neutral in shape (T =−0.90–0.25) (Figs. I.8b and I.9). The orientation of magnetic fabric is homogeneous–magnetic foliations strike ~NE–SW and dip moderately to steeply ~NW, whereas magnetic lineations plunge gently to the ~W–WSW (Figs. I.9 and I.10a and d).

In Domain 2, the degree of anisotropy is in the range 1.04–1.19. The shape parameter is between −0.48 and 0.88, so the AMS ellipsoids have neutral to oblate shapes (Figs. I.8b and I.9). Magnetic foliations exhibit four main orientations: (1) ~NNW–SSE dipping steeply ~ENE, (2) ~WNW–ESE dipping gently ~NNE, (3) ~WNW–ESE dipping steeply ~NNE, and (4) ~E–W dipping moderately to steeply ~N (Fig. I.9). These orientations correspond to four distinct maxima of k3 axes on the stereonet (Fig. I.10e) and can be correlated with the rather scattered distribution of cleavage in Domain 2 (Fig. I.5). Magnetic lineations cluster in three maxima plunging gently ~WSW, steeply ~NE, and gently ~NNW (Figs. I.9 and I.10b).

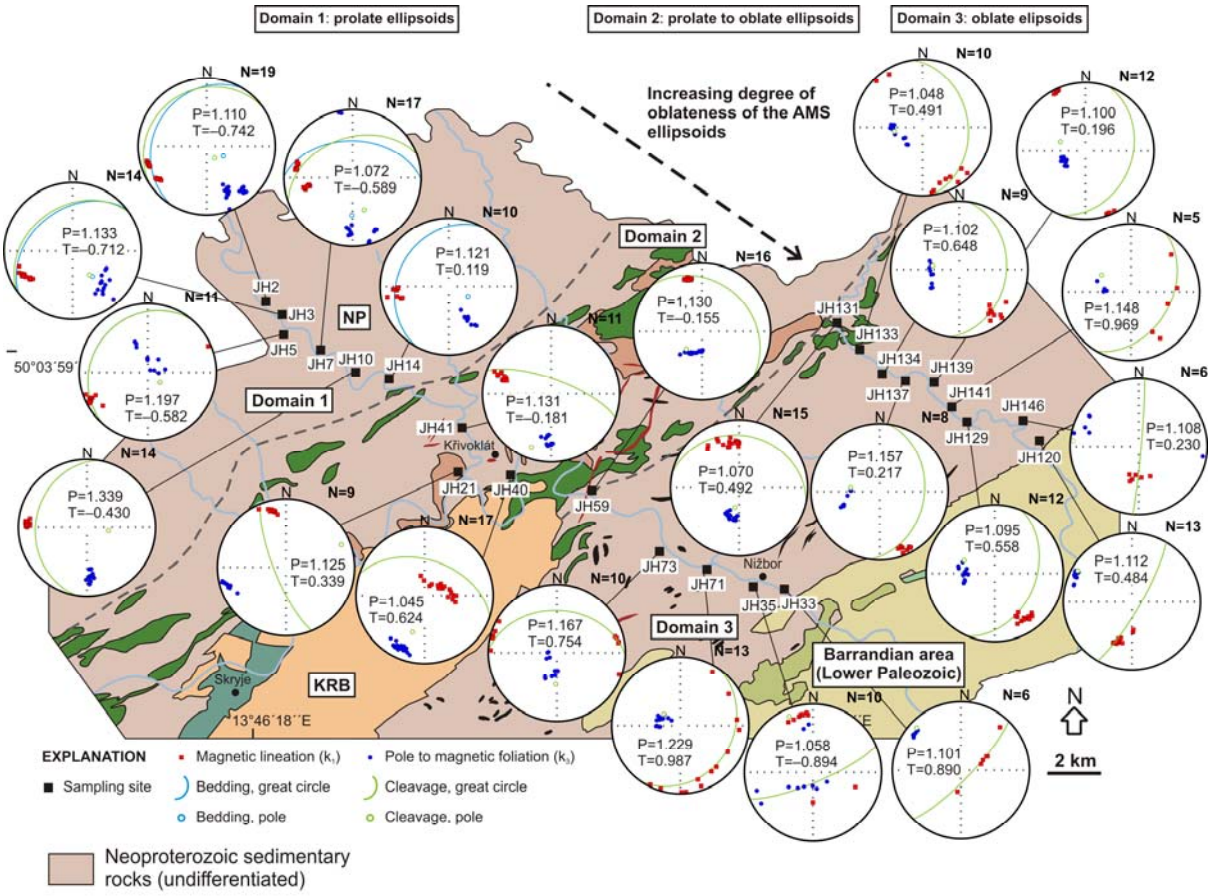

Fig. I.9. Map of the northwestern margin of the Barrandian area showing AMS sample locations, mean P and T parameters at each sampling site, and orientation of magnetic lineations (k1) and poles to magnetic foliations (k3) in stereonets (equal area projection, lower hemisphere, geographic coordinate system).

In Domain 3, the degree of anisotropy is in the range of 1.04–1.31. The shape parameter ranges between 0.10 and 0.99, which means that the AMS ellipsoids have only oblate shapes (Fig. I.8b). On the stereonet, magnetic foliations cluster around two maxima, one corresponding to cleavage striking ~NW–SE to ~N–S and dipping gently ~NE, and the other to ~NE–SWcleavage dipping steeply ~SE (Figs. I.9 and I.10f). Magnetic lineations are subhorizontal but their trends scatter widely (Figs. I.9 and I.10c).

In summary, the following general trends are revealed by the magnetic fabric survey in the Barrandian Neoproterozoic: (1) The degree of anisotropy (P) varies noticeably from 1.04 (almost isotropic samples) up to 1.31 (Fig. I.8b). (2) The shape of the AMS ellipsoid changes significantly from the ~NW to the ~SE, with values of T in both map view (Fig. I.9) or

AMS plot (Fig. I.8b), clearly increasing from Domain 1 to Domain 3, i.e., from prolate through neutral to weakly oblate to significantly oblate AMS ellipsoids. (3) The orientation of the magnetic fabric corresponds well to mesoscopic structures with magnetic foliations having nearly the same orientations as bedding or cleavage and magnetic lineations having similar orientations as lineations measured in outcrop.

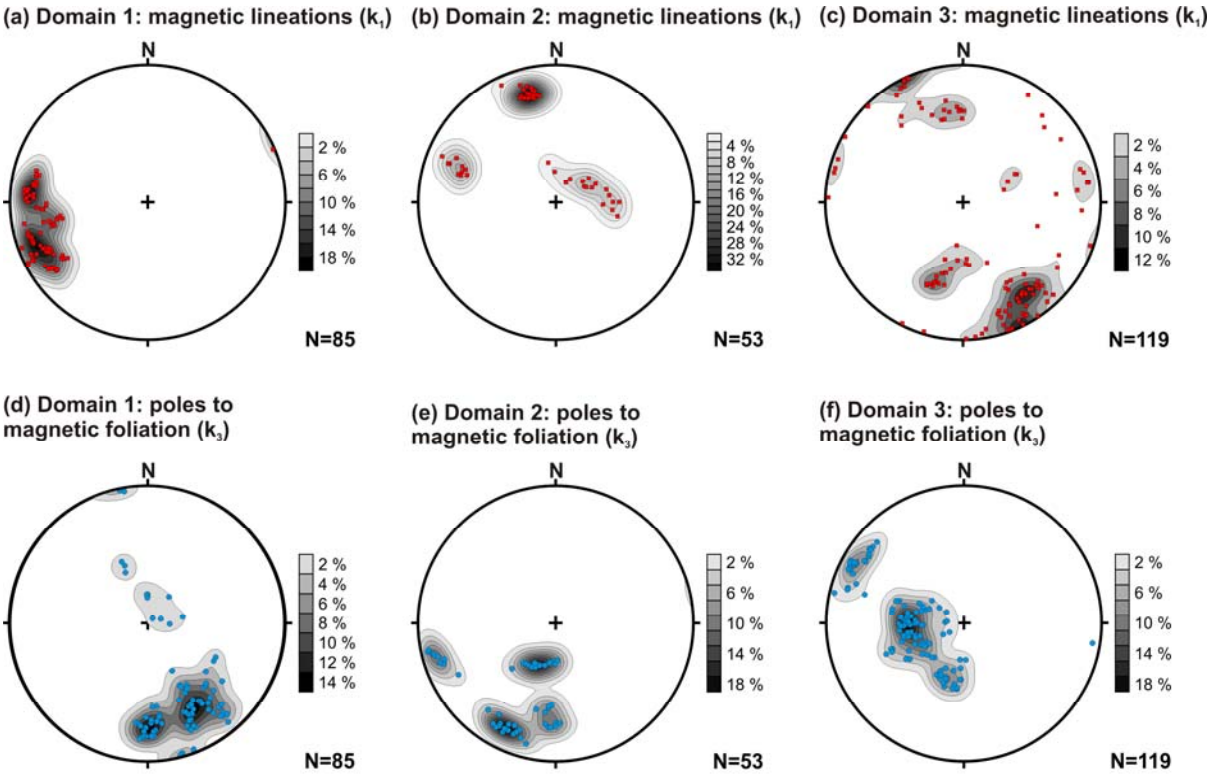

Fig. I.10. Stereonets (equal area projection, lower hemisphere) summarizing orientation of magnetic lineations (k1) and poles to magnetic foliations (k3) for Domains 1−3.

6. Microstructures

Microstructures within the Neoproterozoic and Lower Paleozoic rocks were examined at 17 stations along two ~NW–SE transects in order to characterize mineral assemblages, deformation mechanisms, and cleavage development across the three structural domains. Below we describe four representative samples that are typical of each

domain and which document a striking microstructural gradient from NW to SE.

6.1. Sample JH7—graywacke from Domain 1

The graywacke is composed chiefly of quartz, plagioclase, K-feldspar, sericite, and partly chloritized clastic biotite (Fig. I.11a). The fine-grained quartz and sericite matrix encloses irregularly shaped, subangular detrital porphyroclasts (up to 0.2mmin size) of feldspar, quartz, and acid volcanic rocks. Quartz is recrystallized in pressure shadows of the porphyroclasts to form grains with significantly reduced grain-size (down to 25µm). The cleavage is rough and developed as short, discontinuous cleavage domains defined by seams of extremely fine-grained dark material enveloping the large detrital grains (spaced disjunctive cleavage of Powell, 1979; Passchier and Trouw, 2005).

6.2. Sample JH41—graywacke from Domain 2

The main minerals in the sample are quartz, plagioclase, sericite, K-feldspar, and calcite (Fig. I.11b). The rock exhibits a weak lamination: laminae composed of large irregular clasts (up to 0.2mm in size) set in a coarse-grained graywacke matrix alternate with fine-grained silty laminae enclosing significantly smaller detrital grains. The graywacke material is mingled with broken-off shale fragments (presumably micro-scale slump structures; Cháb and Pelc, 1968). Cleavage is largely localized in finer-grained laminae, forming anastomosing but continuous cleavage domains (Fig. I.11b).

6.3. Sample JH139—metagraywacke from Domain 3

The metagraywacke is composed of quartz, plagioclase (mostly albite), biotite, muscovite, chlorite, epidote and actinolite, with titanite and microcline as accessory minerals (Fig. I.11c). Acicular actinolite has grown at the expense of detrital hornblende in the pressure shadows of quartz and feldspar porphyroclasts. Such a mineral assemblage

indicates lower greenschist facies conditions with stable chlorite, albite, epidote, and actinolite. The metagreywacke also contains flattened clasts of black shale, siltstone, and devitrified volcanic glass. No sedimentary textures are preserved. Instead, the rock has been penetratively deformed by closely spaced smooth to anastomosing (around larger subangular grains) cleavage domains defined by ultra-fine-grained dark seams wrapping around larger grains (Fig. I.11c). The cleavage is enhanced by the alignment of biotite grains and flattened siltstone clasts in the microlithons.

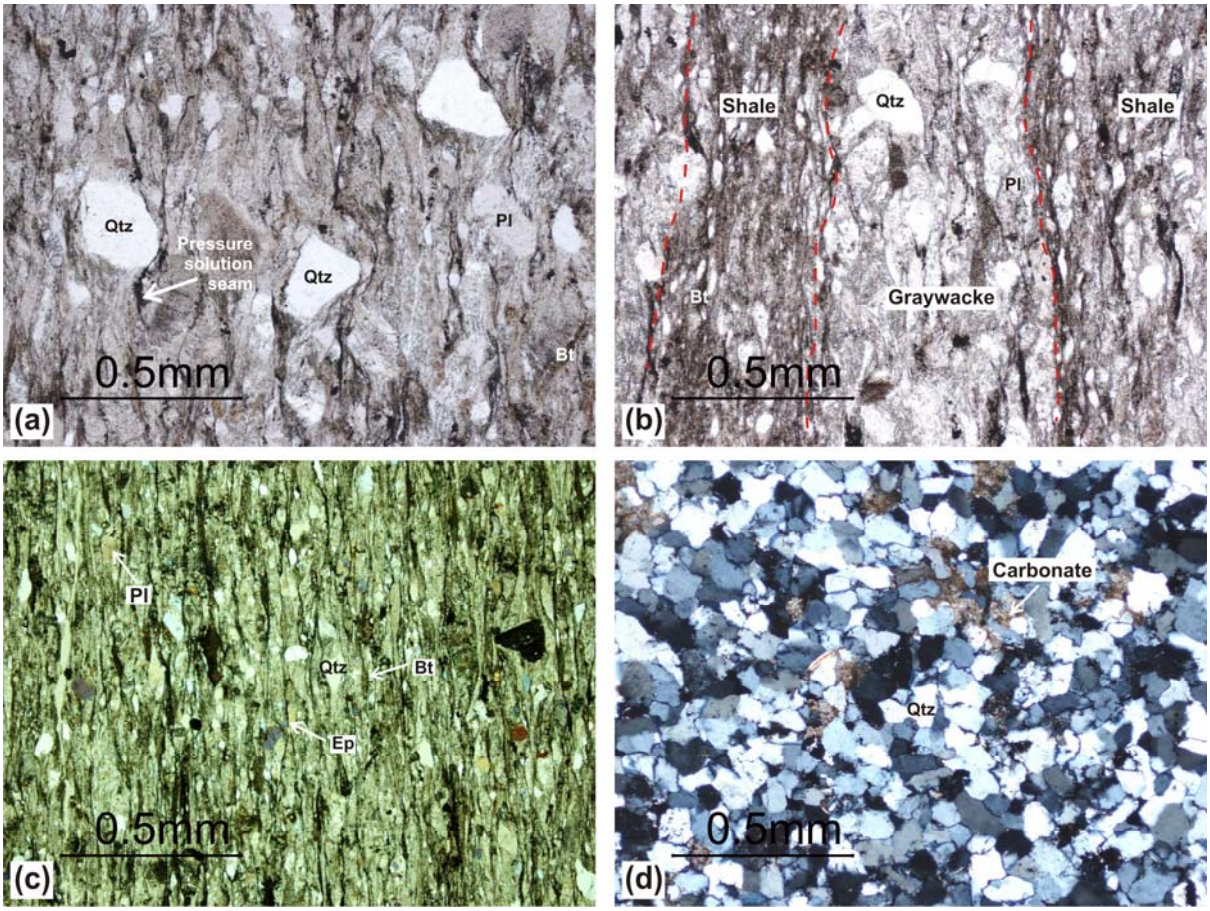

Fig. I.11. Microphotographs showing contrasting deformation structures and mineral assemblages in (a) Neoproterozoic graywackes in Domain 1, (b) finely laminated graywackes in Domain 2, (c) metagraywackes in Domain 3, and (d) Ordovician quartzite. Mineral symbols and abbreviations after by Kretz (1983), see Fig. I.3 for sample locations.

In the Neoproterozoic rocks, the deformational microstructures are characterized by

increasing volume and smoothness of cleavage domains from the NW to the SE. In addition, the degree of regional metamorphism increases to the SE as documented by syntectonic growth of chlorite and epidote in Domains 2 and 3.

6.4. Sample JH28—undeformed Ordovician quartzite

The rock is well-sorted, composed predominantly of quartz with almost no matrix preserved. Calcite and tourmaline occur as accessory minerals (Fig. I.11d). The quartz grains, approximately 0.1mm in size, have irregular boundaries and show only weak undulatory extinction (Fig. I.11d). In contrast to the Neoproterozoic rocks, the quartzite is virtually undeformed with no micro-scale evidence for recrystallization or cleavage.

7. Discussion

7.1. Criteria used to separate Cadomian from Variscan deformation

The following criteria firmly establish the Cadomian age of deformation structures (described above) in the Neoproterozoic basement along the northwestern margin of the Barrandian area. (1) An angular unconformity exists between the steep pervasive cleavage in the Neoproterozoic slates developed under prehnite–pumpellyite to lower greenschist facies conditions (Cháb and Bernardová, 1974; Cháb et al., 1995; this study) and the only gently to moderately tilted and internally unstrained Middle Cambrian and Ordovician strata (Fig. I.7a). (2) The ?Cambro–Ordovician felsic dikes cut across the cleavage with knife-sharp discordant contacts and also enclose wall-rock xenoliths with cleavage (Fig. I.7b). (3) The angular unconformity between the cleavage in the Neoproterozoic rocks and bedding in the Lower Paleozoic rocks is expressed both at map-scale (Fig. I.5) and in the mean directions calculated from the structural data. In Domain 3, the cleavage is folded about an 038°-trending axis that makes an angle of 29° to the mean strike of the overlying Lower Paleozoic

strata (067°). (4) The 40° angular divergence exists between the mean Lower Paleozoic fold axis and conjugate kink bands superposed on the flat-lying cleavage (Fig. I.7d and e; mean strike of kink axial planes is 027°). (5) The Middle Cambrian and Lower Ordovician strata and Cambro–Ordovician extrusive rocks of the Křivoklát–Rokycany volcanic complex (KRVC in Fig. I.5), which overlap the structural domains (Domains 1–3), constrain the age of early movements along the boundary faults and domain juxtaposition to the pre-Middle Cambrian. In general, however, the ~NE–SW faults in the Cadomian basement (presumably including the Domains 1–3 boundaries) may have been later reactivated during Early Paleozoic basin formation and subsequent Variscan structural inversion (Chlupáč et al., 1998).

In contrast to the above, Variscan deformation recorded in the adjacent Lower Paleozoic rocks is non-penetrative and characterized by a simple fold style. Variscan folding resulted only in moderate tilting of the bedding in the Lower Ordovician siliciclastic rocks to the SE about a 067°-trending axis (Fig. I.5), and in the reorientation (steepening) of the Cadomian cleavage and kinkbands superposed onto the cleavage in the adjacent Neoproterozoic basement (Fig. I.5).

7.2. Tectonic model for the Teplá–Barrandian Neoproterozoic accretionary wedge

As summarized in Table 1, the three structural domains defined in this paper differ significantly in lithology, style and intensity of deformation, and degree of Cadomian regional metamorphism. The amount of finite shortening, as revealed by cleavage intensity and progressive flattening of the AMS ellipsoid, and temperature conditions of deformation generally increase to the SE from prehnite–pumpellyite up to lower greenschist facies conditions (T~250–350 °C; Cháb and Bernardová, 1974; Suchý et al., 2007). Based on these

data and the newly defined lithotectonic zonation we propose the following kinematic model for the TBU accretionary wedge during the Cadomian orogeny (Fig. I.12).We adopt the paleo-subduction zone polarity and timing of deformation events proposed by Dörr et al. (2002) and Sláma et al. (2008), which are consistent with our structural data (Fig. I.12a).

Domain	**Lithology**	**Stratigraphy**	**Structures**					**Mineral assemblage**
			Bedding	Cleavage	Magnetic foliation	Magnetic lineation	AMS ellipsoid	
1	Flysch-like alternating graywackes and shales	Blovice Fm.[1] Rakovník G.[2] Kralovice–Rakovník belt[3] Flysch facies[4]	(1) ~ENE–WSW (2) ~NE–SW	Spaced disjunctive, bedding-parallel	Dips moderately to steeply to the ~N–NW	Plunges shallowly to the ~W–WSW	Prolate	Weak burial metamorphism Qtz, Plg, Kfs, Ser
2	Graywackes and slates, olistoliths, slump structures, basalt bodies	Blovice Fm.[1] Zvíkovec G.[2] Radnice–Kralupy belt[3] Volcanogenic facies[4]	Variable, ~E–W dominant	Anastomosing, continuous ENE–WSW to ESE–WNW (2) ENE–WSW to ESE–WNW	Dips moderately to the ~NE	Three distinct orientations, dominant lineation plunges shallowly to the NNW	Neutral to weakly oblate	Lower greenschist facies Qtz, Plg, Kfs, Ser, Chl, Ep
3	Slates with graywackes, chert lenses	Blovice Fm.[1] Úslava G.[2] Zbiroh–Šárka belt[3] Monotonous facies[4]	No bedding preserved due to pervasive deformation	Smooth, poles create a girdle around axis 38°/17°, cleavage steepens near the contact with Lower Paleozoic	Dips gently to the ~NE	Subhorizontal with variable trend, dominant SSE	Oblate	Lower greenschist facies Qtz, Plg, Kfs, Ser, Chl, Ep, Mu, Amp
Barrandian Lower Paleozoic	Shales, siltstones, sandstones, basalts, andesites	Lower Ordovician	Homogeneous, mean strike 66°, dip to the SSE	No cleavage or bedding-parallel in shale interbeds	No data	No data	No data	Clastic grains, no metamorphic minerals

Table 1. Characteristics of structural domains (Domains 1–3) and overlying Lower Paleozoic rocks along the northwestern margin of the Barrandian area. Lithostratigraphy after [a]Mašek (2000), [b]Holubec (1995), [c]Röhlich (1965), [d]Cháb and Pelc (1968).

The northwesterly Domain 1 is both the most outboard (trenchward) unit. It has never been significantly buried within the wedge (Fig. I.12b) and experienced only weak deformation and folding. Both the tilt of the bedding to the ~NW and the bedding-parallel low-temperature cleavage formed by pressure solution in slate interbeds are the result of

flexural-slip folding. The cleavage is associated with an ~E–W magnetic lineation and prolate shapes of the AMS ellipsoid (Figs. I.8b and I.9). In terms of orientation, the magnetic lineation corresponds to the mesoscopic lineation and both are interpreted to represent the bedding-oblique flexural-slip direction. Compared to the slate interbeds, the internal strain recorded by the graywackes during flexural-slip folding was weak since the degree of anisotropy P is generally low.

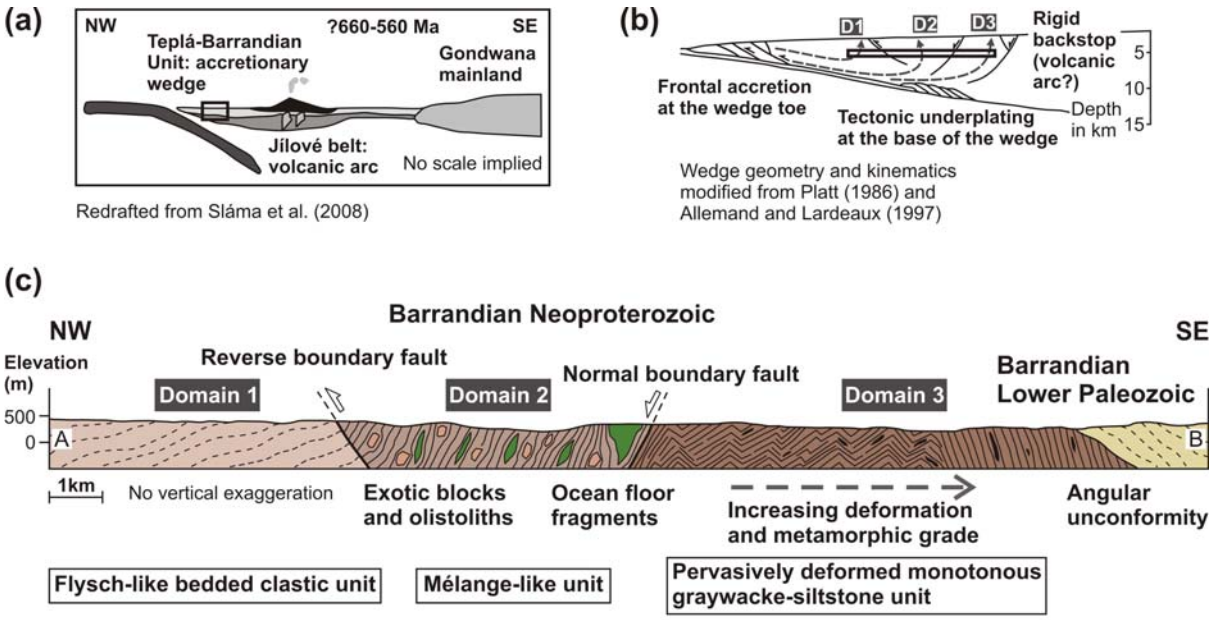

Fig. I.12. Tentative tectonic model for the Teplá–Barrandian Unit as a Cadomian accretionary wedge between a subduction zone to the NW and a volcanic arc to the SE (present-day coordinates). (a) Interpretation of an overall geotectonic setting of the Teplá−Barrandian Unit during Cadomian orogeny after Sláma et al. (2008). Bold rectangle indicates presumed position of the study area. (b) Simplified Platt (1986) kinematic model for an accretionary wedge showing inferred position and differential burial−exhumation trajectories (dashed gray lines) of the three structural domains (D1−D3) described in this paper. Bold rectangle represents interpreted position of cross-section in Fig. I.12c. (c) Simplified interpretive cross-section along line A−B (location shown in Fig. I.3). The three structural domains are interpreted to represent contrasting units juxtaposed within the accretionary wedge along localized boundary faults. The total amount of displacement and throw along the boundary faults are unknown.

In contrast to Domain 1, the central mélange-like Domain 2 is characterized by heterogenous intense deformation and predominantly ~E–W relic bedding and cleavage associated with neutral shapes of the AMS ellipsoids (Figs. I.8b and I.9). Mesoscopic lineation

is almost absent, suggesting a flattening strain associated with the cleavage development. The magnetic lineation is interpreted to represent the intersection of mesoscopic cleavage and bedding and presumably corresponds to the common axis of phyllosilicate grains in various stages of reorientation. This interpretation is consistent with the lack of mesoscopic stretching lineation and absence of evidence for flexural slip. Thus, the AMS lineations cannot represent a mineral (stretching) lineation (e.g., Parés and van der Pluijm, 2002). Magnetic foliations correspond to the cleavage, both recording heterogenous deformation during dominantly ~N–S shortening. Syntectonic growth of chlorite along cleavage planes suggests increased regional metamorphism (prehnite–pumpellyite to lower greenschist facies conditions) relative to Domain 1 (Fig. I.12b).

Hence, we envision the evolution of central Domain 2 as involving: (1) graywacke-argillite mélange formation by the mingling of broken-off sedimentary rocks and pieces of ocean floor, (2) burial to depths corresponding to prehnite–pumpellyite to lower greenschist facies conditions, and (3) later heterogenous ductile deformation with dominant ~N–S shortening. The mélange formation and heterogeneous deformation may have taken place in the subduction channel (e.g., Cloos, 1982; Cowan, 1985; Cloos and Shreve, 1988a,b), however, the weak ~N–S shortening is also recorded in graywackes of Domain 1 at higher structural levels. Subsequently, Domain 2 was exhumed and thrust over Domain 1 as a rigid block along a highly localized ~NE–SW-trending fault (Figs. I.7f and I.12b and c).

The most inboard (arcward) but lithologically monotonous Domain 3 was also buried to depths corresponding to the lower greenschist facies conditions (indicated by the syntectonic growth of epidote, actinolite and albite; Fig. I.11c) where it was pervasively overprinted by flattening strain as evidenced by an intensely developed, ~SE-dipping cleavage and oblate AMS ellipsoids (Figs. I.8b and I.9). Continued shortening produced

contractional kink-bands and chevron folds (Fig. I.7c and d) superimposed on the greenschist-facies cleavage. Exhumation of Domain 3 was accommodated by a major ~NE–SW normal fault (Figs. I.7g and I.12b and c).

Taken together,we interpret this structural history to record discrete deformational events and differential exhumation of the three structural domains from various depths within the accretionary wedge during active subduction in a manner analogous to that theoretically elaborated by Platt (1986). The NW-directed thrusting of Domain 2 over Domain 1 is thought to have been caused by accretion at the wedge front, whereas the SE-dipping cleavage and exhumation of Domain 3 is interpreted to record inclined pervasive shortening during tectonic underplating and subsequent horizontal extension of the rear of the wedge (Fig. I.12b; e.g., Platt, 1986; Cloos and Shreve, 1988a,b; Allemand and Lardeaux, 1997). It is important to note, however, that the exact timing of these processes is unknown and that the structural history of the wedge was likely much more complex (e.g., Braid et al., in press).

Combining our structural data with recent high-precision geochronology (Sláma et al., 2008), we suggest that the overall convergent setting and intraoceanic subduction-driven processes lasted from ?660–560Ma as recorded in the Kralupy–Zbraslav Group, although the main phase of shortening was coeval with syntectonic flysch sedimentation at ~560–530Ma (Sláma et al., 2008). In the overlying flysch succession of the Štěchovice Group (Fig. I.2), clastic material was derived from both the arc and the nearby continental crust (Sláma et al., 2008), suggesting telescoping of the accretionary wedge–arc system between an arriving aseismic ridge or oceanic plateau to the N or NW and a rigid backstop to the SE (?continental basement; Figs. I.1d and I.12a). The syntectonic flysch sedimentation continued until ~530Ma in a southeasterly short-lived retroarc basin (Sláma et al., 2008). The deformation

and sedimentation thus progressively migrated in the wedge/arc system from the NW to the SE, i.e., towards the presumed continent (Gondwana mainland in Fig. I.12a). Boninite dikes cutting across the graywackes contain ~540Ma zircons and are overlain by Middle Cambrian strata, suggesting that the mid-ocean ridge entered the trench and caused anomalous thermal conditions in the overriding lithospheric mantle.

A more precise paleogeographic reconstruction of the original subduction zone geometry, accretionary wedge width, and extent of the volcanic arc is, unfortunately, hindered by extensive Variscan (Late Devonian to Early Carboniferous) reworking of the TBU margins and possible rotations of the entire TBU block (e.g., Edel et al., 2003).

7.3. Comparison of the Teplá–Barrandian unit with related Cadomian terranes

Since the TBU is a component of the Cadomian–Avalonian belt with affinities to the Armorican Terrane Assemblage (e.g., Tait et al., 1997; Franke and Zelazniewicz, 2002; Drost et al., 2004, 2007; Kalvoda et al., 2008; Sláma et al., 2008), we briefly compare its tectonic evolution to that of the two geologically most closely related terranes (the adjacent Saxothuringia and the Armorica s.s.; Fig. I.1a), emphasizing the main differences in order to highlight the uniqueness of some aspects of the TBU.

The Neoproterozoic basement of the Saxothuringian unit (exposed in the Lausitz block and North Saxon Anticline) comprises three lithotectonic units interpreted as a backarc basin, a retroarc basin with a related remnant basin, and a shelf-basin with passive margin deposits (e.g., Linnemann and Romer, 2002; Buschmann et al., 2006; Linnemann et al., 2007, 2008a,b,c). Accretionary wedge sediments and a related magmatic arc have not been preserved, but the existence of an arc is reflected in the composition of the backarc basin sediments. A recent tectonic model proposed by Linnemann et al. (2007) for the

Saxothuringian unit assumes the co-existence of amagmatic arc, backarc basin, and a passive margin during subduction at ~570 Ma, followed by a collision of the arc with the continent, and subsequent closure of backarc basin to form a foldand- thrust belt with related retroarc basin at ~543Ma (see Figs. 13 and 14 in Linnemann et al., 2007). The final stages of the Cadomian orogeny were accompanied by intrusions of granitoid plutons into the sedimentary successions at ~570–560Ma and ~540–530 Ma.

The North Armorican Massif (Armorica s.s.), a classic area where the Cadomian orogeny was first defined (Bertrand, 1921), is an assemblage of four terranes separated by steep ductile shear zones and brittle faults (e.g., Strachan et al., 1989; D'Lemos et al., 1990; Treloar and Strachan, 1990; Brown, 1995; Miller et al., 1999; Ballévre et al., 2001; Chantraine et al., 2001; Samson et al., 2005; Linnemann et al., 2008b). The most outboard (northwestern) part of the Massif is made up of ~2Ga Icartian basement, interpreted as a detached fragment of the West African Craton, and a volcanic arc built on this basement (Samson et al., 2005; Linnemann et al., 2008b). The accretionary wedge is not exposed, but is assumed to lie offshore further to the N. To the S, sediments of an intra-arc basin and magmatic rocks that lack an ancient basement are present (Linnemann et al., 2008b). The two southernmost terranes represent a backarc basin with LP–HT metamorphic rocks and numerous granitoid plutons, and are separated from the Central Armorican Massif by the Variscan North Armorican Shear Zone. A tectonic model proposed for these terranes invokes oblique subduction of an aseismic ridge or island arc at ~610Ma beneath an active continental margin, leading to segmentation of the margin, sinistral transpression, and intracrustal melting producing migmatites and granitoids in the backarc region (Brown, 1995).

Comparison of the TBU with these two regions shows that subduction, arc

magmatism, and regional deformation broadly overlapped in time along the Cadomian active margin. But there are several striking differences: (1) Pre-Cadomian continental basement is not exposed in the TBU, contrary to the ~2Ga Icartian gneisses of the Armorican Massif. Instead, seismic anisotropy data indicate the TBU to be underlain by attenuated mantle lithosphere with its own mantle fabric distinct from that of adjacent units (Babuška et al., in press). In addition, seismic profiles show significant subhorizontal to SSE-dipping reflections in the TBU at depth, a seismic pattern similar to subduction–accretion complexes in modern arcs (Tomek et al., 1997). The geophysical data are thus consistent with the presumed accretionary wedge model for the TBU during the Cadomian orogeny. (2) Unlike the Armorican Massif, backarc volcanic complexes, LP–HT metamorphic core complexes, and extensive granitoid magmatism have not been found in association with the Cadomian evolution of the TBU. This would suggest a rather limited amount of backarc extension, perhaps due to flat-slab subduction. (3) In both the North Armorican Massif and Saxothuringia, oblique Cadomian subduction of oceanic lithosphere is assumed, producing large-scale strike-slip shear zones separating individual lithotectonic units. In contrast, no evidence has been found in the TBU for significant Cadomian strike-slip movements, suggesting frontal subduction with the trenchward margin of the TBU oriented at a high angle to the subduction vector in this part of the Cadomian belt.

8. Conclusions

(1) Three contrasting lithotectonic units (Domains 1–3) occur in the central part of the TBU that differ in lithology (flysch-like, graywacke–argillite mélange with pieces of ocean floor, and monotonous siliciclastic), style and intensity of deformation, magnetic fabric, and in the degree of regional metamorphism. The amount of finite shortening and the temperature conditions of deformation generally increase from the NW to the SE across

these units, i.e., from the unmetamorphosed Domain 1 to the lower greenschist facies Domain 3.

(2) The boundaries between the adjacent domains are major antithetic brittle faults: the Domain 1/2 boundary is a thrust fault associated with top-to-the-NW movement (Domain 2 over Domain 1), whereas the Domain 2/3 boundary is a normal fault (Domain 2 down, Domain 3 up). The domains are overstepped by the Middle Cambrian and Lower Ordovician successions and Cambro–Ordovician volcanic rocks, constraining the age for domain juxtaposition and early movements along the boundary faults to the pre-Middle Cambrian (Late Cadomian).

(3) We interpret Domains 1–3 as allochtonous tectonic slices of an accretionary wedge at the northern active margin of Gondwana during the Late Neoproterozoic Cadomian orogeny (~660–540 Ma) that were differentially exhumed from various depths within the wedge during subduction. The NW-directed thrusting of Domain 2 over the most outboard Domain 1 may have been caused by accretion at the wedge front, whereas the exhumation of the arcward Domain 3 may record shortening during underplating and subsequent extension at the rear of the wedge. This model may also explain the uplift and erosion of older sedimentary rocks of the Kralupy–Zbraslav Group and volcanic arc rocks of the Jílové Belt, and the shift of sedimentation to the SE, where a small retroarc basin formed during the terminal Neoproterozoic/Early Cambrian. The intrusion of boninite dikes bracketed between ~540 and 520 Ma may reflect the ridge–trench collision and the transition from destructive to transform margin during Early/Middle Cambrian. Such a kinematic scenario would suggest that the Cadomian wedges developed in a manner identical to Phanerozoic and modern accretionary margins.

(4) Compared to related Armorican-type terranes, the TBU lacks exposed continental

basement, evidence for strike-slip shearing, extensive backarc plutonism and LP–HT metamorphism and anatexis, which could be interpreted as a result of frontal flat-slab Cadomian subduction.

(5) Finally, our study emphasizes that the TBU may represent the best preserved fragment of an accretionary wedge in the entire Avalonian–Cadomian belt and may therefore provide unique insight into the style, kinematics, and timing of accretionary processes along the Avalonian–Cadomian belt. Further research should focus on the larger-scale kinematic pattern linked to a petrologic study of regional metamorphism to better understand the details of the P–T evolution of different segments of the wedge, and on precise geochronology of the volcanic rocks in Domains 1–3 to reconstruct their stratigraphic relations as a time constraint for tectonic models.

References

Allemand, P., Lardeaux, J.M., 1997. Strain partitioning and metamorphism in a deformable orogenic wedge: application to the Alpine belt. Tectonophysics 280, 157–169.

Babuška, V., Fiala, J., Plomerová, J., in press. Bottom to top lithosphere structure and evolution of western Eger Rift (Central Europe). Int. J. Earth Sci., doi:10.1007/s00531-009r-r0434-4.

Ballévre, M., Le Goff, E., Hébert, R., 2001. The tectonothermal evolution of the Cadomian belt of northern Brittany, France: a Neoproterozoic volcanic arc. Tectonophysics 331, 19–43.

Bertrand, L., 1921. Les anciennes mers de la France et leurs depots. Flammarion, Paris, 190 pp.

Braid, J.A., Murphy, B.J., Quesada, C., in press. Structural analysis of an accretionary prism in a continental collisional setting, the Late Paleozoic Pulo do Lobo Zone, Southern Iberia. Gondwana Res., doi:10.1016/j.gr.2009.09.003.

Brown, M., 1995. The late-Precambrian geodynamic evolution of the Armorican segment of the Cadomian belt (France): distortion of an active continental margin during south-west directed convergence and subduction of a bathymetric high. Géol. France 3, 3–22.

Buschmann, B., Elicki, O., Jonas, P., 2006. The Cadomian unconformity in the Saxo–Thuringian Zone, Germany: palaeogeographic affinities of Ediacaran (terminal Neoproterozoic) and Cambrian strata. Precambrian Res. 147, 387–403.

Cháb, J., 1993. General problems of the TB (Teplá–Barrandian) Precambrian, Bohemian Massif, the Czech Republic. Bull. Geosci. 68, 1–6.

Cháb, J., Bernardová, E., 1974. Prehnite and pumpellyite in the Upper Proterozoic basalts of the north-western part of the Barrandian region (Czechoslovakia). Krystalinikum 10, 53–66.

Cháb, J., Pelc, Z., 1968. Lithology of Upper Proterozoic in the NW limb of the Barrandian area. Krystalinikum 6, 141–167.

Cháb, J., Suchý , V., Vejnar, Z., 1995. Metamorphic evolution (the Teplá–Barrandian Zone). In: Dallmeyer, R.D., Franke, W.,Weber, K. (Eds.), Pre-Permian Geology of Central and Eastern Europe. Springer-Verlag, Berlin/Heidelberg/New York, pp. 392–397.

Chadima, M., Pruner, P., Šlechta, S., Grygar, T., Hirt, A.M., 2006. Magnetic fabric variations in Mesozoic black shales, Northern Siberia, Russia: possible paleomagnetic implications. Tectonophysics 418, 145–162.

Chaloupský , J., Chlupáč, I., Mašek, J., Waldhausrová, J., Cháb, J., 1995. Stratigraphy of the Teplá–Barrandian zone (Bohemicum). In: Dallmeyer, R.D., Franke, W., Weber, K. (Eds.), Pre-Permian Geology of Central and Eastern Europe. Springer, Berlin/Heidelberg/New York, pp. 379–391.
Chantraine, J., Egal, E., Thieblemont, D., Le Goff, E., Guerrot, C., Ballévre, M., Guennoc, P., 2001. The Cadomian active margin (North Armorican Massif, France): a segment of the North Atlantic Panafrican belt. Tectonophysics 331, 1–18.
Chlupáč, I., Havlíček, V.,Kříž, J., Kukal, Z., Štorch, P., 1998. Palaeozoic of the Barrandian (Cambrian–Devonian). Czech Geological Survey, Prague, 183 pp.
Cloos, M., 1982. Flow melanges: numerical modeling and geologic constraints on their origin in the Franciscan subduction complex. Geol. Soc. Am. Bull. 93, 330–345.
Cloos, M., Shreve, R.L., 1988a. Subduction-channel model of prism accretion, melange formation, sediment subduction, and subduction erosion at convergent plate pargins: 1. Background and description. PAGEOPH 128, 455–500.
Cloos, M., Shreve, R.L., 1988b. Subduction-channel model of prism accretion, melange formation, sediment subduction, and subduction erosion at convergent plate margins: 2. Implications and discussion. PAGEOPH 128, 501–545.
Cocks, L.R.M., Torsvik, T.H., 2002. Earth geography from 500 to 400 million years ago. A faunal and palaeomagnetic review. J. Geol. Soc. London 159, 631–644.
Cowan, D.S., 1974. Deformation and metamorphism of the Franciscan subduction zone complex northwest of Pacheco Pass, California. Geol. Soc. Am. Bull. 85, 1623–1634.
Cowan, D.S., 1985. Structural styles in Mesozoic and Cenozoic melanges in the Western Cordillera of North America. Geol. Soc. Am. Bull. 96, 451–462.
Dallmeyer, R.D., Urban, M., 1998. Variscan vs Cadomian tectonothermal activity in northwestern sectors of the Teplá–Barrandian zone, Czech Republic: constraints from 40Ar/39Ar ages. Geol. Rundsch. 87, 94–106.
D'Lemos, R.S., Strachan, R.A., Topley, C.G., 1990. The Cadomian Orogeny in the North Armorican Massif: a brief review. In: D'Lemos, R.S., Strachan, R.A., Topley, C.G. (Eds.), The Cadomian Orogeny, vol. 51. Geol. Soc. London Spec. Publ., pp. 3–12.
Dörr, W., Zulauf, G., in press. Elevator tectonics and orogenic collapse of a Tibetan style plateau in the European Variscides: the role of the Bohemian shear zone. Int. J. Earth Sci., doi:10.1007/s00531-008-0389-x.
Dörr, W., Fiala, J., Vejnar, Z., Zulauf, G., 1998. U–Pb zircon ages and structural development of metagranitoids of the Teplá crystalline complex—evidence for pervasive Cambrian plutonism within the Bohemian Massif (Czech Republic). Geol. Rundsch. 87, 135–149.
Dörr, W., Zulauf, G., Fiala, J., Franke, W., Vejnar, Z., 2002. Neoproterozoic to Early Cambrian history of an active plate margin in the Teplá–Barrandian unit—a correlation of U–Pb isotopic-dilution-TIMS ages (Bohemia, Czech Republic). Tectonophysics 352, 65–85.
Dostal, J., Patočka, F., Pin, C., 2001. Middle/Late Cambrian intracontinental rifting in the central West Sudetes, NE Bohemian Massif (Czech Republic): geochemistry and petrogenesis of the bimodal metavolcanic rocks. Geol. J. 36, 1–17.
Drost, K., Linnemann, U., McNaughton, N., Fatka, O., Kraft, P., Gehmlich, M., Tonk, Ch., Marek, J., 2004. New data on the Neoproterozoic–Cambrian geotectonic setting of the Teplá–Barrandian volcano-sedimentary successions: geochemistry, U–Pb zircon ages, and provenance (Bohemian Massif, Czech Republic). Int. J. Earth Sci. 93, 742–757.
Drost, K., Romer, R.L., Linnemann, U., Fatka, O., Kraft, P., Marek, J., 2007. Nd–Sr–Pb isotopic signatures of Neoproterozoic—early Paleozoic siliciclastic rocks in response to changing geotectonic regimes: a case study from the Barrandian area (Bohemian Massif, Czech Republic). In: Linnemann, U., Nance, D., Kraft, P., Zulauf, G. (Eds.), The Evolution of the Rheic Ocean: From Avalonian–Cadomian Active Margin to Alleghenian–Variscan Collision. Geol. Soc. Am. Spec. Paper 423, pp. 191–208.
Dubanský, A., 1984. Determination of the radiogenic age by the K–Ar method (geochronological data from the Bohemian Massif in the ČSR region). Sbor. Věd. prací Vys. šk. báňské 30, 137–170 (in Czech).
Edel, J.B., Schulmann, K., Holub, F.V., 2003. Anticlockwise and clockwise rotations of the Eastern Variscides accommodated by lithospheric wrenching: palaeomagnetic and structural evidence. J. Geol. Soc. London 160, 209–218.
Fatka, O., Gabriel, Z., 1991. Microbiota from siliceous stromatolitic rocks of the Barrandian Proterozoic (Bohemian Massif). J. Min. Geol. 36, 143–148.
Fiala, F., 1977. The Upper Proterozoic volcanism of the Barrandian area and the problem of spilites. J. Geol. Sci., Geol. 30, 2–247.
Franke, W., Zelazniewicz, A., 2002. Structure and evolution of the Bohemian arc. In: Winchester, J.A., Pharaoh,

T.C., Verniers, J. (Eds.), Palaeozoic amalgamation of Central Europe, vol. 201. Geol. Soc. London Spec. Publ., pp. 279–293.
Geyer, G., Elicki, O., Fatka, O., Zylinska, A., 2008. Cambrian. In: McCann, T. (Ed.), The Geology of Central Europe, vol. 1: Precambrian and Palaeozoic. Geological Society, London, pp. 155–202.
Holubec, J., 1995. Structure (the Teplá–Barrandian Zone). In: Dallmeyer, R.D., Franke, W., Weber, K. (Eds.), Pre-Permian Geology of Central and Eastern Europe. Springer-Verlag, Berlin/Heidelberg/New York, pp. 392–397.
Hrouda, F., 1982. Magnetic anisotropy of rocks and its application in geology and geophysics. Geophys. Surv. 5, 37–82.
Hsü, K.J., 1968. Principles of mélanges and their bearing on the Franciscan-Knoxville paradox. Geol. Soc. Am. Bull. 79, 1063–1074.
Jakeš, P., Zoubek, J., Zoubková, J., Franke, W., 1979. Graywackes and metagraywackes of the Teplá–Barrandian proterozoic area. J. Geol. Sci., Geol. 33, 83–122.
Jelínek, V., 1981. Characterization of magnetic fabric of rocks. Tectonophysics 79, 563–567.
Kachlík, V., Patočka, F., 1998. Cambrian/Ordovician intracontinental rifting and Devonian closure of the rifting generated basins in the Bohemian Massif realms. Acta Univ. Carol., Geol. 42, 433–441.
Kalvoda, J., Bábek, O., Fatka, O., Leichmann, J., Melichar, R., Nehyba, S., Špaček, P., 2008. Brunovistulian terrane (Bohemian Massif, Central Europe) from late Proterozoic to late Paleozoic: a review. Int. J. Earth Sci. 97, 497–518.
Kettner, R., 1923. Cambrian of the Skreje–Tejřovice area. Sbor. Stát. geol. Úst. Čs. Republ. 3, 5–63 (in Czech).
Kettner, R., Slavík, F., 1929. New section through Algonkian and Cambrian near Tejřovice. Rozpravy II. třídy České akademie věd 38, 1–30 (in Czech).
Košler, J., Bowes, D.R., Farrow, C.M., Hopgood, A.M., Rieder, M., Rogers, G., 1997. Constraints on the timing of events in the multi-episodic of the Teplá–Barrandian complex, western Bohemia, from integration of deformational sequence and Rb–Sr isotopic data. N. Jb. Miner., Mh. 5, 203–220.
Kretz, R., 1983. Symbols for rock forming minerals. Am. Miner. 68, 277–279.
Kříbek, B., Pouba, Z., Skoček, V., Waldhausrová, J., 2000. Neoproterozoic of the Teplá–Barrandian Unit as a part of the Cadomian orogenic belt: a review and correlation aspects. Bull. Czech Geol. Surv. 75, 175–196.
Krs, M., Krsová, M., Pruner, P., Chvojka, R., Havlíček, V., 1987. Palaeomagnetism, palaeogeography and the multicomponent analysis of middle and upper Cambrian rocks of the Barrandian in the Bohemian Massif. Tectonophysics 139, 1–20.
Krs, M., Pruner, P., Man, O., 2001. Tectonic and paleogeographic interpretation of the paleomagnetism of Variscan and pre-Variscan formations of the Bohemian Massif, with special reference to the Barrandian terrane. Tectonophysics 332, 93–114.
Lang, M., 2000. Composition of Proterozoic greywackes in the Barrandian. Bull. Czech Geol. Surv. 75, 205–216.
Linnemann, U., Romer, R.L., 2002. The Cadomian orogeny in Saxo-Thuringia, Germany: geochemical and Nd–Sr–Pb isotopic characterization of marginal basins with constraints to geotectonic setting and provenance. Tectonophysics 352, 33–64.
Linnemann, U., McNaughton, N.J., Romer, R.L., Gehmlich, M., Drost, K., Tonk, C., 2004. West African provenance for Saxo-Thuringia (Bohemian Massif): did Armorica ever leave pre-Pangean Gondwana? U/Pb-SHRIMP zircon evidence and the Ndisotopic record. Int. J. Earth Sci. 93, 683–705.
Linnemann, U., Gerdes, A., Drost, K., Buschmann, B., 2007. The continuum between Cadomian orogenesis and opening of the Rheic Ocean: constraints from LA-ICP-MS U–Pb zircon dating and analysis of plate-tectonic setting (Saxo-Thuringian zone, northeastern Bohemian Massif, Germany). In: Linnemann, U., Nance, D., Kraft, P., Zulauf, G. (Eds.), The Evolution of the Rheic Ocean: From Avalonian–Cadomian active margin to Alleghenian–Variscan Collision. Geol. Soc. Am. Spec. Paper 423, pp. 61–96.
Linnemann, U., Pereira, F., Jeffries, T.E., Drost, K., Gerdes, A., 2008a. The Cadomian orogeny and the opening of the Rheic Ocean: the diacrony of geotectonic processes constrained by LA-ICP-MS U–Pb zircon dating (Ossa-Morena and Saxo-Thuringian Zones, Iberian and Bohemian Massifs). Tectonophysics 461, 21–43.
Linnemann, U., D'Lemos, R.S., Drost, K., Jeffries, T., Gerdes, A., Romer, R.L., Samson, S.D., Strachan, R.A., 2008b. Cadomian tectonics. In: McCann, T. (Ed.), The Geology of Central Europe, vol. 1: Precambrian and Palaeozoic. Geological Society, London, pp. 103–154.
Linnemann, U., Drost, K., Elicki, O., Gaitzsch, B., Gehmlich, M., Hahn, T., Kroner, U., Romer, R.L., 2008c. Das Saxothuringikum. Museum für Mineralogie und Geologie, Dresden, 163 pp.
Martín-Hernández, F., Hirt, A.M., 2003. The anisotropy of magnetic susceptibility in biotite, muscovite and chlorite single crystals. Tectonophysics 367, 13–28.
Mašek, J., 2000. Stratigraphy of the Proterozoic of the Barrandian area. Bull. Czech Geol. Surv. 75, 197–200.
McCann, T. (Ed.), 2008. The Geology of Central Europe, vol. 1: Precambrian and Palaeozoic. Geological Society,

London, 748 pp.
Miller, B.V., Samson, S.D., D'Lemos, R.S., 1999. Time span of plutonism, fabric development, and cooling in a Neoproterozoic magmatic arc segment: U–Pb age constraints from syn-tectonic plutons, Sark, Channel Islands, UK. Tectonophysics 312, 79–95.
Murphy, J.B., Eguiluz, L., Zulauf, G., 2002. Cadomian orogens, peri-Gondwanan correlatives and Laurentia–Baltica connections. Tectonophysics 352, 1–9.
Murphy, J.B., Pisarevsky, S.A., Nance, R.D., Keppie, J.D., 2004. Neoproterozoic–Early Paleozoic evolution of peri-Gondwanan terranes: implications for Laurentia–Gondwana connections. Int. J. Earth Sci. 93, 659–682.
Murphy, J.B., Gutierrez-Alonso, G., Nance, R.D., Fernandez-Suarez, J., Keppie, J.D., Quesada, C., Strachan, R.A., Dostal, J., 2006. Origin of the Rheic Ocean: rifting along a Neoproterozoic suture? Geology 34, 325–328.
Nagata, T., 1961. Rock Magnetism. Maruzen, Tokyo, 350 pp.
Nance, R.D., Murphy, J.B., 1994. Constraining basement isotopic signatures and the palinspastic restoration of peripheral orogens: example from the Neoproterozoic Avalonian–Cadomian belt. Geology 22, 617–620.
Nance, R.D., Murphy, J.B., Strachan, R.A., D'Lemos, R.S., Taylor, G.K., 1991. Late Proterozoic tectonostratigraphic evolution of the Avalonian and Cadomian terranes. Precambrian Res. 53, 41–78.
Osozawa, S., Morimoto, J., Flower, M.F.J., 2009. "Block-in-matrix" fabrics that lack shearing but possess composite cleavage planes: a sedimentary mélange origin for the Yuwan accretionary complex in the Ryukyu island arc, Japan. Geol. Soc. Am. Bull. 121, 1190–1203.
Parés, J.M., van der Pluijm, B.A., 2002. Evaluating magnetic lineations (AMS) in deformed rocks. Tectonophysics 350, 283–298.
Passchier, C.W., Trouw, R.A.J., 2005. Microtectonics. Springer-Verlag, Berlin, 325 pp.
Patočka, F., Štorch, P., 2004. Evolution of geochemistry and depositional settings of Early Palaeozoic siliciclastics of the Barrandian (Teplá–Barrandian Unit, Bohemian Massif, Czech Republic). Int. J. Earth Sci. 93, 728–741.
Patočka, F., Pruner, P., Štorch, P., 2003. Palaeomagnetism and geochemistry of Early Palaeozoic rocks of the Barrandian (Teplá–Barrandian Unit, Bohemian Massif): palaeotectonic implications. Phys. Chem. Earth 28, 735–749.
Pin, C., Waldhausrová, J., 2007. Sm–Nd isotope and trace element study of Late Proterozoic metabasalts ("spilites") from the Central Barrandian domain (Bohemian Massif, Czech Republic). In: Linnemann, U., Nance, D., Kraft, P., Zulauf, G. (Eds.), The Evolution of the Rheic Ocean: From Avalonian–Cadomian Active Margin to Alleghenian–Variscan Collision. Geol. Soc. Am. Spec. Paper 423, pp. 231–247.
Pin, C., Kryza, R., Oberc-Dziedzic, T., Mazur, S., Turniak, K., Waldhausrová, J., 2007. The diversity and geodynamic significance of Late Cambrian (ca. 500 Ma) felsic anorogenic magmatism in the northern part of Bohemian Massif: a review based on Sm–Nd isotope and geochemical data. In: Linnemann, U., Nance, D., Kraft, P., Zulauf, G. (Eds.), The Evolution of the Rheic Ocean: From Avalonian–Cadomian Active Margin to Alleghenian–Variscan Collision. Geol. Soc. Am. Spec. Paper 423, pp. 209–229.
Platt, J.P., 1986. Dynamics of orogenic wedges and the uplift of high-pressure metamorphic rocks. Geol. Soc. Am. Bull. 97, 1037–1053.
Pouba, Z., Kříbek, B., 1986. Organic matter and the concentration of metals in Precambrian stratiform deposits of the Bohemian Massif. Precambrian Res. 33, 225–237.
Pouba, Z., Kříbek, B., Pudilová, M., 2000. Stromatolite-like cherts in the Barrandian Upper Proterozoic: a review. Bull. Czech Geol. Surv. 75, 285–296.
Powell, C.M., 1979. A morphological classification of rock cleavage. Tectonophysics 58, 21–34.
Röhlich, P., 1965. Geologische Probleme des mittelböhmischen Algonkiums. Geologie 14, 373–403.
Samson, S.D., D'Lemos, R.S., Miller, B.V., Hamilton, M.A., 2005. Neoproterozoic palaeogeography of the Cadomia and Avalon terranes: constraints from detrital zircon U–Pb ages. J. Geol. Soc. London 162, 65–71.
Sláma, J., Dunkley, D.J., Kachlík, V., Kusiak, M.A., 2008. Transition from island-arc to passive setting on the continental margin of Gondwana: U–Pb zircon dating of Neoproterozoic metaconglomerates from the SE margin of the Teplá–Barrandian Unit, Bohemian Massif. Tectonophysics 461, 44–59.
Štědrá, V., Kachlík, V., Kryza, R., 2002. Coronitic metagabbros of the Mariánské Lázně Complex and Teplá Crystalline Unit: inferences for the tectonometamorphic evolution of the western margin of the Teplá–Barrandian Unit, Bohemian Massif. In: Winchester, J.A., Pharaoh, T.C., Verniers, J. (Eds.), Palaeozoic amalgamation of Central Europe. Geol. Soc. London Spec. Publ. 201, pp. 217–237.
Štorch, P., 2006. Facies development, depositional settings and sequence stratigraphy across the Ordovician–Silurian boundary: a new perspective from the Barrandian area of the Czech Republic. Geol. J. 41, 163–192.
Strachan, R.A., Treloar, P.J., Brown, M., D'Lemos, R.S., 1989. Cadomian terrane tectonics and magmatism in the Armorican Massif. J. Geol. Soc. London 146, 423–426. Suchý , V., Sýkorová, I., Melka, K., Filip, J., Machovič, V.,

2007. Illite “crystallinity” maturation of organic matter and microstructural development associated with lowest-grade metamorphism of Neoproterozoic sediments in the Teplá–Barrandian unit, Czech Republic. Clay Miner. 42, 503–526.
Tait, J.A., Bachtadse, V., Franke, W., Soffel, H.C., 1997. Geodynamic evolution of the European Variscan fold belt: palaeomagnetic and geological constraints. Geol. Rundsch. 87, 585–598.
Tarling, D.H., Hrouda, F., 1993. The Magnetic Anisotropy of Rocks. Chapman and Hall, London, 217 pp.
Timmermann, H., Štědrá, V., Gerdes, A., Noble, S.R., Parrish, R.R., Dörr, W., 2004. The problem of dating high-pressure metamorphism: a U–Pb isotope and geochemical study on eclogites and related rocks of the Mariánské Lázně Complex, Czech Republic. J. Petrol. 45, 1311–1338.
Timmermann, H., Dörr, W., Krenn, E., Finger, F., Zulauf, G., 2006. Conventional and in situ geochronology of the Teplá crystalline unit, Bohemian Massif: implications for the processes involving monazite formation. Int. J. Earth Sci. 95, 629–647.
Tomek, Č., Dvořáková, V., Vrána, S., 1997. Geological interpretation of the 9HR and 503M seismic profiles in western Bohemia. In: Vrána, S., Štědrá, V. (Eds.), Geological Model of Western Bohemia Related to the KTB Borehole in Germany. J. Geol. Sci., Geol., vol. 47, pp. 43–50.
Torsvik, T.H., Cocks, L.R.M., 2004. Earth geography from 400 to 250 Ma: a palaeomagnetic, faunal and facies review. J. Geol. Soc. London 161, 555–572.
Treloar, P.J., Strachan, R.A., 1990. Cadomian strike-slip tectonics in NE Brittany. In: D’Lemos, R.S., Strachan, R.A., Topley, C.G. (Eds.), The Cadomian Orogeny, vol. 51. Geol. Soc. London Spec. Publ., pp. 151–168.
Venera, Z., Schulmann, K., Kröner, A., 2000. Intrusion within a transtensional tectonic domain: the Čistá granodiorite (Bohemian Massif)—structure and rheological modelling. J. Struct. Geol. 22, 1437–1454.
Vidal, P., Auvray, B., Charlot, R., Fediuk, F., Hameurt, J., Waldhausrová, J., 1975. Radiometric age of volcanics of the Cambrian “Křivoklát Rokycany” complex (Bohemian Massif). Geol. Rundsch. 64, 563–570.
von Raumer, J.F., Stampfli, G.M., 2008. The birth of the Rheic Ocean—Early Palaeozoic subsidence patterns and subsequent tectonic plate scenarios. Tectonophysics 461, 9–20.
von Raumer, J.F., Stampfli, G.M., Borel, G., Bussy, F., 2002. Organization of pre-Variscan basement areas at the north-Gondwanan margin. Int. J. Earth. Sci. 91, 35–52.
von Raumer, J.F., Stampfli, G.M., Bussy, F., 2003. Gondwana-derived microcontinents—the constituents of the Variscan and Alpine collisional orogens. Tectonophysics 365, 7–22.
Vrána, S., Štědrá, V. (Eds.), 1997. Geological model of western Bohemia related to the KTB borehole in Germany. J. Geol. Sci., Geol. 47, 240 pp.
Waldhausrová, J., 1966. The volcanites of the Křivoklát–Rokycany Zone. In: Fediuk, F., Fišera, M. (Eds.), Paleovolcanites of the Bohemian Massif, pp. 145–151.
Waldhausrová, J., 1971. The chemistry of the Cambrian volcanics in the Barrandian area. Krystalinikum 8, 45–75.
Waldhausrová, J., 1984. Proterozoic volcanics and intrusive rocks of the Jílové Zone (Central Bohemia). Krystalinikum 17, 77–97.
Winkler, A., Florindo, F., Sagnotti, L., 1996. Inverse to normal magnetic fabric transition in an upper Miocene marly sequence from Tuscany, Italy. Geophys. Res. Lett. 23, 909–912.
Worm, H.U., Clark, D., Dekkers, M.J., 1993. Magnetic susceptibility of pyrrhotite: grain size, field and frequency dependence. Geophys. J. Int. 114, 127–137.
Wortman, G.L., Samson, S.D., Hibbard, J.P., 2000. Precise U–Pb zircon constraints on the earliest magmatic history of the Carolina terrane. J. Geol. 108, 321–338.
Žák, J., Schulmann, K., Hrouda, F., 2005. Multiple magmatic fabrics in the Sázava pluton (Bohemian Massif, Czech Republic): a result of superposition of wrench dominated regional transpression on final emplacement. J. Struct. Geol. 27, 805–822.
Zulauf, G., 1997. From very low-grade to eclogite-facies metamorphism: tilted crustal sections as a consequence of Cadomian and Variscan orogeny in the Teplá–Barrandian unit (Bohemian Massif). Geotekt. Forsch. 89, 1–302.
Zulauf, G., Dörr, W., Fiala, J., Vejnar, Z., 1997. Late Cadomian crustal tilting and Cambrian transtension in the Teplá–Barrandian unit (Bohemian Massif, Central European Variscides). Geol. Rundsch. 86, 571–587.
Zulauf, G., Schritter, F., Riegler, G., Finger, F., Fiala, J., Vejnar, Z., 1999. Age constraints on the Cadomian evolution of the Teplá–Barrandian unit (Bohemian Massif) through electron microprobe dating of metamorphic monazite. Zt. Deutsch. Geol. Ges. 180, 627–639.

CHAPTER 2

Jaroslava Hajná, Jiří Žák, Václav Kachlík: Structure and stratigraphy of the Teplá–Barrandian Neoproterozoic, Bohemian Massif: a new plate-tectonic reinterpretation.

Gondwana Research 19, 495–508, 2011

Structure and stratigraphy of the Teplá–Barrandian Neoproterozoic, Bohemian Massif: a new plate-tectonic reinterpretation

Jaroslava Hajná[1], Jiří Žák[1, 2], Václav Kachlík[1]

[1] *Institute of Geology and Paleontology, Faculty of Science, Charles University, Albertov 6, Prague, 12843, Czech Republic*

[2] *Czech Geological Survey, Klárov 3, Prague, 11821, Czech Republic*

Abstract

The Teplá–Barrandian unit (TBU) of the Bohemian Massif exposes a section across the once extensive Avalonian–Cadomian belt, which bordered the northern active margin of Gondwana during late Neoproterozoic. This paper synthesizes the state-of-the-art knowledge on the Cadomian basement of the TBU to redefine its principal component units, to revise an outdated stratigraphic scheme, and to interpret this scheme in terms of a recent plate-tectonic model for the Cadomian orogeny in the Bohemian Massif. The main emphasis of this paper is on an area between two newly defined fronts of the Variscan pervasive deformation to the NW and SE of the Barrandian Lower Paleozoic overlap successions. This area has escaped the pervasive Variscan (late Devonian to early Carboniferous) ductile reworking and a section through the Cadomian orogen is here superbly preserved.

The NW segment of the TBU consists of three juxtaposed allochthonous belts of unknown stratigraphic relation (the Kralovice–Rakovník, Radnice–Kralupy, and Zbiroh–Šárka belts), differing in lithology, complex internal strain patterns, and containing sedimentary

and tectonic mélanges with blocks of diverse ocean floor (meta-)basalts. We summarize these three belts under a new term the Blovice complex, which we believe represents a part of an accretionary wedge of the Cadomian orogen.

The SE segment of the TBU exposes the narrow Pičín belt, which is probably a continuation of the Blovice complex from beneath the Barrandian Lower Paleozoic, and a volcanic arc sequence (the Davle Group). Their stratigraphic relation is unknown. Flysch units (the Štěchovice Group and Svrchnice Formation) overlay the arc volcanics, and both units contain material derived from volcanic arc. The former was also sourced from the NW segment, whereas the latter contains an increased amount of passive margin continental material. In contrast to the Blovice complex, the flysch experienced only weak Cadomian deformation.

The new lithotectonic zonation fits the following tectonic scenario for the Cadomian evolution of the TBU well. The S- to SE-directed Cadomian subduction beneath the TBU led to the involvement of turbidites, chaotic deposits, and 605 ± 39 Ma ocean floor in the accretionary wedge represented by the Blovice complex. The accretionary wedge formation mostly overlapped temporally with the growth of the volcanic arc (the Davle Group) at ~620–560 Ma. Upon cessation of the arc igneous activity, the rear of the wedge and some elevated portions of the arc were eroded to supply the deep-water flysch sequences of the Štěchovice Group, whereas the comparable Svrchnice Formation (~560 to <544 Ma) was deposited in a southeasterly remnant basin close to the continental margin. The Cadomian orogeny in the TBU was terminated at ~550–540 Ma by slab break-off, by final attachment of the most outboard ~540 Ma oceanic crust, and by intrusion of ~544–524 Ma boninite dikes marking the transition from the destructive to transform margin during the early/middle Cambrian.

Keywords: *Avalonian–Cadomian belt; Bohemian Massif; Cadomian orogeny; Neoproterozoic; Teplá–Barrandian unit*

1. Introduction

The supracrustal Teplá–Barrandian unit (TBU) in the center of the Bohemian Massif (Fig. II.1) is one of the best preserved, that is, not pervasively overprinted by younger deformation and metamorphism, components of the Avalonian–Cadomian belt which developed along the northern active margin of Gondwana during the late Neoproterozoic (Cryogenian to Ediacaran; ~750–540 Ma; e.g., Nance et al., 1991; Nance and Murphy, 1994; Wortman et al., 2000; Murphy et al., 2002, 2004, 2006; Linnemann and Romer, 2002; von Raumer et al., 2002; Linnemann et al., 2007, 2008a, b). Understanding the sedimentary record, stratigraphy, and large-scale structure of the Cadomian basement of the TBU is thus of prime importance not only for interpreting its geotectonic setting during the Cadomian orogeny but also for global stratigraphic correlations across the Avalonian–Cadomian belt and for the late Neoproterozoic to early Palaeozoic paleogeography of the Gondwana-derived Cadomian terranes (Armorica, Saxo-Thuringia, Teplá–Barrandian or “Perunica”; e.g., Tait et al., 1997; Franke and Zelazniewicz, 2002; Drost et al., 2004, 2007, in press; Kalvoda et al., 2008; Sláma et al., 2008; Fatka and Mergl, 2009). Consequently, the TBU has received considerable scientific interest over the past few years (e.g., Zulauf, 1997; Zulauf et al., 1997, 1999; Kříbek et al., 2000; Dörr et al., 2002; Patočka et al., 2003; Patočka and Štorch, 2004; Drost et al., 2004, 2007, in press; Aïfa et al., 2007; Pin and Waldhausrová, 2007; Suchý et al., 2007; Drost, 2008; Linnemann et al., 2008b; Sláma et al., 2008).

The stratigraphy of the TBU Neoproterozoic has long been considered well established, and a “conventional” subdivision of the TBU into lithostratigraphic units has been widely

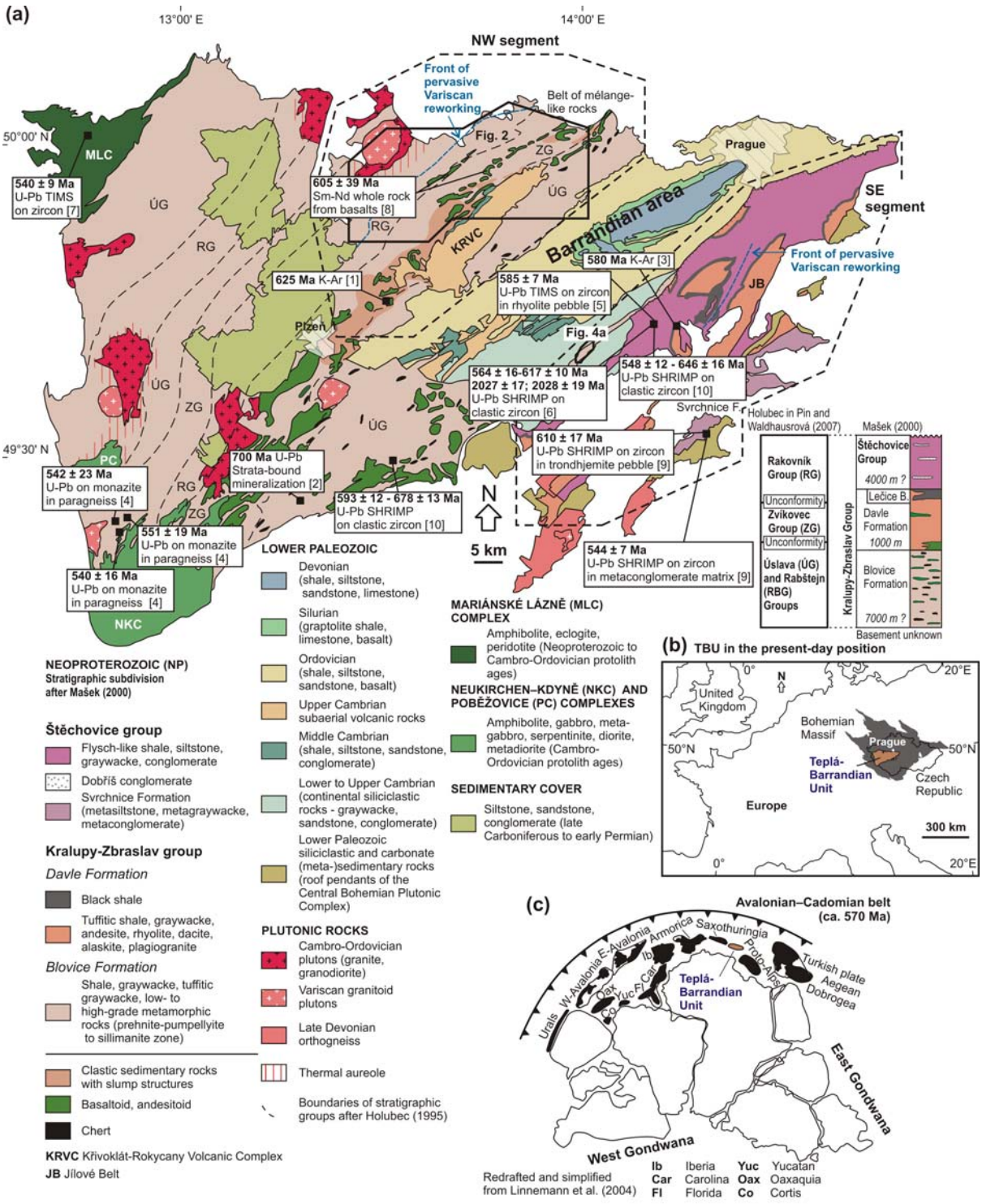

Fig. II.1. (a) A simplified geologic map of the Teplá–Barrandian unit (TBU) with geochronologic data from its Neoproterozoic basement. This map redrafted from Geologic map of the Czech Republic, at a scale of 1:500,000, published by the Czech Geological Survey in 2007. Lithologic units in the explanation are arranged in a stratigraphic order following Mašek (2000), and dashed lines on the map correspond to the lithostratigraphic belts of J. Holubec (cited in Pin and Waldhausrová, 2007). The inset shows a comparison of the two main lithostratigraphic concepts proposed for the Barrandian Neoproterozoic. (b) The present-day position of the TBU in the central Bohemian Massif. (c) The inferred paleogeographic position of the TBU within the Avalonian–Cadomian belt on the active northern margin of Gondwana during the late Neoproterozoic (after Linnemann et al., 2004). Source of geochronologic data: (1) Dubanský et al. (1984), (2) Ordynec et al. (1984), (3) Vlašímský & Fiala cited in Mašek (2000), (4) Zulauf et al. (1999), (5) Dörr et al. (2002), (6) Drost et al. (2004), (7)

Timmermann et al. (2004), (8) Pin and Waldhausrová (2007), (9) Sláma et al. (2008), (10) Drost et al. (2010).

adopted in both scientific papers and geologic maps (see fig. 2.37 in Kachlík, 2008 for a detailed comparison of published stratigraphic columns and Röhlich, 2000 for discussion). The "conventional" scheme was proposed by Mašek and Zoubek (1980) and Mašek (2000; inset in Fig. II.1a) and divides the Teplá–Barrandian Neoproterozoic into the presumably oldest Blovice and younger Davle Formations. Both formations contain abundant volcanic rocks and are merged into the Kralupy–Zbraslav Group, which is overlain conformably by the flysch-like Štěchovice Group that is devoid of volcanic rocks and spans the latest Neoproterozoic to the earliest Cambrian (Fig. II.1a; Cháb and Pelc, 1968; Fiala, 1977, 1978; Jakeš et al., 1979; Konzalová, 1981; Pacltová, 1990; Fatka and Gabriel, 1991; Cháb, 1993; Pelc and Waldhausrová, 1994; Waldhausrová, 1997; Kříbek et al., 2000; Dörr et al., 2002; Sláma et al., 2008).

A completely different, and not widely appreciated, view on the TBU stratigraphy was introduced by Holubec (1966, 1995). In the latest version of his hypothesis, the Neoproterozoic rocks are subdivided into three lithostratigraphic groups (referred to as the Rabštejn–Úslava, Rakovník, and Zvíkovec Groups; inset in Fig. II.1a), which are interpreted as several hundred meter thick sedimentary megacycles separated by two major unconformities. As a result of several phases of superposed Cadomian folding, the presumed unconformities have been steeply tilted and the groups now define the ~NE–SW-trending belts on the map (Fig. II.1a; Holubec, 1968).

Our field observations and detailed structural mapping of large areas to the NW and SE of the Barrandian Lower Paleozoic over the past ten years prompted us to challenge the existing stratigraphic concepts. For brevity, we use the descriptive terms "the NW and SE segments" for these two areas (their extent is outlined in Fig. II.1a) with the notion that

comparable units and structures may also continue to other parts of the TBU. Unlike our previous structural study on the NW segment (Hajná et al., 2010), this paper correlates the principal field, lithologic, geochemical, and structural characteristics of component lithotectonic units across both segments of the TBU and, as a frame for future studies, synthesizes the state-of-the-art knowledge on the Teplá–Barrandian Neoproterozoic. Furthermore, two fronts of the pervasive Variscan reworking are newly and precisely defined between which the Cadomian basement is not at all or only weakly overprinted by the Variscan ductile deformation. For this "low-Variscan-strain" area, we introduce a new lithotectonic zonation and reinterpret the large-scale structure and stratigraphy of the Teplá–Barrandian Neoproterozoic. Finally, we put these stratigraphic inferences into the context of a recent plate-tectonic model for the Cadomian accretionary orogen as preserved in the TBU.

2. A refined lithotectonic zonation of the Barrandian Neoproterozoic

Below we describe a newly defined lithotectonic zonation and critically evaluate the stratigraphic relations among the low-grade units in both segments of the Teplá–Barrandian Neoproterozoic. The lithostratigraphy and structural pattern were examined in an area between the two fronts of the Variscan pervasive deformation to the NW and SE (shown as dashed lines in map in Fig. II.1a) where the Cadomian basement has not been affected by the pervasive Variscan overprint. In the remainder of the TBU, the Variscan deformation and metamorphism was so intense that the original stratigraphic relations and structures in the Neoproterozoic rocks are largely obscured.

The criteria used in this paper to define the individual lithotectonic units are (1) geologic setting and spatial position in the Neoproterozoic basement of the TBU, (2) lithology, textures, composition, and inferred depositional environment of sedimentary

rocks, (3) composition and textures of volcanic rocks (if present), (4) the presence or absence of specific rock assemblages and marker horizons, (5) the style and intensity of Cadomian deformation, (6) the degree of Cadomian regional metamorphism, and (7) the nature of the outer contacts (depositional conformable, depositional unconformable, faulted, concealed).

2.1. Lithotectonic units in the NW segment of the TBU

In the NW segment of the TBU (assigned entirely to the single Blovice Formation of the Kralupy–Zbraslav Group by Mašek, 2000), the Neoproterozoic basement between the front of the Variscan pervasive deformation to the NW and the Barrandian Lower Paleozoic overlap sequences to the SE (Fig. II.2) consists of three contrasting ~NE–SW-trending lithotectonic units. These units are termed here the Kralovice–Rakovník, Radnice–Kralupy, and Zbiroh–Šárka belts after Röhlich (1965) and correspond to Domains 1–3 of Hajná et al. (2010), respectively. The northwesterly front of the Variscan pervasive deformation is represented by the Krakovec shear zone (KSZ in Fig. II.2). This zone, named and defined in this paper for the first time (but will be dealt with in a great detail elsewhere), overprints a wide thermal aureole of the ~505 Ma Tis granite (Pb–Pb zircon evaporation age; Venera et al., 2000) and is thus of the post-late Cambrian (perhaps the Late Devonian) age. Along this ductile shear zone, higher-grade phyllites (a chlorite to biotite zone displaying the Late Devonian cooling ages after Dallmeyer and Urban, 1998) are thrust obliquely to the NE over the Kralovice–Rakovník belt.

The Kralovice–Rakovník belt (~Domain 1 of Hajná et al., 2010) is a very-low-grade bedded sequence of rhythmically alternating graywackes, slates, and siltstones (Fig. II.3a), which were presumably deposited as deep-water turbidites and gravity flows (Cháb and Pelc, 1968) sourced from a volcanic arc. The average thickness of graywacke beds typically ranges from 20 cm to less than a meter. The thickness of the slate interbeds varies from

centimeters to decimeters.

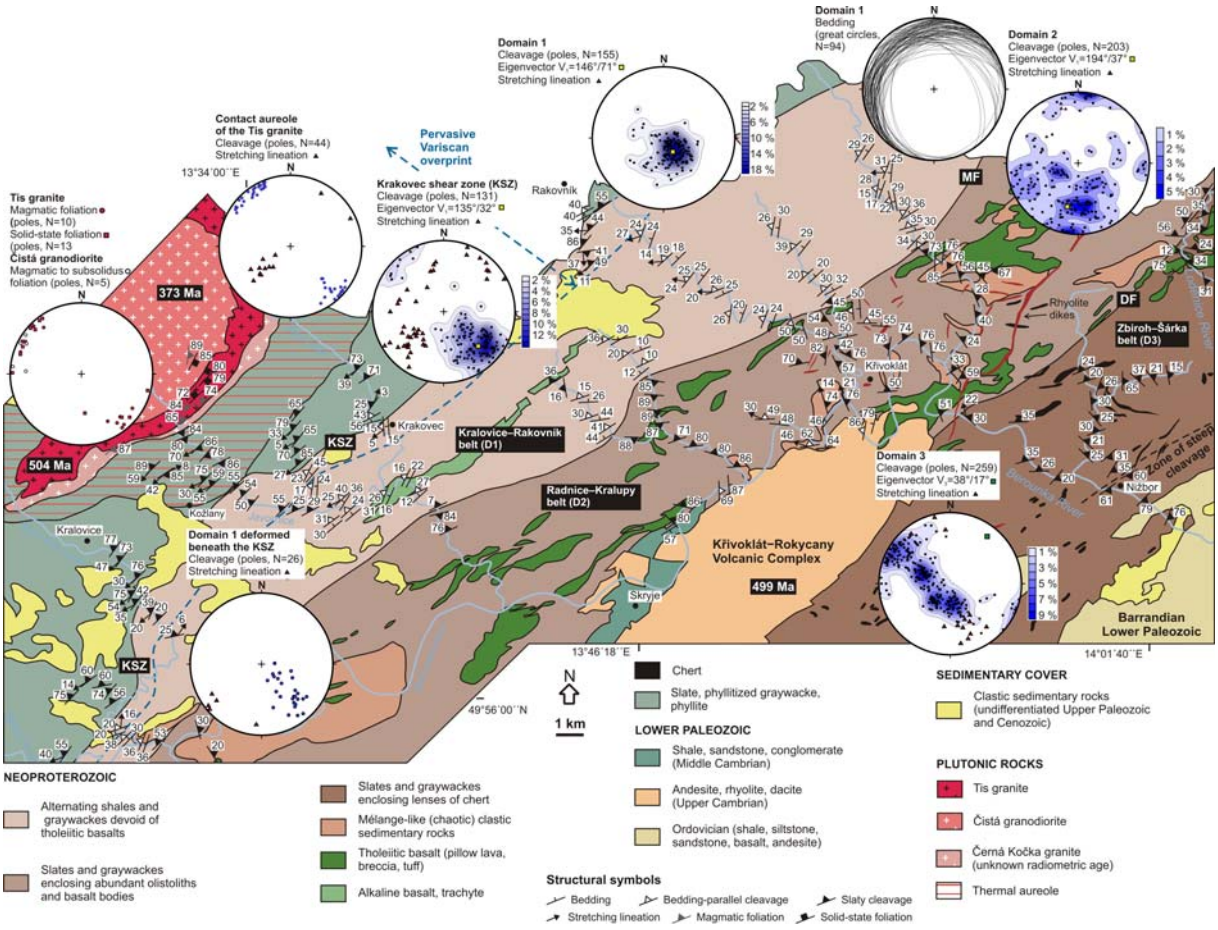

Fig. II.2. A structural map of the NW segment of the TBU showing well-preserved contrasting Cadomian structures in the Kralovice–Rakovník, Radnice–Kralupy, and Zbiroh–Šárka belts overlain unconformably by the Lower Paleozoic rocks to the SE. In contrast, the Cadomian basement to the NW of the Variscan Krakovec shear zone (KSZ) has been pervasively affected by the Variscan (perhaps Late Devonian) deformation and metamorphism. Stereonets (equal area projection, lower hemisphere) show orientation of bedding, cleavage, stretching lineation, and magmatic and subsolidus foliations in the post-Cadomian granitoids. DF – Družec fault, MF – Městečko fault.

The Kralovice–Rakovník belt is devoid of volcanic rocks except for a few NE–SW-trending km-scale elongated bodies of alkali basalt and trachybasalt to trachyandesite. Felsic trachytes (up to 70 wt% of SiO_2) are rare. The field and structural relations of these bodies to the host graywackes have not been examined in detail and still remain unknown. The fractionated LREE vs. HREE pattern; the enrichment in Nb, Ta, and incompatible elements; and the high to moderate εNd values (from +3.8 to +5.1) as well as the low Th/Nb values of

basaltic members are compatible with more evolved within-plate magmas (e.g., OIB) generated by a low-degree of partial melting from an LREE-enriched mantle with no subduction-related components (Pin and Waldhausrová, 2007). The εNd_{600} of felsic trachytes is about +3.2, which may be a result of minor crustal assimilation during magma differentiation.

In sedimentary rocks, the bedding dips gently to moderately to the ~W to ~NW implying that the Cadomian deformation was weak resulting only in the tilt of bedding and formation of bedding-parallel cleavage in the soft slate interbeds. However, the deformation varies along trend of this belt as its southwesternmost (?deeper) section is characterized by abundant, recumbent, tightly to isoclinally folded quartz veins, a boudinage of competent graywacke beds, and intensely developed flat-lying cleavage even in the graywackes (J. Hajná and J. Žák, new mapping and unpublished data). These features imply a significant vertical shortening and subhorizontal shearing associated with an increased fluid flow at the base of the belt.

The Radnice–Kralupy belt (~Domain 2 of Hajná et al., 2010) is the most complex unit in terms of lithology and structural pattern consisting predominantly of bedded or massive graywackes (Fig. II.3b), slates, and siltstones with lenses of limestone, chert, and black shales. In places, the graywackes exhibit chaotic (micro-)textures and contain syn-sedimentary slump structures and structurally isolated exotic blocks (graywacke or chert blocks embedded in slates) that are interpreted as olistoliths (Cháb and Pelc, 1968; Mašek, 2000; Fig. II.3c). Pebbles from debris flow deposits found within the Radnice–Kralupy belt are composed of various types of intrabasinal graywackes with variable texture and composition (e.g., graywackes rich in redeposited volcanogenic material, detrital muscovite, biotite-bearing graywackes, epidote- and amphibole-rich graywackes, graywackes with

cleavage fabric, graphitic shales, cherts) mixed with pebbles of deformed leucotonalites, contact metamorphosed biotite-cordierite hornfelses, and cordierite-bearing metagreywackes. The clast compositions indicate mixing of intrabasinal and island arc sources of the clastic material and its rapid recycling (typical of accretionary wedges).

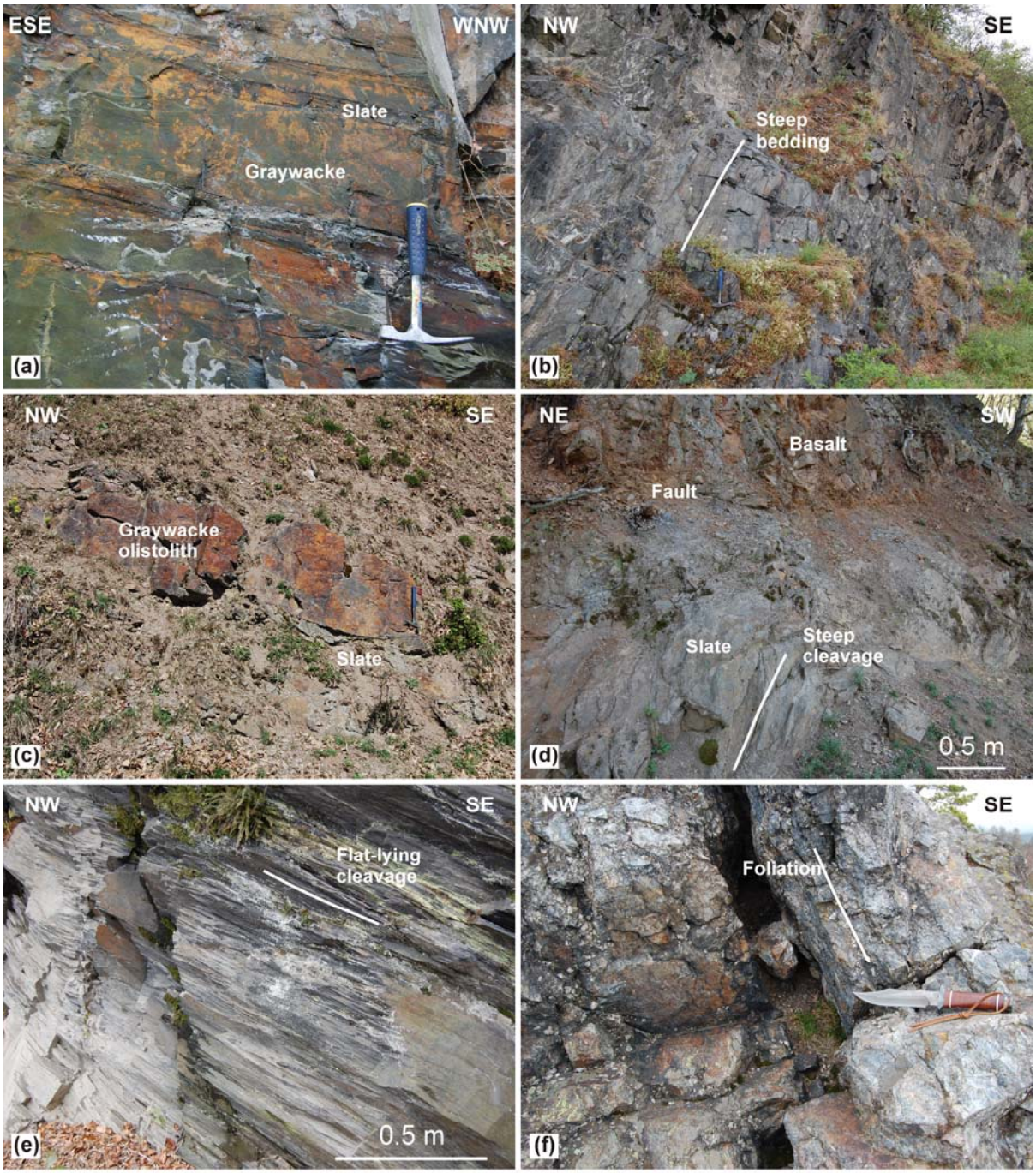

Fig. II.3. The lithologic and structural features of the Neoproterozoic rocks in the NW segment of the TBU. (a) The bedding in only gently tilted alternating graywackes and slates typical of the Kralovice–Rakovník belt. The

cleavage is localized in incompetent thin slate interbeds; Žákův mlýn. Hammer for scale. (b) The steep bedding and bedding-parallel cleavage in the graywacke–slate sequence; Nezabudické skály in the Radnice–Kralupy belt. Hammer for scale. (c) The graywacke olistoliths in slate, the Radnice–Kralupy belt; Klíčava dam. Hammer for scale. (d) The basalt body thrust over slate. Note that the fault plane truncates the steep slaty cleavage, the Radnice–Kralupy belt; Klíčava dam. (e) The homogeneous pervasive cleavage in slate, the Zbiroh–Šárka belt; Malé Kyšice. (f) The weakly foliated chert in the Zbiroh–Šárka belt; Vraní skála. SOG Bowie 2.0 knife for scale.

Both the massive and bedded graywackes are typically preserved as larger (up to several hundreds of meters) lenses or boudins enclosed in intensely deformed finer-grained slates and graywackes. The bedded graywackes are folded into upright folds ranging from tight to isoclinal with intensely developed bedding-parallel, axial-planar cleavage. The host slates are characterized by pervasive cleavage steeply dipping to the N (thus at a high angle to the belt boundaries), which transposes the original bedding or fine-scale lamination.

Volcanic rocks occur as abundant up to km-scale lens-shaped to irregular bodies in the graywackes or slates (Fig. II.3d). In terms of composition and texture, the volcanic rocks correspond mostly to tholeiitic to moderately enriched (meta-)basalts, whereas alkali basalts are rare. The (meta-)basalts are mostly hydrothermally altered and occur as massive and pillow lavas, breccias, hydrothermal breccias containing both disseminated and massive volcanogenic sulphides, and peperites (Fiala, 1977; Fiala, 1987; Pin and Waldhausrová, 2007). The lack of contact metamorphism and tectonic contacts between the (meta-)basalts and the intensely sheared host slates suggest that a great majority of these bodies are allochtonous blocks emplaced either tectonically (e.g., Fig. II.3d) or via gravitational sliding as olistoliths.

According to REE patterns, trace-element geochemistry, and Sm–Nd isotopes, the (meta-)basalts in the Radnice–Kralupy belt can be classified into four different groups (Pin and Waldhausrová, 2007). The first group exhibits a strongly LREE-depleted pattern and depletion in Th and Nb typical of N-MORB´s. The εNd values range from +8 to +9.3, which

implies a primitive mantle source with no significant interactions with crustal melts, but the negative Zr and Ti anomalies and Ti/V ratios suggest an influence of a suprasubduction zone setting. Thus, Pin and Waldhausrová (2007) interpreted these magmas as having been generated by partial melting of a depleted mantle that was metasomatized and fluxed by a hydrous component from a subducting oceanic plate. The second group exhibits negative anomalies in incompatible elements (Th, Nb, La, Ce), lower εNd values (+7.8 to +8.3), and higher Th/Nb ratios, which are probably due to higher crustal contamination by low-radiogenic greywackes. The third group is comprised of moderately LREE-enriched (meta-)basalts with a positive Nb anomaly and higher Zr/Nb ratios, and εNd ranges from +6.7 to +8.2. Low Th/Nb ratios preclude significant crustal contamination. The fourth group includes minor and strongly LREE-enriched alkali basalts with no associated fractionated felsic rocks.

On either side, the Radnice–Kralupy belt is bounded by major brittle faults: a thrust fault to the NW, which is associated with the top-to-the-NW movement over the Kralovice–Rakovník belt, and a normal fault against the Zbiroh–Šárka belt to the SE (Fig. II.2; Hajná et al., 2010). Importantly, the Radnice–Kralupy belt is overlain unconformably by the middle Cambrian marine successions and Cambro–Ordovician subaerial volcanic rocks (the youngest rhyolite lavas were dated at 499 ± 4 Ma; Drost et al., 2004), which constrain the pre-middle Cambrian (Cadomian) age for early movements along these boundary faults.

The Zbiroh–Šárka belt (~Domain 3 of Hajná et al., 2010) is lithologically monotonous as compared to the Radnice–Kralupy belt and is dominated by (meta-)graywackes, (meta-)siltstones, and slates (Fig. II.3e). Volcanic rocks are absent. Lenses of chert meters to tens of meters wide and up to several hundred meters long and enclosed in the clastic sedimentary rocks are typical of this belt (Fig. II.3f). The cherts exhibit a wide range of synsedimentary textures (massive, veined, brecciated, and finely laminated) and their origin has been

debated. The presence of microfossils resembling radiolaria (Rodič, 1931) supports a biogenic silica accumulation for some thinly-bedded types, whereas Kettner (1932) and Vajner (1961) suggested that the cherts precipitated directly from silica-rich hydrothermal solutions linked to volcanic activity. Some cherts also originated during diagenetic processes via capture and precipitation of hydrothermal solutions in impermeable black shales. According to Pouba (1978), Pouba et al. (2000), Skoček and Pouba (2000), and Vavrdová (2000), at least some of the cherts are geysirites and stiriolites while others represent silicified limestones, evaporites, and stromatolites rimming the submarine volcanic elevations.

The clastic sedimentary rocks (distal turbidites) indicate a deep-water depositional environment (Cháb and Pelc, 1968) with the source material derived from a volcanic arc. The cherts may have formed in both deep-water (hydrothermal cherts of abiotic origin) and a shallow-water lagoonal environment (stromatolitic cherts; Pouba et al., 2000). Compared to the above two belts, the mineral assemblages in graywackes involve stable chlorite in strain shadows, both clastic and newly grown albite and epidote, and scarce actinolite formed at the expense of clastic hornblende, which all suggests a relatively higher grade of the Cadomian regional metamorphism corresponding up to the lower greenschist facies conditions (Hajná et al., 2010).

The clastic sedimentary rocks in this belt are characterized by an intensely developed pervasive cleavage dipping moderately to the SE and NW mostly with no macroscopically discernible bedding or lamination, which implies that both the finite strain and peak conditions of the Cadomian regional metamorphism generally increase from the NW to the SE, i.e., from the uppermost, very-low-grade Kralovice–Rakovník belt to the lower greenschist facies Zbiroh–Šárka belt.

To the SE, the belt is overlain unconformably by only gently tilted basal Ordovician (Tremadocian) siliciclastic rocks (Fig. II.1a and II.2) and thus may continue further underneath the Barrandian Lower Paleozoic.

In all three belts, the clastic sedimentary rocks exhibit the lowest chemical maturity within the TBU (Sláma et al., 2008), with the εNd_{570} values ranging from –7.2 (Drost et al., 2007) to –1.0 (Pin and Waldhausrová, 2007). Such a wide range of εNd_{570} values corresponds to a rather heterogeneous pile/mélange of sedimentary rocks. The trace-element and chondrite-normalized REE patterns of graywackes are characterized by enrichment in incompatible elements and LREE (Ba, Rb, Th), negative anomalies of Nb, Ta, Sr, P, Ti, and strong fractionation of LREE/HREE (Sláma et al., 2008). All these features, together with high Na_2O/K_2O ratio, suggest a significant amount of island-arc-derived material (Jakeš et al., 1979; Lang, 2000; Drost et al., 2004; Drost, 2008) mixed with a minor amount of recycled sedimentary material (some detrital zircons were derived from Paleoproterozoic to Archean sources; Drost et al., 2010) and basic volcanic rocks (causing local enrichment in MgO, Cr, and higher Zr/Hf ratios).

2.2. Lithotectonic units in the SE segment of the TBU

Deciphering the large-scale structure of the Neoproterozoic basement becomes more complex in the SE segment of the TBU due to the heterogeneous Variscan deformation and emplacement of the early Carboniferous granitoids (Žák et al., 2005, 2009). It has been shown that the intensity of the Variscan finite strain increases significantly to the southeast where up to 60 % of the shortening was calculated in the aureoles of Variscan plutons (Rajlich et al., 1988; Žák et al., 2005). Hence, the Cadomian deformation and field relationships in the multiply deformed Neoproterozoic rocks can only be detected in domains of the low Variscan strain just southeast of the Barrandian Lower Paleozoic (Fig.

II.1a).

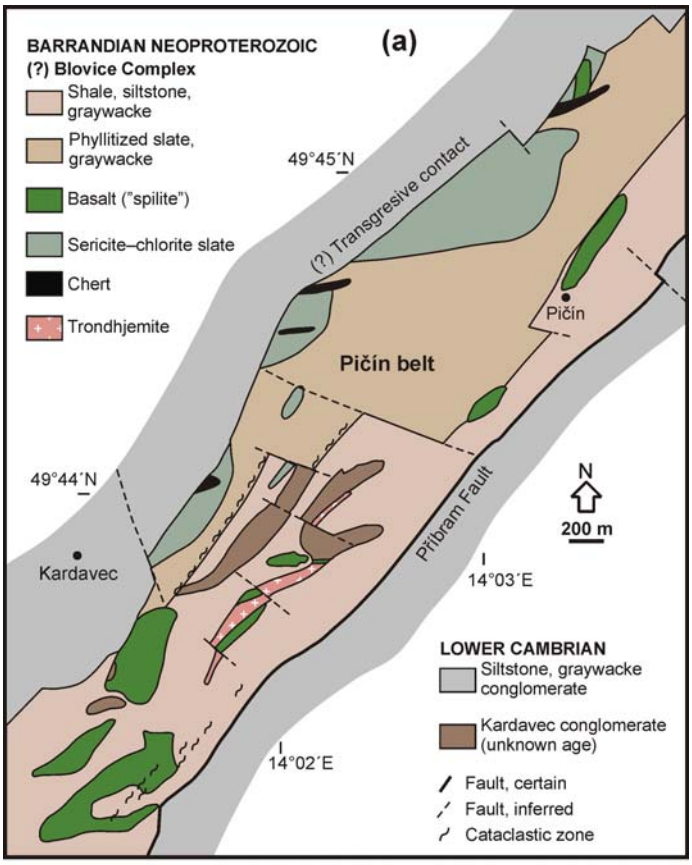

Fig. II.4. (a) A geologic map of the central part of the Pičín belt. This map was redrafted from a Geologic map at a 1:25,000 scale, sheet Rosovice (published by the Czech Geological Survey in 1986). (b) The foliated chert with quartz veins in the Pičín belt; near Hluboš. Swiss Army penknife (9 cm long) for scale.

In the Neoproterozoic basement of the SE segment of the TBU, the following four major lithotectonic or lithostratigraphic units can be recognized.

The Pičín belt (a new name for "the second slate belt" first described in 19th century) is a poorly exposed, narrow NE–SW-trending belt of phyllitized metagraywackes, slates, cherts, tuffitic rocks, and metabasalts overlain unconformably by the Lower Cambrian continental "molasse-type" siliciclastic rocks to the NW (Fig. II.4a). The opposite, southeastern margin of the belt is juxtaposed against the Lower Cambrian along a Variscan fault. Its contact with the adjacent Štěchovice Group near the northeastern termination of the belt is not exposed, and its nature thus remains unknown (Fig. II.4a). The cherts, locally strongly foliated, are a distinct rock type occurring here in several ~E–W-

elongated lenses (Fig. II.4b), which are parallel to the ~E–W trending chevron folds and kink bands in slates as described by Rajlich (1988).

In the remainder of the SE segment of the TBU, the Neoproterozoic units are well exposed and exhibit clear-cut stratigraphic relationships.

The Davle Group (newly renamed in this study instead of the "Davle Formation" to reflect the complexity and protracted time of the volcanism) is an approximately 1000–2000 m (Mašek, 2000) thick volcanic sequence that emerges from beneath the overlying Štěchovice Group in the cores of several major antiforms (Fig. II.1a). The sequence includes low-Ti tholeiitic and high-alumina basalts, rare boninite dikes, calc-alkaline andesites, dacites, and Na-rhyolites capped by felsic pyroclastic rocks (banded and massive ash-flow and ash-fall deposits as well as coarse-grained lithic pyroclastic and epiclastic breccias). The uppermost member of the Davle Group (and thus of the whole Kralupy–Zbraslav Group of Mašek and Zoubek, 1980) is a 50–200 m thick horizon of silicified black shales (the Lečice beds; Fig. II.1a), which cap the volcanic sequence and pass into the overlying siliciclastic rocks of the Štěchovice Group.

The most important of the large-scale antiforms is the Jílové Belt (Fig. II.1a), a ~NNE–SSW-trending, ~65 km long and ~3–5 km wide volcanic complex consisting of basalt to rhyolite lava flows and felsic pyroclastic rocks in its upper part. An integral component of the belt, not found elsewhere, are large bodies of Na-rich leucotonalite, plagiogranite, and alaskite (Fediuk, 2004; Fig. II.5a, b) that were interpreted as shallow-level intrusions into the volcanic edifice (Röhlich, 1998). Their age has not been constrained by radiometric methods due to the lack of zircons, but pebbles of comparable leucotonalites in the Vletice conglomerates (Sláma et al., 2008; see below) yielded an age 610 ± 17 Ma (Sláma et al., 2008). High positive εNd values of the leucotonalites and Na-plagiogranites suggest that

these rocks represent highly fractionated melts derived from the depleted mantle in an island arc setting (Ch. Pin, personal communication, 2009).

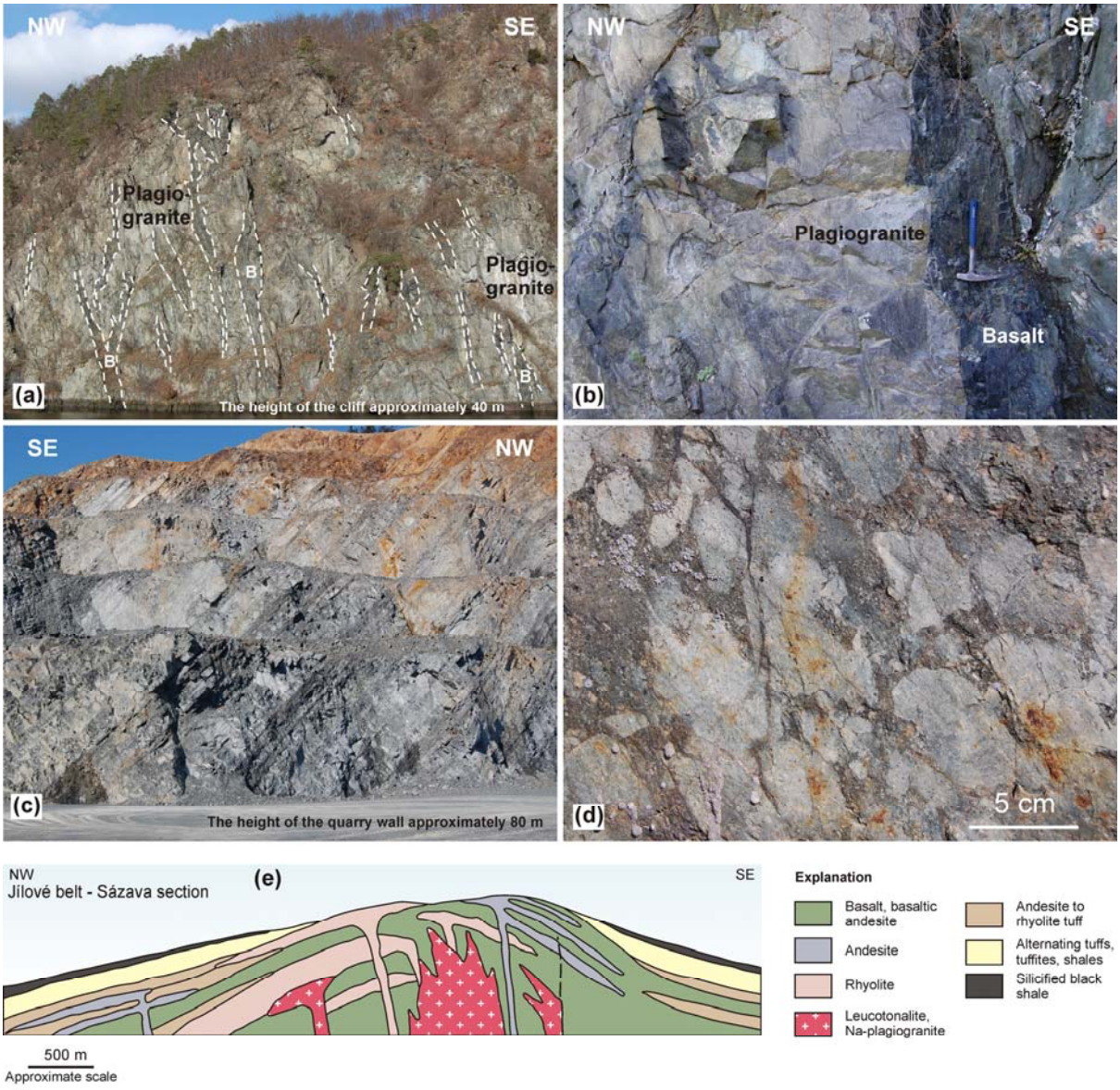

Fig. II.5. The lithologic features of the Davle Group in the SE segment of the TBU. (a) Alternating volcanic arc basalts and associated plagiogranites of the Jílové Belt. The steep attitude of lithologic contacts is a result of the Variscan (early Carboniferous) deformation; Slapy. B – basalt. (b) The steep contact of basalt with plagiogranite in the Jílové Belt; Slapy. Hammer for scale. (c) A thick sequence of alternating banded felsic tuffs, volcanic breccias, and graywackes of the Davle Group; Zbraslav quarry. (d) The volcanic breccia of the Jílové Belt (close-up); Štěchovice dam. (e) A greatly idealized, restored section across the northern part of the Jílové belt volcanic arc sequence showing alternating lavas of various composition, shallow-level intrusions of plagiogranites, tonalites, and trondhjemites, which are all capped by a thin horizon of silicified black shales (redrafted from Röhlich, 1998).

The Jílové Belt has been severely shortened in the ~WNW–ESE direction as indicated

by the pervasive, steep ~NNE–SSW cleavage associated with the subhorizontal ~NNE–SSW stretching lineation, steep lithologic contacts (Fig. II.5a, b), and finite strain estimations yielding shortening of up to 60 % (Rajlich et al., 1988; Žák et al., 2005). This regional deformation, previously thought to be of the Neoproterozoic (Cadomian) age (Morávek and Röhlich, 1971), was synchronous with the emplacement of the early Carboniferous granitoids and is thus a result of the Variscan orogeny (Rajlich, 1988; Rajlich et al., 1988; Žák et al., 2005, 2009). In contrast to the intense Variscan reworking of the Jílové Belt, the pyroclastic deposits of the Davle Group to the NW experienced only weak Variscan shortening leading to a moderate tilt of the banding in the cleavage-free tuffs (Fig. II.5c, d).

The Davle Group and especially the Jílové Belt play a key, but often neglected, role for understanding the polarity and timing of the Cadomian orogeny in the Bohemian Massif. The volcanic sequences hosting the shallow-level leucotonalite and alaskite intrusions (Fig. II.5e) were interpreted to represent an upper section through a Cadomian volcanic arc developed on oceanic crust close to the continental margin around 660–560 Ma (Waldhausrová, 1984; Sláma et al., 2008; Hajná et al., 2010). No other Cadomian volcanic arc has been found in the neighboring Saxothuringian and Moldanubian units of the Bohemian Massif.

The Štěchovice Group (Fig. II.1a; up to ~4000–5000 m thick; Mašek, 2000) comprises rhythmically alternating shales, siltstones, and graywackes (Fig. II.6a). Volcanic rocks are absent except for thin tuffitic beds (Mašek, 2000; Dörr et al., 2002). Syn-sedimentary textures (e.g., graded bedding, flute marks, and slump structures; Fig. II.6b) and inferred depositional settings (turbidites, debris flows, and mudflows) are indicative of relatively deep-water flysch-like sedimentation (Röhlich, 1964). The rhythmically bedded siliciclastic sequences are in many places interrupted by meters to tens of meters thick, massive bodies

of unsorted polymictic conglomerates (the Dobříš conglomerates) containing pebbles of graywackes and slates (96 %; Sláma et al. 2008), cherts, felsic volcanic rocks (Fig. II.6c, d), and granitoids of unknown origin (Fiala, 1948). The conglomerate bodies commonly have a sharp erosional base (Fig. II.6c) and were interpreted as episodic submarine debris flows transporting material eroded from the elevated land (perhaps by fluvial systems) to the deeper parts of the basin (Röhlich, 1964; Chlupáč, 1993; Dörr et al., 2002).

Geochronologic studies on detrital zircons from the conglomerates revealed an abundance of Neoproterozoic zircon grains (71 % of the analyzed population with distinct maxima at ~615, ~600, and ~570 Ma) and fewer Archean and Paleoproterozoic grains (Drost et al., in press) reflecting an increasing importance of the island arc source material. As a whole, sedimentary rocks of the Štěchovice Group were derived from slightly more evolved sources as compared to those in the NW segment of the TBU though their HREE and HFSE patterns mostly overlap (Kachlík, 1992; Sláma et al., 2008).

The Štěchovice Group is spatially restricted to the SE segment of the TBU and overlies the Davle Group conformably (Fig. II.1a). This stratigraphic contact is indisputable, well exposed, and precisely mapped on a regional scale (defined by the Lečice beds) and corroborates the fact that the Štěchovice Group occupies the highest stratigraphic position in the entire SE segment of the TBU. Its upper (transgressive) contact against the overlying Lower Cambrian or Ordovician strata is not exposed anywhere. The northwestern boundary of the Štěchovice Group is a major thrust fault (the Závist thrust), whereas the southeastern boundary is an intrusive contact with the early Carboniferous granitoids.

In a sharp contrast to the pervasively deformed units in the NW segment of the TBU, the Cadomian deformation recorded in the flysch-like Štěchovice Group is extremely weak. The intensity of the Cadomian strain does not generally exceed the pencil cleavage stage

(corresponding to the incipient shortening; Ramsay and Huber, 1987; Parés and van der Pluijm, 2002) as corroborated by both field observations and finite strain estimations on conglomerates in areas of the low Variscan overprint (Rajlich et al., 1988; Žák et al., 2005).

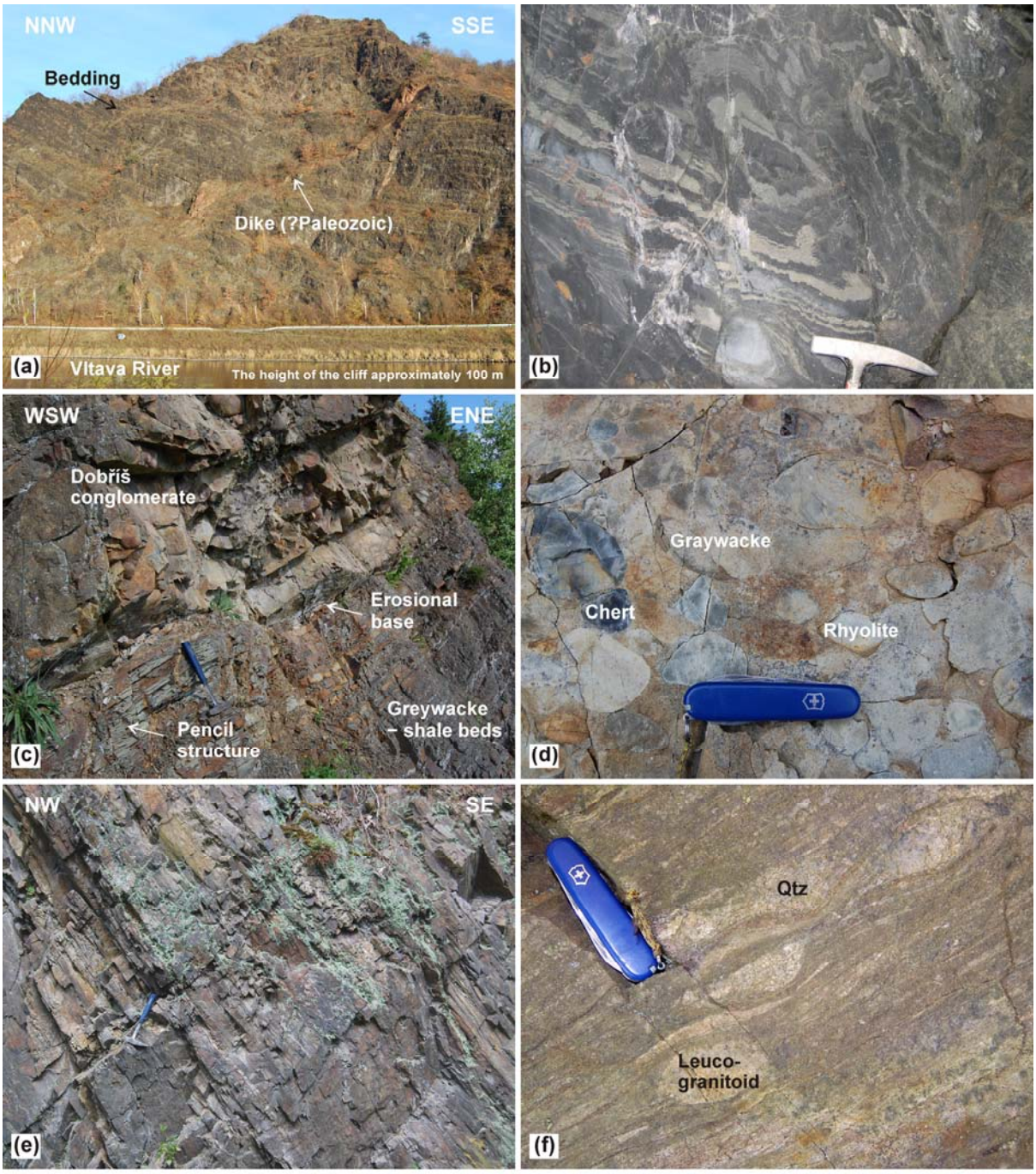

Fig. II.6. The lithologic and structural features of the Štěchovice Group in the SE segment of the TBU. (a) A weakly deformed and gently to moderately tilted sequence of alternating graywackes, siltstones, and shales; Zvolská Homole. (b) Synsedimentary slump structures in siltstones ; Zbraslav. Hammer for scale. (c) A thick layer of the Dobříš conglomerate with a sharp erosional base against the underlying weakly deformed

graywacke-shale beds; Jezírko quarry. Hammer for scale. (d) A polymictic Dobříš conglomerate (close-up); Jezírko quarry. Swiss Army penknife for scale. (e) Alternating metasiltstones and metagraywackes of the Svrchnice Formation; Vletice area. The metasedimentary rocks have been affected by contact metamorphism and deformation synchronous with the emplacement of early Carboniferous granitoids. Hammer for scale. (f) The Vletice conglomerate (close-up) containing clasts of leucogranitods, quartzite, and quartz (Qtz); Vletice area. Swiss Army penknife for scale.

The Svrchnice Formation (Fig. II.1a; approximate thickness of >1000 m), in a roof pendant of the early Carboniferous Central Bohemian Plutonic Complex, is represented by a flysch-like sequence of alternating metasiltstones, metagreywackes, and metaconglomerates (Fig. II.6e, f) that is comparable to the Štěchovice Group of the SE segment of the TBU (Sláma et al., 2008). An important difference exists, however, in the composition of the clasts in the conglomerates. Unlike the Dobříš conglomerates of the Štěchovice Group (Fig. II.6d), the medium- to coarse-grained pebbly metasandstones and matrix-supported metaconglomerates (the Vletice metaconglomerates, Fig. II.6f; Fiala, 1948) are characterized by the prevalence of clasts derived from mature continental crust (quartz, quartzites, granitoids, limestones; see Sláma et al., 2008 for details). Radiometric dating of detrital zircons from the matrix of the conglomerates yielded age maxima at ~600 Ma and ~544 Ma. This finding suggests that the sedimentation of the Svrchnice Formation may have continued until the earliest Cambrian; thus, these metasediments represent probably the youngest part of the entire Teplá–Barrandian Neoproterozoic.

Additional differences from the Štěchovice Group include the presence of low-Ti basalts and boninite sills (Fediuk, 1991; Kachlík, 1992; Vítková and Kachlík, 2001) and the absence of the underlying marker horizon of black shales (the Lečice beds; Fig. II.1a). The emplacement age of the boninites and low-Ti metabasalts is bracketed between 544 ± 7 Ma (maximum age of the host metagreywackes; Sláma et al., 2008) and 524 ± 8.8 Ma (age of metarhyolites within the overlying Cambrian succession; V. Kachlík and D. Dunkley, unpublished data).

The Svrchnice Formation is overlain unconformably by the lower Cambrian to Middle Devonian strata. All the units have been affected extensively by the Variscan (Late Devonian to early Carboniferous) contact metamorphism and regional deformation (Chlupáč, 1989; Kachlík, 1992; Sláma et al., 2008).

3. Discussion

The recent extensive research into the evolution of the Avalonian–Cadomian orogenic belt, and its significance for the opening of the Rheic Ocean (e.g., the IGCP project No. 497 "The Rheic Ocean and its correlatives"; see Nance et al., 2010 for an overview), has also involved the TBU as one of the key segments of the Cadomian active margin. The outstanding issues we address below regarding the Neoproterozoic evolution of the TBU include the polarity of the Cadomian orogen as preserved in TBU, the significance of the lithotectonic and lithostratigraphic units in the Teplá–Barrandian Neoproterozoic defined in this paper, and the tectonic development of the Cadomian orogen in the TBU through time.

3.1. Polarity of the Cadomian orogen in the Bohemian Massif

The direction of the Cadomian oceanic subduction and the location of the subduction zone, fore-arc, volcanic arc, back-arc regions, and Gondwana mainland in relation to the present-day basement geology of the TBU have long been a matter of controversy. According to one view, it was assumed that the subduction zone was located to the SE of the TBU (present-day coordinates are used throughout), with the NW-directed subduction of the oceanic crust beneath the TBU and an island arc represented by the Davle Group. In this hypothesis, the sedimentary rocks of the Blovice Formation would represent the northwesterly back-arc basin fill (Kříbek et al., 2000). In contrast, Zulauf (1997), Dörr et al. (2002), Timmermann et al. (2004), Sláma et al. (2008), Hajná et al. (2010), and Drost et al. (in press) argued for the S- to SE-directed subduction (from the N or NW). The tectonic

significance of the Davle Group remains identical to the previous hypothesis (volcanic arc), but the sedimentary rocks of the Blovice Formation are interpreted as an accretionary wedge and the Svrchnice Formation as a remnant basin close to the Gondwana mainland (Sláma et al., 2008).

As the issue of subduction polarity is central to understanding the Cadomian orogeny in the Bohemian Massif, below we expand on the latter and our strongly preferred hypothesis by listing multiple arguments in support of the S- to SE-directed Cadomian subduction beneath the TBU.

(1) The northwesternmost tip of the TBU is made up of the Mariánské Lázně Complex (MLC in Fig. II.1a), a part of which was dated by Timmermann et al. (2004) at 540 ± 9 Ma (Fig. II.1a). This complex was interpreted to represent a late-Cadomian oceanic crust attached to the northwestern TBU prior to the emplacement of the within-plate gabbros at ~500 Ma (Štědrá et al., 2002; Timmermann et al., 2004; Sláma et al., 2008). In contrast, the opposite, southeastern margin of the TBU hosts the Cadomian volcanic arc (the Davle Group; Fig. II.1a, 7a) and is adjacent to the southeasterly high-grade Moldanubian unit that contains slivers of a 2.1 Ma continental basement (Wendt et al., 1993). Despite the TBU margins have been intensely reworked during the Variscan orogeny (Dörr and Zulauf, 2010 and references therein), such a spatial distribution of the main lithotectonic units in the TBU is consistent with the ocean and trench located to the N–NW and the Gondwana mainland (specifically, the Trans-Saharan mobile belt according to Drost et al., in press) to the S–SE.

(2) Our structural studies revealed that striking differences exist between both segments of the TBU in the intensity, style, and spatial pattern of the Cadomian deformation, as exemplified by the area between the fronts of the Variscan pervasive deformation (Fig. II.1a, II.7a). While the NW segment is characterized by tectonic

juxtaposition of variously deformed allochtonous belts (the Kralovice–Rakovník, Radnice–Kralupy, and Zbiroh–Šárka belts) that are commonly affected by pervasive cleavage (Fig. II.3e) and display complex internal strain patterns (Fig. II.2) typical of accretionary wedges (e.g., Braid et al., 2010), the Cadomian deformation was weak in the SE segment as recorded in the sedimentary rocks of the Štěchovice Group off the front of the Variscan pervasive deformation (Fig. II.6c, d). In short, the Cadomian deformation is discontinuous across boundaries of the individual lithotectonic units in the NW segment, and its intensity drops abruptly in the younger units of the SE segment (Fig. II.7a). Hence, the major deforming zone of the Cadomian orogen in the TBU was the NW segment, which most likely represents an accretionary wedge in the outboard (frontal) position facing the subduction zone.

(3) As early as in the 1960s, abundant chaotic deposits, slump structures, and olistoliths (Fig. II.3c) were described by Cháb and Pelc (1968) as an integral component of the Radnice–Kralupy belt. The significance of these structures, however, could not be fully appreciated at the dawn of plate tectonics. Importantly, this belt also includes tectonically emplaced fragments of the ocean floor in strongly sheared slate and a graywacke matrix (Fig. II.3d) and mixed with lenses of chert, limestone, and black shales (Hajná et al., 2010; J. Hajná and J. Žák, new mapping and unpublished data). The ocean floor (meta-)basalts that now occur together as closely spaced blocks have contrasting geochemical signatures and originated from different sources in various tectonic settings (NMORBs, depleted basalts influenced by suprasubduction zone fluids, and rare alkali within-plate basalts derived from an enriched mantle; Pin and Waldhausrová, 2007). The Radnice–Kralupy belt was thus recently interpreted as involving both sedimentary and tectonic mélanges (Hajná et al., 2010), which are typical components of subduction-related accretionary complexes (e.g., Silver and Beutner, 1980; Cloos, 1982; Cowan, 1985, Kusky and Bradley, 1999; Ujiie, 2002;

Braid et al., 2010; Osozawa et al., 2009; Yamamoto et al., 2009; Festa et al., 2010; Ghikas et al., 2010). No such rock assemblages have been found in the SE segment of the TBU.

(4) Although the detrital zircon ages and the abundance of (meta-)sedimentary clasts in the Neoproterozoic sedimentary rocks point to multiple sources changing through time (see details in Drost et al., in press) and rapid sediment recycling, a consistent shift exists in the lithology of clasts in conglomerates. Rare conglomerates in the Blovice complex and the Dobříš conglomerates in the Štěchovice Group are dominated by intrabasinal and arc-derived clasts (Fig. II.6d; Chlupáč, 1993; Dörr et al. 2002), whereas the southeasterly Vletice metaconglomerate of the Svrchnice Formation (Fig. II.6f) is composed of clasts derived from both the volcanic arc and the mature continental crust (presumably Gondwana mainland; Sláma et al., 2008).

(5) The 9HR deep seismic profile in the ~NW–SE direction across the entire TBU (Tomek et al., 1997) shows significant subhorizontal to SSE-dipping reflections at depth. This seismic pattern was interpreted as being similar to subduction–accretion complexes in modern arcs (Tomek et al., 1997) and thus is consistent with the S- to SE-directed subduction of oceanic crust beneath the accretionary wedge (represented by the NW segment of the TBU).

(6) All the paleogeographic reconstructions of the Avalonian–Cadomian belt agree that the Gondwana mainland laid approximately south of the belt (Nance et al., 1991; Nance and Murphy, 1994; Tait et al., 1994; Wortman et al., 2000; Robardet, 2003; Murphy et al., 2002, 2004, 2006; Linnemann and Romer, 2002; von Raumer et al., 2002; Linnemann et al., 2007, 2008a, b; Fatka and Mergl, 2009). A large amount of post-Cadomian clockwise rotation of the entire TBU lithosphere would be required to place the NW segment of the TBU to the back-arc position with respect to the Jílové belt volcanic arc (now to the SE) and to rotate

the NW segment away from the (southerly) Gondwana mainland (see fig. 7 in Kříbek et al., 2000). No paleomagnetic data exist for the Teplá–Barrandian Neoproterozoic, and the data from the overlying Lower Paleozoic are still far from being conclusive to exclude either paleogeographic configuration due to the strong early Carboniferous remagnetization (e.g., Tait et al., 1995, 1997; Krs et al., 1987, 2001; Aïfa et al., 2007; Edel et al., 2003).

3.2. A new tectonic–stratigraphic scheme for the Teplá–Barrandian Neoproterozoic

The above described lithotectonic zonation and inferred plate-tectonic setting of the component units of the Teplá–Barrandian Neoproterozoic suggest that the existing, strictly non-tectonic stratigraphic schemes (e.g., Mašek, 2000) cannot apply as previously envisaged. First, we have shown that the NW segment of the TBU, entirely assigned to the "Blovice Formation", is a package of contrasting fault-bounded allochtonous units (Figs. II.2, II.7a, b; Hajná et al., 2010; this study). Second, the radiometric ages of (meta-)basalts (Sm–Nd model ages), black shales, and age of graywackes as inferred from the age spectra of detrital zircons scatter widely (although some of the scatter may be attributed to large uncertainties on the data; e.g., Pin and Waldhausrová, 2007; Pašava and Amov, 1993; Drost et al., in press) implying a time span of at least tens of millions of years for this single "formation". Third, it is generally difficult or even impossible to apply basic stratigraphic principles to restore the original stratigraphic and temporal relations among lithotectonic units in accretionary wedges and mélanges (e.g., Hsü, 1968; Festa et al., 2010). In the absence of index fossils, stratigraphic contacts, and high-precision radiometric ages, this statement applies in particular for the Kralovice–Rakovník, Radnice–Kralupy, and Zbiroh–Šárka belts. These lithotectonic units thus might have been originally deposited in separate environments at different times and then diachronously buried, exhumed, and welded together within the

accretionary wedge. Obviously, the “Blovice Formation” cannot be considered as a single lithostratigraphic unit. We thus coin a new term the “Blovice complex” to embrace all the allochtonous lithotectonic belts that make up the Cadomian basement of the NW segment of the Teplá–Barrandian Neoproterozoic and to emphasize their different lithology, deformation patterns, and unknown stratigraphic relations (Fig. II.7b).

The Blovice complex probably underlies the entire Barrandian Lower Paleozoic as its southeasternmost exposure may be represented by the Pičín belt (Fig. II.4). Aside from the Pičín belt, lithostratigraphy can be well established in the remainder of the SE segment of the TBU with the arc volcanic complexes of the Davle Group and its uppermost member (the Lečice beds) conformably overlain by the flysch sequence of the Štěchovice Group (Fig. II.7a, b). It is important to note that the contact of the Pičín belt against the Davle Group and Štěchovice Group is not exposed, and has never before been observed, leaving the stratigraphic relations between the Blovice complex and the other lithostratigraphic units in the SE segment of the TBU unknown (Mašek, 2000; Fig. II.7b). It follows that the term Kralupy–Zbraslav Group merges rocks of unknown stratigraphic relations across both segments of the TBU and is thus rather problematic and should be abandoned.

The lithotectonic belts of the Blovice complex continue further to the NE and SW of the area examined in detail here (Fig. II.1a; see also Röhlich, 1965). Our reconnaissance mapping suggests, however, that large along-strike variations may exist in their lithology, structure, and metamorphic grade, which is a common feature in accretionary wedges. In addition, the Variscan reworking increases significantly towards the TBU margins, which makes the reconstruction of the Cadomian structures and stratigraphic relations much more difficult. It is the focus of our ongoing research to examine these variations and to correlate structures across large portions of the Cadomian basement of the TBU.

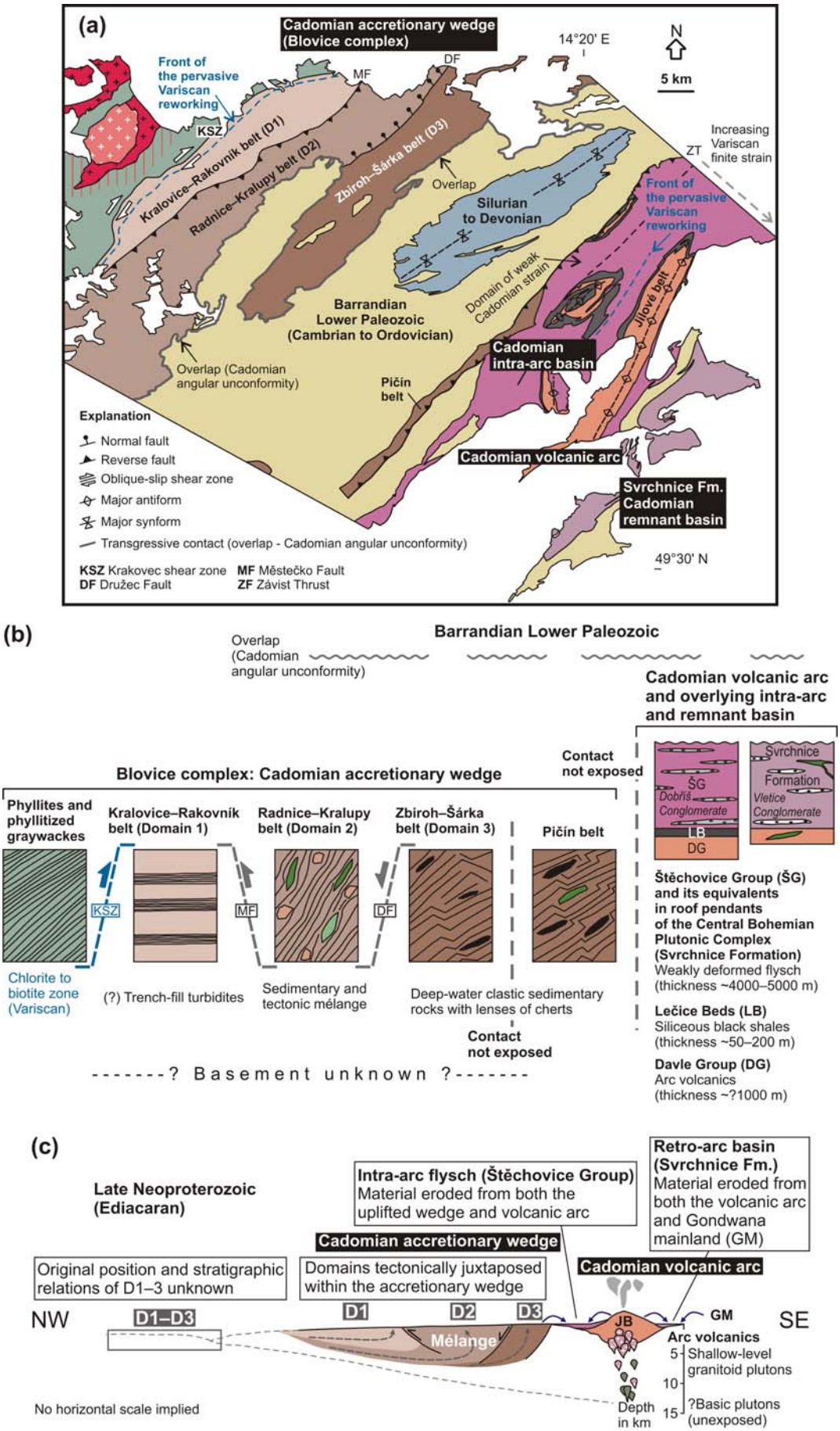
(a)
Cadomian accretionary wedge (Blovice complex)
14°20' E
N
5 km
Front of the pervasive Variscan reworking
KSZ
MF
DF
Kralovice–Rakovník belt (D1)
Radnice–Kralupy belt (D2)
Zbiroh–Šárka belt (D3)
Overlap
Silurian to Devonian
ZT
Increasing Variscan finite strain
Front of the pervasive Variscan reworking
Domain of weak Cadomian strain
Jílové belt
Barrandian Lower Paleozoic (Cambrian to Ordovician)
Overlap (Cadomian angular unconformity)
Cadomian intra-arc basin
Pičín belt
Cadomian volcanic arc
Svrchnice Fm. Cadomian remnant basin
49°30' N
Explanation
Normal fault
Reverse fault
Oblique-slip shear zone
Major antiform
Major synform
Transgressive contact (overlap - Cadomian angular unconformity)
KSZ Krakovec shear zone
MF Městečko Fault
DF Družec Fault
ZF Závist Thrust
(b)
Barrandian Lower Paleozoic
Overlap (Cadomian angular unconformity)
Cadomian volcanic arc and overlying intra-arc and remnant basin
Contact not exposed
Svrchnice Formation
ŠG
Dobříš Conglomerate
Vletice Conglomerate
LB
DG
Blovice complex: Cadomian accretionary wedge
Phyllites and phyllitized graywackes
Kralovice–Rakovník belt (Domain 1)
Radnice–Kralupy belt (Domain 2)
Zbiroh–Šárka belt (Domain 3)
Pičín belt
KSZ
MF
DF
Chlorite to biotite zone (Variscan)
(?) Trench-fill turbidites
Sedimentary and tectonic mélange
Deep-water clastic sedimentary rocks with lenses of cherts
Contact not exposed
-------? Basement unknown ?-------
Štěchovice Group (ŠG) and its equivalents in roof pendants of the Central Bohemian Plutonic Complex (Svrchnice Formation)
Weakly deformed flysch (thickness ~4000–5000 m)
Lečice Beds (LB)
Siliceous black shales (thickness ~50–200 m)
Davle Group (DG)
Arc volcanics (thickness ~?1000 m)
(c)
Late Neoproterozoic (Ediacaran)
Intra-arc flysch (Štěchovice Group)
Material eroded from both the uplifted wedge and volcanic arc
Retro-arc basin (Svrchnice Fm.)
Material eroded from both the volcanic arc and Gondwana mainland (GM)
Cadomian accretionary wedge
Cadomian volcanic arc
Original position and stratigraphic relations of D1–3 unknown
Domains tectonically juxtaposed within the accretionary wedge
NW
D1–D3
D1
D2
D3
JB
GM
SE
Mélange
Arc volcanics
5
Shallow-level granitoid plutons
10
15
?Basic plutons (unexposed)
Depth in km
No horizontal scale implied

Fig. II.7. (a) A simplified geologic map to show a geotectonic interpretation of the Neoproterozoic (Cadomian) lithotectonic and lithostratigraphic units of the TBU. The Cadomian structures are well preserved between the NW and SE front of the Variscan pervasive deformation. (b) A new proposal of a tectonostratigraphic scheme for the NW and SE segments of the Teplá–Barrandian Neoproterozoic. See text for discussion. (c) The inferred position and tectonic significance of the component units of the Teplá–Barrandian Neoproterozoic within the Cadomian orogen as preserved in the TBU. See text for discussion.

Also taking into account the Svrchnice Formation in a roof pendant of the Variscan granitoids, we newly summarize the inferences on the structure and stratigraphy of the Teplá–Barrandian Neoproterozoic in Fig. II.7b. This synoptic diagram portrays lithology, internal structure, the nature of contacts, stratigraphic relations where known, and a plate-tectonic interpretation of the component units in both segments of the TBU as described in this paper. The lithotectonic units (belts) of the NW segment have an unknown vertical extent, are bounded by tectonic contacts or overlain trangressively by the Barrandian Lower Paleozoic, and are strongly deformed except for the Kralovice–Rakovník belt. The intense deformation also prevents from establishing the younging direction in most cases. Thus, stratigraphic columns for each belt cannot be constructed. Furthermore, the contact between the Pičín belt and Davle and Štěchovice groups is not exposed. Given these uncertainties, the units in the NW and SE segments of the TBU are shown only schematically with no vertical dimension or temporal and stratigraphic relations implied.

3.3. Structure and stratigraphy of the Teplá–Barrandian Neoproterozoic in a plate-tectonic context

Our new views on structure and stratigraphy of the Teplá–Barrandian Neoproterozoic fit the following plate-tectonic scenario recently proposed for the Cadomian orogeny in the TBU well (Zulauf, 1997; Dörr et al., 2002; Sláma et al., 2008; Hajná et al., 2010; Drost et al., in press).

The ocean floor (meta-)basalts found in the Radnice–Kralupy belt have contrasting

geochemical signatures compatible with intra-oceanic supra-subduction zone and within-plate settings (Pin and Waldhausrová, 2007). These (meta-)basalts were thus brought together as tectonic blocks (e.g., Fig. II.3d) within the accretionary wedge as represented by the Blovice complex (Fig. II.7c). The subduction of these fragments of diverse oceanic crust was most likely broadly synchronous with the sedimentation of the trench-fill turbidites (the Kralovice–Rakovník belt), chaotic slump deposits (the Radnice–Kralupy belt), and monotonous chert–graywacke sequences (the Zbiroh–Šárka belt). Detrital zircons in one sample from these sedimentary rocks indicate approximate age of deposition at ~635 to ~620 Ma (Drost et al., in press). All these units record multiple episodes of rapid recycling of the arc-derived material followed by differential burial, heterogeneous deformation, and exhumation within the wedge (Fig. II.7c; Hajná et al., 2010).

The 605 ± 39 Ma (meta-)basalts (Pin and Waldhausrová, 2007) have been involved in the accretionary wedge implying that its formation, at least partly, temporally overlapped with the main phase of volcanic arc growth and its coeval erosion (the Davle Group) to the SE around ~620–560 Ma (Fig. II.7c; Sláma et al., 2008; Drost et al., in press). The arc igneous activity had largely ceased at about 560 Ma, while both the rear of the wedge and some elevated portions of the arc continued to be extensively eroded supplying the deep-water flysch sequence of the Štěchovice Group (Fig. II.7c; the Dobříš conglomerates contain both arc-derived felsic volcanic rocks and chert clasts that are unique to the Blovice complex; Figs. II.2, II.3f, II.4). At the same time, the arc-derived and continental margin-derived detritus was deposited in a southeasterly remnant basin (the Svrchnice Formation; Fig. II.7c). Deposition of the Štěchovice Group and Svrchnice Formation may have continued into the earliest Cambrian.

The Cadomian orogeny in the TBU was terminated at ~550–540 Ma by slab breakoff

and associated metamorphism in its southern and northwestern part (Zulauf et al., 1999; Dörr et al., 2002), by final attachment of the ~540 Ma oceanic crust to northwesternmost margin of the TBU (Štědrá et al., 2002; Timmermann et al., 2004; Sláma et al., 2008), and by intrusion of boninite dikes between ~544–524 Ma (Sláma et al., 2008). The latter may reflect the ridge–trench collision and the transition from a destructive to transform margin during the early/middle Cambrian.

4. Conclusions

The Neoproterozoic (Cadomian) basement of the Teplá–Barrandian unit reveals a complex structure and mostly unclear stratigraphic relations of its components.

The NW segment of the TBU is a package of juxtaposed allochtonous belts (the Kralovice–Rakovník, Radnice–Kralupy, and Zbiroh–Šárka belts) that have been variously deformed and display complex internal strain patterns typical of accretionary wedges. We summarize these three belts, and comparable units elsewhere in the TBU, under a new term the Blovice complex.

In the SE segment of the TBU, the Pičín belt, which may represent the southeasternmost exposure of the Blovice complex, is in unknown relation to the volcanic arc sequence, which was newly renamed as the Davle Group. The latter is overlain conformably by the flysch sedimentary rocks of the Štěchovice Group and its retro-arc (or remnant basin) equivalent in a roof pendant of the Variscan granitoids (the Svrchnice Formation). The flysch sequences have only been affected a little by the Cadomian deformation.

The structural and stratigraphic relations are consistent with the S- to SE-directed Cadomian subduction beneath the TBU that have lead to the involvement of trench-fill turbidites, chaotic deposits, and diverse ocean floor (meta-)basalts into the accretionary

wedge represented by the Blovice complex. The accretionary wedge formation temporally overlapped with the growth and coeval erosion of the volcanic arc (the Davle Group) around ~620–560 Ma. Upon cessation of the arc igneous activity, the rear of the wedge and some elevated portions of the arc were eroded to supply the deep-water flysch sequences of the Štěchovice Group (~560 to <544 Ma), whereas the comparable Svrchnice Formation was deposited in a southeasterly retro-arc basin largely sourced from the nearby continental margin. The Cadomian orogeny in the TBU was terminated around ~550–540 Ma by slab breakoff, by final attachment of the most outboard ~540 Ma oceanic crust, and by intrusion of ~544–524 Ma boninite dikes marking the transition from a destructive to transform margin during the early/middle Cambrian.

References

Aïfa, T., Pruner, P., Chadima, M., Štorch, P., 2007. Structural evolution of the Prague synform (Czech Republic) during Silurian times: an AMS, rock magnetism, and paleomagnetic study of the Svatý Jan pod Skalou dikes. Consequences for the nappes emplacement. In: Linnemann, U., Nance, D., Kraft, P., Zulauf, G. (Eds.) The evolution of the Rheic Ocean: from Avalonian–Cadomian active margin to Alleghenian–Variscan collision. Geological Society of America Special Paper, 423, 249–265.

Braid, J.A., Murphy, B.J., Quesada, C., 2010. Structural analysis of an accretionary prism in a continental collisional setting, the Late Paleozoic Pulo do Lobo Zone, Southern Iberia. Gondwana Research, 17, 422–439.

Cháb, J., 1993. General problems of the TB (Teplá–Barrandian) Precambrian, Bohemian Massif, the Czech Republic. Bulletin of the Czech Geological Survey, 68, 1–6.

Cháb, J. and Pelc, Z., 1968. Lithology of Upper Proterozoic in the NW limb of the Barrandian area. Krystalinikum, 6, 141–167.

Chlupáč, I., 1989. Stratigraphy of the Sedlčany–Krásná Hora Metamorphic "Islet" in Bohemia (Proterozoic? to Devonian). Journal of Mineralogy and Geology, 34, 1–16.

Chlupáč, I., 1993. Geology of the Barrandian – a field trip guide. Senckenberg-Buch 69, W. Kramer.

Cloos, M., 1982. Flow mélanges: numerical modeling and geologic constraints on their origin in the Franciscan subduction complex. Geological Society of America Bulletin, 93, 330–345.

Cowan, D.S., 1985. Structural styles in Mesozoic and Cenozoic mélanges in the Western Cordillera of North America. Geological Society of America Bulletin, 96, 451–462.

Dallmeyer, R.D. and Urban, M., 1998. Variscan vs Cadomian tectonothermal activity in northwestern sectors of the Teplá–Barrandian zone, Czech Republic: constraints from $^{40}Ar/^{39}Ar$ ages. Geologische Rundschau, 87, 94–106.

Dörr, W., Zulauf, G., Fiala, J., Franke, W., Vejnar, Z., 2002. Neoproterozoic to Early Cambrian history of an active plate margin in the Teplá–Barrandian unit – a correlation of U–Pb isotopic-dilution-TIMS ages (Bohemia, Czech Republic). Tectonophysics, 352, 65–85.

Dörr, W. and Zulauf, G., 2010. Elevator tectonics and orogenic collapse of a Tibetan-style plateau in the European Variscides: the role of the Bohemian shear zone. International Journal of Earth Sciences, 99, 299–325.

Drost, K., Linnemann, U., McNaughton, N., Fatka, O., Kraft, P., Gehmlich, M., Tonk, Ch., Marek, J., 2004. New data on the Neoproterozoic–Cambrian geotectonic setting of the Teplá–Barrandian

volcano-sedimentary successions: geochemistry, U–Pb zircon ages, and provenance (Bohemian Massif, Czech Republic). International Journal of Earth Sciences, 93, 742–757.
Drost, K., Romer, R.L., Linnemann, U., Fatka, O., Kraft, P., Marek, J., 2007. Nd–Sr–Pb isotopic signatures of Neoproterozoic–Early Paleozoic siliciclastic rocks in response to changing geotectonic regimes: a case study from the Barrandian area (Bohemian Massif, Czech Republic). In: Linnemann, U., Nance, D., Kraft, P., Zulauf, G. (Eds.), The evolution of the Rheic Ocean: from Avalonian–Cadomian active margin to Alleghenian–Variscan collision. Geological Society of America Special Paper, 423, pp. 191–208.
Drost, K., 2008. Sources and geotectonic setting of Late Neoproterozoic–Early Paleozoic volcano-sedimentary successions of the Teplá–Barrandian unit (Bohemian Massif): evidence from petrographical, geochemical, and isotope analyses. Geologica Saxonica, 54, 1–165.
Drost, K., Gerdes, A., Jeffries, T., Linnemann, U., Storey, C., in press. Provenance of Neoproterozoic and early Paleozoic siliciclastic rocks of the Teplá–Barrandian unit (Bohemian Massif): evidence from U–Pb detrital zircon ages. Gondwana Research, doi:10.1016/j.gr.2010.05.003
Dubanský, A., 1984. Determination of the radiogenic age by the K–Ar method (geochronological data from the Bohemian Massif in the ČSR region). Collection of Scientific Works of Technical University of Ostrava, Mining and Geological Series, 30, 137–170.
Edel, J.B., Schulmann, K., Holub, F.V., 2003. Anticlockwise and clockwise rotations of the Eastern Variscides accommodated by lithospheric wrenching: palaeomagnetic and structural evidence. Journal of the Geological Society, London, 160, 209–218.
Fatka, O. and Gabriel, Z., 1991. Microfossils from siliceous stromatolitic rocks of the Barrandian Proterozoic (Bohemian Massif). Journal of Mineralogy and Geology, 36, 143–148.
Fatka, O., Mergl, M., 2009. The 'microcontinent' Perunica: status and story 15 years after conception. In: Bassett, M.G. (Ed.), Early Palaeozoic peri-Gondwana terranes: new insights from tectonics and biogeography. Geological Society, London, Special Publications, 325, 65–101.
Fediuk, F., l99l. Pre-Variscan boninite metavolcanics in the Bohemian Massif. Ofioliti, 16, l27–128.
Fediuk, F., 2004. Alaskites and related rocks in the Proterozoic Jílové Belt of central Bohemia. Krystalinikum, 30, 27–50.
Festa, A., Pini, G. A., Dilek, Y., Codegone, G., 2010. Mélanges and mélange-forming processes: a historical overview and new concepts. International Geological Review, 52, 1040–1105.
Fiala, F., 1948. Algonkian conglomerates in central Bohemia. Bulletin of the Central Geological Survey, 15, 399–612.
Fiala, F., 1977. The Upper Proterozoic volcanism of the Barrandian area and the problem of spilites. Journal of Geological Sciences, Geology, 30, 2–247.
Fiala, F., 1978. Chemistry of the earlier magmatic rocks from the Železné hory Mts. Correlation of the Proterozoic and Paleozoic stratiform deposits, 5, 25–39.
Fiala, F., 1987. Structures and textures of the Upper Proterozoic volcanics of the Barrandian area. Journal of Geological Sciences, Geology, 42, 9–40.
Franke, W. and Zelazniewicz, A., 2002. Structure and evolution of the Bohemian arc. In: Winchester, J.A., Pharaoh, T.C., Verniers, J. (Eds.), Palaeozoic amalgamation of Central Europe. Geological Society, London, Special Publications, 201, 279–293.
Ghikas, C., Dilek, Y., Rassios, A. E., 2010. Structure and tectonics of subophiolitic mélanges in the western Hellenides (Greece): implications for ophiolite emplacement tectonics. International Geological Review, 52, 423–453.
Hajná, J., Žák, J., Kachlík, V., Chadima, M., 2010. Subduction-driven shortening and differential exhumation in a Cadomian accretionary wedge: the Teplá–Barrandian unit, Bohemian Massif. Precambrian Research, 176, 27–45.
Holubec, J., 1966. Stratigraphy of the Upper Proterozoic in the core of the Bohemian Massif. Transactions of the Czechoslovak Academy of Sciences, Mathematical and Natural Science Series, 76, 43–62.
Holubec, J., 1968. Structural development of the geosynclinal Proterozoic and its relations to the deeper zones of the Earth's crust. Transactions of the Czechoslovak Academy of Sciences, Mathematical and Natural Science Series, 78, 3–77.
Holubec, J., 1995. Structure (the Teplá–Barrandian Zone). In: Dallmeyer, R.D., Franke, W., Weber, K. (Eds.), Pre-Permian geology of Central and Eastern Europe, Springer, Berlin, Heidelberg, New York, 392–397.
Hsü, K.J., 1968. Principles of mélanges and their bearing on the Franciscan–Knoxville paradox. Geological Society of America Bulletin, 79, 1063–1074.
Jakeš, P., Zoubek, J., Zoubková, J., Franke, W., 1979. Graywackes and metagraywackes of

the Teplá–Barrandian Proterozoic area. Journal of Geological Sciences, Geology, 33, 83–122.
Kachlík, V., 1992. Litostratigraphy, paleogeography, and metamorphism of roof pendants in the NE part of the Central Bohemian Pluton. Unpublished Ph.D. thesis, Charles University in Prague.
Kachlík, V., 2008. Teplá–Barrandian Unit (Moldanubian Zone). In: McCann, T. (Ed.), The Geology of Central Europe, Volume 1: Precambrian and Paleozoic. Geological Society, London, 68–75.
Kalvoda, J., Bábek, O., Fatka, O., Leichmann, J., Melichar, R., Nehyba, S., Špaček, P., 2008. Brunovistulian terrane (Bohemian Massif, Central Europe) from late Proterozoic to late Paleozoic: a review. International Journal of Earth Sciences, 97, 497–518.
Kettner, R., 1932. The issue of the Precambrian in Bohemia. Journal of the National Museum (Prague), Natural History Series, 35–43.
Konzalová, M., 1981. Some Late Precambrian microfossils from the Bohemian Massif and their correlation. Precambrian Research, 15, 43–62.
Kříbek, B., Pouba, Z., Skoček, V., Waldhausrová, J., 2000. Neoproterozoic of the Teplá–Barrandian Unit as a part of the Cadomian orogenic belt: a review and correlation aspects. Bulletin of the Czech Geological Survey, 75, 175–196.
Krs, M., Krsová, M., Pruner, P., Chvojka, R., Havlíček, V., 1987. Palaeomagnetism, palaeogeography and the multicomponent analysis of Middle and Upper Cambrian rocks of the Barrandian in the Bohemian Massif. Tectonophysics, 139, 1–20.
Krs, M., Pruner, P., Man, O., 2001. Tectonic and paleogeographic interpretation of the paleomagnetism of Variscan and pre-Variscan formations of the Bohemian Massif, with special reference to the Barrandian terrane. Tectonophysics, 332, 93–114.
Kusky, T. and Bradley, D., 1999. Kinematic analysis of mélange fabrics: examples and applications from the McHugh Complex, Kenai Peninsula, Alaska. Journal of Structural Geology, 21, 1773–1796.
Lang, M., 2000. Composition of Proterozoic greywackes in the Barrandian. Bulletin of the Czech Geological Survey, 75, 205–216.
Linnemann, U. and Romer, R.L., 2002. The Cadomian orogeny in Saxo-Thuringia, Germany: geochemical and Nd–Sr–Pb isotopic characterization of marginal basins with constraints to geotectonic setting and provenance. Tectonophysics, 352, 33–64.
Linnemann, U., McNaughton, N.J., Romer, R.L., Gehmlich, M., Drost, K., Tonk, C., 2004. West African provenance for Saxo-Thuringia (Bohemian Massif): did Armorica ever leave pre-Pangean Gondwana? – U/Pb-SHRIMP zircon evidence and the Nd-isotopic record. International Journal of Earth Sciences, 93, 683–705.
Linnemann, U., Gerdes, A., Drost, K., Buschmann, B., 2007. The continuum between Cadomian orogenesis and opening of the Rheic Ocean: constraints from LA-ICP-MS U-Pb zircon dating and analysis of plate-tectonic setting (Saxo-Thuringian zone, northeastern Bohemian Massif, Germany). In: Linnemann, U., Nance, D., Kraft, P., Zulauf, G. (Eds.), The evolution of the Rheic Ocean: from Avalonian–Cadomian active margin to Alleghenian–Variscan collision. Geological Society of America Special Paper, 423, 61–96.
Linnemann, U., Pereira, F., Jeffries, T.E., Drost, K., Gerdes, A., 2008a. The Cadomian orogeny and the opening of the Rheic Ocean: the diacrony of geotectonic processes constrained by LA-ICP-MS U–Pb zircon dating (Ossa-Morena and Saxo-Thuringian Zones, Iberian and Bohemian Massifs). Tectonophysics, 461, 21–43.
Linnemann, U., D´Lemos, R.S., Drost, K., Jeffries, T., Gerdes, A., Romer, R.L., Samson, S.D., Strachan, R.A., 2008b. Cadomian tectonics. In: McCann, T. (Ed.), The geology of Central Europe. Volume 1: Precambrian and Palaeozoic. Geological Society, London, 103–154.
Mašek, J., 2000. Stratigraphy of the Proterozoic of the Barrandian area. Bulletin of the Czech Geological Survey, 75, 197–204.
Mašek, J. and Zoubek, J., 1980. Proposal of stratigraphical terms for stratigraphical units of the Barrandian Proterozoic. Bulletin of the Czech Geological Survey, 55, 121 – 123.
Morávek, P. and Röhlich, P., 1971. Geology of the northern part of the Jílové zone. Journal of Geological Sciences, Geology, 20, 101–145.
Murphy, J.B., Eguiluz, L., Zulauf, G., 2002. Cadomian orogens, peri-Gondwanan correlatives and Laurentia–Baltica connections. Tectonophysics, 352, 1–9.
Murphy, J.B., Pisarevsky, S.A., Nance, R.D., Keppie, J.D., 2004. Neoproterozoic–Early Paleozoic evolution of peri-Gondwanan terranes: implications for Laurentia–Gondwana connections. International Journal of Earth Sciences, 93, 659–682.
Murphy, J.B., Gutiérrez-Alonso, G., Nance, R.D., Fernandez-Suarez, J., Keppie, J.D., Quesada, C., Strachan, R.A., Dostal, J., 2006. Origin of the Rheic Ocean: rifting along a Neoproterozoic suture? Geology, 34, 325–328.

Nance, R.D., Murphy, J.B., Strachan, R.A., D'Lemos, R.S., Taylor, G.K., 1991. Late Proterozoic tectonostratigraphic evolution of the Avalonian and Cadomian terranes. Precambrian Research, 53, 41–78.
Nance, R.D. and Murphy, J.B., 1994. Constraining basement isotopic signatures and the palinspastic restoration of peripheral orogens: example from the Neoproterozoic Avalonian–Cadomian belt. Geology, 22, 617–620.
Nance, R.D., Gutiérrez-Alonso, G., Keppie, J.D., Linnemann, U., Murphy, J.B., Quesada, C., Strachan, A., Woodcock, N.H., 2010. Evolution of the Rheic Ocean. Gondwana Research, 17, 194–222.
Ordynec, G.J., Žukova, V.I., Habásko, J., 1984. Prevariscan uranium mineralisation in the Proterozoic of the Bohemian Massif. Journal of Mineralogy and Geology, 29, 69–77.
Osozawa, S., Morimoto, J., Flowe, M. F. J., 2009. "Block-in-matrix" fabrics that lack shearing but possess composite cleavage planes: a sedimentary mélange origin for the Yuwan accretionary complex in the Ryukyu island arc, Japan. Geological Society of America Bulletin, 121, 1190–1203.
Pacltová., B., 1990. Late Proterozoic organic remains from the Mítov locality. Journal of Palynology, 91, 261–276.
Parés, J.M. and van der Pluijm, B.A., 2002. Evaluating magnetic lineations (AMS) in deformed rocks. Tectonophysics, 350, 283–298.
Pašava, J. and Amov, B., 1993. Isotopic composition of lead in Proterozoic anoxic metasedimentary and volcanogenic rocks from the Bohemian Massif (Czech Republic) with metallogenetic implications. Chemical Geology, 109, 293–304.
Patočka, F., Pruner, P., Štorch, P., 2003. Palaeomagnetism and geochemistry of Early Palaeozoic rocks of the Barrandian (Teplá–Barrandian Unit, Bohemian Massif): palaeotectonic implications. Physics and Chemistry of the Earth, 28, 735–749.
Patočka, F. and Štorch, P., 2004. Evolution of geochemistry and depositional settings of Early Palaeozoic siliciclastics of the Barrandian (Teplá–Barrandian Unit, Bohemian Massif, Czech Republic). International Journal of Earth Sciences, 93, 728–741.
Pelc, Z. and Waldhausrová, J., 1994. Geochemical characteristics of volcanics of the Barrandian Upper Proterozoic in the Chudenice–Nepomuk region (SW Bohemia). Journal of Geological Sciences, Geology, 46, 5–21.
Pin, C. and Waldhausrová, J., 2007. Sm–Nd isotope and trace element study of Late Proterozoic metabasalts ("spilites") from the Central Barrandian domain (Bohemian Massif, Czech Republic). In: Linnemann, U., Nance, D., Kraft, P., Zulauf, G. (Eds.), The evolution of the Rheic Ocean: from Avalonian–Cadomian active margin to Alleghenian–Variscan collision. Geological Society of America Special Paper, 423, pp. 231–247.
Pouba, Z., 1978. Stromatolites, geysirites or stiriolites in the Czech Proterozoic. Correlation of the Proterozoic and Paleozoic stratiform deposits, 5, 71–80.
Pouba, Z., Kříbek, B., Pudilová, M., 2000. Stromatolite-like cherts in the Barrandian Upper Proterozoic: a review. Bulletin of the Czech Geological Survey, 75, 285–296.
Rajlich, P., 1988. Tectonics of the NW border of the Central Bohemian Pluton and the Variscan transpression of the Bohemicum block structure. Journal of Geological Sciences, Geology, 43, 9–72.
Rajlich, P., Schulmann, K., Synek, J., 1988. Strain analysis of conglomerates in the Central Bohemian shear zone. Krystalinikum, 19, 119–134.
Ramsay, J. and Huber, M., 1987. The techniques of modern structural geology. Academic Press, London.
Robardet, M., 2003. The Armorica 'microplate': fact or fiction? Critical review of the concept and contradictory palaeobiogeographical data. Palaeogeography, Palaeoclimatology, Palaeoecology, 195, 125–148.
Rodič, I., 1931. Radiolaria of siliceous shales in central Bohemia. Lotos, 73, 167–172.
Röhlich, P., 1964. Submarine slides and mudflows in the youngest Algonkian of Central Bohemia. Journal of Geological Sciences, Geology, 6, 89–121.
Röhlich, P., 1965. Geologic problems of the central Bohemian Algonikan. Geologie, 14, 373–403.
Röhlich, P., 1998. The Jílové belt: a Neoproterozoic volcanic rift zone in central Bohemia. Acta Universitatis Carolinae, Geologica, 42, 489–493.
Röhlich, P., 2000. Some stratigraphic problems of the Barrandian Neoproterozoic. Bulletin of the Czech Geological Survey, 75, 201–204.
Silver, E. A. and Beutner, E., C., 1980. Melanges. Geology, 8, 32–34.
Skoček, V. and Pouba, Z., 2000. Neoproterozoic sedimentary carbonates and their silicified equivalents: Barrandian, Czech Republic. Bulletin of the Czech Geological Survey, 75, 241–260.
Sláma, J., Dunkley, D. J., Kachlík, V., Kusiak, M.A., 2008. Transition from island-arc to

passive setting on the continental margin of Gondwana: U–Pb zircon dating of Neoproterozoic metaconglomerates from the SE margin of the Teplá–Barrandian Unit, Bohemian Massif, Tectonophysics, 461, 44–59.
Štědrá, V., Kachlík, V., Kryza, R., 2002. Coronitic metagabbros of the Mariánské Lázně Complex and Teplá Crystalline Unit: interferences for the tectonometamorphic evolution of the western margin of the Teplá–Barrandian Unit, Bohemian Massif. In: Winchester, J.A., Pharaoh, T.C., Verniers, J., (Eds.), Paleozoic amalgamation of Central Europe. Geological Society, London, Special Publications, 201, 217–237.
Suchý, V., Sýkorová, I. Melka, K., Filip, J., Machovič, V., 2007. Illite "crystallinity" maturation of organic matter and microstructural development associated with lowest-grade metamorphism of Neoproterozoic sediments in the Teplá–Barrandian unit, Czech Republic. Clay Minerals, 42, 503–526.
Tait, J., Bachtadse, V., Soffel, H., 1994. New palaeomagnetic constraints on the position of central Bohemia during Early Ordovician times. Geophysical Journal International, 116, 131–140.
Tait, J., Bachtadse, V., Soffel, H., 1995. Upper Ordovician palaeogeography of the Bohemian massif: implications for Armorica. Geophysical Journal International, 122, 211–218.
Tait, J.A., Bachtadse, V., Franke, W., Soffel, H.C., 1997. Geodynamic evolution of the European Variscan fold belt: palaeomagnetic and geological constraints. Geologische Rundschau, 87, 585–598.
Timmermann, H., Štědrá, V., Gerdes, A., Noble, S.R., Parrish, R.R., Dörr, W., 2004. The problem of dating high-pressure metamorphism: a U–Pb isotope and geochemical study on eclogites and related rocks of the Marianské Lázně Complex, Czech Republic. Journal of Petrology, 45, 1311–1338.
Tomek, Č., Dvořáková, V., Vrána, S., 1997. Geological interpretation of the 9HR and 503M seismic profiles in western Bohemia. In: Vrána, S., Štědrá, V. (Eds.), Geological model of western Bohemia related to the KTB borehole in Germany. Journal of Geological Sciences, Geology, 47, 43–50.
Ujiie, K., 2002. Evolution and kinematics of an ancient décollement zone, mélange in the Shimanto accretionary complex of Okinawa Island, Ryukyu Arc. Journal of Structural Geology, 24, 937–952.
Vajner, V., 1961. Siliceous oolitic rock from the Proterozoic of the SE wing of the Barrandian at Říčany. Journal of Mineralogy and Geology, 6, 77–79.
Vavrdová, M., 2000. Microfossils in carbonaceous cherts from Barrandian Neoproterozoic (Blovice Formation, Czech Republic). Bulletin of the Czech Geological Survey, 75, 351–360.
Venera, Z., Schulmann, K., Kröner, A., 2000. Intrusion within a transtensional tectonic domain: the Čistá granodiorite (Bohemian Massif) – structure and rheological modelling. Journal of Structural Geology, 22, 1437–1454.
Vítková, P. and Kachlík, V., 2001. Petrology and geochemistry of high-Mg mafic metavolcanics sequence of the Sedlčany–Krásná Hory metamorphic "Islet", Central Bohemian Pluton, Czech Republic. Krystalinikum, 27, 7–25.
von Raumer, J.F., Stampfli, G.M., Borel, G., Bussy, F., 2002. Organization of pre-Variscan basement areas at the north-Gondwanan margin. International Journal of Earth Sciences, 91, 35–52.
Waldhausrová, J., 1984. Proterozoic volcanics and intrusive rocks of the Jílové Zone (Central Bohemia). Krystalinikum, 17, 77–97.
Waldhausrová., J., 1997. Geochemistry of volcanics (metavolcanics) in the western part of the TBU Precambrian and their original geotectonic setting. In: Vrána, S., Štědrá, V., (Eds.), Geological model of western Bohemia related to the KTB borehole in Germany. Journal of Geological Sciences, Geology, 47, 85–90.
Wendt, J. I., Kröner, A., Fiala, J., Todt, W., 1993. Evidence from zircon dating for existence of approximately 2.1 Ga old crystalline basement in southern Bohemia, Czech Republic. Geologische Rundschau, 82, 42–50.
Wortman, G.L., Samson, S.D., Hibbard, J.P., 2000. Precise U–Pb zircon constraints on the earliest magmatic history of the Carolina terrane. Journal of Geology, 108, 321–338.
Yamamoto, Y., Nidaira, M., Ohta, Y., Ogawa, Y., 2009. Formation of chaotic rock units during primary accretion processes: examples from the Miura–Boso accretionary complex, central Japan. Island Arc, 18, 496–512.
Zulauf, G., 1997. From very low-grade to eclogite-facies metamorphism: tilted crustal sections as a consequence of Cadomian and Variscan orogeny in the Teplá–Barrandian unit (Bohemian Massif). Geotektonische Forschungen, 89, 1–302.
Zulauf, G., Dörr, W., Fiala, J., Vejnar, Z., 1997. Late Cadomian crustal tilting and Cambrian transtension in the Teplá–Barrandian unit (Bohemian Massif, Central European Variscides). Geologische Rundschau, 86, 571–587.
Zulauf, G., Schritter, F., Riegler, G., Finger, F., Fiala, J., Vejnar, Z., 1999. Age constraints on the Cadomian evolution of the Teplá–Barrandian unit (Bohemian Massif) through electron microprobe dating of metamorphic monazite. Zeitschrift der Deutschen Geologischen Gesellschaft, 180, 627–639.

Žák, J., Schulmann, K., Hrouda, F., 2005. Multiple magmatic fabrics in the Sázava pluton (Bohemian Massif, Czech Republic): a result of superposition of wrench-dominated regional transpression on final emplacement. Journal of Structural Geology, 27, 805–822.
Žák, J., Dragoun, F., Verner, K., Chlupáčová, M., Holub, F.V., Kachlík, V., 2009. Forearc deformation and strain partitioning during growth of a continental magmatic arc: the northwestern margin of the Central Bohemian Plutonic Complex, Bohemian Massif. Tectonophysics, 469, 93–111.

CHAPTER 3

Jaroslava Hajná, Jiří Žák, Václav Kachlík, Wolfgang Dörr, Axel Gerdes: Neoproterozoic to early Cambrian Franciscan-type mélanges in the Teplá–Barrandian unit, Bohemian Massif: evidence of modern-style accretionary processes along the Cadomian active margin of Gondwana?

Manuscript in preparation for Precambrian Research

Neoproterozoic to early Cambrian Franciscan-type mélanges in the Teplá–Barrandian unit, Bohemian Massif: evidence of modern-style accretionary processes along the Cadomian active margin of Gondwana?

Jaroslava Hajná[1] , Jiří Žák[1], Václav Kachlík[1], Wolfgang Dörr[2], Axel Gerdes[2, 3]

[1] *Institute of Geology and Paleontology, Faculty of Science, Charles University, Albertov 6, Prague, 12843, Czech Republic*

[2] *Institute of Geosciences, Goethe University, Altenhöferallee 1, Frankfurt am Main, 60438, Germany*

[3] *Department of Earth Sciences, Stellenbosch University, Private Bag X1, Matieland 7602, South Africa*

Abstract

Mélanges have been reported from a variety of modern tectonic settings and, importantly, are a hallmark of the Franciscan-type subduction–accretion complexes. Going back in time to Precambrian, well-documented examples of mélanges become extremely scarce. This paper describes in detail such ancient, Cadomian mélanges newly recognized in the Teplá–Barrandian unit of the Bohemian Massif. The mélanges are of dual, sedimentary and tectonic origin and include voluminous olistostromal successions of graywackes interpreted to represent gravity flow deposits presumably along the trench slope. The clast compositions indicate multiple episodes of mixing of arc-derived and deepwater (?pelagic) material. Moreover, abundant bodies of (meta-)basalts, interpreted as dismembered

seamount chains, were emplaced tectonically into various structural levels of this sedimentary mélange by two different mechanisms. At the upper level, the irregular bodies of basalts were offscraped, only weakly deformed, and incorporated in the sedimentary matrix that exhibits steep cleavage indicating horizontal pure shear shortening (flattening strain). In contrast, at the lower level, disc-shaped and closely spaced basalt bodies are ductilely sheared and reworked into a flat-lying fabric suggesting horizontal ductile flow, presumably in a subduction channel during flat-slab oceanic subduction. Our new U–Pb ages also revealed an extended duration of the mélange-forming processes, starting at around 630–?650 Ma and spanning till the early Cambrian (~527 Ma). We conclude that the sedimentary–tectonic mélanges and the inferred mélange-forming process are identical to those that operate along modern active margins and, in general, reveal a great potential as excellent markers to prove the modern-style subduction in Precambrian settings.

Keywords: *Accretionary wedge; Cadomian orogeny; Bohemian Massif; Mélange; Ophiolite; Teplá–Barrandian unit*

1. Introduction

Mélanges are mapable bodies with the along-strike dimension varying from tens of meters to hundred of kilometers that consist of compositionally diverse inclusions chaotically mixed in a significantly finer grained siliciclastic or serpentinite matrix (block-in-matrix fabric; e.g., Hsü, 1968; Silver and Beutner, 1980; Raymond, 1984; Cowan, 1985; Wakabayashi and Medley, 2004; Osozawa et al., 2009; Festa et al., 2010a; Wakabayashi, 2011). The composition and metamorphic grade of the mixed inclusions may vary considerably from the very-low-grade, prehnite-pumpellyite through blueschist to eclogite

facies or even mantle-derived rocks. The extensive stratal disruption to even entirely chaotic nature of mélanges implies that they are specific tectonic objects that do not obey common stratigraphic principles such as superposition and lateral continuity (Hsü, 1968). Although mélanges occur in a variety of tectonic settings, they are most typically an important lithotectonic element of accretionary wedges above subduction zones. The most remarkable and extensively studied examples include Mesozoic to Cenozoic mélanges in the circum-Pacific realm, such as the Franciscan complex, California (e.g., Hsü, 1968; Cowan, 1974; Kleist, 1974; Cowan and Gucwa, 1975; Page, 1975; Platt, 1975; Fox, 1976; Platt et al., 1976; Aalto, 1981; Tarduno et al., 1985; Wakabayashi, 1999; Wakabayashi, 2008; Wakabayashi, 2011), the Shimanto belt, Japan (Ueda et al., 2000; Ujiie et al., 2000; Ujiie, 2002; Osozawa et al., 2009; Yamamoto et al., 2009), Tararua Range and the Balloon mélange, New Zealand (Orr et al., 1991; Jongens et al., 2003), Chilean forearc in the Andean region (Wilson et al., 1989, Glodny et al., 2005), or in the Alpine–Himalayan belt (Burg et al., 2008; Festa et al., 2010b, Festa, 2011; Perroti et al., 2011). In contrast, earlier, Precambrian mélange systems which would corroborate the operation of modern plate tectonic processes have been only rarely documented and examined in detail. The Precambrian examples include Mesoproterozoic to Neoproterozoic ophilitic mélanges of the Arabian–Nubian shield (Shackleton et al., 1980; Al-Shanti and Gass, 1983), blueschist-bearing mélanges of the Bou Azzer inlier, Anti-Atlas Mountains, Morocco (Hefferan et al., 2002), and tectonic mélange in the Schreiber–Hemlo greenstone belt of the Superior province, Canada (Polat and Kerrich, 1999).

As the composition, geometry, and internal structure vary greatly among the known examples of supra-subduction zone mélanges, the same applies for the inferred mélange-forming processes. In the supra-subduction zone settings, mélanges have been interpreted

as a result of: (1) gravitational sliding and disruption of the semi-consolidated sediment to produce olistostromes (e.g., Hsü and Schlanger, 1971; Page and Suppe, 1981; Cowan, 1985; Marroni and Pandolfi, 2001; Festa et al., 2010a), (2) mud or serpentinite diapirism governed by lateral and vertical density contrasts (Orange, 1990), (3) tectonic mixing due to variable material displacement paths within accretionary wedges (Cloos, 1982; Wakabayashi, 2011), and (4) deformation and movement along broad tabular fault or shear zones that commonly cut across accretionary wedges (Wakabayashi, 2011).

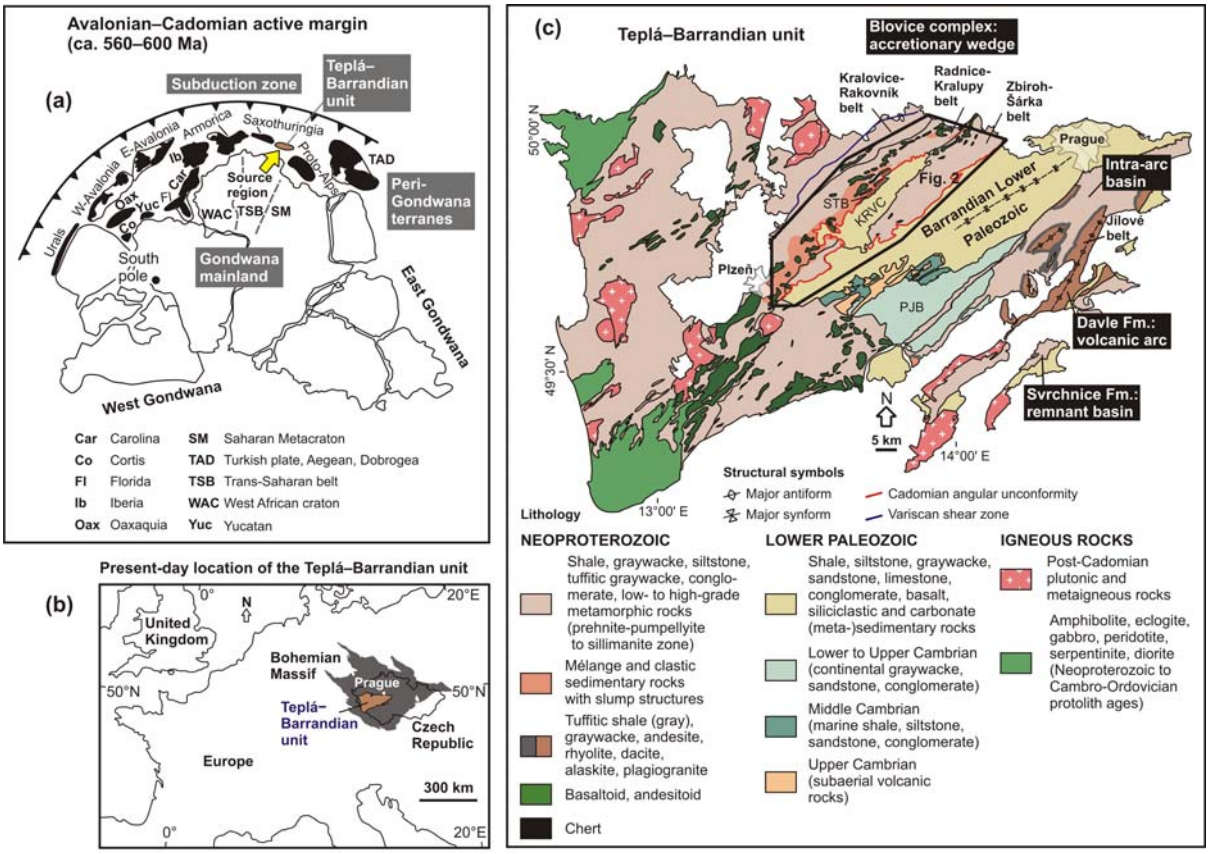

Fig. III.1. (a) Inferred paleogeographic position of the Teplá–Barrandian unit within the Avalonian–Cadomian belt on the northern active margin of Gondwana during the late Neoproterozoic (after Linnemann et al., 2004). (b) The present-day position of the TBU in the central Bohemian Massif. (c) Simplified geologic map of the Teplá–Barrandian unit (TBU). This map was redrafted from geologic map of the Czech Republic, at a scale of 1:500,000, published by the Czech Geological Survey in 2007.

This paper supplements the yet scarce information on Precambrian mélanges with a detailed study of sedimentary and tectonic mélanges newly recognized in the Cadomian

basement of the Teplá–Barrandian unit, Bohemian Massif (Fig. III.1). These mélanges define a distinct lithotectonic belt which consists of abundant slivers of ocean floor and lenses of chert and limestone mixed with olistostromal shale to graywacke matrix (the Radnice–Kralupy belt, RKB in Fig. III.2) and which resembles in many aspects the `classic' Fransciscan Complex of California and Oregon. After a brief introduction into the geologic background and basic petrography of the mélange rocks, we describe five areas representing an upper to lower structural levels of the mélange belt. We also summarize the existing geochronologic information from this belt and present new U–Pb zircon ages that surprisingly indicate an extended time span of the mélange formation lasting from the late Neoproterozoic till the early Cambrian. Finally, we use this Barrandian case example as a basis for discussion of mélange formation and accretionary processes in an ancient, Precambrian to early Cambrian active margin setting in comparison with modern suprasubduction zone environments.

2. Geologic setting

The supracrustal Teplá–Barrandian unit (TBU) in the center of the Bohemian Massif (Fig. III.1b and c) is one of the best preserved components of the Avalonian–Cadomian belt which developed along the northern active margin of Gondwana during the late Neoproterozoic to the earliest Cambrian (Nance et al., 1991; Nance et al., 2010) and references therein; Fig. III.1a). The basement of the TBU is unique in that it exposes almost a complete section across the Cadomian active margin from a remnant ophiolite complex to the NW, through an accretionary wedge, to a volcanic arc and intra-arc and back arc basins to the SE (Fig. III.1c; present-day coordinates are used throughout this paper). The accretionary wedge, referred to as the Blovice complex by (Hajná et al., 2011), underlies the largest portion of this unit (Fig. III.1c). In a broad zone between a Variscan shear zone to the NW and Barrandian Lower Paleozoic overlap successions to the SE (Fig. III.1c), the wedge has

been only weakly or even at all affected by the pervasive Variscan deformation and metamorphism (Hajná et al., in press), thus superbly preserving the original Cadomian lithologies and structures. This north-central part of the accretionary wedge consists here of three fault-bounded NE–SW-trending lithotectonic belts (Fig. III.2) that differ in lithology, internal structure, magnetic fabric, and perhaps also in grade of the Cadomian regional metamorphism (see Hajná et al., 2010 for details). From northwest to southeast, these belts are:

(1) The Kralovice–Rakovník belt (KRB in Fig. III.2) is characterized by very low-grade monotonous succesion of graywackes rhytmically alternating with minor slates and siltstones deposited as deep-water turbidites and gravity flows (Cháb and Pelc, 1968). This belt is devoid of volcanic rocks except for only a few NE–SW-trending km-scale elongated bodies of alkali basalt and trachybasalt to trachyandesite (Fig. III.2). Well-preserved shallowly-dipping bedding, synsedimentary textures, and general lack of pervasive deformation suggest that the Kralovice–Rakovník belt is the least deformed and presumably structurally the uppermost unit in the accretionary wedge.

(2) In contrast, the central Radnice–Kralupy belt (RKB in Fig. III.2), which hosts the mélanges dealt with in this paper, is lithologically the most diverse and structurally the most complex unit of the entire Teplá–Barrandian Neoproterozoic. The belt consists predominantly of strongly deformed graywackes with minor breccias and conglomerates, shales to slates, and siltstones commonly displaying chaotic (micro-)textures and synsedimentary slump structures (Cháb and Pelc, 1968). The clast compositions indicate mixing of intrabasinal and island arc sources of the clastic material (Jakeš et al., 1979; Lang, 2000; Drost et al., 2004; Drost, 2008; Drost et al., 2011). This belt is characterized by a block-in-matrix fabric as it contains numerous structurally isolated blocks of massive graywackes,

limestones, and cherts embedded in argillaceous matrix (Cháb and Pelc, 1968; Mašek, 2000), and abundant up to km-scale lens-shaped to irregular bodies of ocean-floor, variously altered (meta-)basalts (Fig. III.2). The basalt bodies show diverse compositions ranging from tholeiitic (N-MORB-like), interpreted as being derived from a primitive mantle source in a suprasubduction zone setting, through moderately LREE-enriched basalts with significant crustal contamination to LREE-enriched alkali basalts (Pin and Waldhausrová, 2007). The basalts are in places closely spatially associated or even interlayered with silicified shales, cherts, and metal-rich black shales (Pašava and Amov, 1993; Pašava et al., 1996).

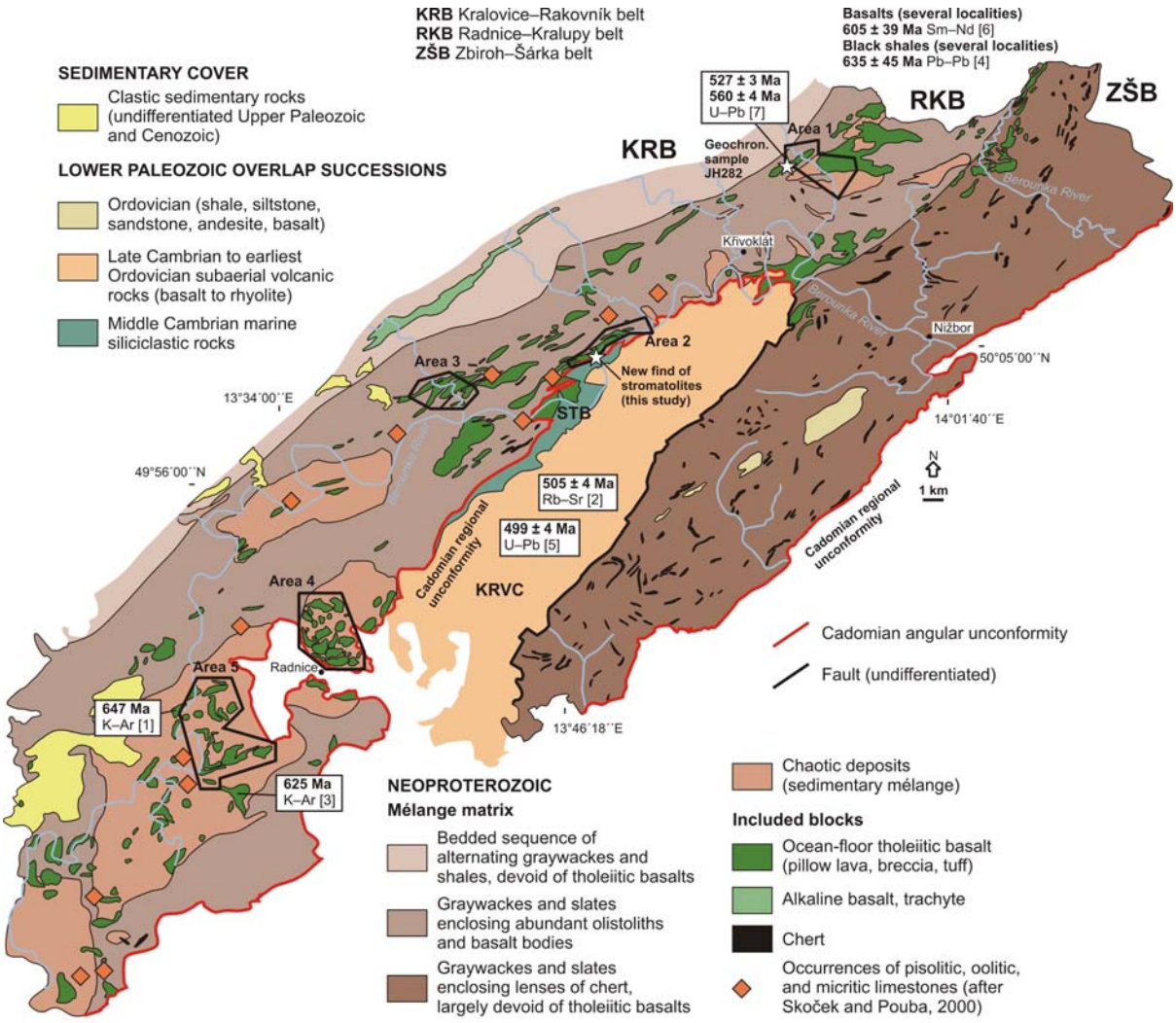

Fig. III.2. Simplified geologic map of the study area with geochronologic data from its Neoproterozoic basement and localities of limestones. Geology compiled from Geologic map of the Křivoklát area 1:50,000

published by the Czech Geological Survey in 1997, and geologic map of the Czech Republic 1:50,000, sheets Zdice, Kladno, Beroun, Plasy, Plzeň, Hořovice. Source of geochronologic data: (1) Šmejkal (1964); (2) Dornsiepen (1979); (3) Dubanský et al. (1984); (4) Pašava and Amov (1993); (5) Drost et al. (2004); (6) Pin and Waldhausrová 2007; (7) this study.

(3) The southeasterly Zbiroh–Šárka belt (ZŠB in Fig. III.2) is lithologically uniform but strongly deformed, dominated by slates, siltstones, and graywackes interpreted as distal turbidites sourced from a volcanic arc and deposited in a deepwater environment (Cháb and Pelc, 1968). The siltstone–slate–graywacke matrix encloses numerous structurally isolated meter- to hundreds of meters-long lenses of chert and, in contrast to the other belts, volcanic rocks are entirely absent. The cherts are typically extensively fractured, veined, and in some cases foliated. The chert/host contacts are rarely exposed, but we found several outcrops where the cherts form isolated meter-sized blocks embedded in the strongly deformed slate matrix. In all observed cases, the chert–slate contacts were knife-sharp and the nearby slate showed no evidence of percolation of siliceous hydrothermal fluids.

3. Petrography and microstructures of the mélange rocks

Going down to the hand sample- to micro-scale, we describe below some important petrographic and primary microstructural features of the matrix sedimentary rocks and of the basalt inclusions (Figs. III.3 and III.4). The rocks under study have been heterogeneously deformed along the Radnice–Kralupy belt and have also been affected by the Cadomian regional metamorphism ranging from very low (anchimetamorphic; (Suchý et al., 2007) through the prehnite–pumpellyite to the lower greenschist facies conditions (Cháb and Pelc, 1968; Cháb and Bernardová, 1974). The preservation of their primary features thus largely depends on their strain history and degree of regional metamorphic overprint.

3.1. Siliciclastic mélange matrix

Three main types of breccias and conglomerates can be distinguished on the basis of clast

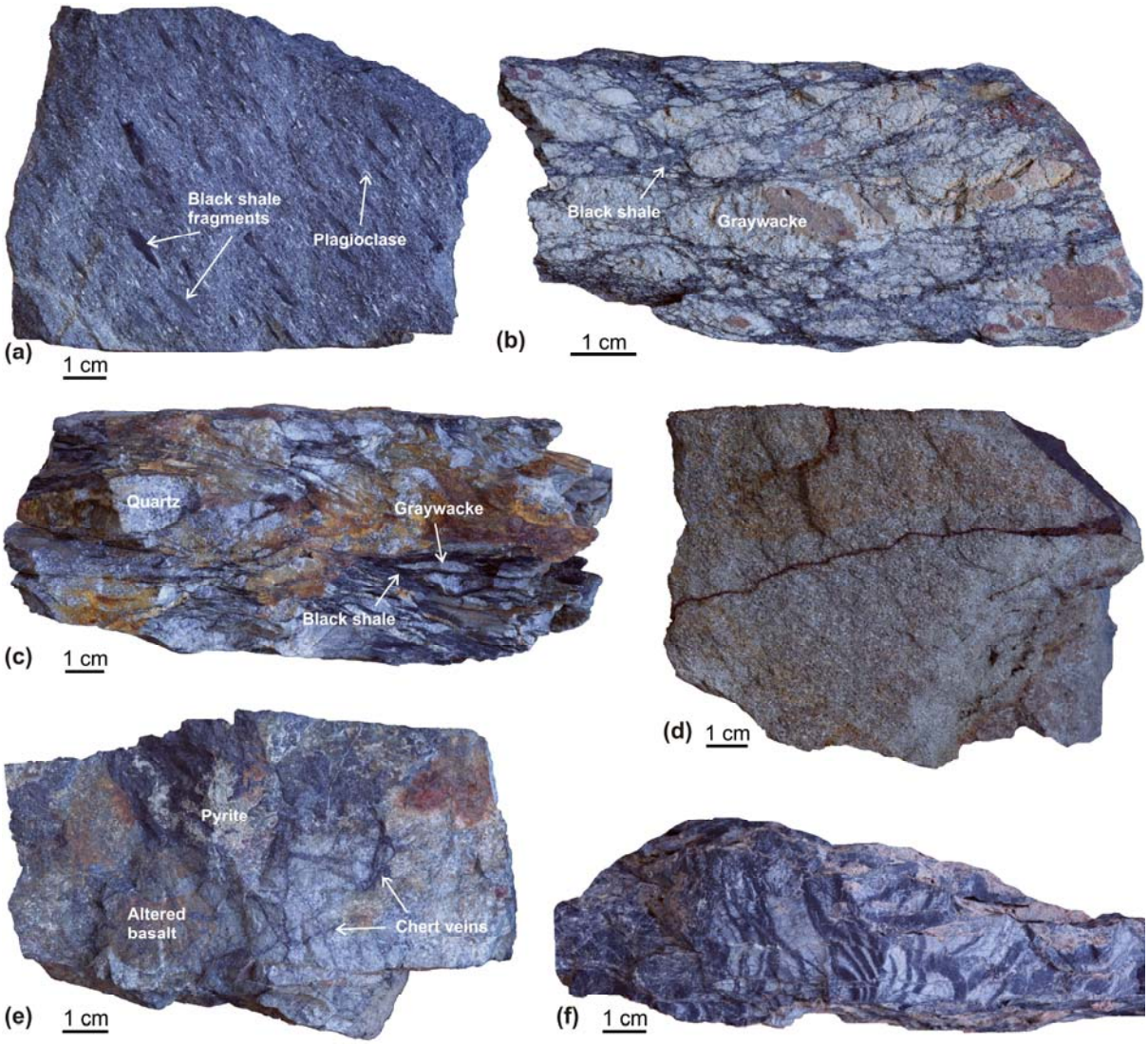

Fig. III.3. Hand samples of main lithological types of the Radnice–Kralupy mélange belt. (a) Graywacke matrix-supported breccia with black shale fragments. Area 1, Klíčava creek, [WGS84 coordinates: N50° 6'18.41", E13°53'9.49"]. (b) Black shale matrix-supported conglomerate with graywacke clasts. Area 4, Near Kamenec, [WGS84 coordinates: N49°52'45.96", E13°36'33.41"]. (c) Black shale matrix-supported conglomerate with quartz and graywacke clasts. Area 5, right bank of the Berounka River, near Nynice, [WGS84 coordinates: N49°50'45.40, E13°31'30.74"] (d) Massive graywacke. Area 1, Klíčava creek, [WGS84 coordinates: N50° 6'18.41", E13°53'9.49"]. (e) Hydrothermal breccia with altered basalt matrix. Area 1, section along Klíčava dam, [WGS84 coordinates: N50° 4'31.38", E13°56'24.56"]. (f) Stromatolite bearing chert. Area 2, left bank of the Berounka River, near Týřovice, [WGS84 coordinates: N49°59'34.24", E13°47'6.02"].

and matrix composition: (1) Most common are matrix-supported breccias that contain angular to subangular black shale fragments, typically 0.5–3 cm in size, set in coarse grained graywacke matrix (Figs. III.3a and III.4a). The black shales in these breccias commonly exhibit cleavage planes truncated along the clast margins and discordant to cleavage in the graywacke matrix. (2) Another type of conglomerates consists of larger, up to 5–6 cm in size,

rounded graywacke fragments set in very fine grained black shale matrix (Figs. III.3b and III.4b). (3) Only in a few places, we found strongly deformed, matrix-supported conglomerates that contain rounded clasts, up to 3–5 cm in size, of arc-related plutonic rocks (mostly trondhjemites) and vein quartz (Fig. III.3c). Under the microscope, the graywacke to siltstone matrix in all types also contains smaller (up to 0.2 mm in size) irregular clasts of acid volcanic rocks, cherts, graywackes, and shales mixed with grains of quartz, plagioclase, and mica (Figs. III.3a and III.4a).

Finer grained siliciclastic rocks of the Radnice–Kralupy belt are dominated by massive to poorly bedded graywackes (Fig. III.3d). The graywackes show clast compositions comparable to breccias and conglomerates, with the clast size varying from 150 μm to 2.5 mm, and commonly exhibit chaotic texture. A detailed account on the graywacke petrography and geochemistry is given in Cháb and Pelc (1968, 1973), Jakeš et al. (1979), and Lang (2000). Shales are composed of fine-grained silty matrix with clasts of up to 0.05 mm in size and of the same composition as those in graywackes (Fig. III.4d). Relic fine-scale lamination may commonly be preserved. Black shales can be described as mudstone with intercalations of silty or even sandy material, commonly exhibiting a fine-scale lamination defined by dark, pyrite-rich laminae alternating lighter laminae rich in volcanogenic detritus (Fig. III.4c).

3.2. Included basalt blocks

The basalts mapped in this study include two main textural types: (1) Macroscopically aphanitic (massive) basalt which shows ophitic texture under the microscope, defined by plagioclase laths set in pyroxene or glassy matrix (Fig. III.4e). This type also contains well developed spherolites. The glassy matrix is commonly altered into a mixture of carbonatized and sericitized plagioclase. (2) Hydrothermal breccias with the matrix composed of laths and

spherolites of sericitized plagioclase set in the strongly altered glass (Figs. III.3e and III.4f).

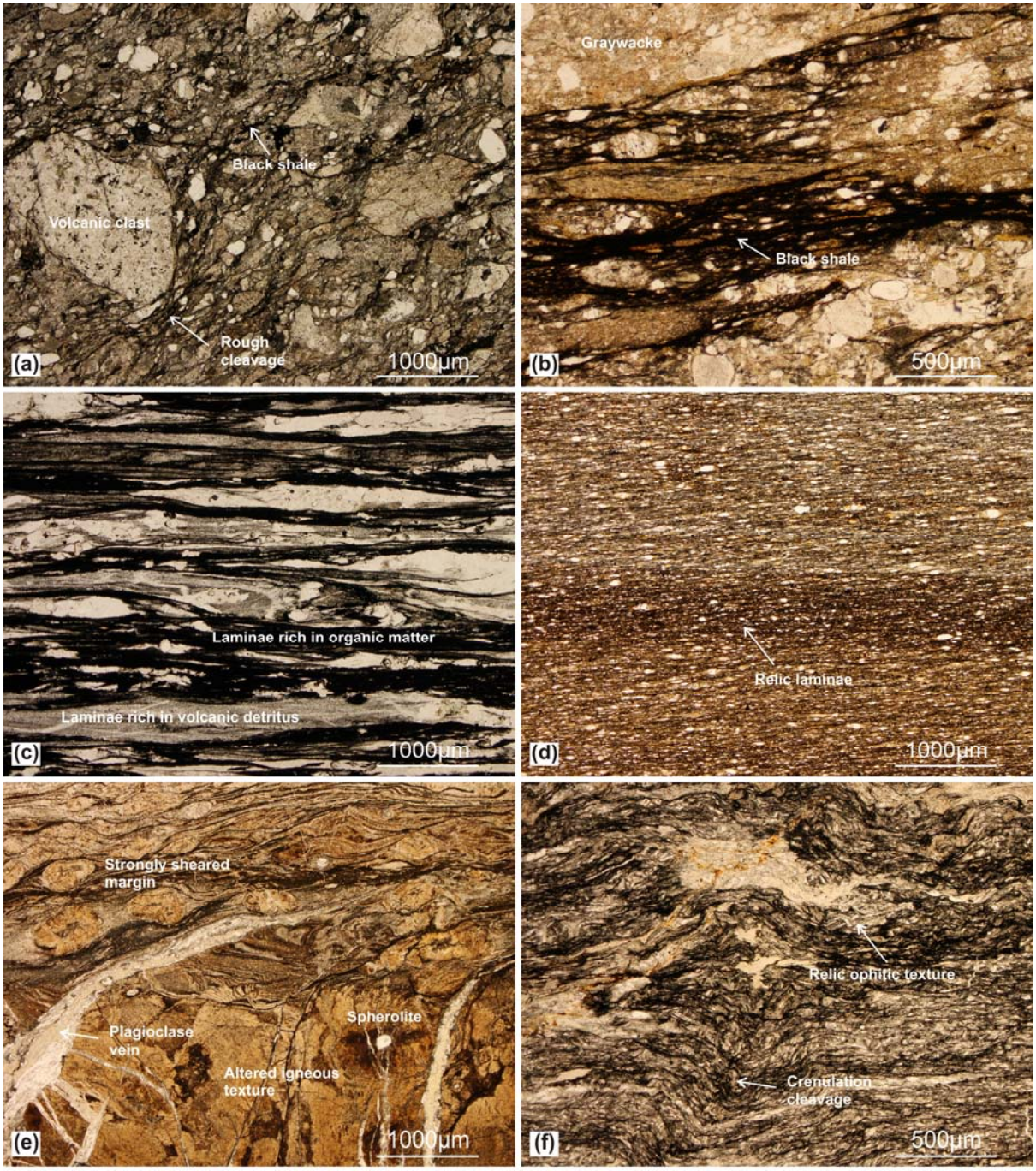

Fig. III.4. Microphotographs showing main structures and mineral assemblages of rocks in the Radnice–Kralupy mélange belt. (a) Rough cleavage domains developed around angular clasts of acid volcanic clasts and black shale fragments in graywacke matrix-supported breccia. Area 1, Klíčava creek, [WGS84 coordinates: N50° 6'18.41", E13°53'9.49"]. (b) Disjunctive cleavage developed in the black shale matrix wrapping around graywacke clasts in black shale matrix-supported breccia. Area 4, near Kamenec, [WGS84 coordinates: N49°52'45.96", E13°36'33.41"]. (c) Black shale costinting of alternating laminae rich in organic matter and laminae rich in volcanic detritus. Area 5, near Sedlecko, [WGS84 coordinates: N49°48'37.96", E13°31'49.03"]. (d) Relics of lamination in fine-grained siltstone. Area 4, near Mostiště, [WGS84 coordinates: N49°52'28.34", E13°37'28.24"]. (e) Spherolitic basalt with preserved igneous texture and strongly deformed margin. Area 4,

near Hlohovice, [WGS84 coordinates: N49°53'4.82", E13°36'55.66"]. (f) Altered basalt with relics of ophitic texture and well developed crenulation cleavage. Area 5, near Sedlecko, [WGS84 coordinates: N49°48'37.96", E13°31'49.03"].

4. New U–Pb geochronology of the mélange rocks

4.1. Overview of the existing gechronology and sample description

The lack of suitable lithologies in all the three belts causes that the existing radiometric ages are extremely scarce or are weighed down by large errors. The ages include a K–Ar ages of 647 Ma and 625 Ma (errors not given) and a Sm–Nd age of 605 ± 39 Ma for basalts (Fig. III.2; Šmejkal, 1964; Dubanský et al., 1984; Pin and Waldhausrová, 2007, respectively) and a Pb–Pb age of 635 ± 45 Ma for the black shales (Fig. III.2; Pašava and Amov, 1993). Consequently, any new geochronologic information to better constrain the age of the Blovice complex and the minimum age of the involved mélanges is desirable. In search for some more reliable radiometric ages, we sampled seven localities of zirconium-rich (meta-)basalts or volcanogenic graywackes in various parts of the complex; only one sample yielded sufficient amount of zircons. This sample JH282 is a volcanogenic graywacke (Fig. III.5) from the locality Požáry near Křivoklát (WGS84 coordinates are E13°53.878´; N50°04.350´), previously mapped as a metabasalt of the northern part of the Radnice–Kralupy belt. The graywacke is composed of angular quartz and albitized plagioclase clasts (up to 300 µm in size) and abundant clasts of felsic volcanic rocks, chert, and black shales (up to 1 mm in size; Fig. III.5). The clasts are set in a fine grained sandy matrix (grain size varies from 45 to 130 µm) which is a mixture of quartz, plagioclase, chert, and tuffitic material (Fig. III.5). Zircon and some opaque minerals are present as an accessory phase. On the basis of clast composition and microstructure, the sample is undistinguishable from other graywackes widespread in the Radnice–Kralupy belt. About thirty kilograms of this rock was

crushed, sieved (<400 µm), and further processed on a wet shaking table to concentrate the heavy minerals.

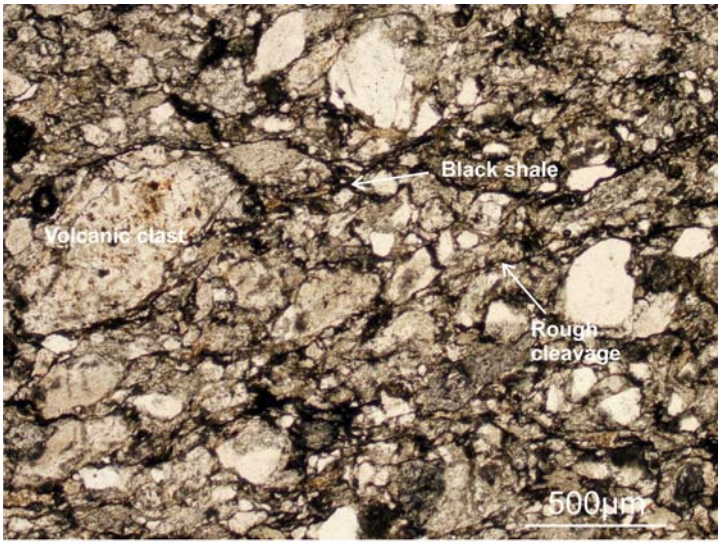

Fig. III.5. Microphotograph of volcanogenic graywacke sample used for gochronologic dating. Poorly developed rough cleavage domains wrap aroung volcanic clasts and black shale fragments. Area 1, near Požáry, [WGS84 coordinates: N50° 4'21.04", E13°53'52.66"].

4.2. Analytical methods

Uranium, thorium, and lead isotope analyses were carried out by laser ablation – inductively coupled plasma–mass spectrometry (LA–ICP–MS) at the Goethe University, Frankfurt am Main, Germany, using a method described in Gerdes and Zeh (2006, 2009). The analyses were performed with a ThermoScientific Element 2 sector field ICP-MS coupled to a Resolution M-50 (Resonetics) 193 nm ArF excimer laser (CompexPro 110, Coherent) system. Data were acquired in time resolved – peak jumping – pulse counting / analogue mode over 480 mass scans, with a 20 second background measurement followed by 21 second sample ablation. The laser spot sizes were 23 µm in diameter. Sample surface was cleaned directly before each analysis by three pulses pre-ablation. Ablation was performed in a 0.6 L min^{-1} He stream, which was mixed directly after the ablation cell with 0.07 L min^{-1} N and 0.68 L min^{-1} Ar prior introduction into the Ar plasma of the SF-ICPMS. The gases all had a purity of 99.999 % and no homogenizer was used for mixing the gases to prevent smoothing of the

signal. The signal was tuned for maximum sensitivity for Pb and U while keeping oxide production, monitored as $^{254}UO/^{238}U$, below 0.3 %. The sensitivity achieved was in the range of 8000–12000 cps/µg g^{-1} for ^{238}U with a 23 µm spot size, at 5.5 Hz and 5–6 J cm^{-2}. The typical penetration depth was about 14–20 µm. The two-volume ablation cell (Laurin Technic, Australia) of the M50 enables detection and sequential sampling of heterogeneous grains (e.g., growth zones) during time resolved data acquisition, due to its quick response time of <1s (time until maximum signal strength was achieved) and wash-out (< 99 % of previous signal) time of <3s. With a depth penetration of ~0.6 µm s^{-1} and a 0.46 s integration time (4 mass scans = 0.46 s = 1 integration) any significant variation of the Pb/Pb and U/Pb in the µm scale is detectable.

Raw data were corrected offline for background signal, common Pb, laser induced elemental fractionation, instrumental mass discrimination, and time-dependent elemental fractionation of Pb/U using an in-house MS Excel spreadsheet program (Gerdes and Zeh, 2006, 2009). A common-Pb correction based on the interference- and background-corrected ^{204}Pb signal and a model Pb composition (Stacey and Kramers, 1975) was carried out. The ^{204}Pb content for each ratio was determined in three different ways. First it was estimated by subtracting the average mass 204 signal, obtained during the 20 second baseline acquisition, which mostly results from ^{204}Hg in the carrier gas (ca. 2000 cps), from the mass 204 signal of the respective ratio. Due to the high Hg background this method results in rather high detection limits for the ^{204}Pb. Therefore, in case of Th/U < 0.3 the ^{208}Pb signal was used to determine the ^{204}Pb content by subtracting the radiogenic ^{208}Pb calculated from the Th signal and the $^{206}Pb/^{238}U$ age. For analyses with high Th/U (> 3) or with $^{206}Pb/^{238}U$ < 0.02 and Th/U > 0.3 the ^{204}Pb content is estimated from the non radiogenic ^{207}Pb calculated from the $^{206}Pb/^{238}U$ (or $^{208}Pb/^{232}Th$) age and the ^{206}Pb signal assuming a concordant analysis.

Reported uncertainties (2σ) of the $^{206}Pb/^{238}U$ ratio were propagated by quadratic addition of the external reproducibility (2 SD) obtained from the standard zircon GJ-1 (n = 16–20; 2 SD ~1.2%) during the analytical session and the within-run precision of each analysis (2 SE; standard error). In case of the $^{207}Pb/^{206}Pb$ we used a ^{207}Pb signal dependent uncertainty propagation (see Gerdes and Zeh, 2009). The $^{207}Pb/^{235}U$ ratio is derived from the normalized and error propagated $^{207}Pb/^{206}Pb$ and $^{206}Pb/^{238}U$ ratios assuming a $^{238}U/^{235}U$ natural abundance ratio of 137.88 and the uncertainty derived by quadratic addition of the propagated uncertainties of both ratios. The quality and accuracy of the method was verified by analyses of the reference zircon Plešovice which yielded concordia ages of 337.2 ± 1.9 Ma (n = 8), in perfect agreement with the published value of Sláma et al. (2008a). Concordia diagrams (2σ error ellipses), concordia ages and upper intercept ages (95% confidence level) were calculated using the Isoplot/Ex 2.49 software (Ludwig, 2011).

4.3. Results

Seventy two detrital zircon grains were analyzed in total. Eight zircons (0.11 % of the analyzed population) yielded discordant $^{207}Pb–^{206}Pb$ ages ranging from Paleoproterozoic (2013 ± 20 Ma) to late Neoproterozoic (578 ± 64 Ma; Fig. III.6). The $^{206}Pb–^{238}U$ ages from the remaining 64 zircons were concordant and show two pronounced peaks on the frequency histogram, corresponding to late Neoproterozoic (Ediacaran) and early Cambrian (Terreneuvian, Fortunian to stage 2) ages. The calculated concordia ages are 560 ± 4 Ma and 527 ± 3, respectively (Fig. III.6). At variance with the well-established field relations (note that the Kralupy–Radnice belt is unconformably overlain by paleontologically constrained mid-Cambrian shales), three zircons (0.04 % of the analyzed population) yielded a concordia age of 508 ± 7 Ma (middle Cambrian, Series 3, stage 5). It is thus not clear whether these three youngest zircons mark the minimum age of deposition (unlikely) or whether the

respective $^{206}Pb/^{238}U$ ages were affected by some Pb loss.

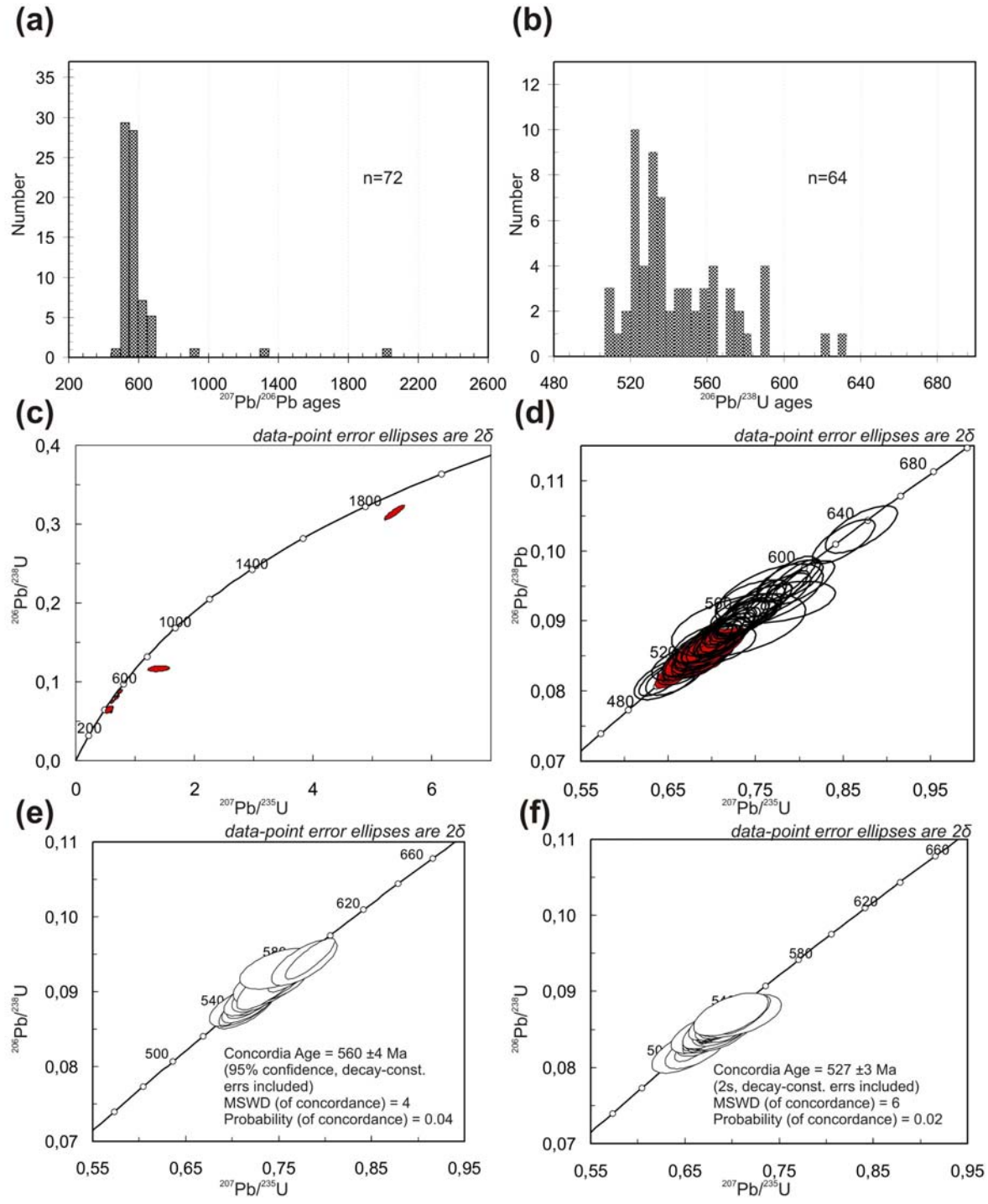

Fig. III.6. Graphs summarizing our geochronologic data from sample JH282. (a) Number of detrital zircon grains analyzed in total and their $^{207}Pb/^{206}Pb$ ratios. (b) Number of concordant detrital zircon grains and their $^{207}Pb/^{206}Pb$ ratios. (c) Diagram of discordant zircon grains. (d) Diagram of all concordant zircon grains. (e) Concordia diagram for zircons of Ediacaran age. (f) Concordia diagram for zircons of Cambrian age.

5. Structure of the Radnice–Kralupy ophiolitic mélange belt

Five separate areas were newly mapped along about 45 km of the Radnice–Kralupy belt at the scale of 1:10,000 (Figs. III.7 and III.8; see Fig. III.2 for location of the areas). This detailed mapping revealed that the lithologic features, shape, size, spatial distribution and contact relations of basalt bodies, fabric orientation and symmetry, and structural style vary significantly along strike of the belt. Below, we describe these variations from northeast to southwest.

5.1. Northeastern portion of the belt (areas 1–2)

The northeastern Radnice–Kralupy belt is characterized by the presence of only a few scattered larger basalt bodies that are typically highly irregular and up to several kilometers across in the map (area 1; Fig. III.7a). An order-of-magnitude smaller, typically tens of meters to several hundreds of meters in length, basalt bodies are elliptical in the map and elongated NE–SW (Fig. III.7a). The basalts have well-preserved magmatic texture and include massive, pillowed, variolitic, and flow-brecciated autoclastic lavas. In some places, the basalts are net-veined by mm-thick veinlets of chert to form fine-scale hydrothermal breccias with disseminated massive sulfides (Fig. III.3e). The basalts are chiefly non-foliated with the exception of weak disjunctive cleavage, defined by chlorite and actinolite fibers, that is only locally developed in the matrix and wraps around the pillows. This observation is consistent with the individual pillows being commonly spherical to weakly ellipsoidal with large aspect ratios suggesting none or only minor ductile deformation of the basalts. Instead, the basalts are commonly cut by a dense network of mesoscale faults, non-systematic joints, or calcite veins.

In contrast, the host sedimentary rocks are heterogeneously deformed depending on the original proportion of graywacke and shale in the succession prior to deformation. The

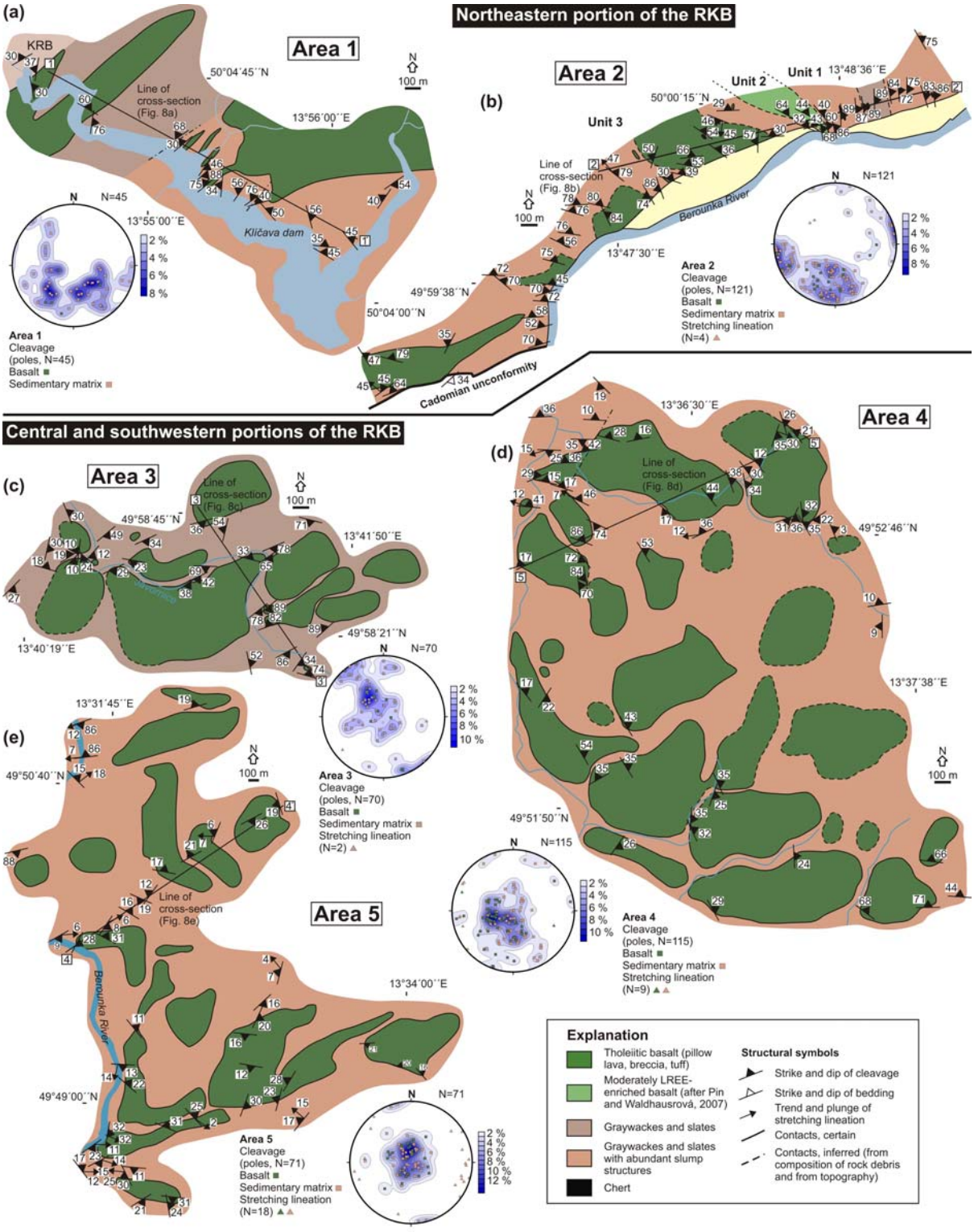

Fig. III.7. Structural maps of areas 1–5 in the Radnice–Kralupy mélange belt (RKB) and stereonets (equal area projection, lower hemisphere) summarizing orientation of cleavage planes and lineations. Geology in area 1 and 5 modified after geologic map of the Křivoklát area 1:50,000 published by the Czech Geological Survey in 1997 and geologic map of the Czech Republic 1:50,000, sheets Plasy, Plzeň, geology in area 2–4 based on new mapping by Hajná and Žák (this study).

graywacke-dominated successions commonly preserve continuous bedding on the

outcrop-scale with the shale interbeds being strongly cleaved (Fig. III.9a) whereas the monotonous shale-dominated successions exhibit a pervasive, slaty cleavage. The shales may also enclose meter-scale isolated blocks of chert or graywacke (Fig. III.9b). The cleavage orientation varies greatly but tends to dip moderately to the NW or NE (Figs. III.7a and III.8a). The fabric ellipsoid is oblate as macroscopic lineation is not developed on cleavage planes.

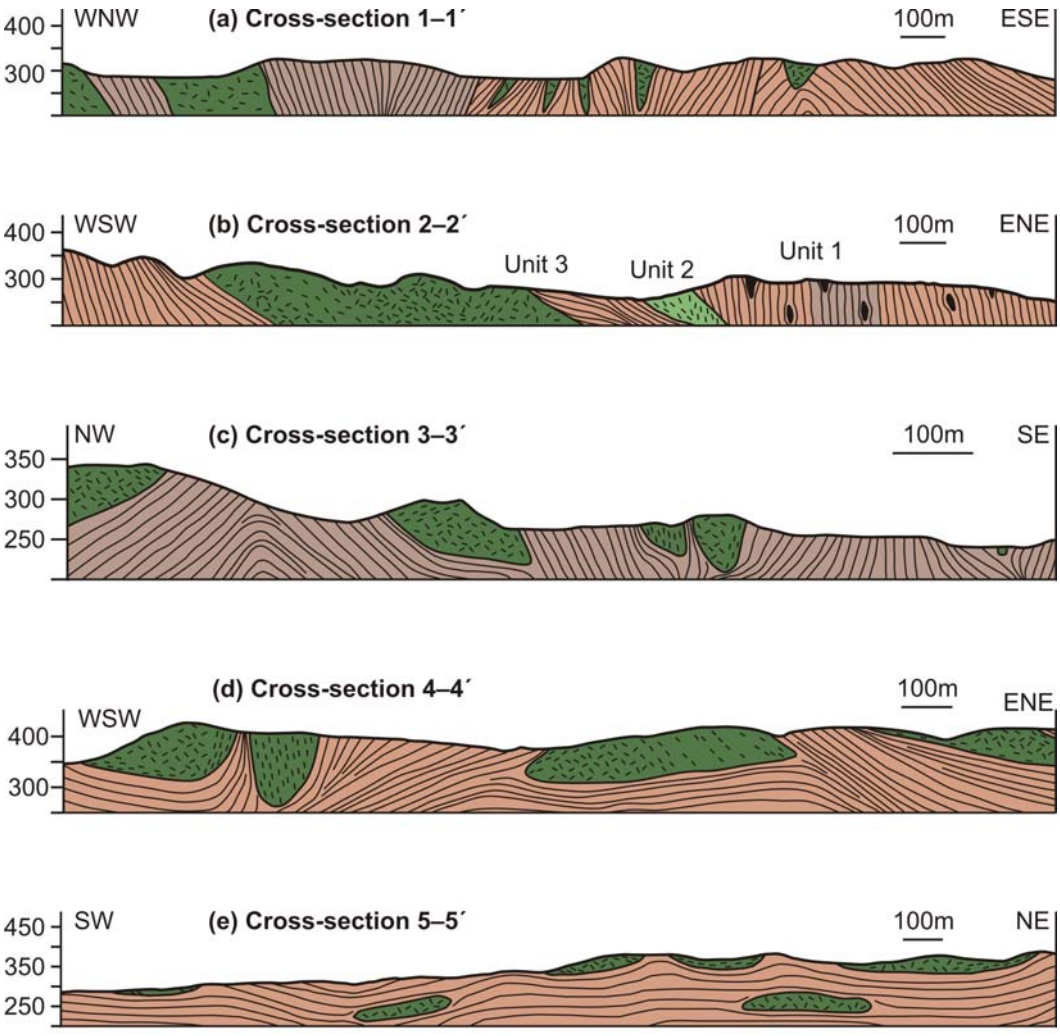

Fig. III.8. Schematic cross-sections of areas 1–5. See Fig. III.7 for location.

We also found several exposures of the basalt/slate contacts. In all cases the contacts

are narrow, dm-thick brittle faults that are discordant to and sharply truncate the slaty cleavage (Fig. III.9c). In other cases, although the contacts are not exposed, the slates in the immediate vicinity of even km-sized basalt bodies show no sign of contact-metamorphic heating.

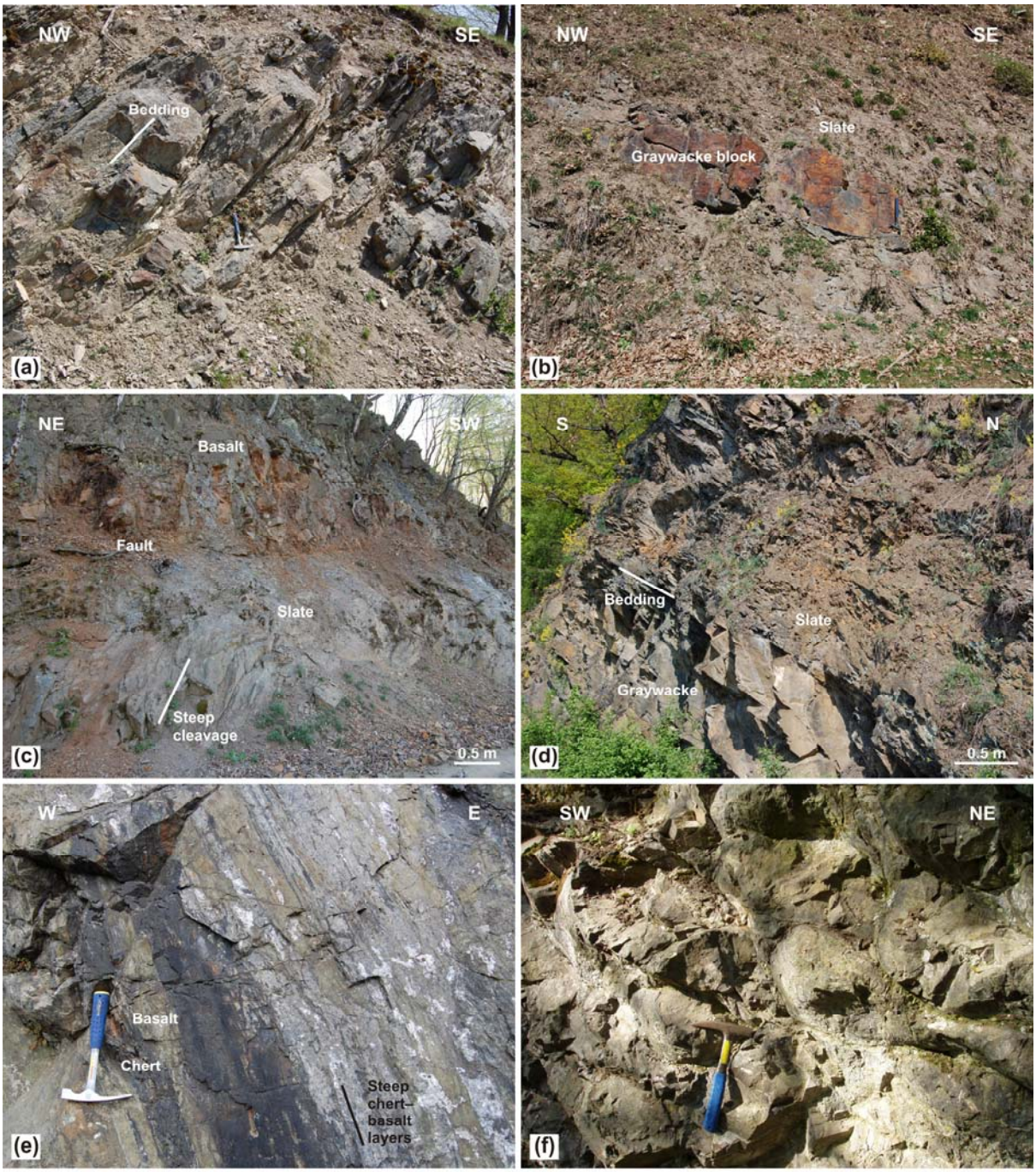

Fig. III.9. Characteristic lithologic and structural features of the Neoproterozoic rocks in the northeastern portion of the Radnice–Kralupy mélange belt. (a) Graywacke dominated successions with well preserved

bedding parallel with cleavage developed in thin slate interbeds. Area 1, section along Klíčava dam, [WGS84 coordinates: N50° 4'36.26", E13°54'49.11"]. Hammer for scale. (b) Graywacke blocks (interpreted as olistoliths) in the slate matrix. Area 1, section along Klíčava dam. [WGS84 coordinates: N50° 4'12.48", E13°56'7.82"]. Hammer for scale. (c) Faulted contact between slate and basalt. The fault truncates cleavage in slate. Area 1, section along Klíčava dam. [WGS84 coordinates: N50° 4'43.67", E13°54'25.27"]. (d) Bedded sequence of alternating graywackes and slates. Unit 1 in Area 2, Nezabudické skály, near Nezabudice. [WGS84 coordinates: N50° 1'19.19", E13°50'3.86"]. (e) Strongly altered and deformed basalt intercalated by dark chert. Unit 2 in Area 2, Kněžská skála, near Nezabudice. [WGS84 coordinates: N50° 0'7.98", E13°48'33.68"]. Hammer for scale. (f) Weakly deformed pillow basalt. Unit 3 in Area 2, Čertova skála, near Hracholusky. [WGS84 coordinates: N49°59'49.17", E13°47'28.92"]. Hammer for scale.

This structural pattern changes and becomes more complex some 10 km farther to the southwest along the belt (area 2; Figs. III.7b and III.8b). Here, we mapped a 2 km long continuous section along the Berounka River (Fig. III.7b) which exposes a package of three distinct units from northeast to southwest:

(1) A structurally upper succession of graywackes and slates (Fig. III.9d) with abundant black shale interbeds and minor, up to several meters thick fault-bounded lenses of chert (Unit 1 in Figs. III.7b and III.8b). This succession is entirely devoid of basalt inclusions and is characterized by a pervasive cleavage dipping steeply to the E (Fig. III.7b).

(2) The base of the sedimentary succession is underlain by an elongated, curvilinear body of basalt (Unit 2 in Figs. III.7b and III.8b). In the map, this body is about 250 m wide and trends NW–SE but then pinches out to the southeast while it reorients to the NNW–SSE trend (Fig. III.7b). The basalt itself is strongly altered and differs significantly from those in the remainder of the section. It exhibits massive, non-pillowed texture but consists of multiple dm- to m-thick layers interstratified with the dark chert (Fig. III.9e). In terms of composition, it corresponds to the moderately LREE-enriched group of presumably within-plate basalts (sample UP-1 in Pin and Waldhausrová, 2007). Moreover, this stratiform basalt–chert package is intensely deformed, the layers dip moderately to the NE but as the basalt body pinches out they are tightly folded and dip steeply to the ENE (Figs. III.7b and III.8b).

(3) The structurally lowermost and most extensive unit of the section comprises four major (several hundreds of meters in length) and a few minor (several meters to tens of meters in length) bodies of basalt (Unit 3 in Figs. III.7b and III.8b), geochemically corresponding to the N-MORB-like LREE-depleted group of Pin and Waldhausrová (2007; their sample UP-2), embedded in a slate-dominated sedimentary succession. The basalts are frequently pillowed and exhibit generally weak ductile shortening as inferred from the spherical to weakly ellipsoidal pillows (Fig. III.9f) and weakly foliated matrix which contrasts sharply with the pervasively deformed host slate. The slaty cleavage reorients along the examined section. The cleavage dips moderately to the NE below the unit 2 whereas it dips moderately to steeply to the N farther to the southwest (Figs. III.7b and III.8b). Lineation is only rarely developed. The slaty cleavage and the weak cleavage in the basalts are generally concordant (Figs. III.7b and III.8b), but locally the cleavage may wrap around the basalt bodies and become complexly folded or reoriented near the basalt/slate contacts. Importantly, all the above units 1–3 are unconformably overlain by the middle Cambrian marine siliciclastic rocks of the Skryje–Týřovice basin (STB; Figs. III.2 and III.7b) that are attributed to the upper Stage 5 to lower Drummian Stage (ca. 508–504 Ma; Fatka et al., 2011) or by a late Cambrian to earliest Ordovician volcanic complex (Fig. III.2; dated at 505 ± 4 Ma using Rb–Sr whole-rock; (Vidal et al., 1975) recalculated by Dornsiepen (1979), and at 499 ± 4 Ma using U–Pb on zircons (Drost et al., 2004). Both overlying successions lack any ductile deformation and are only gently to moderately tilted (see Hajná et al., 2010 for details).

5.2. Central and southwestern portion of the belt (areas 3–5)

The southwestern half of the Radnice–Kralupy belt differs significantly from that of described above. The areas 3–5 are characterized by abundant basalt bodies that are

typically several hundred of meters across, are commonly rounded, sub-circular to weakly elliptical to amoeboid in plan view (Figs. III.2 and III.7c–e), and have a generally flat-lying attitude (Fig. III.8c–e). In three-dimensions, the basalts bodies are thus approximately tabular or disc-shaped inclusions. Compared to areas 1 and 2, the basalt bodies are closely spaced, only meters to tens of meters apart in some cases (Figs. III.2 and III.7c–e). The internal deformation of the basalts bodies is weak in area 3 where they contain relic pillows with fracture cleavage developed only along margins. In contrast, in areas 4 and 5 they are intensely ductilely deformed and exhibit continuous cleavage and strongly flattened pillows near margins (Fig. III.10a), grading into less deformed interior with preserved igneous textures, including massive, variolitic, and autoclastic and hydrothermal chert–basalt breccias. In many cases, however, the basalts are extensively transformed into greenstones, that is, they are overprinted by a pervasive foliation defined by chlorite and actinolite fibers (Fig. III.4f).

The basalt bodies are embedded in the predominantly chlorite–sericite slate, corresponding to the lower greenschist facies conditions, commonly interbedded with metal-rich black shales, minor graywackes, conglomerates, and scattered chert lenses. Although strongly overprinted by the lower greenschist facies deformation, these rocks may locally preserve relics of the syn-sedimentary chaotic slump structures.

Both the (meta-)basalts and the host chlorite–sericite slates are characterized by a predominantly flat-lying foliation (Fig. III.7c–e) and strongly developed stretching or mineral lineation (Fig. III.10b) defined by stretched clasts or by chlorite and actinolite fibers, respectively. In some cases, however, foliation in the (meta-)basalts is discordant to that in the host slates. The lineation plunges shallowly to the NE to SE (Fig. III.7c–e). In many places, strong linear fabric in the host slates dominates and they exhibit a pencil structure (Fig.

III.10c) or intensely developed crenulation lineation.

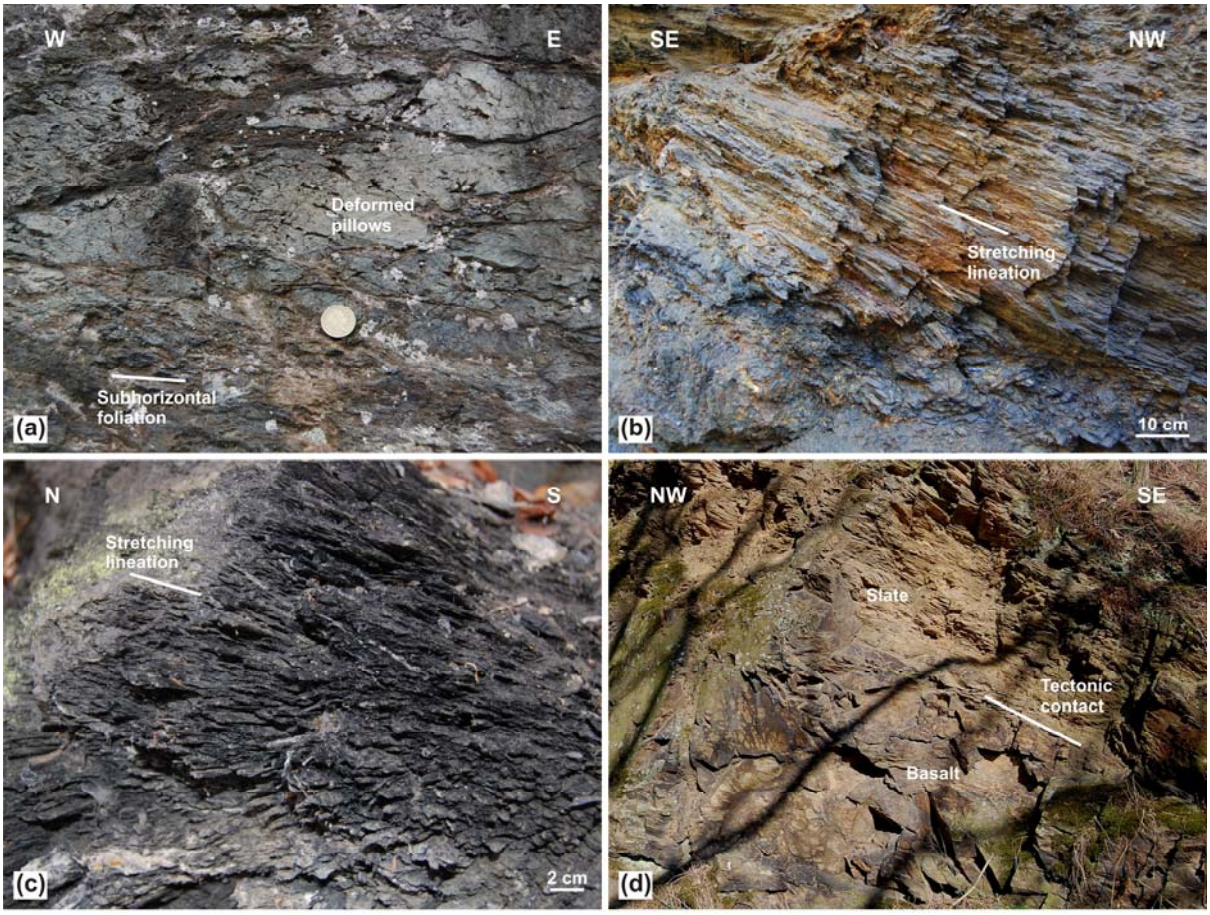

Fig. III.10. Characteristic lithologic and structural features of the Neoproterozoic rocks in the southwestern portion of the Radnice–Kralupy mélange belt. (a) Pervasive cleavage in altered matrix around pillows. Area 5, Všenice, [WGS84 coordinates: N49°49'12.07", E13°33'58.01"]. Sterling for scale. (b) Strong subhorizontal stretching lineation in black shale. Area 5, Lužnice creek, near Sedlecko, [WGS84 coordinates: N49°48'37.96", E13°31'49.03"]. (c) Pencil structure in black shale. Area 5, right bank of the Berounka River, near Sedlecko, [WGS84 coordinates: N49°48'44.17", E13°31'37.45"]. (d) Basalt/slate tectonic contact. Area 5, near Střapole, [WGS84 coordinates: N49°48'30.52", E13°32'12.67"].

All the (meta-)basalt/slate contacts observed on outcrops are sub-horizontal and also strongly sheared with no evidence of contact metamorphism (Fig. III.10d). Moreover, significant competence contrast between basalts and host slates creates a remarkable surface topography in areas 3–5. The topography is characterized by rounded steeply sloping buttes made up by basalt (Fig. III.11), closely resembling serpentinite `knockers' of the Franciscan Complex, California, and surrounded by wide flats underlain by or narrow valleys

deeply incised into slate (Fig. III.11).

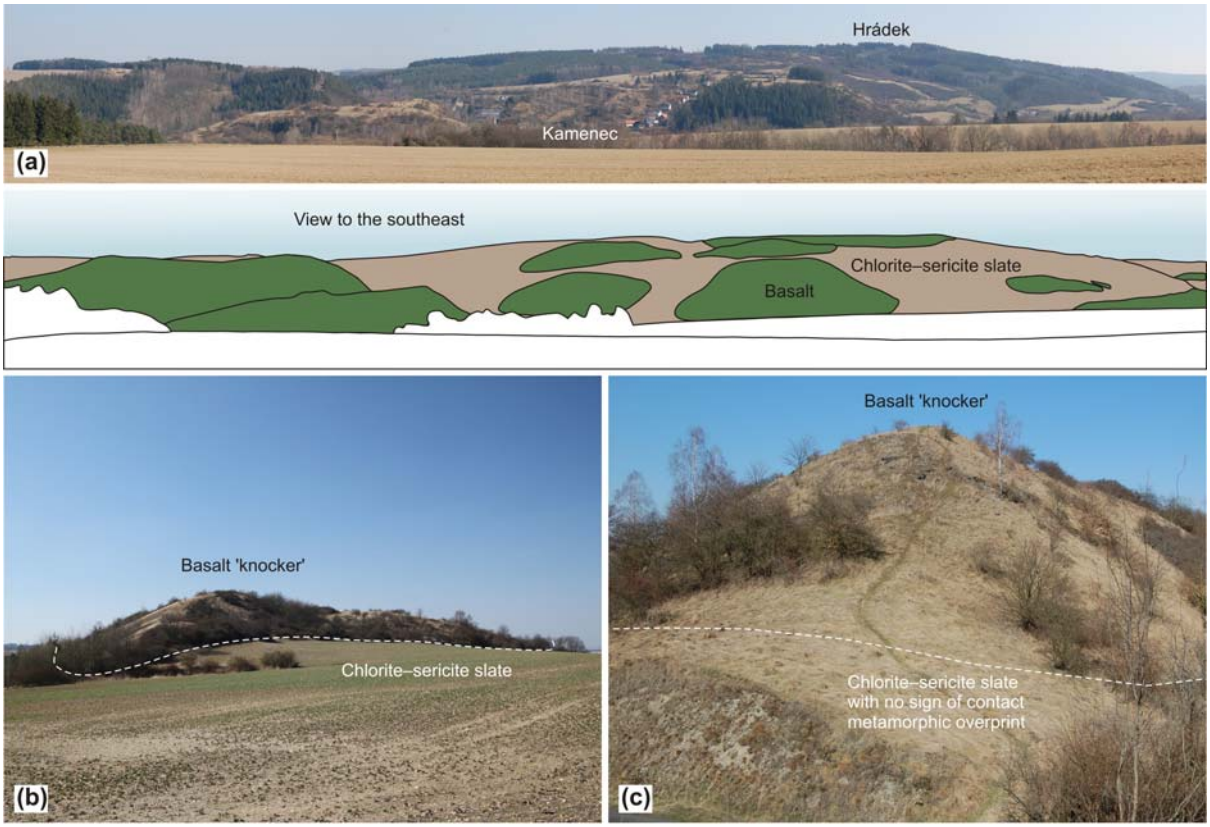

Fig. III.11. (a) Panoramic view on and schematic line drawing of mélange landscape (Kamenec, Area 4) with buttes or ʽknockers' of basalt surrounded by more eroded slate matrix. (b) Close-up view on a basalt`knocker' projecting upward from a flat area underlain by soft slates. (c) Sharp subhorizontal contact (covered by grass) between a basalt body flat and strongly deformed underlying slate.

6. Discussion

6.1. Mechanisms of mélange formation in the Radnice–Kralupy belt

The composition and structures of the mélange rocks described above suggest that two main end-member types of mélanges and inferred mélange-forming processes can be identified in the Radnice–Kralupy belt.

First, the massive to thickly bedded graywackes commonly show chaotic textures and were interpreted as deepwater turbidites as early as in the late 1960s (Cháb and Pelc, 1968). We concur with this interpretation and suggest that the depositional processes mostly included

gravity driven debris flows (submarine slides) along the upper wedge slope, transporting material from an eroded volcanic arc towards the wedge toe and trench (Fig. III.12). Furthermore, isolated meter-scale blocks of chert and graywackes occur in some places scattered in the strongly deformed slate matrix (Fig. III.9b). We interpret these blocks as olistoliths, in agreement with the inferred olistostromal origin of at least some graywacke succesions. We have also shown that some graywackes frequently contain angular clasts of cleaved metal-rich black shales (Figs. III.3a and III.4a), interpreted as deposited in a deepwater (pelagic?) anoxic environment (Pašava et al., 1996). This implies that the deepwater sediments must have been incorporated in the accretionary wedge, deformed, carried up to the wedge surface (Fig. III.12), and eroded by and mixed with the gravity-driven debris flows largely composed of the terrigenous arc-derived detritus. Vice versa, some black shales contain rounded pebbles of graywacke (Figs. III.3b and III.4b) suggesting deposition into and mixing of the (semi-)consolidated terrigenous arc-derived graywacke material with deepwater pelagic shales. These inferences suggest repeated recycling of the sedimentary material in the accretionary wedge (Fig. III.12).

Second, numerous meter- to kilometer-scale basalt bodies are included in this olistotromal graywacke matrix (Figs. III.2, III.7, III.8, and III.11). In all cases we encountered, the basalt/host contacts were tectonic and no evidence was found for contact metamorphism in the host slates (Figs. III.9c, III.10d, and III.11b and c). Furthermore, there are three intriguing facts regarding these oceanic (ophiolitic) rocks in the Radnice–Kralupy belt. (1) Basalt clasts are largely absent as major constituents of the (meta-)sedimentary rocks. (2) All the basalt bodies we mapped consist solely of lavas (commonly pillowed; Fig. III.9f), however, no deeper section of the oceanic lithosphere such as sheeted dikes, plutonic rocks, or even lithospheric mantle has been discovered in the Radnice–Kralupy belt. (3) The

basalts involved in the belt show contrasting geochemical composition and were interpreted as having been generated in different plate-tectonic settings. One compositional group includes basalts of intra-oceanic back arc basin whereas the other group includes within-plate basalts that lack suprasubduction zone signature (Pin and Waldhausrová, 2007). It is fascinating to note that basalts assigned to the different plate-tectonic environments, with the sites of their origin possibly spaced hundreds of kilometers apart, are now juxtaposed to within a less than 1 km in the Radnice–Kralupy belt (Figs. III.7b and III.8b). (4) The peak Cadomian regional metamorphism of the basalts in the Radnice–Kralupy belt, at least according to the present knowledge, does not exceed the lower greenschist facies conditions. The absence of blueschist or eclogite facies rocks would thus favor a flat-slab subduction (see also Hajná et al., 2010). We interpret these observations as follows.

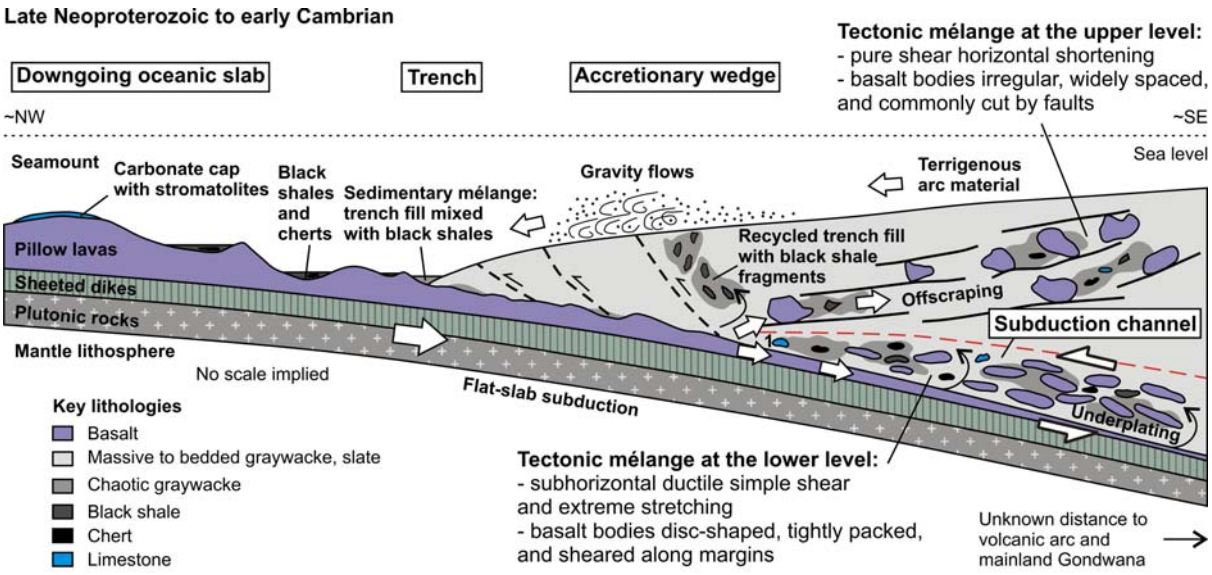

Fig. III.12. Idealized model for the origin of sedimentary and tectonic mélanges in the Radnice–Kralupy belt; see text for discussion.

No exposures of deeper section of the oceanic lithosphere suggests that only the very superficial layer was plucked from the top of the subducting oceanic plate upon entering the

subduction zone (Fig. III.12). We thus speculate that the subducted slab must have had a rugged topography, either faulted or covered by seamounts composed of thick packages of pillow lavas. We favor the latter interpretation which is further supported by the occurences of pisolitic and oolitic limestones that are included together with the basalts in the mélange (Figs. III.2 and III.12). The limestones may represent dismembered relics of the uppermost, shallow water carbonate rims or lagoons on top of the seamounts (Fig. III.12). An additional argument for the seamount origin of at least some basalts would be the presence of silicified stromatolites, newly found in a close proximity of the pillowed, N-MORB-like basalts (Figs. III.2 and III.3f), corroborating that rocks from the near tidal zone were mixed with the ocean floor fragments in the mélange. Without dealing with the plate-tectonic context, a similar reconstruction was also proposed by Pouba et al. (2000) to explain the origin of the stromatolite-bearing cherts in a correlative unit to the southeast of the Radnice–Kralupy belt. These authors envisioned the cherts and stromatolites as having been formed in shallow water lagoonal environment along flanks of volcanic elevations rising above the sea level.

The `seamount scrape-off' model also provides an elegant explanation for the overall architecture of the Blovice accretionary wedge, that consists of several NE–SW-trending crustal-scale belts where ocean-floor-bearing (`ophiolitic') mélanges alternate with graywacke-dominated belts devoid of basalts (Figs. III.1c and III.2). We may speculate that the`ophiolitic' belts, with the Radnice–Kralupy belt as the most notable example, represent several originally linear, trench-parallel seamount chains that entered the subduction zone and were accreted successively, alternating with periods of deposition and accretion of trench-fill deposits.

Importantly, two contrasting basalt/host contact relationships were observed in the

Radnice–Kralupy belt. In areas 1 and 2, the basalt bodies are irregular in shape, widely spaced, commonly bounded by faulted contacts, and only weakly strained (Figs. III.2, III.7a and b, III.8a and b, and III.9c and f). This suggests that they were never significantly buried and ductilely deformed in the accretionary wedge. Our interpretation is thus that areas 1 and 2 represent an upper structural level of the wedge, with the basalts having been offscraped and displaced as rigid bodies along faults that commonly truncate steep cleavage in the previously deformed slates (Fig. III.12). In contrast, the basalts in areas 4 and 5 are disc-shaped, closely spaced, and intensely ductilely deformed within the flat-lying fabric (Figs. III.2, III.7d and e, III.8d and e, and III.11a). The host slates show strongly developed stretching lineation (Fig. III.10b and c) compatible with their extreme shearing. We interpret areas 4 and 5 to represent the lower structural level of the wedge, where the basalt were plucked from the top of the subducting oceanic slab and intensely sheared together with the host slates in the subduction channel (Fig. III.12). The ductile flow of the matrix and strain coupling between the basalts and slates also resulted in the local accumulations and tight packing of the individual basalt bodies (Figs. III.2, and III.7d and e), as opposed to their more scattered occurrence at the upper structural level (Fig. III.2).

Examining fabric symmetry and orientation also reveals that the different levels of the accretionary wedge record two different strain paths. The steep cleavage and oblate fabric ellipsoid (areas 1 and 2) imply pure shear horizontal flattening strain prior to and during emplacement of the basalt bodies in the upper structural level, whereas the flat-lying plane strain to prolate fabric (areas 4 and 5) implies subhorizontal simple shear associated with a strong stretching component in the lower level above the subducting plate. An intermediate case between these two is perhaps represented by area 3, preserving both steep and flat fabrics. Exposure of the various structural levels along the same belt, with the

depth increasing generally to the southwest, may be explained by late Cadomian northeastward tilting of the belt along major bounding faults (Zulauf et al., 1997). The tilting must have occurred before mid- to late-Cambrian as the ~504–508 Ma Cambrian shales and overlying late-Cambrian to early Ordovician volcanic rocks overstep the belt.

6.2. Geochronologic constraints for the mélange formation

A combination of the existing and our new U–Pb zircon ages points to a protracted time span of more than 100 M.y. for the mélange formation and growth of the Cadomian accretionary wedge in the Teplá–Barrandian unit (see Zulauf et al., 1999; Dörr et al., 2002; Sláma et al., 2008; Hajná et al., 2010 for details). The Cadomian subduction and wedge development perhaps commenced at around ?650–635 Ma, as inferred from a deposition age of comparable graywackes to the southeast of the Radnice–Kralupy belt (Drost et al., 2011). The mélange also includes fragments of 647 Ma, 625 Ma, and 605 ± 39 Ma ocean floor (Fig. III.2; Pin and Waldhausrová, 2007). A significant peak of subduction-related arc volcanism at around 560 Ma is recorded by a pronounced population of detrital zircons in our dated sample (560 ± 4 Ma; Fig. III.6), in agreement with the radiometric ages of arc volcanic rocks reported from the southeastern TBU (568 ± 3 Ma; (Dörr et al., 2002). Surprisingly, the statistically significant population of early Cambrian detrital zircons (527 ± 3 Ma) in the dated sample implies that the deposition, deformation, and erosion of at least some parts of the accretionary wedge lasted till the early Cambrian (note that this entire portion of the TBU was previously considered as Neoproterozoic in age). A similar conclusion that the Cadomian processes spanned in a back arc basin along the southeastern margin of the TBU till the early Cambrian was previously reached by Sláma et al. (2008b). These new geochronologic data thus strongly support a critical reappraisal of the stratigraphic relations between the northwestern and southeastern segments of the Cadomian basement of the

TBU, exposed to the NW and SE of the Lower Paleozoic overlap successions, respectively (Fig. III.1), and prove that both segments evolved separately but the depositional processes overlapped in time (as proposed by Röhlich, 2000; see Hajná et al., 2011 for detailed discussion). While the northeastern segment was still an active accretionary wedge at around 527 Ma (this study), the southeastern segment of TBU was already elevated above the sea level and was extensively eroded. The erosion is exemplified by a >4000 m thick early Cambrian continental, molasse-type siliciclastic succession of the Příbram–Jince basin (PJB in Fig. III.2), inferred to have been deposited as alluvial fans in intra-montane depressions (Havlíček, 1971; Kukal, 1971). The separate evolution of both segments, as well as the latest processes in the Cadomian accretionary wedge, were terminated prior to the middle Cambrian (ca. 508–504 Ma) when both areas were largely peneplenized and invaded by a short time marine trangression.

6.3. Mélanges as markers of modern-style plate tectonics in the Precambrian?

The above interpretations suggest that both sedimentary (olistostromal) mixing and tectonic offscraping and underplating were involved in the formation of the Radnice–Kralupy mélange belt (Fig. III.12) and perhaps also in the entire Blovice accretionary complex. The inferred dual sedimentary–tectonic origin of this Neoproterozoic/early Cambrian mélange associated with rapid recycling of material within the accretionary wedge is identical to processes that operate along modern, Mesozoic to Cenozoic active margins in the circum-Pacific rim. Indeed, several authors proposed a modern style of active margin processes for the development of the Avalonian–Cadomian belt on the basis of comparison with the North American Cordillera or Japanese Islands (Nance et al., 2002; Linnemann et al., 2008). Using the Radnice–Kralupy belt as a case example, we propose that the presence of similar dual

sedimentary–tectonic mélanges would be a compelling evidence in support of oceanic subduction and may be sought after to reveal the operation of modern style plate tectonics in older Precambrian settings (see, e.g., Cawood et al., 2006; Ernst, 2007; Stern, 2008 for discussion).

7. Conclusions

The Franciscan-type mélanges newly recognized in the Radnice–Kralupy belt are of dual, sedimentary and tectonic origin and allow a detailed reconstruction of processes in a fossil accretionary wedge.

The voluminous olistostromal successions of graywackes that exhibit chaotic texture and slates containing graywacke and chert olistoliths are interpreted to represent gravity flow deposits (submarine slides) presumably along the trench slope. The clast compositions indicate multiple episodes of mixing of arc-derived and deepwater (?pelagic) material.

Moreover, abundant bodies of (meta-)basalts, interpreted as dismembered seamount chains, were emplaced tectonically into various structural levels of this sedimentary mélange by two different mechanisms. At the upper level, the irregular bodies of basalts were offscraped, only weakly deformed, and incorporated in the sedimentary matrix that exhibits steep cleavage indicating horizontal shortening (flattening strain). In contrast, at the lower level, disc-shaped and closely spaced basalt bodies are ductilely sheared and reworked into a flat-lying fabric suggesting horizontal ductile flow, presumably in a subduction channel during flat-slab oceanic subduction. Our new U–Pb ages also revealed an extended duration of the mélange-forming processes, starting at around 630–?650 Ma and spanning till the early Cambrian (~527 Ma).

The inferred mélange-forming process are identical to those that operate along modern active margins. In general, this notion reveals potential of sedimentary–tectonic

mélanges as excellent markers to prove the modern-style subduction in Precambrian settings.

References

Aalto, K.R., 1981. Multistage melange formation in the Fraciscan Complex, northernmost California. Geology, 9, 602–607.

Al-Shanti, A.M., Gass, I.G., 1983. The Upper Proterozoic ophiolite melange zones of the easternmost Arabian shield. J. Geol. Soc. London 140, 867–876.

Burg, J.P., Bernoulli, D., Smit, J., Dolati, A., Bahroudi, A., 2008. A giant catastrophic mud-and-debris flow in the Miocene Makran. Terra Nova 20, 188–193.

Cawood, P.A., Kröner, A., Pisarevsky, S.A., 2006. Precambrian Plate Tectonics: Criteria and Evidence. GSA Today, 16, 4–11.

Cháb, J., Pelc, Z., 1968. Lithology of Upper Proterozoic in the NW limb of the Barrandian area. Krystalinikum 6, 141–167.

Cháb, J., Pelc, Z., 1973. Proterozoic graywackes in NW flank of the Barrandian. J. Geol. Sci. 25, 7–84.

Cháb, J., Bernardová, E., 1974. Prehnite and pumpellyite in the Upper Proterozoic basalts of the north-western part of the Barrandian region (Czechoslovakia). Krystalinikum 10, 53–66.

Cloos, M., 1982. Flow melanges: numerical modeling and geologic constraints on their origin in the Franciscan subduction complex, California. Geol. Soc. Am. Bull. 93, 330–345.

Cowan, D.S., 1974. Deformation and metamorphism of Franciscan subduction zone complex northwest of Pacheco Pass, California. Geol. Soc. Am. Bull. 85, 1623–1634.

Cowan, D.S., 1985. Structural styles in Mesozoic and Cenozoic melanges in the western Cordillera of North America. Geol. Soc. Am. Bull. 96, 451–462.

Cowan, D.S., Page, B.M., 1975. Recycled Franciscan material in Franciscan melange west of Paso Robles, California. Geol. Soc. Am. Bull. 86, 1089–1095.

Dornsiepen, U.,F., 1979. Rb–Sr whole rock ages within the European Hercynian, a review. Krystalinikum 14, 33–49.

Dörr, W., Zulauf, G., Fiala, J., Franke, W., Vejnar, Z., 2002. Neoproterozoic to Early Cambrian history of an active plate margin in the Teplá–Barrandian unit - a correlation of U–Pb isotopic-dilution-TIMS ages (Bohemia, Czech Republic). Tectonophysics, 352, 65–85.

Drost, K., Linnemann, U., McNaughton, N., Fatka, O., Kraft, P., Gehmlich, M., Tonk, Ch., Marek, J., 2004. New data on the Neoproterozoic - Cambrian geotectonic setting of the Teplá–Barrandian volcano-sedimentary successions: geochemistry, U–Pb zircon ages, and provenance (Bohemian Massif, Czech Republic). Int. J. Earth Sci. 93, 742–757.

Drost, K., 2008. Sources and geotectonic setting of Late Neoproterozoic - Early Paleozoic volcano-sedimentary successions of the Teplá–Barrandian unit (Bohemian Massif): evidence frompetrographical, geochemical, and isotope analyses. Geologica Saxonica 54, 1–165.

Drost, K., Gerdes, A., Jeffries, T., Linnemann, U., Storey, C., 2011. Provenance of Neoproterozoic and early Paleozoic siliciclastic rocks of the Teplá–Barrandian unit (Bohemian Massif): Evidence from U–Pb detrital zircon ages. Gondwana Res. 19, 213–231.

Dubanský, A., 1984. Determination of the radiogenic age by the K–Ar method (geochronological data from the Bohemian Massif in the ČSR region). Collection of Scientific Works of Technical University of Ostrava: Mining and Geological Series 30, 137–170.

Ernst, W.G., 2007. Speculations on evolution of the terrestrial lithosphere-asthenosphere system - Plumes and plates. Gondwana Res. 11, 38–49.

Fatka, O., Micka, V., Szabad, M., Vokáč, V., Vorel, T., 2011. Nomenclature of Cambrian lithostratigraphy of the Skryje–Týřovice basin. Bull. Geosci. 86, 841–858.

Festa, A., Pini, G.A., Dilek, Y., Codegone, G., 2010a. Mélanges and mélange-forming processes: a historical overview and new concepts. International Geology Review 52, 1040–1105.

Festa, A., Pini, G.A., Dilek, Y., Codegone, G., Vezzani, L., Ghisetti, F., Lucente, C.C., Ogata, K., 2010b. Peri-Adriatic mélanges and their evolution in the Tethyan realm. International Geology Review 52, 369–403.

Festa, A., 2011. Tectonic, sedimentary, and diapiric formation of the Messinian melange: Tertiary Piedmont

Basin (northwestern Italy). In: Wakabayashi, J., Dilek, Y. (Eds.), Melanges: Processes of Formation and Societal Significance: Geol. Soc. Am. Spec. Pap. 480, 215–232.
Fox, K.F., 1976. Melanges in Franciscan Complex, a product of triple-junction tectonics. Geology 4, 737–740.
Gerdes, A., Zeh, A., 2006. Combined U–Pb and Hf isotope LA-(MC-)ICP-MS analyses of detrital zircons: comparison with SHRIMP and new constraints for the provenance and age of an Armorican metasediment in Central Germany. Earth and Planetary Science Letters 249, 47–61.
Gerdes, A.,Zeh, A., 2009. Zircon formation versus zircon alteration - New insights from combined U–Pb and Lu-Hf in-situ La-ICP-MS analyses of Archean zircons from the Limpopo Belt. Chemical Geology 261, 230–243.
Glodny, J., Lohrmann, J., Echtler, H., Gräfe, K., Seifert, W., Collao, S., Figueroa, O., 2005. Internaldynamics of apaleoaccretionary wedge: insights from combined isotope tectonochronology and sandbox modelling of the South-Central Chilean forearc. Earth and Planetary Science Letters 231, 23–39.
Gucwa, P.R., 1975. Middle to Late Cretaceous sedimentary mélange, Franciscan Complex, northern California. Geology 3, 105–108.
Hajná, J., Žák, J., Kachlík, V., Chadima, M., 2010. Subduction-driven shortening and differential exhumation in a Cadomian accretionary wedge: The Teplá–Barrandian unit, Bohemian Massif. Precambrian Res. 176, 27–45.
Hajná, J., Žák, J., Kachlík, V., 2011. Structure and stratigraphy of the Teplá–Barrandian Neoproterozoic, Bohemian Massif: a new plate-tectonic reinterpretation. Gondwana Res. 19, 495–508.
Havlíček, V., 1971. Stratigraphy of the Cambrian of Central Bohemia. J. Geol. Sci., Geol. 20, 7–52.
Hefferan, K.P., Admou, H., Hilal, R., Karson, J., Saquaque, A., Samson, S., Kornprobst, J., 2002. Proterozoic blueschist-bearing mélange in the Anti-Atlas Mountains, Morocco. Precambrian Res. 118, 179–194.
Hsü, K.J., 1968. Principles of mélanges and their bearing on the Franciscan–Knoxville paradox. Geol. Soc. Am. Bull. 79, 1063–1974.
Hsü, K.J., Schlanger, S.O., 1971. Ultrahelvetic Flysch sedimentation and deformation related to plate tectonics. Geol. Soc. Am. Bull. 82, 1207–1218.
Jakeš, P., Zoubek, J., Zoubková, J., Franke, W., 1979. Graywackes and metagraywackes of the Teplá–Barrandian Proterozoic area. J. Geol. Sci., Geol. 33, 83–122.
Jongens, R., Bradshaw, J.D., Fowler, A.P., 2003, The Balloon Melange, northwest Nelson: Origin, structure, and emplacement: New Zealand Journal of Geology and Geophysics 46, 437–448.
Kleist, J.R., 1974. Deformation by soft-sediment extension in the Coastal belt, Franciscan Complex. Geology 2, 501–504.
Kukal, Z. 1971. Sedimentology of Cambrian deposits of the Barrandian area. J. Geol. Sci., Geol. 20, 53–100.
Lang, M., 2000. Composition of Proterozoic greywackes in the Barrandian. Bull. Czech Geol. Surv. 75, 205–216.
Linnemann, U., Pereira, F., Jeffries, T.E., Drost, K., Gerdes, A., 2008. The Cadomian orogeny and the opening of the Rheic Ocean: the diacrony of geotectonic processes constrained by LA-ICP-MS U–Pb zircon dating (Ossa-Morena and Saxo-Thuringian Zones, Iberian and Bohemian Massifs). Tectonophysics 461, 21–43.
Marroni, M., Pandolfi, L., 2001. Debris flow and slide deposits at the top of the Internal Liguride ophiolitic sequence, Northern Apennines, Italy: a record of frontal tectonic erosion in a fossil accretionary wedge. Island Arc 10, 9–21.
Mašek, J., 2000. Stratigraphy of the Proterozoic of the Barrandian area. Bull. Czech Geol. Surv. 75, 197–204.
Nance, R.D., Murphy, J.B., Keppie, J.D., 2002. Cordilleran model for the evolution of Avalonia. Tectonophys 352, 11–32.
Nance, R.D., Gutierrez-Alonso, G., Keppie, J.D., Linnemann, U., Murphy, J.B., Quesada, C., Strachan, R.A., Woodcock, N.H., 2010. Evolution of the Rheic Ocean. Gondwana Res. 17, 194–222.
Nance, R.D., Murphy, J.B., Strachan, R.A., D'Lemos, R.S., Taylor, G.K., 1991. Late Proterozoic tectonostratigraphic evolution of the Avalonian and Cadomian terranes. Precambrian Res. 53, 41–78.
Orange, D.L., 1990. Criteria helpful in recognizing shear-zone and diapiric mélanges: examples from the Hoh accretionary complex, Olympic Peninsula, Washington. Geol. Soc. Am. Bull. 102, 935–951.
Orr, T.O.H., Korsch, R.J., Foley, L.A., 1991. Structure of melange and associated units in the Torlesse accretionary wedge, Tararua Range, New Zealand: New Zealand Journal of Geology and Geophysics 34, 61–72.
Osozawa, S., Morimoto, J., Flower, M.F.J., 2009. "Block-in-matrix" fabrics that lack shearing but possess composite cleavage planes: a sedimentary mélange origin for the Yuwan accretionary complex in the Ryukyu island arc, Japan. Geol. Soc. Am. Bull. 121, 1190–1203.
Page, B.M., Suppe, J., 1981. The Pliocene Lichi melange of Taiwan - its plate-tectonic and olistostromal origin.

American Journal of Science 281, 193–227.
Pašava, J., Hladíková, J., Dobeš, P., 1996. Origin of Proterozoic metal-rich black shales from the Bohemian Massif, Czech Republic. Economic Geology 91, 63–79.
Perroti, E., Bertok, C., d'Atri, A., Martire, L., Piana, F., Catanzariti, R., 2011. A tectonically-induced Eocene sedimentary mélange in the West Ligurian Alps, Italy. Tectonophysics, doi:10.1016./j.tecto.2011.09.005.
Pin, C., Waldhausrová, J., 2007. Sm–Nd isotope and trace element study of Late Proterozoic metabasalts ("spilites") from the Central Barrandian domain (Bohemian Massif, Czech Republic). Geol. Soc. Am. Spec. Paper 423, 231–247.
Platt, J.B., Liou, J.G., Page, B.M., 1976. Franciscan blueschist-facies metaconglomerate, Diablo Range, California. Geol. Soc. Am. Bull. 87, 581–591.
Platt, J.P., 1975. Metamorphic and deformational processes in Franciscan Complex, California: some insights from Catalina schist terrane. Geol. Soc. Am. Bull. 86, 1337–1347.
Polat, A., Kerrich, R., 1999. Formation of an Archean tectonic mélange in the Schreiber-Hemlo greenstone belt, Superior Province, Canada: Implications for Archean subduction-accretion process. Tectonics 18, 733–755.
Pouba, Z., Kříbek, B., Pudilová, M., 2000. Stromatolite-like cherts in the Barrandian
Upper Proterozoic: a review. Bull. Czech Geol. Surv. 75, 285–296.
Shackleton, M.R., Ries, A.C., Graham, R.H., Fitches, W.R., 1980. Late Precambrian ophiolitic mélange in the eastern desert of Egypt. Nature 285, 472–474.
Silver, E.A., Beutner, E.C., 1980. Mélanges. Geology 8, 32–34.
Sláma, J., Košler, J., Condon, D. J., Crowley, J. L., Gerdes, A., Hanchar, J. M., Horstwood, M. S. A., Morris, G. A., Nasdala, L., Norberg, N., Schaltegger, U., Schoene, B., Tubrett, M. N., Whitehouse, M. J., 2008a. Plešovice zircon - a new natural reference material for U–Pb and Hf isotopic microanalysis. Chemical Geology 249, 1–35.
Sláma, J., Dunkley, D.J., Kachlík, V., Kusiak, M.A., 2008b. Transition from island-arc to passive setting on the continental margin of Gondwana: U–Pb zircon dating of Neoproterozoic metaconglomerates from the SE margin of the Teplá–Barrandian Unit, Bohemian Massif. Tectonophysics 461, 44–59.
Stern, R.J, 2008. Modern-style plate tectonics began in Neoproterozoic time: An alternative interpretation of Earth's tectonic history. Geol. Soc. Am. Spec. Paper 440, 265–280.
Suchý, V., Sýkorová, I., Melka, K., Filip, J., Machovič, V., 2007. Illite 'crystallinity', maturation of organic matter and microstructural development associated with lowest-grade metamorphism of Neoproterozoic sediments in the Teplá–Barrandian unit, Czech Republic. Clay Minerals 42, 503–526.
Šmejkal, Z., 1964. The age of some igneous and metamorphic rocks of the Bohemian Massif determined by K–Ar method (Part 2). J. Geol. Sci., Geol. 4, 121–136.
Tarduno, J.A., McWilliams, M., Debiche, M.G., Sliter, W.V., Blake, M.C., 1985. Franciscan Complex Calera limestones: accreted remnants of Farallon Plate oceanic plateaus. Nature 317, 345–347.
Ueda, H., Kawamura, M., Niida, K., 2000. Accretion and tectonic erosion processes revealed by the mode of occurrence and geochemistry of greenstones in the Cretaceous accretionary complexes of the Idonnappu Zone, southern central Hokkaido, Japan. Island Arc 9, 237–257.
Ujiie, K., 2002. Evolution and kinematics of an ancient decollement zone, melange in the Shimanto accretionary complex of Okinawa Island, Ryukyu Arc. J. Struct. Geol. 24, 937–952.
Ujiie, K., Hisamitsu, T., Soh, W., 2000. Magnetic and structural fabrics of the melange in the Shimanto accretionary complex, Okinawa Island: implication for strain history during decollement-related deformation. Journal of Geophysical Research 105, 25729 –25741.
Vidal, P., Auvray, B., Charlot, R., Fediuk, F., Hameurt, J., Waldhausrová, J., 1975. Radiometric age of volcanics of the Cambrian "Křivoklát-Rokycany" complex (Bohemian Massif). Geol. Rundsch. 64, 563–570.
Wakabayashi, J., 1999. Subduction and the rock record: concepts developed in the Franciscan Complex, California. In: Moores, E.M., Sloan, D., Stout, D.L. (Eds.), Classic Cordilleran concepts: a view from California. Geol. Soc. Am. Spec. Paper 338, 123–133.
Wakabayashi, J., 2008. Franciscan Complex, California: problems in recognition of melanges and the gap between research knowledge and professional practice. American Rock Mechanics Association 2008, 1–12.
Wakabayashi, J., 2011. Mélanges of the Franciscan Complex, California: diverse structural settings, evidence for sedimentary mixing, and their connection to subduction processes. In: J. Wakabayashi and Y. Dilek (Eds), Mélanges: processes of formation and societal significance. Geol. Soc. Am. Spec. Paper 480, 117–141.
Wakabayashi, J., Medley, E.W., 2004. Geological characterization of melanges for practitioners. Felsbau 22, 10–18.
Wilson, T.J., Hanson, R.E., Grunow, A.M., 1989. Multistage melange formation within an accretionary complex, Diego Ramirez Islands, southern Chile. Geology 17, 11–14.
Yamamoto, Y., Nidaira, M., Ohta, Y., Ogawa, Y., 2009. Formation of chaotic rock units during primary accretion

processes: examples from the Miura–Boso accretionary complex, central Japan. Island Arc 18, 496–512.
Zulauf, G., Dorr, W., Fiala, J., Vejnar, Z., 1997. Late Cadomian crustal tilting and Cambrian transtension in the Teplá–Barrandian unit (Bohemian Massif, Central European Variscides). Geol. Rundsch. 86, 571–584.
Zulauf, G., Schritter, F., Riegler, G., Finger, F., Fiala, J., Vejnar, Z., 1999. Age constraints on the Cadomian evolution of the Teplá–Barrandian unit (Bohemian Massif) through electron microprobe dating of metamorphic monazite. Zt. Deutsch. Geol. Ges. 150, 627–639.

CHAPTER 4

Jiří Žák, Petr Kraft, Jaroslava Hajná: Timing, styles, and kinematics of Cambro-Ordovician extension in the Teplá–Barrandian Unit, Bohemian Massif, and its bearing on the opening of the Rheic Ocean.

International Journal of Earth Sciences, in review

Timing, styles, and kinematics of Cambro–Ordovician extension in the Teplá–Barrandian Unit, Bohemian Massif, and its bearing on the opening of the Rheic Ocean

Jiří Žák[1] *, Petr Kraft*[1]*, Jaroslava Hajná*[1]

[1]*Institute of Geology and Paleontology, Faculty of Science, Charles University, Albertov 6, Prague, 12843, Czech Republic*

Abstract

This paper describes late Cambrian dikes and Early Ordovician volcano-sedimentary successions of the Prague Basin, Bohemian Massif, to constrain the timing and kinematics of break-up of the northern margin of Gondwana. Andesitic dikes indicate minor E–W crustal extension in the late Cambrian whereas the Tremadocian to Darriwilian lithofacies distribution and linear array of depocentres suggest opening of this Rheic Ocean rift-related basin during the NW–SE pure shear-dominated extension. This kinematic change was accompanied by the onset of basic submarine volcanism, presumably resulting from decompression mantle melting as the amount of extension increased. These inferences challenge some previous models for the Cambro–Ordovician rifting of the northern Gondwanan margin as a process that passed continuously from the Cadomian subduction and was diachronous from west to east. Instead, we conclude that the incipient extension may have been triggered by the onset of subduction of the Iapetus Ocean at around 510 Ma, after a significant time lag from the Cadomian subduction, and that the advanced extension was broadly coeval (Tremadocian to Darriwilian) along the Avalonian–Cadomian belt.

Various amounts of extension resulted in the break-up and drift of some terranes while other portions of the belt remained adjacent to Gondwana.

Keywords: *Anisotropy of magnetic susceptibility (AMS); Bohemian Massif; extension; Rheic Ocean; rifting; Teplá–Barrandian unit*

1. Introduction

It has been widely accepted that the Avalonian–Cadomian orogenic belt that had developed along the northern periphery of Gondwana during the late Neoproterozoic and the earliest Cambrian (Fig. IV.1a; ~750–530 Ma) began to break-up during the Cambrian and early Ordovician times (e.g., Pin and Marini 1993; Furnes et al. 1994; Kachlík and Patočka 1998; Crowley et al. 2000; Dostal et al. 2001; Murphy et al. 2002, 2004, 2006; von Raumer et al. 2002, 2003; Etxebarria et al. 2006; Keppie et al. 2006; Drost et al. 2007; Drost 2008; Linnemann et al. 2008a, b; Nance and Linnemann 2008; von Raumer and Stampfli 2008; Nance et al. 2010). This process was associated with orogen-wide extension of the northern Gondwana lithosphere (composed mostly of accreted volcanic arcs, arc-related basins, and continental fragments) and was followed by the opening of the Rheic Ocean and subsequent equator-ward drift of both mainland Gondwana and the intervening crustal fragments, which were later involved in the Variscan–Alleghenian–Quachita orogenic belt (Fig. IV.1b; see Nance et al. 2010 for a detailed overview).

The Ordovician opening of the Rheic Ocean was thus a key geodynamic event in the Early Paleozoic. Although the incipient rifting stages and associated bimodal magmatism are now fairly well documented in terms of chronology, petrogenesis of the (meta-)igneous complexes, and paleogeography in many of the Gondwana-derived microplates (Fig. IV.1a),

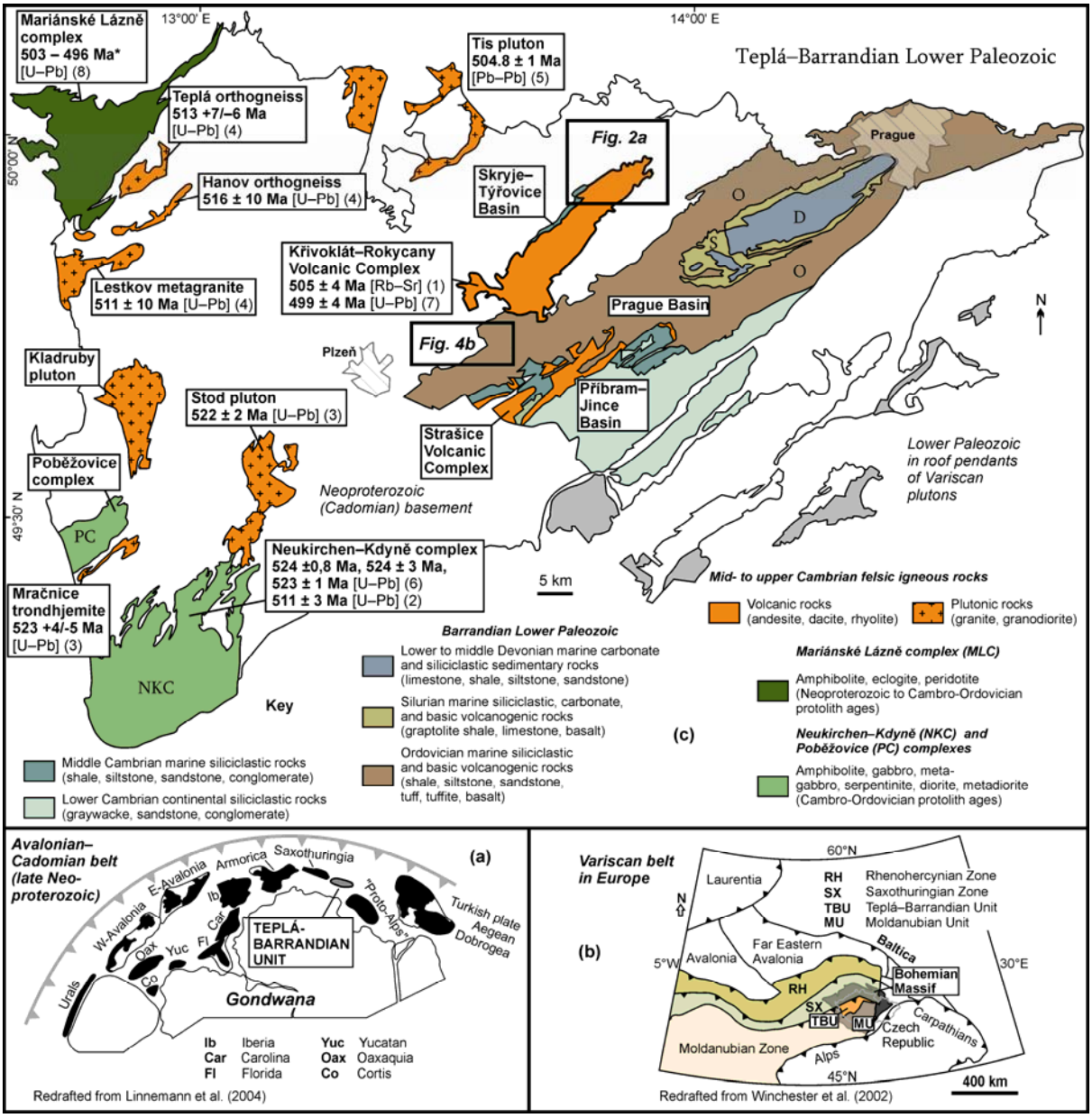

Fig. IV.1. (a) Paleogeographic position of the Teplá–Barrandian Unit (TBU) within the Avalonian–Cadomian belt on the active northern margin of Gondwana during the late Neoproterozoic Era (after Linnemann et al. 2004). (b) Greatly simplified map of basement structure and Variscan lithotectonic zonation of Europe showing main units and suture zones in the Bohemian Massif; modified after Winchester (2002). (c) Simplified geological map of the Teplá–Barrandian Unit, central Bohemian Massif, highlighting the middle Cambrian to early Ordovician igneous complexes hosted in the Neoproterozoic (Cadomian) basement, two separate early to middle Cambrian sedimentary basins (Příbram–Jince, Skryje–Týřovice), and overlying Ordovician to middle Devonian volcano-sedimentary successions of the Prague Basin. The dikes examined in this study intrude the Neoproterozoic and early Ordovician rocks to the NNE and SSW of the late Cambrian Křivoklát–Rokycany Volcanic Complex. Geology based on Geological map of the Czech Republic 1:500,000 published by the Czech Geological Survey in 2007. Source of geochronologic data: (1) Dornsiepen (1979), (2) Gebauer (1993), (3) Zulauf et al. (1997), (4) Dörr et al. (1998), (5) Venera et al. (2000), (6) Dörr et al. (2002), (7) Drost et al. (2004), (8) Timmermann et al. (2006).

such as the Acatlán complex, Mexico (e.g., Nance et al. 2007; Keppie et al. 2008; Ortega-

Obregon et al. 2010), Avalonia (e.g., Prigmore et al. 1997; Nance et al. 2002; Verniers et al. 2002; Pollock et al. 2009; Thompson et al. 2010), Ossa Morena (e.g., Silva and Pereira 2004; Chichorro et al. 2008; López-Guijarro et al. 2008; Sánchez-García et al. 2008, 2010; Fernández et al. in press) and Saxothuringian zones (e.g., Kachlík and Patočka, 1998; Patočka and Smulikowski 2000; Patočka et al. 2000; Dostal et al. 2001; Kemnitz et al. 2002; Linnemann et al. 2007, 2008a, b), the driving forces, plate kinematics, and exact timing of the Rheic Ocean opening still remain controversial.

One of the more easterly recognized crustal fragments derived from the Avalonian–Cadomian belt is the upper-crustal Teplá–Barrandian Unit (TBU) of the central Bohemian Massif (Fig. IV.1b, c). The Neoproterozoic basement of the TBU is overlain unconformably by the Lower Paleozoic (Cambrian to middle Devonian) volcano-sedimentary successions but was also intruded by mid- to late Cambrian (~504–524 Ma) granitoid plutons and is capped by two major upper Cambrian to Lower Ordovician subaerial volcanic complexes (Fig. IV.1c). This paper describes field observations and structural data from dikes that are closely associated with one of the volcanic complexes, specifically, the Křivoklát–Rokycany Volcanic Complex (KRVC; Fig. IV.1c). Unlike the other Cambro–Ordovician metaigneous complexes that are widespread in the Bohemian Massif (see Pin et al. 2007 for detailed overview and references), the dikes examined here are unique in that they have not been affected by the Variscan deformation and metamorphism. Thus they provide the missing key information on the geometry of the Cambro–Ordovician extension in this portion of the northern Gondwana margin. Observations on the dikes were combined from two separate areas to the northeast and southwest of the KRVC (Fig. IV.1c) where the dikes intrude the Neoproterozoic basement and the Ordovician siliciclastic sedimentary successions of the Prague Basin, respectively. On the basis of structural relationships combined with anisotropy of magnetic

susceptibility (AMS), detailed graptolite biostratigraphy and taphonomy, and lithofacies distribution in their Ordovican host rocks, we examine the dikes as markers of the Cambro–Ordovician regional extension across in the TBU. The dikes also allow inferences on the reorientation of the principal extension directions (present-day coordinates are used throughout this paper) during the initial stages of rifting and thus on the development of Early Paleozoic sedimentary basins in the TBU. Finally, broader implications are discussed, with the possible role and kinematics of slab-pull of the Iapetus Ocean as a driving force for this orogen-wide Cambro–Ordovician extension in the Avalonian–Cadomian belt.

2. The Křivoklát–Rokycany Volcanic Complex

The late Cambrian to earliest Ordovician Křivoklát–Rokycany Volcanic Complex (KRVC) has been interpreted to have formed in an incipient intra-plate rift. It is considered to be the best preserved, that is, not overprinted by Variscan ductile deformation and metamorphism, example of the Cambro¬–Ordovician igneous activity in the Bohemian Massif. The volcanic rocks unconformably overlie the Neoproterozoic (Cadomian) basement and overlap various stratigraphic levels of the middle Cambrian marine succession of the Skryje–Týřovice Basin (Figs. IV.1c, IV.2a), attributed to the upper Stage 5 to lower Drummian Stage (ca. 508–504 Ma; Chlupáč et al. 1998; Geyer et al. 2008; Fatka and Mergl 2009; Fatka et al. 2011; O. Fatka, pers. comm. 2011). The overlap suggests sea regression and differential uplift and erosion of fault-bounded basement blocks prior to the effusive volcanic activity. In turn, the volcanic rocks are overlain by and contained as clasts in the basal Ordovician (Tremadocian) siliciclastic marine successions of the southeasterly Prague Basin (Fig. IV.1c; Waldhausrová 1971; Chlupáč et al. 1998; Pin et al. 2007). These stratigraphic relations support the existing geochronologic data that constrain the age of the KRVC as 505 ± 4 Ma (Rb–Sr whole-rock data of Vidal et al. 1975 recalculated by Dornsiepen 1979) and 499 ± 4 Ma

(U–Pb on zircons, rhyolite; Drost et al. 2004).

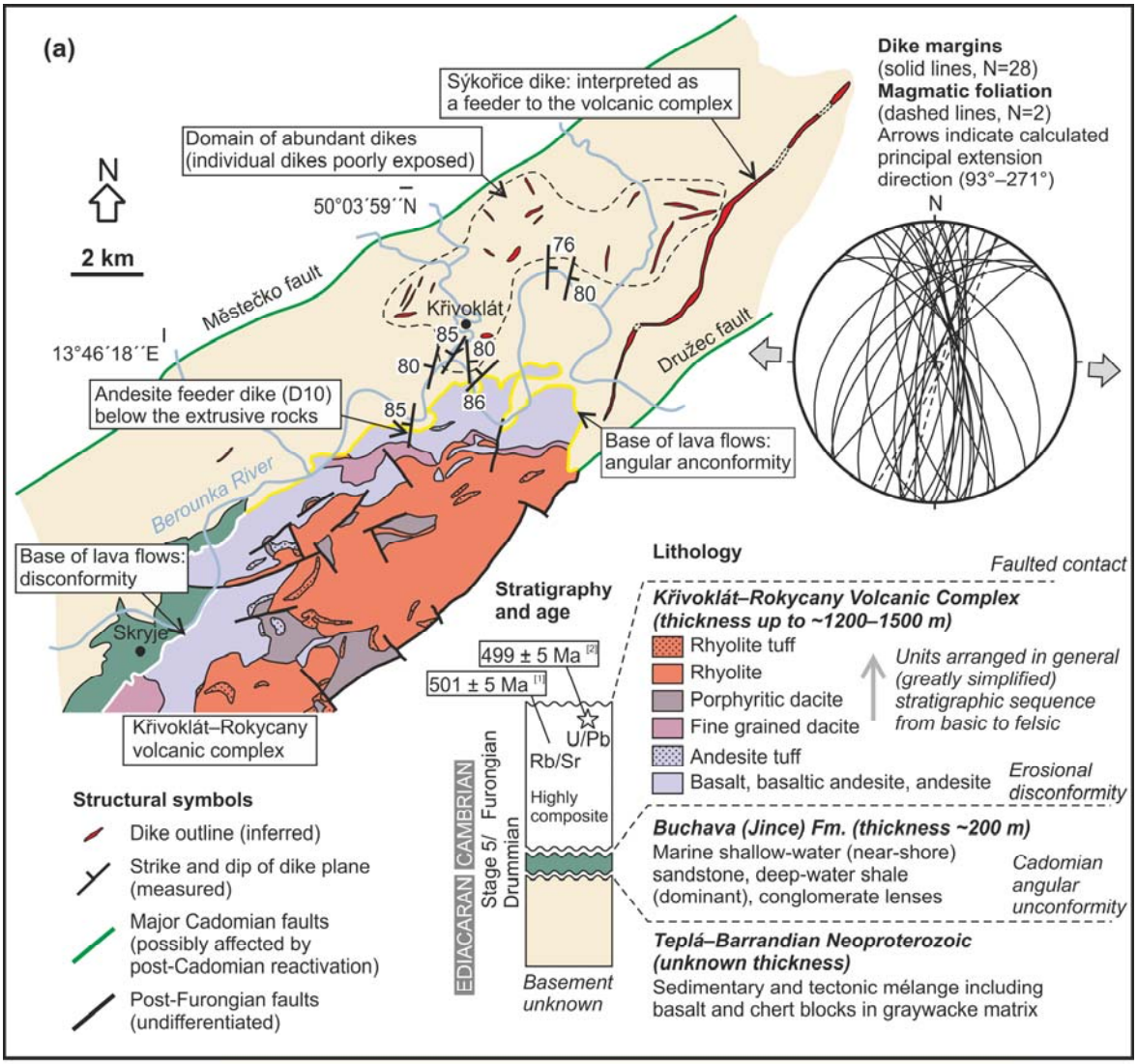

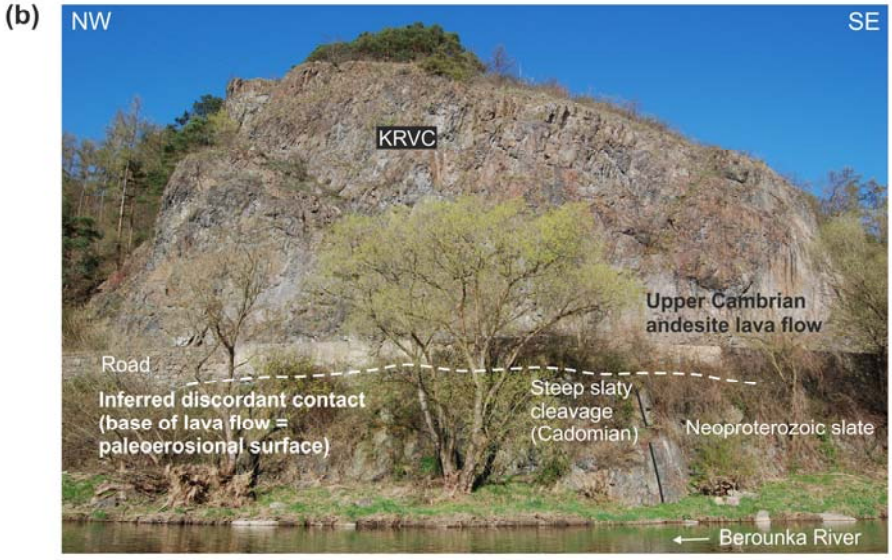

Fig. IV.2. (a) Simplified geological map of the northern part of the Křivoklát–Rokycany Volcanic Complex which overlies unconformably the Neoproterozoic basement and disconformably the marine siliciclastic rocks (dominated by shales) of the Skryje–Týřovice Basin; geology based on Geological map of the Křivoklát area 1:50,000 published by the Czech Geological Survey in 1997. The complex consists of multiple chiefly intermediate to felsic lava flows and minor pyroclastic rocks (see the inset stratigraphic column). Stereonet (equal area, lower hemisphere projection) shows orientation of andesite dikes (dike–host contacts) and margin-parallel magmatic foliations defined by flattened vesicles and alignment of feldspar phenocrysts in the dikes. (b) Subhorizontal base of an undeformed andesitic lava flow overlying the Neoproterozoic slate that is pervasively deformed and exhibits a steeply dipping cleavage; Berounka River valley near Višňová-Hájek. KRVC Křivoklát–Rokycany Volcanic Complex.

The KRVC consists of a package of subaeric lava flows, ignimbrites, and minor pyroclastic rocks up to 1500 m thick erupted in a relative, and greatly generalized, succession from aphanitic dacites, basaltic andesites and andesites to porphyritic dacite, rhyodacite, and rhyolite (Waldhausrová 1971). The petrogenesis of these volcanic rocks remains to be fully studied but may have involved melting of both mantle and crustal sources (including the Neoproterozoic basement graywackes) and assimilation and fractional crystallization in crustal magma chambers (Vidal et al. 1975; Patočka et al. 1993; Drost et al. 2004; Pin et al. 2007). A detailed account on paleomagnetism is given in Krs et al. (1988).

The KRVC trends NE–SW (Figs. IV.1c, IV.2a); its northwestern margin is defined by the base of the lowest lava flows (Fig. IV.2b) while along the southeastern margin the complex has presumably been truncated by a concealed (inferred) fault of uncertain sense of movement (Fig. IV.2a). The volcanic rocks are entirely devoid of any Variscan (Late Devonian to early Carboniferous) ductile deformation and have only been gently to moderately tilted in some places. The dip of the base of the complex or of internal lithologic contacts varies mainly between 0° and ~30° at most. In addition, the volcanic rocks and associated dikes commonly contain well-preserved vesicles implying no significant burial since the late Cambrian Period. Altogether this suggests that the particular basement block occupied by the KRVC has not been significantly buried or affected by the Variscan and post-Variscan deformations.

3. Field and structural observations on the dikes

3.1. Dikes in the northeastern extension of the KRVC (the Křivoklát area)

About thirty intermediate to felsic dikes were previously mapped in the Neoproterozoic basement around the northeastern end of the KRVC (Fig. IV.2a), suggesting not only their close spatial and temporal association with the late Cambrian extrusive rocks. In this study, we examined most of these dikes in detail, although only a few dikes appeared to be sufficiently well exposed for a magnetic fabric study and could be used as reliable and particularly telling examples for tectonic interpretations. These representative dikes (1) show a clear spatial relationship and are close to the KRVC, (2) are compositionally and texturally comparable to the volcanic rocks, (3) preserve intrusive contacts not altered or affected by Variscan or post-Variscan brittle deformation, and (4) have not been significantly tilted or rotated. The latter point is documented by subhorizontal host rock markers (bedding, lithologic contacts) in the overlying units (Fig. IV.2b).

Two major dikes were found to the northeast of the KRVC. One dike (station D10; Fig. IV.2a) composed of locally vesicular andesite, trends N–S, and is subvertical with thickness of about 15 m. Local topographic relief reveals that the dike exposure is located only several tens of meters below the flat base of the lowermost andesitic lavas of the KRVC (Fig. IV.2a) and hence it could be interpreted as a feeder to the overlying andesitic flows. The other ˙Sýkořice dike' is up to several tens of meters thick and extends for at least 10 km along strike from the eastern margin of the KRVC (Fig. IV.2a). Although locally curvilinear in plan view, the dike trends NE–SW and dips steeply to the ESE in its southern segment (Fig. IV.3a). The dike is composed of granite porphyry comparable to the younger rhyolite lavas along

the southeastern margin of the KRVC (Fig. IV.2a) and was thus interpreted as a feeder zone to these volcanic rocks as early as in the 1930s (Kodym 1936; see also Melichar 2004).

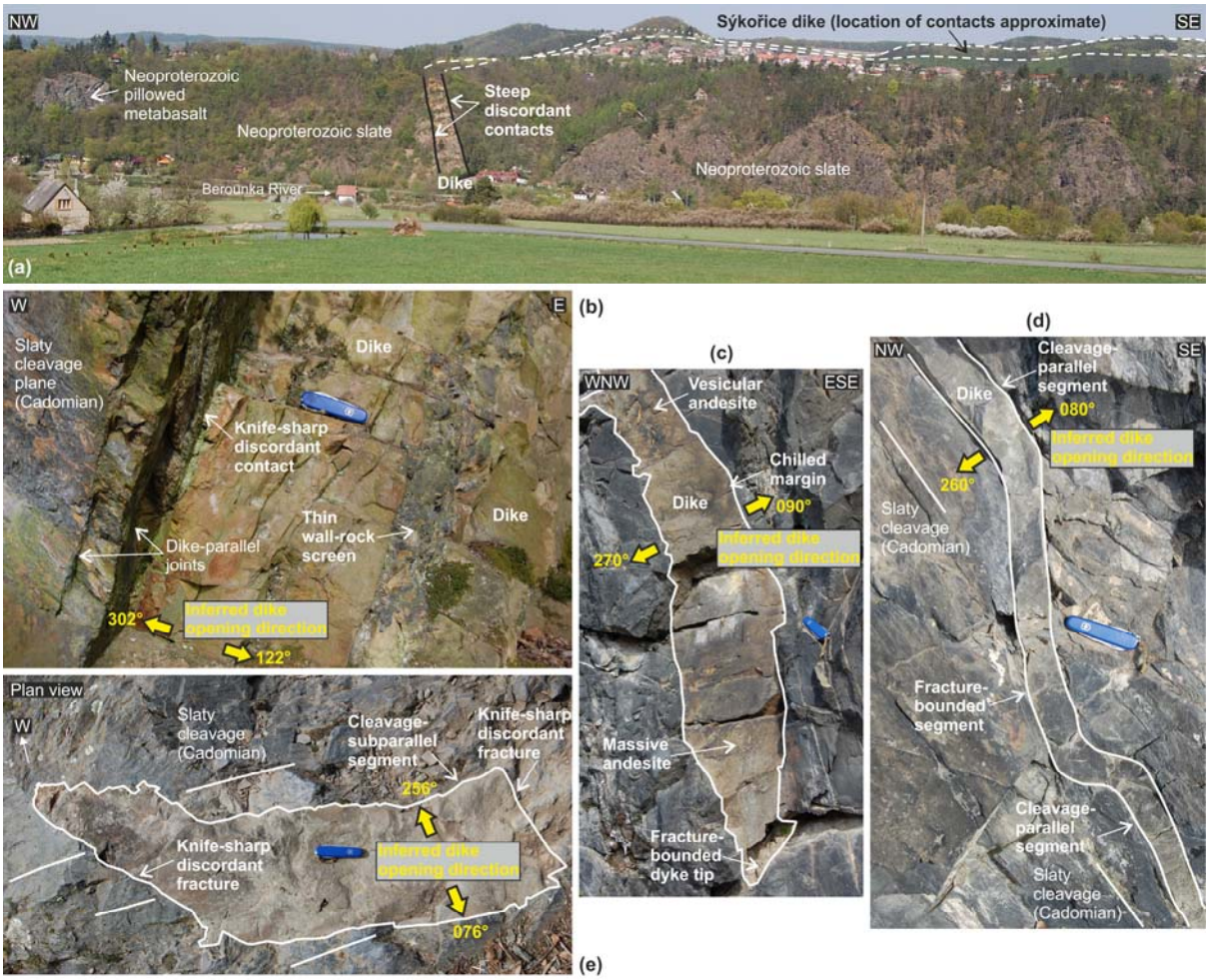

Fig. IV.3. Andesite and granite porphyry dikes associated with the Křivoklát–Rokycany Volcanic Complex. (a) Distant view on the Sýkořice granite porphyry dike; Berounka River valley northeast of Račice. (b) Close-up view on margin of a composite andesite dike that truncates the pre-existing (Cadomian) slaty cleavage in the host rock. Swiss Army penknife (9 cm long) for scale; Berounka River valley north Roztoky u Křivoklátu. (c–e) Close-up views on andesite dikes that consist of segments parallel to the host rock cleavage and fracture-bounded segments discordant to the cleavage. The dike margins indicate approximately E–W dilation during emplacement. Swiss Army penknife (9 cm long) for scale; Berounka River valley northeast of Roztoky u Křivoklátu.

In addition, we documented several minor, locally vesicular andesite dikes that intrude the Neoproterozoic basement only a few tens of meters away from the northernmost margin of the andesite lava flows (Fig. IV.2a). These dikes range from decimeters to several meters in thickness and display exceptionally well-exposed intrusive

contacts (Fig. IV.3b–e). The dikes are generally steep and strike N–S (Fig. IV.2a) and always have a knife-sharp contacts with the host rock. In detail, however, the contact geometry may vary from simple, planar and discordant to the pre-existing (Cadomian) slaty cleavage in the host rock (Fig. IV.3b) to more complex cases where the dikes are segmented, where they consist of cleavage-parallel segments alternating on a decimeter scale with segments bounded by brittle fractures (Fig. IV.3c, d). Irregularities in fitting the opposite dike margins back together yields dike opening directions ranging from 76°(256°) to 90° (270°) in three cases and 122°(302°) in one case (Fig. IV.3b–e). The former directions are remarkably consistent with the minimum eigenvector of normals to all the measured dikes (93° or 273°; Fig. IV.2a), which could represent a ˙statistical' principal extension direction assuming dike opening perpendicular to the dike margins.

3.2. Dikes in the southwestern extension of the KRVC (the Rokycany area)

Rare, scattered basic and felsic dikes and sills intrude both the Neoproterozoic and Lower Ordovician (Tremadocian to Sandbian) host rocks to the southwest of the KRVC (Figs. IV.1c, IV.4, IV.5). The lower Ordovican siliciclastic successions of the southwestern Prague Basin are also accompanied by voluminous submarine effusive and explosive volcanic rocks with the main peak in volcanic activity in the early Darriwillian Age (Fig. IV.4c). These volcanic rocks have exclusively within-plate transitional to MORB-like basaltic compositions (Fiala 1971; Patočka et al. 1993, 1994; Chlupáč et al. 1998), which contrasts with the predominantly intermediate to felsic subaerial volcanic rocks of the KRVC.

Compared to the above, the dikes have commonly been more significantly affected by post-emplacement (Variscan or later) alteration, fracturing, brittle reactivation along margins, and have been tilted by up to 45° as inferred from the attitude of nearby bedding.

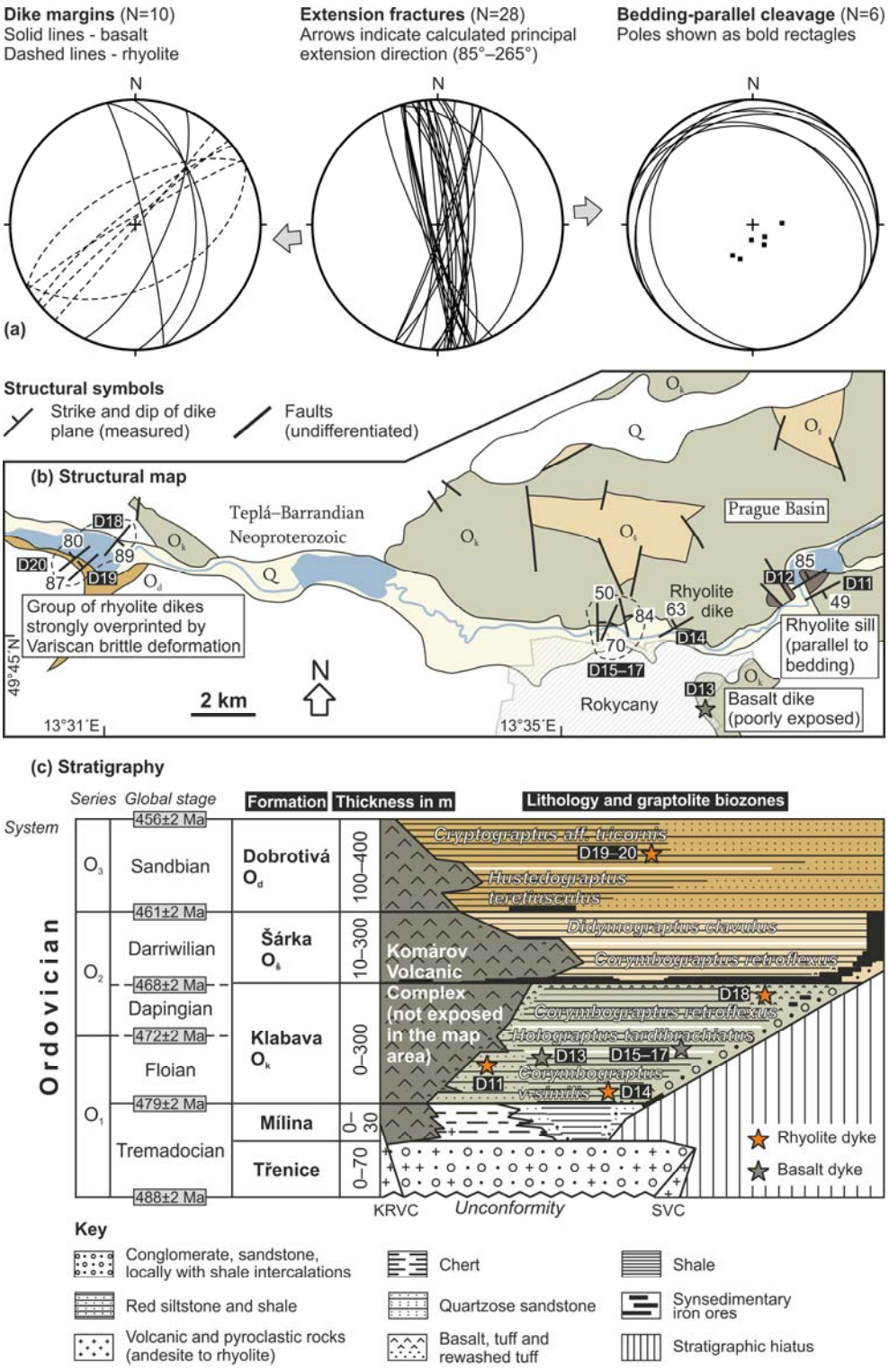

Fig. IV.4. (a) Stereonets (equal area, lower hemisphere projection) showing orientation of both basic and felsic dikes in the Rokycany area to the SSW of the Křivoklát–Rokycany Volcanic Complex, and extension fractures and host rock bedding-parallel cleavage associated with basalt dikes D15–17. (b) Simplified geological map showing location and setting of dikes in the Rokycany area; geology based on the Czech Geological Survey 1:50,000 map, sheet 12-33 Plzeň. (c) Detailed stratigraphic chart integrating lithostratigraphy and graptolite biostratigratigraphy for the Lower Ordovician volcano-sedimentary successions of the southwestern Prague Basin; modified after Kraft and Kraft (2003). The basalt and rhyolite dikes (indicated by stars) were found at various stratigraphic levels precisely constrained by graptolite biozones. Along with the Komárov volcanic complex, the dikes reveal a general compositional schift from felsic to basic during Floian to Sandbian, with the

peak of the submarine basaltic volcanism in the Dapingian to Darriwilian. Radiometric ages taken from the latest version of the International Stratigraphic Chart published in 2009 (www.stratigraphy.org).

Thus they provide poor information on the dike opening and regional principal extension directions. However, the dikes occur at various stratigraphic levels of the Ordovician rocks (Fig. IV.4c) while they change in composition from felsic to basic up the stratigraphic succession. In combination with the detailed graptolite biostratigraphy, these dikes are thus key markers in deciphering temporal changes in tectonic setting and magma composition during the progressive Cambro–Ordovician extension.

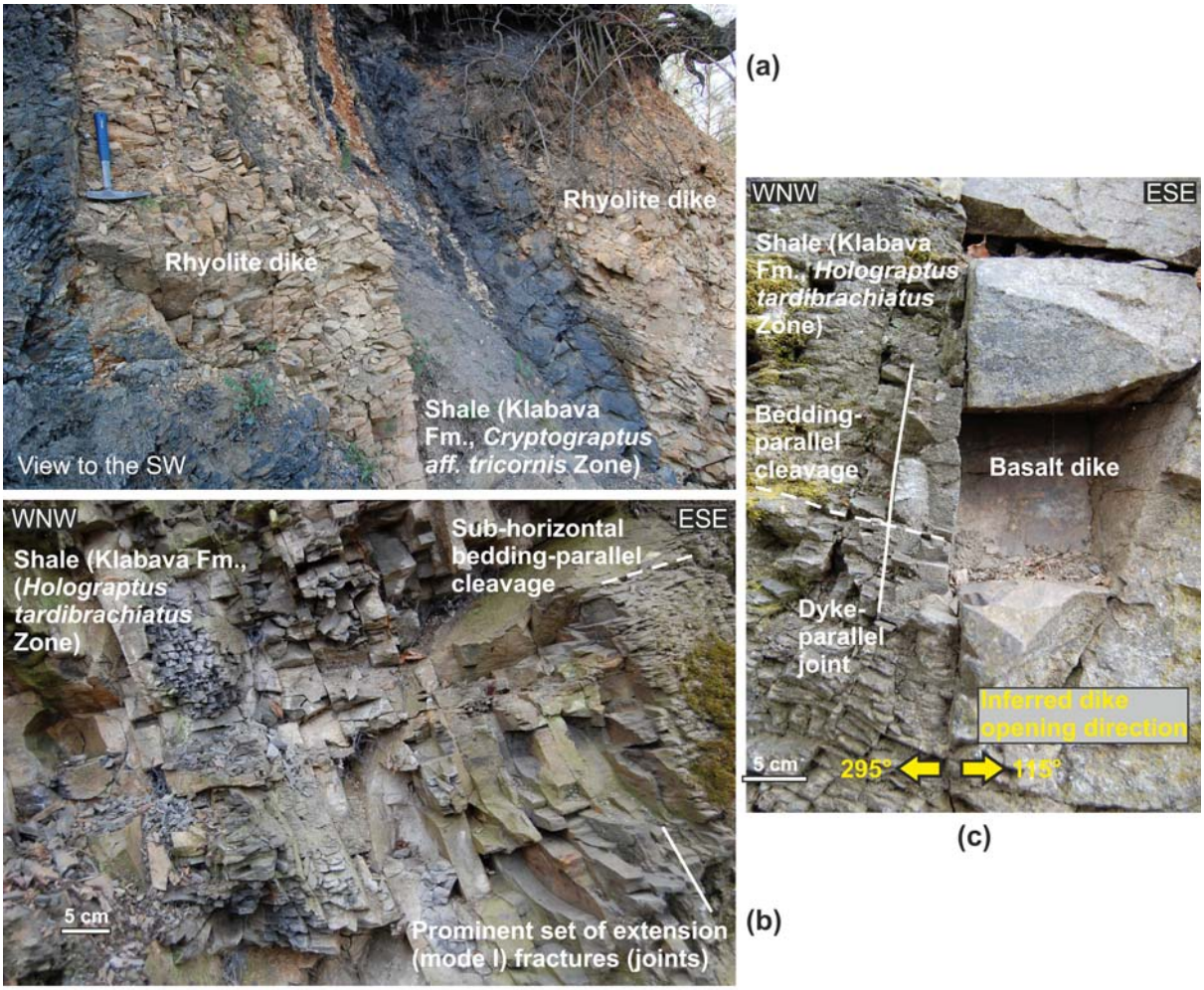

Fig. IV.5. (a) The youngest rhyolite dikes (D19–20) found in the Rokycany area. The dikes have been intensely overprinted by post-emplacement, presumably Variscan brittle deformation. Ejpovice; hammer for scale. (b) A prominent set of extension fractures associated with basalt dikes D15–17. (c) The sub-horizontal bedding-parallel cleavage indicates little Variscan tilt of the host rock and thus approximately original orientation of the

basalt dikes D15–D17; Husovy sady, Klabava River valley in Rokycany.

The stratigraphically lowest basalt dikes intrude various graptolite biozones of the Klabava Formation (Floian to Dapingian) together with rhyolite dikes (Fig. IV.4c). However, the rhyolite dikes disappear up the sequence with the stratigraphically highest rare rhyolite dikes found in the Cryptograptus aff. tricornis Zone of the Dobrotivá Formation (lower Sandbian; Fig. IV.4c). This is the youngest reported occurence yet of felsic dikes within the Lower Paleozoic of the Prague Basin, with the overlying successions being entirely dominated by basic or even mafic igneous rocks (Fiala 1971, 1976; Patočka et al. 1993, 1994; Chlupáč et al. 1998; Tasáryová et al. 2010a, b, 2011).

Only one locality in the area exposes basalt dikes (D15–17; Figs. IV.4a, b, IV.5c) that lack the Variscan and post-Variscan overprint. These dikes intrude shales of the Klabava Formation (the Hologratus tardibrachiatus Zone; Figs. IV.4c, IV.5b, c) that display subhorizontal fine-scale lamination and weak bedding-parallel cleavage (Figs. IV.4a, IV.5b) suggesting that they have not been significantly tilted. The dikes are steep, strike N–S, and are up to 70 cm thick. Importantly, the dikes are parallel to a prominent set of subvertical N–S-trending and closely spaced joints (mode I, extension fractures; Fig. IV.5b).

4. Magnetic fabric of selected dikes

Examining internal fabric in dikes by means of the anisotropy of magnetic susceptibility (AMS; for reviews and principles of the method see Hrouda 1982; Rochette et al. 1992; Tarling and Hrouda 1993; Borradaile and Jackson 2010) has been proven to be a valuable source of information on magma flow directions, growth history of dike-hosting fractures, and principal strain axes of regional extension during dike emplacement (e.g., Cañón-Tapia 2004; Cañón-Tapia and Chávez-Álvarez 2004; Chadima et al. 2009 and

references therein). In this contribution, we use the AMS to complement our structural observations and to describe quantitatively the internal (magnetic) fabric in selected dikes. The dikes were sampled only in the Křivoklát area northeast of the KRVC (Fig. IV.6) where they have not been significantly affected by Variscan and post-Variscan brittle deformation. The sampling strategy was to cover dikes of both andesite and rhyolite compositions, focusing on major dikes, and also to sample various domains across individual dikes. Importantly, the sampled dikes exhibit magmatic microstructure with no evidence of solid-state deformation (Fig. IV.7).

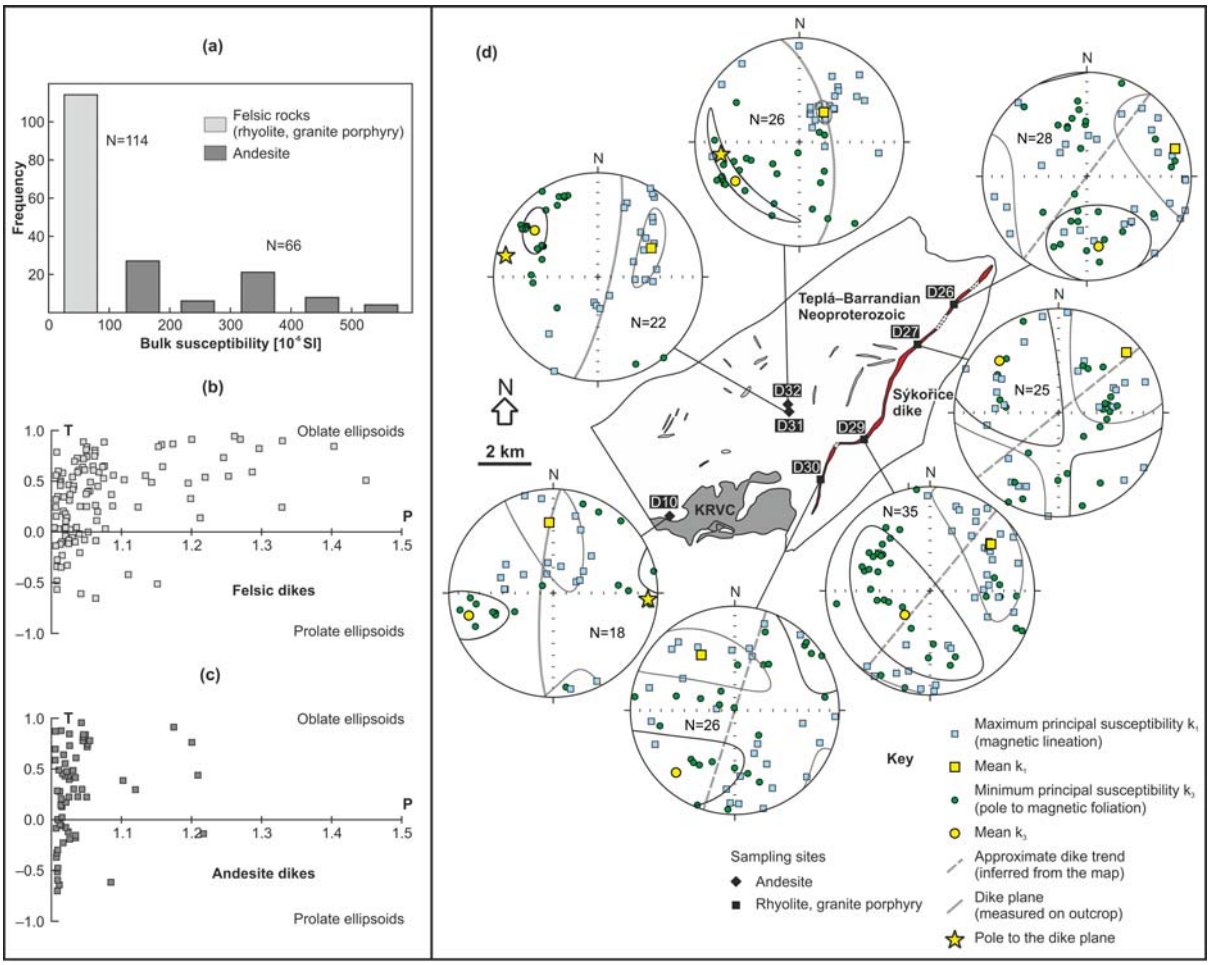

Fig. IV.6. Magnetic susceptibility data from andesite and granite porphyry dikes hosted in the Cadomian basement to the NNE of the Křivoklát–Rokycany Volcanic Complex. (a) Histogram of the bulk magnetic susceptibility for all analyzed specimens. (b) Magnetic susceptibility P–T plot for specimens from the Sýkořice dike (granite porphyry). (c) Magnetic susceptibility P–T plot for specimens from andesite dikes. (d) Map showing location of stations and orientation of the maximum and minimum principal susceptibilities in equal

area, lower hemisphere stereographic projections. KRVC Křivoklát–Rokycany Volcanic Complex.

The AMS is mathematically described as a symmetric second rank tensor, which can be visualized as an ellipsoid; its semi-axis lengths, k1 ≥ k2 ≥ k3, are termed the principal susceptibilities and their orientations, K1, K2, K3, are denoted as the principal directions. Such an ellipsoid defines a magnetic fabric where the maximum direction (K1) is denoted as magnetic lineation and the plane perpendicular to the minimum direction (K3) and containing the maximum and intermediate directions (K1, K2) is denoted as magnetic foliation. The AMS data are further characterized by several parameters (Tarling and Hrouda 1993, p. 18–19). We used the bulk susceptibility (kb = (k1 + k2 + k3) / 3), degree of anisotropy (P = k1 / k3), and anisotropy shape parameter (T = 2ln(k2 / k3) / ln(k1 / k3) – 1). If 1>T>0 then the AMS ellipsoid is oblate, whereas for 0>T>–1 the AMS ellipsoid is prolate. The AMS data are presented in a concise form in Fig. IV.6.

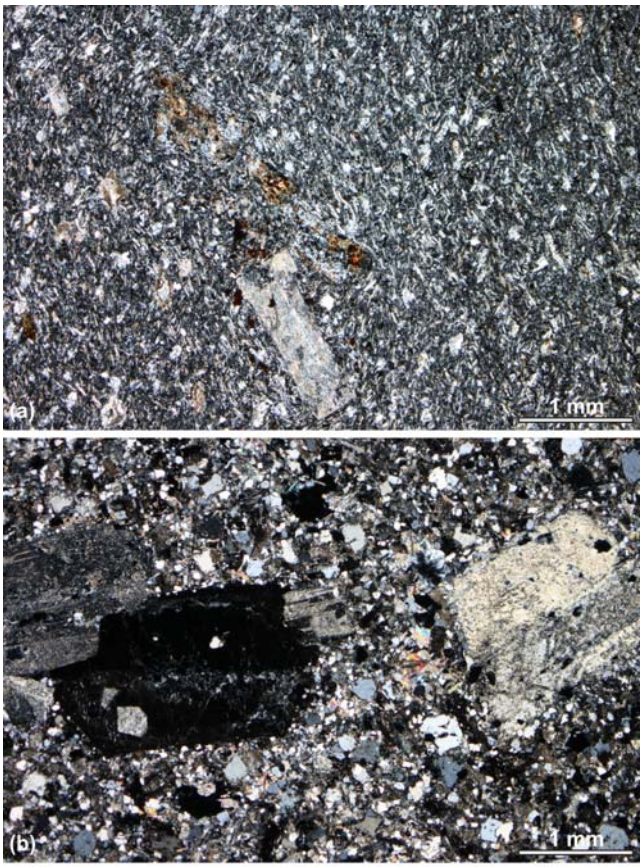

Fig. IV.7. Magmatic microstructures of the analyzed dike rocks. (a) Andesite with abundant euhedral phenocrysts of plagioclase set in an originally glassy but now largely sericitized and chloritized groundmass with minor opaque grains. The phenocrysts were aligned during magmatic flow. Dike D31 (see Fig. IV.6d for location), crossed polars. (b) Granite porphyry with largely sericitized subhedral K-feldspar phenocrysts set in a fine-grained holocrystalline groundmass with opaque grains. Dike D28 (see Fig. IV.6d for location), crossed polars.

The bulk susceptibility is low in all analyzed specimens but differs according to rock composition. Felsic rocks (rhyolite, granite porphyry) exhibit a restricted

range of the bulk susceptibility on the order of 10–5 SI (Fig. IV.6a) whereas andesitic rocks are characterized by an order of magnitude higher susceptibility ranging from 110 to 592 × 10–6 (Fig. IV.6a). In the felsic rocks, such low susceptibility values indicate that the AMS is dominated by paramagnetic minerals, most likely biotite. The andesites contain accessory magnetite, typically less than 1 % volume (Waldhausrová et al. 1971). Thus a minor ferromagnetic contribution to the total AMS cannot be excluded and may also account for the slightly elevated bulk susceptibility. Both the felsic and intermediate dikes exhibit predominantly oblate shapes of the AMS ellipsoid (79 and 29 % of the analyzed specimens, respectively; Fig. IV.6b, c). The degree of anisotropy is, however, noticeably elevated in the felsic dikes. One data group is characterized by the P parameter from 1.004 to 1.088 (78 % of the data) but one data group exhibits the P parameter from 1.104 to 1.449 (Fig. IV.6b). In contrast, the andesitic dikes mostly have the P parameter less than 1.05 (5% anisotropy, 83 % of specimens; Fig. IV.6c).

In terms of orientation of the principal susceptibilities, the N–S andesite dikes (stations D10, D31, D32) exhibit `normal' magnetic fabric of Rochette (1992, 1999). That is, magnetic foliations are subparallel to the dike plane whereas magnetic lineations, though scattered, lay along to the dike plane and plunge steeply to moderately (Fig. IV.6d). The Sýkořice granite porphyry dike, sampled at four stations along its strike (Fig. IV.6d), shows more complex magnetic fabric characterized by significantly more scattered principal susceptibilities at each station. In addition, the dike margins are not exposed, except at one outcrop (Fig. IV.3a). Thus the AMS cannot be precisely compared with the local contact orientation. Nevertheless, most magnetic lineations at all but one station (D30) tend to plunge shallowly with their mean orientations close to the approximate trend of the dike, and poles to magnetic foliations define broad bands about the mean lineation on stereonets

(Fig. IV.6d).

5. Facies development and depocentres in the Lower Ordovician successions of the southwestern Prague Basin

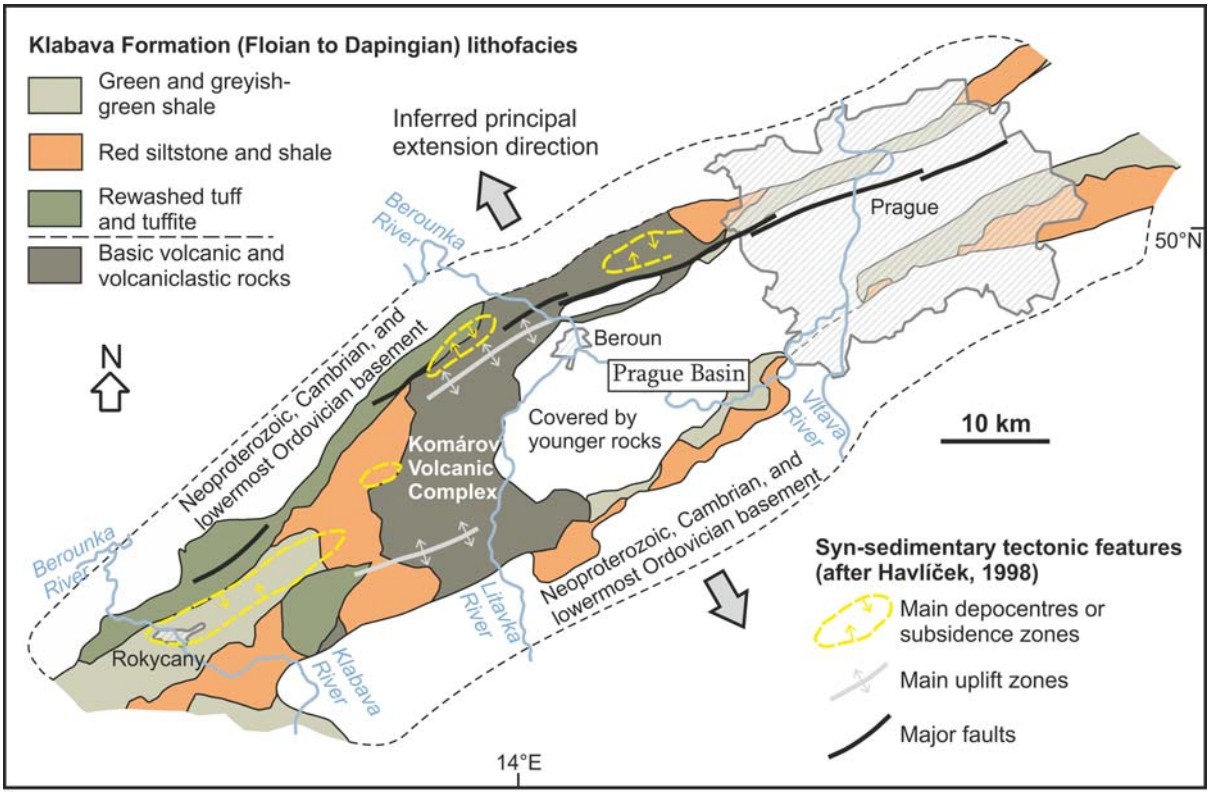

Fig. IV.8. Map of lithofacies of the Klabava Formation in the Prague Basin. The southwestern part of the basin, generally little affected by Variscan folding, exhibits NE–SW elongated depocenters and synsedimentary uplift zones (horsts) that are parallel to the basin axis and are compatible with NW–SE pure shear-dominated extension. Modified from Havlíček (1998).

In contrast to the N–S-trending dikes, the Lower/Middle Ordovician volcano-sedimentary successions were deposited on multiple fault-bounded basement blocks that generally strike NE–SW. This is best exemplified by the Lower/Middle Ordovician facies distribution in the southwestern Prague Basin (Fig. IV.7). The NE–SW strike is well-documented by the elongation (in plan view) of the basal Třenice and Mílina formations (see Fig. IV.4c for their lithology and stratigraphic position), which are of limited spatial extent

and form a narrow, NE–SW-trending belt (on the map) which was presumably terminated against an ancient shoreline (Havlíček 1981; see also fig. 18 in Havlíček 1998). The subsequent differentiation of the basin led to its along-strike segmentation into several independent narrow sub-basins, each with different specific facies patterns. The individual facies are elongated NE–SW (Fig. IV.8), parallel to the strike of the controlling master faults. Moreover, within the each sub-basin, shallower facies surrounded by deeper ones indicate transient paleohighs (Kraft and Kraft 2003) and the distribution of some indicative fossils reflects paleobathymetry (Kraft and Kraft 2006). In both cases, these features follow an overall basement architecture and indicate the NE–SW orientation of the faulted basement blocks.

6. Discussion

6.1. Interpretation of the early tectonic development of the Prague Basin

The structural and AMS data from the dikes combined with the detailed Lower Ordovician stratigraphy and lithofacies distribution suggest the following scenario for the Cambro–Ordovician extension in the Teplá–Barrandian Unit and for the initial development of the Prague Basin (Fig. IV.9).

First, we have shown that the andesitic dikes, correlated with the earliest volcanic rocks of the KRVC (younger than ca. 504 Ma), consistently indicate an E–W principal extension during dike emplacement (present-day coordinates are used throughout the manuscript) and dike opening nearly perpendicular to the dike margins (Figs. IV.2a, IV.3c–e). The same applies for a group of younger basalt dikes that intrude the Lower to Middle Ordovician rocks of the Klabava Formation (Figs. IV.4a, b, IV.5b, c). Moreover, the AMS

analysis revealed steep magnetic lineations and margin-subparallel magnetic foliations in the andesite dikes (`normal' magnetic fabric of Rochette 1992, 1999; Fig. IV.6d). Assuming the simplest relationship between the AMS and magma flow pattern (i.e. magnetic lineations parallel to the flow lines), magnetic fabric is consistent with steep magma flow and with the dikes representing feeder zones to the overlying andesitic lavas. In the absence of kinematic indicators, it can only be assumed that the magma flowed largely upwards.

A younger stage of igneous activity in the KRVC is represented by rhyolites (dated at 499 ± 4 Ma; Drost et al. 2004) and the Sýkořice granite porphyry dike (Figs. IV.2a, IV.3a). However, this dike reveals generally subhorizontal magnetic lineations consistent with lateral magma flow (Fig. IV.6d). The dike may thus be an off-shoot from an intrusive center (located beneath the KRVC?) rather than a feeder to the rhyolitic lavas. Sparse, volumetrically negligible felsic magmatism lasted till at least Sandbian time (>461 Ma; Fig. IV.4c), having been progressively replaced by voluminous, predominantly basic volcanism. In summary, the overall scarcity and narrowness of both the intermediate and felsic dikes indicate fairly minor E–W crustal extension during the late Cambrian (Fig. IV.9a).

An entirely different style and orientation of the principal extension is recorded by the depocenters and facies distribution in the Lower Ordovician of the Prague Basin (Fig. IV.8). Havlíček (1981) and Kraft and Kraft (2003) suggested that the Lower Ordovician siliciclastic and pyroclastic rocks were deposited in a NE–SW terndingrift setting. The basin developed on eroded Cadomian basement, interpreted as an accretionary wedge (Hajná et al. 2010, 2011), presumably through reactivation of inherited NE–SW-trending Cadomian faults. As documented by the facies distribution, the basin floor was composed of multiple basement blocks that consistently had shoulders on the SE side and their seaward side facing to the NW. Elongation of the variously subsided basement blocks and a linear array of

depocenters parallel to the basin axis are compatible with the NW–SE, pure shear-dominated extension during the initial basin development (Fig. IV.8; see also Kříž 1992). However, the total amount of extension remains unknown. As no deep oceanic lithosphere is exposed in the TBU, the extension in the Prague Basin probably did not develop into a wider oceanic domain but instead this narrow rift-related basin was underlain by thinned Cadomian crust (Fig. IV.8b).

Taken together, we interpret the dikes and Lower Ordovician rocks of the Prague Basin as recording a major kinematic change in the amount and directions of regional extension from E–W to NW–SE during the Tremadocian to Darriwilian interval (Fig. IV.9). Importantly, this reorientation overlaps with the compositional shift of igneous rocks from intermediate/felsic to basic and with the onset of voluminous basic submarine volcanism (Fig. IV.4c). The latter could be explained as a result of mantle upwelling and replacement of crustal or mixed mantle/crustal magma sources by decompression melting of the asthenospheric mantle as the amount of lithospheric extension increased (Patočka et al. 1993, 1994; Tasáryová et al. 2011; Ilnicki in press, and references therein).

6.2. Broader implications for the opening of the Rheic Ocean

Two end-member geodynamic causes have been recently proposed to explain the Cambro–Ordovician rifting along the northern Gondwanan margin: far-field slab pull due to subduction of the Iapetus Ocean beneath Laurentia or Avalonia (e.g., Nance et al. 2010), or retreat of an oceanic plate steeply subducting beneath northern Gondwana (e.g., Fernández et al. in press). Whereas these models invoke the opposite polarity and/or location of oceanic subduction, they identically assume a continuous transition from the Cadomian orogeny to transform and passive margin (e.g., Dörr et al. 2002; Nance et al. 2002, 2010; Linnemann et al. 2008a, b). However, a synthesis of the existing geological and

geochronologic data from the TBU points to a significantly more complex succession of tectonic events. The cessation of the Cadomian subduction and volcanic arc activity is well constrained in the TBU at around 560 Ma (Sláma et al. 2008). Subsequent slab break-off and gravitational collapse of the Cadomian orogen took place at ~550–540 Ma (Zulauf 1997; Zulauf et al. 1997, 1999), and its extensive erosion is indicated by marine and continental siliciclastic successions of the late Ediacaran and early Cambrian age, respectively (Patočka and Štorch 2004). As shown in this study, the incipient Cambro–Ordovician extension is recorded by the KRVC and associated dikes at around 504–495 Ma (Fig. IV.2a), or possibly earlier by ~524–505 Ma granitoid intrusions (Figs. IV.1c, IV.9a; Dörr et al. 1998), but the advanced extension accompanied by basaltic sea-floor volcanism commenced in the Floian to early Darriwilian ages (~461–479 Ma; Figs. IV.4c, IV.9b). In other words, there is at least a ~36–55 My, but more likely ~50–60 My, gap between the cessation of the Cadomian subduction-related arc magmatism and the onset of Cambro–Ordovician rifting. The tectonic regime of the TBU during this time span remains unclear. Zulauf et al. (1997, 1999) proposed an overall WSW–ENE dextral transtension during ca. 540–510 Ma whereas others argued for at least short periods of compression as documented by complex subsidence and uplift patterns of the individual fault-bounded basement blocks (Havlíček 1981; Patočka et al. 1994). Furthermore, the Floian to early Darriwilian extension and basaltic volcanism in the Prague Basin exactly overlap with the rift–drift transition of Avalonia from Gondwana (Prigmore et al. 1997; Verniers et al. 2002; Pollock et al. 2009; Thompson et al. 2010). The above implies that the both the western (Avalonia) and eastern (the Teplá–Barrandian) portions of the Avalonian–Cadomian orogenic belt began to break up nearly simultaneously, which is at variance with hypotheses suggesting diachronous opening of the Rheic Ocean from west to east (e.g., Linnemann et al. 2008a, b).

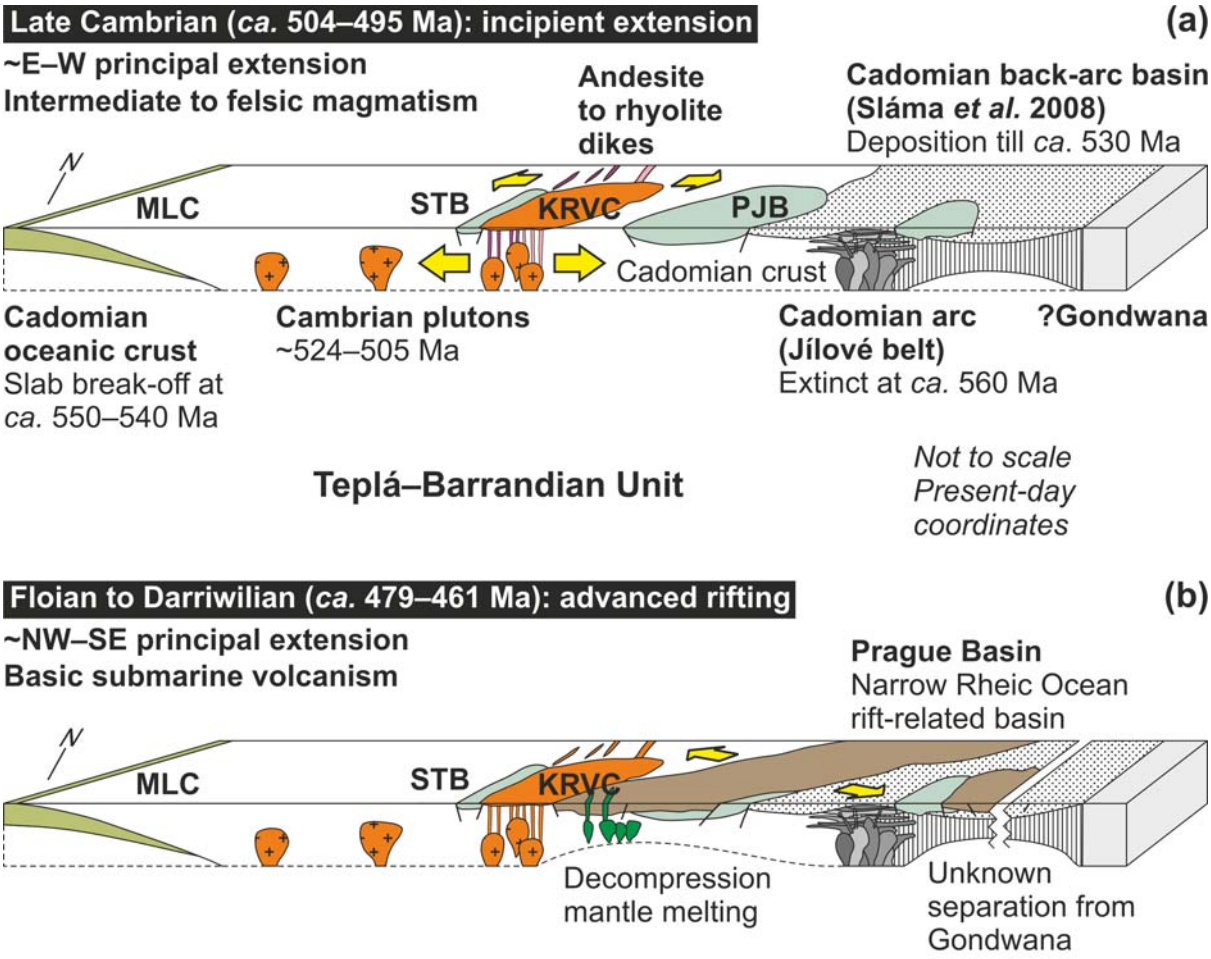

Fig. IV.9. Schematic cartoon to show the principal lithotectonic elements, the inferred styles and timing of extension, and its relation to magmatic events in the Teplá–Barrandian Unit during the late Cambrian a to early Ordovician times b. The Prague Basin is interpreted as a part of the Rheic Ocean rift system. KRVC Křivoklát–Rokycany Volcanic Complex, MLC Mariánské Lázně complex (ophiolite assemblage), PJB Příbram–Jince Basin, STB Skryje–Týřovice Basin.

Consequently, the data and interpretations presented above from the TBU are consistent with the following alternative scenario for the Cambro–Ordovician extension in the Avalonian–Cadomian belt. Given the time gap of several tens of millions of years between the termination of Cadomian subduction-related volcanism and the onset of advanced rifting in the TBU, we can exclude slab roll-back as a driving force for the extension. More likely, the extension was triggered by the onset of subduction of the Iapetus Ocean at around 510 Ma (Nance et al. 2010). This event may be recorded in the TBU by the emplacement of the andesitic dikes which indicate the E–W principal extension (Figs. IV.2a,

IV.3c–e, IV.9a). Furthermore, we suggest that the continuing slab-pull of the Iapetus subduction system may have created a wholesale and broadly coeval extension along the Avalonian–Cadomian belt, leading to complete detachment of Avalonia and its drift away from the Gondwana mainland. This later event was perhaps associated with the NW–SE principal extension in the TBU. Such a reorientation of the principal extension directions from E–W to NW–SE in the TBU during ca. 504–480 Ma could be explained in several ways. First, the entire TBU could have rotated anti-clockwise about vertical axis while the orientation of the far-field pull remained constant. Such an anti-clockwise rotation was inferred for the entire Gondwana by Nance et al. (2002). This explanation is, however, at variance with the existing paleomagnetic data that suggest exactly the opposite, clock-wise rotation of the TBU during the middle Cambrian to early Ordovician (Krs et al. 1997; Patočka et al. 2003). Second, the direction of the far-field slab-pull could have switched clock-wise while the TBU was fixed (attached to Gondwana?); this alternative is not constrained by any existing data. Last, the extension could have been heterogeneous with the principal directions varying from one location to another.

No doubt, Avalonia was entirely separated and drifted away from Gondwana (Nance et al. 2002, 2010; Pollock et al. 2009; Thompson et al. 2010). However, Linnemann et al. (2004) suggested that Saxothuringia remained attached or was close to the Gondwana mainland from the Neoproterozoic until the Carboniferous. A similar uncertainty exists regarding the amount of extension in the TBU and thus its displacement from Gondwana. The Prague Basin, located entirely inside the TBU and interpreted as an intracontinental Rheic Ocean rift-related basin, cannot represent an oceanic domain floored by oceanic lithosphere and separating the TBU from Gondwana. The clue is hidden along the southeastern margin of the TBU where a Cadomian (late Ediacaran to earliest Cambrian)

back-arc basin was presumed by Sláma et al. (2008). This already thinned Cadomian lithosphere could then serve as a locus for subsequent more advanced rifting, sea-floor spreading, and separation of the TBU from Gondwana during the late Cambrian and early Ordovician times. Indeed, a narrow oceanic domain referred to as `the Gföhl Ocean' was placed between the TBU and the adjacent Moldanubian unit (a portion of Gondwana?) in some plate-tectonic reconstructions (e.g., Franke 1999, 2000, 2006). However, no true ophiolite complexes were found along the Teplá–Barrandian/Moldanubian boundary suggesting that the TBU may have remained close to Gondwana during the early Palaezoic times, at variance with the `Perunica' far-travelled terrane model (e.g., Havlíček et al. 1994; Fatka and Mergl 2009).

7. Conclusions

Rare N–S andesitic dikes, interpreted as being feeders to the associated extrusive rocks of the Křivoklát–Rokycany Volcanic Complex (ca. 504–495 Ma), indicate that the principal crustal extension was approximately E–W in the Teplá–Barrandian Unit during the late Cambrian Period and that the magnitude of this extension was fairly minor. The andesitic magmatism evolved to rhyolitic which waned before the Tremadocian but lasted sporadically till at least Sandbian time (>461 Ma). In contrast, the lithofacies distribution and linear array of depocenters in the Lower Ordovician of the Prague Basin suggest deposition in a rift-related basin developed as a response to the NW–SE pure shear-dominated extension. This Tremadocian to Darriwilian kinematic change was accompanied by a flare-up of basic submarine volcanism, presumably resulting from decompression melting of the lithospheric mantle as the amount of extension increased.

We conclude that the incipient E–W extension in the Teplá–Barrandian Unit may have been triggered by the onset of subduction of the Iapetus Ocean at around 510 Ma.

Subsequently, the continuing slab-pull of the Iapetus subduction system may have created a broadly coeval, as opposed to diachronous, extension along the whole Avalonian–Cadomian belt between the Tremadocian and the Darriwilian. In the Teplá–Barrandian Unit, this event is perhaps manifested by the NW–SE-directed development of the Rheic Ocean rift-related Prague Basin. The amount of extension varied along the Avalonian–Cadomian belt, resulting either in the complete break-up and drift of some crustal fragments while other portions of the belt remained close to Gondwana. Indeed, the absence of ophiolite complexes inside and to the southeast of the Teplá–Barrandian Unit indicates that it may never have drifted far from the Gondwana mainland.

References

Borradaile GJ, Jackson M (2010) Structural geology, petrofabrics and magnetic fabrics (AMS, AARM, AIRM). J Struct Geol 32:1519–1551

Cañón-Tapia E (2004) Anisotropy of magnetic susceptibility of lava flows and dykes: a historical account. In: Martín-Hernández F, Lüneburg CM, Aubourg C, Jackson M (eds) Magnetic fabric: methods and applications. Geol Soc London Spec Publ 238:205–225

Cañón-Tapia E, Chávez-Álvarez MJ (2004) Theoretical aspects of particle movement in flowing magma: implication for the anisotropy of magnetic susceptibility of dykes and lava flows. In: Martín-Hernández F, Lüneburg CM, Aubourg C, Jackson M (eds) Magnetic fabric: methods and applications. Geol Soc London Spec Publ 238:227–249

Chadima M, Cajz V, Týcová P (2009) On the interpretation of normal and inverse magnetic fabric in dikes: examples from the Eger Graben, NW Bohemian Massif. Tectonophysics 466:47–63

Chichorro M, Pereira MF, Díaz-Azpiroz M, Williams IS, Fernández C, Pin C, Silva JB (2008) Cambrian ensialic rift-related magmatism in the Ossa-Morena Zone (Évora-Aracena metamorphic belt, SW Iberian Massif): Sm–Nd isotopes and SHRIMP zircon U–Th–Pb geochronology. Tectonophysics 461:91–113

Chlupáč I, Havlíček V, Kříž J, Kukal Z, Štorch P (1998) Palaeozoic of the Barrandian (Cambrian to Devonian). Czech Geological Survey, Prague, 183 pp

Crowley QG, Floyd PA, Winchester JA, Franke W, Holland JG (2000) Early Palaeozoic rift-related magmatism in Variscan Europe: fragmentation of the Armorican Terrane Assemblage. Terra Nova 12:171–180

Dornsiepen UF (1979) Rb–Sr whole rock ages within the European Hercynian, a review. Krystalinikum 14:33–49

Dörr W, Fiala J, Vejnar Z, Zulauf G (1998) U–Pb zircon ages and structural development of metagranitoids of the Teplá crystalline complex: evidence for pervasive Cambrian plutonism within the Bohemian massif (Czech Republic). Geol Rundsch 87:135–149

Dörr W, Zulauf G, Fiala J, Franke W, Vejnar Z (2002) Neoproterozoic to Early Cambrian history of an active plate margin in the Teplá–Barrandian unit – a correlation of U–Pb isotopic-dilution-TIMS ages (Bohemia, Czech Republic). Tectonophysics 352:65–85

Dostal J, Patočka F, Pin C (2001) Middle/Late Cambrian intracontinental rifting in the central West Sudetes, NE Bohemian Massif (Czech Republic): geochemistry and petrogenesis of bimodal volcanic rocks. Geol J 36:1–17

Drost K (2008) Sources and geotectonic setting of Late Neoproterozoic–Early Paleozoic volcano-sedimentary successions of the Teplá–Barrandian unit (Bohemian Massif): evidence from petrographical, geochemical, and isotope analyses. Geol Saxon 54:1–165

Drost K, Linnemann U, McNaughton N, Fatka O, Kraft P, Gehmlich M, Tonk C, Marek J (2004) New data on the

Neoproterozoic–Cambrian geotectonic setting of the Teplá–Barrandian volcano-sedimentary successions: geochemistry, U–Pb zircon ages, and provenance (Bohemian Massif, Czech Republic). Int J Earth Sci 93:742–757
Drost K, Romer RL, Linnemann U, Fatka O, Kraft P, Marek J (2007) Nd–Sr–Pb isotopic signatures of Neoproterozoic–Early Paleozoic siliciclastic rocks in response to changing geotectonic regimes: a case study from the Barrandian area (Bohemian Massif, Czech Republic). In: Linnemann U, Nance D, Kraft P, Zulauf G (eds) The evolution of the Rheic Ocean: from Avalonian–Cadomian active margin to Alleghenian–Variscan collision. Geol Soc Am Spec Paper 423:191–208
Etxebarria M, Chalot-Prat, Apraiz A, Eguíluz L (2006) Birth of a volcanic passive margin in Cambrian time: rift paleogeography of the Ossa-Morena Zone, SW Spain. Precambrian Res 147:366–386
Fatka O, Mergl M (2009) The 'microcontinent' Perunica: status and story 15 years
after conception. In: Bassett MG (ed) Early Palaeozoic peri-Gondwana terranes: new insights from tectonics and biogeography. Geol Soc London Spec Publ 325:65–101
Fatka O, Micka V, Szabad M, Vokáč V, Vorel T (2011) Nomenclature of Cambrian lithostratigraphy of the Skryje–Týřovice basin. Bull Geosci 86:841–858
Fernández RD, Castiñeiras P, Barreiro JG (in press) Age constraints on Lower Paleozoic convection system: magmatic events in the NW Iberian Gondwana margin. Gondwana Res, doi: 10.1016/j.gr.2011.07.028
Fiala F (1971) Ordovician diabase volcanism and biotite lamprophyres of the Barrandian. J Geol Sci Geol 19:7–97
Fiala F (1976) The Silurian doleritic diabases and ultrabasic rocks of the Barrandian area. Krystalinikum 12:47–77
Franke W (1999) Tectonic and plate tectonic units at the north Gondwana margin: evidence from the Central European Variscides. Abh geol Bundesanst 54:7–13
Franke W (2000) The mid-European segment of the Variscides: tectonostratigraphic units, terrane boundaries and plate tectonic evolution. In: Franke W, Haak V, Oncken O, Tanner D (eds) Orogenic processes: quantification and modelling in the Variscan Belt. Geol Soc London Spec Publ 179:337–354
Franke W (2006) The Variscan orogen in Central Europe: construction and collapse. In: Gee DG, Stephenson RA (eds) European litosphere dynamics. Geol Soc London Memoirs, 333–343
Furnes H, Kryza R, Muszynski A, Pin C, Garmann LB (1994) Geochemical evidence for progressive, rift-related early Palaeozoic volcanism in the western Sudetes. J Geol Soc London 151:91–109
Gebauer, D. 1993. Overview of geochronology. In: Bauberger W (ed) Explanations to the geological map of Bavaria 1:25000, sheet 6439 Tännesberg Bayer, 10–22
Geyer G, Elicki O, Fatka O, Zylinska A (2008) Cambrian. In: McCann T (ed) The geology of Central Europe. Volume 1: Precambrian and Palaeozoic. Geol Soc London, 155–202
Hajná J, Žák J, Kachlík V, Chadima M (2010) Subduction-driven shortening and differential exhumation in a Cadomian accretionary wedge: the Teplá–Barrandian unit, Bohemian Massif. Precambrian Res 176:27–45
Hajná J, Žák J, Kachlík V (2011) Structure and stratigraphy of the Teplá–Barrandian Neoproterozoic, Bohemian Massif: a new plate-tectonic reinterpretation. Gondwana Res 19:495–508
Havlíček V (1981) Development of a linear sedimentary depression exemplified by the Prague Basin (Ordovician–Middle Devonian; Barrandian area – central Bohemia). J Geol Sci Geol 35:7–48
Havlíček V, Vaněk J, Fatka O (1994) Perunica microcontinent in the Ordovician (its position within the Mediterranean Province, series division, benthic and pelagic associations). J Geol Sci Geol 46:23–56
Hrouda F (1982) Magnetic anisotropy of rocks and its application in geology and geophysics. Geophys Surv 5:37–82
Ilnicki S (in press) Amphibolites from the Szklarska Poreba hornfels belt, West Sudetes, SW Poland: magma genesis and implications for the break-up of Gondwana. Int J Earth Sci, doi: 10.1007/s00531-011-0727-2
Kachlík V, Patočka F (1998) Cambrian/Ordovician intracontinental rifting and Devonian closure of the rifting generated basins in the Bohemian Massif realms. Acta Univ Carol Geol 42:433–441
Kemnitz H, Romer RL, Oncken O (2002) Gondwana break-up and the northern margin of the Saxothuringian belt (Variscides of Central Europe). Int J Earth Sci 91:246–259
Keppie JD, Dostal J, Nance RD, Miller BV, Ortega-Rivera A, Lee JKW (2006) Circa 546 Ma plume-related dykes in the □1Ga Novillo Gneiss (east-central Mexico): evidence for the initial separation of Avalonia. Precambrian Res 147:342–353
Keppie JD, Dostal J, Murphy JB, Nance RD (2008) Synthesis and tectonic interpretation of the westernmost Paleozoic Variscan orogen in southern Mexico: from rifted Rheic margin to active Pacific margin. Tectonophysics 461:277–290
Kodym O (1936) Algonkium. In: Čepek L, Hynie O, Kodym O, Matějka A (eds) Explanations to the geological map of the Czechoslovak Republic, sheet 3952 Kladno, 11–20

Kraft P, Kraft J (2003) Facies of the Klabava Formation (?Tremadoc–Arenig) and their fossil content (Barrandian area, Czech Republic). In: Albanesi GL, Beresi MS, Peralta SH (eds) Ordovician from the Andes. INSUGEO, Serie Correlación Geologica 17:309–314
Kraft P, Kraft J (2006) Faunal responses to changes in the Prague Basin during Lower/Middle Ordovician. In: Sennikov NV, Kanygin OT, Obut OT, Kipriyanova TP (eds) Palaeogeography and global correlation of Ordovician events. Academic Publishing House Geo, Novosibirsk, 26–27
Kříž J (1992) Silurian field excursions: Prague Basin (Barrandian), Bohemia. National Museum of Wales, Geological Series, 13, 111 pp
Krs M, Krsová M, Pruner P, Havlíček V (1997) Palaeomagnetism, magnetism and palaeography of the Middle and Upper Cambrian rocks of the Barrandian area in the Bohemian Massif. J Geol Sci Appl Geophys 22:9–48
Krs M, Krsová M, Pruner P (1997) Palaeomagnetism and palaeogeography of the Variscan and pre-Variscan formations of the Bohemian Massif. In: Vrána S, Štědrá V (eds) Geological model of western Bohemia related to the KTB borehole in Germany, J Geol Sci Geol 47:162–173
Linnemann U, McNaughton NJ, Romer RL, Gehmlich M, Drost K, Tonk C (2004) West African provenance for Saxo-Thuringia (Bohemian Massif): did Armorica ever leave pre-Pangean Gondwana? U/Pb-SHRIMP zircon evidence and the Nd-isotopic record. Int J Earth Sci 93:683–705
Linnemann U, Gerdes A, Drost K, Buschmann B (2007) The continuum between Cadomian orogenesis and opening of the Rheic Ocean: constraints from LA-ICP-MS U–Pb zircon dating and analysis of plate-tectonic setting (Saxo-Thuringian zone, northeastern Bohemian Massif, Germany). In: Linnemann U, Nance D, Kraft P, Zulauf G (eds) The evolution of the Rheic Ocean: from Avalonian–Cadomian active margin to Alleghenian–Variscan collision. Geol Soc Am Spec Paper 423:61–96
Linnemann U, Pereira F, Jeffries TE, Drost K, Gerdes A (2008a) The Cadomian Orogeny and the opening of the Rheic Ocean: the diacrony of geotectonic processes constrained by LA-ICP-MS U–Pb zircon dating (Ossa-Morena and Saxo-Thuringian Zones, Iberian and Bohemian Massifs). Tectonophysics 461:21–43
Linnemann U, D'Lemos RS, Drost K, Jeffries T, Gerdes A, Romer RL, Samson SD, Strachan, RA (2008b) Cadomian tectonics. In: McCann T (ed) The geology of Central Europe. Volume 1: Precambrian and Palaeozoic. Geol Soc London, 103–154
López-Guijarro R, Armendáriz M, Quesada C, Fernández-Suárez J, Murphy JB, Pin C, Bellido F (2008) Ediacaran–Palaeozoic tectonic evolution of the Ossa Morena and Central Iberian zones (SW Iberia) as revealed by Sm–Nd isotope systematics. Tectonophysics 461:202–214
Melichar R (2004) Tectonics of the Prague Synform: a hundred years of scientific discussion. Krystalinikum 30:167–187
Murphy JB, Eguiluz L, Zulauf G (2002) Cadomian orogens, peri-Gondwanan correlatives and Laurentia–Baltica connections. Tectonophysics 352:1–9
Murphy JB, Pisarevsky SA, Nance RD, Keppie JD (2004) Neoproterozoic–Early Paleozoic evolution of peri-Gondwanan terranes: implications for Laurentia–Gondwana connections. Int J Earth Sci 93:659–682
Murphy JB, Gutiérrez-Alonso G, Nance RD, Fernández-Suárez J, Keppie JD, Quesada C, Strachan RA, Dostal J (2006) Origin of the Rheic Ocean: rifting along a Neoproterozoic suture? Geology 34:325–328
Nance RD, Linnemann U (2008) The Rheic Ocean: origin, evolution, and significance. GSA Today 18:4–12
Nance RD, Murphy JB, Keppie JD (2002) A Cordilleran model for the evolution of Avalonia. Tectonophysics 352:11–31
Nance RD, Miller BV, Keppie JD, Murphy JB, Dostal J 2007. Vestige of the Rheic Ocean in North America: the Acatlán Complex of southern Mexico. In: Linnemann U, Nance RD, Kraft P, Zulauf G (eds) The evolution of the Rheic Ocean: from Avalonian–Cadomian active margin to Alleghenian–Variscan collision. Geol Soc Am Spec Paper 423:437–452
Nance RD, Gutiérrez-Alonso G, Keppie JD, Linnemann U, Murphy JB, Quesada C, Strachan RA, Woodcock NH (2010) Evolution of the Rheic Ocean. Gondwana Res 17:194–222
Ortega-Obregon C, Murphy JB, Keppie JD (2010) Geochemistry and Sm–Nd isotopic systematics of Ediacaran–Ordovician, sedimentary and bimodal igneous rocks in the western Acatlán Complex, southern Mexico: evidence for rifting on the southern margin of the Rheic Ocean. Lithos 114:155–167
Patočka F, Smulikowski W (2000) Early Palaeozoic intracontinental rifting and incipient oceanic spreading in the Czech/Polish East Krkonoše/Karkonosze Complex, West Sudetes (NE Bohemian Massif). Geol Sudetica 33:1–15
Patočka F, Štorch P (2004) Evolution of geochemistry and depositional settings of Early Palaeozoic siliciclastics of the Barrandian (Teplá–Barrandian Unit, Bohemian Massif, Czech Republic). Int J Earth Sci 93:728–741
Patočka F, Vlašímský P , Blechová K (1993) Geochemistry of Early Paleozoic volcanics of the Barrandian basin (Bohemian Massif, Czech Republic): implications for paleotectonic reconstructions. Jahrb geol Bundesanst 136:873–896

Patočka F, Galle, A, Vavrdová M, Vlašímský P (1994) Early Paleozoic evolution of the Barrandian Terrane, Bohemian Massif, Czech Republic: paleotectonic implications of sedimentary, fossil and volcanic record. J Czech Geol Soc 39:82–83
Patočka F, Fajst M, Kachlík V (2000) Mafic–felsic to mafic–ultramafic Early Palaezoic magmatism of the West Sudetes (NE Bohemian Massif): the South Krkonoše Complex. Z geol Wiss 28:177–210
Patočka F, Pruner P, Štorch P (2003) Palaeomagnetism and geochemistry of Early Palaeozoic rocks of the Barrandian (Tepla-Barrandian Unit, Bohemian Massif): palaeotectonic implications. Phys Chem Earth 28:735–749
Pin C, Marini F (1993) Early Ordovician continental break-up in Variscan Europe: Nd–Sr isotope and trace element evidence from bimodal igneous associations of the Southern Massif Central, France. Lithos 29:177–196
Pin C, Kryza R, Oberc-Dziedzic T, Mazur S, Turniak K, Waldhausrová J (2007) The diversity and geodynamic significance of Late Cambrian (ca. 500 Ma) felsic anorogenic magmatism in the northern part of the Bohemian Massif: a review based on Sm–Nd isotope and geochemical data. In: Linnemann U, Nance RD, Kraft P, Zulauf G (eds) The evolution of the Rheic Ocean: from Avalonian–Cadomian active margin to Alleghenian–Variscan collision. Geol Soc Am Spec Paper 423:209–229
Pollock JC, Hibbard JP, Sylvester PJ (2009) Early Ordovician rifting of Avalonia and birth of the Rheic Ocean: U–Pb detrital zircon constraints from Newfoundland. J Geol Soc London 166:501–515
Prigmore JK, Butler AJ, Woodcock NH (1997) Rifting during separation of Eastern Avalonia from Gondwana: evidence from subsidence analysis. Geology 25:203–206
Rochette P, Jackson M, Aubourg C (1992) Rock magnetism and the interpretation of anisotropy of magnetic susceptibility. Rev Geophys 30:209–226
Rochette P, Aubourg C, Perrin M (1999) Is this magnetic fabric normal? A review and case studies in volcanic formations. Tectonophysics 307:219–234
Sánchez-García T, Quesada C, Bellido F, Dunning GR, del Tanago JG (2008) Two-step magma flooding of the upper crust during rifting: the Early Paleozoic of the Ossa Morena Zone (SW Iberia). Tectonophysics 461:72–90
Sánchez-García T, Bellido F, Pereira MF, Chichorro M, Quesada C, Pin C, Silva JB (2010) Rift-related volcanism predating the birth of the Rheic Ocean (Ossa-Morena zone, SW Iberia). Gondwana Res 17:392–407
Sláma J, Dunkley DJ, Kachlík V, Kusiak MA (2008) Transition from island-arc to passive setting on the continental margin of Gondwana: U–Pb zircon dating of Neoproterozoic metaconglomerates from the SE margin of the Teplá–Barrandian Unit, Bohemian Massif. Tectonophysics 461:44–59
Silva JB, Pereira MF (2004) Transcurrent continental tectonics model for the Ossa-Morena Zone Neoproterozoic–Paleozoic evolution, SW Iberian Massif, Portugal. Int J Earth Sci 93:886–896
Tarling DH, Hrouda F (1993) The magnetic anisotropy of rocks. Chapman and Hall, London, 217 pp
Tasáryová Z, Janoušek V, Frýda J (2010a) Whole-rock geochemistry of the Sv. Jan diabase sills and dykes in the Loděnice–Bubovice area. Geosci Res Reports 2009:256–258
Tasáryová Z, Janoušek V, Frýda J, Manda Š (2010b) Geochemistry of the Silurian effusive volcanics in the Prague Basin. In: Radoň M, Rapprich V (eds) 2. Volcanologic seminar of the Expert Group in Volcanology of the Czech Geological Society. Abstracts and field guide, 47–49
Tasáryová Z, Janoušek V, Frýda J, Manda Š, Štorch P, Trubač J (2011) Geochemical constraints on petrogenesis and geotectonic setting for Silurian basalts of the Prague Synform (Bohemian Massif). Mineral Mag 75:1988
Thompson MD, Grunow AM, Ramezani J (2010) Cambro–Ordovician paleogeography of the Southeastern New England Avalon Zone: implications for Gondwana breakup. Geol Soc Am Bull 122:76–88
Timmermann H, Dörr W, Krenn E, Finger F, Zulauf G (2006) Conventional and in situ geochronology of the Teplá Crystalline unit, Bohemian Massif: implications for the processes involving monazite formation. Int J Earth Sci 95:629–647
Venera Z, Schulmann K, Kröner A (2000) Intrusion within a transtensional tectonic domain: the Čistá granodiorite (Bohemian Massif) – structure and rheological modelling. J Struct Geol 22:1437–1454
Verniers J, Pharaoh T, André L, Debacker TN, de Vos W, Everaerts M, Herbosch A, Samuelson J, Sintubin M, Vecoli M (2002) The Cambrian to mid Devonian basin development and deformation history of Eastern Avalonia, east of the Midlands Microcraton: new data and a review. In: Winchester JA, Pharaoh TC, Verniers J (eds) Palaeozoic amalgamation of Central Europe. Geol Soc London Spec Publ 201:47–93
Vidal P, Auvray B, Charlot R, Fediuk F, Hameurt J, Waldhausrová J (1975) Radiometric age of volcanics of the Cambrian Křivoklát–Rokycany complex (Bohemian Massif). Geol Rundsch 64:563–570
von Raumer JF, Stampfli GM (2008) The birth of the Rheic Ocean–Early Palaeozoic subsidence patterns and subsequent tectonic plate scenarios. Tectonophysics 461:9–20
von Raumer JF, Stampfli GM, Borel G, Bussy F (2002) Organization of pre-Variscan basement areas at the north-

Gondwanan margin. Int J Earth Sci 91:35–52
von Raumer JF, Stampfli GM, Bussy F (2003) Gondwana-derived microcontinents – the constituents of the Variscan and Alpine collisional orogens. Tectonophysics 365:7–22
Waldhausrová J (1971) The chemistry of the Cambrian volcanics in the Barrandian area. Krystalinikum 8:45–75
Zulauf G (1997) From very low-grade to eclogite-facies metamorphism: tilted crustal sections as a consequence of Cadomian and Variscan orogeny in the Teplá–Barrandian unit (Bohemian Massif). Geotekt Forsch 89:1–302
Zulauf G, Dörr W, Fiala J, Vejnar Z (1997) Late Cadomian crustal tilting and Cambrian transtension in the Teplá–Barrandian unit (Bohemian Massif, Central European Variscides). Geologische Rundschau 86:571–584
Zulauf G, Schitter F, Riegler G, Finger F, Fiala J, Vejnar Z (1999) Age constraints on the Cadomian evolution of the Teplá Barrandian unit (Bohemian Massif) through electron microprobe dating of metamorphic monazite. Zeitschr deutsch geol Gesellsch 150:627–639

CHAPTER 5

Jaroslava Hajná, Jiří Žák, Václav Kachlík: Deciphering the Variscan tectonothermal overprint and deformation partitioning in the Cadomian basement of the Teplá–Barrandian unit, Bohemian Massif.

International Journal of Earth Sciences, in press, doi: 10.1007/s00531-012-0753-8

Deciphering the Variscan tectonothermal overprint and deformation partitioning in the Cadomian basement of the Teplá–Barrandian unit, Bohemian Massif

Jaroslava Hajná[1] , Jiří Žák[1] , Václav Kachlík[1], Martin Chadima[2, 3]

[1] *Institute of Geology and Paleontology, Faculty of Science, Charles University, Albertov 6, Prague, 12843, Czech Republic*

[2] *AGICO Inc., Ječná 29, Brno, 62100, Czech Republic*

[3] *Institute of Geology, Academy of Sciences of the Czech Republic, v.v.i., Rozvojová 269, Prague, 16500, Czech Republic*

Abstract

The Teplá–Barrandian unit (TBU) has long been considered as a simply bivergent supracrustal `median massif' above the Saxothuringian subduction zone in the Variscan orogenic belt. This contribution reveals a much more complex style of the Variscan tectonometamorphic overprint and resulting architecture of the Neoproterozoic basement of the TBU. For the first time, we describe the crustal-scale NE–SW-trending dextral transpressional Krakovec shear zone (KSZ) that intersects the TBU and thrusts its higher grade northwestern portion severely reworked by Variscan deformation over a southeastern very low grade portion with well preserved Cadomian structures and only brittle Variscan deformation. The age of movements along the KSZ is inferred as Late Devonian (~380–370 Ma). On the basis of structural, microstructural, and anisotropy of magnetic susceptibility

(AMS) data from the KSZ we propose a new synthetic model for the deformation partitioning in the Teplá–Barrandian upper crust in response to the Late Devonian to early Carboniferous subduction and underthrusting of the Saxothuringan lithosphere. We conclude that the Saxothuringian/Teplá–Barrandian convergence was nearly frontal during ~380–346 Ma and was partitioned into pure shear dominated domains that accommodated orogen-perpendicular shortening alternating with orogen-parallel high-strain domains that accommodated dextral transpression or bilateral extrusion. The syn-convergent shortening of the TBU was terminated by a rapid gravity-driven collapse of the thickened lithosphere at ~346–337 Ma followed by, or partly simultaneous with, dextral strike-slip along the Baltica margin-parallel zones, driven by the westward movement of Gondwana from approximately 345 Ma onwards.

Keywords: *Avalonian–Cadomian belt; Bohemian Massif; shear zone; Teplá–Barrandian unit; transpression; Variscan orogeny*

1. Introduction

The supracrustal Teplá–Barrandian unit (TBU) of the Bohemian Massif is one of the tectonostratigraphic terranes that originated in the Avalonian–Cadomian belt along the northern active margin of Gondwana during the late Neoproterozoic (Fig. V.1; e.g., Nance et al. 1991, 2010; Zulauf 1997; Dörr et al. 2002; Murphy et al. 2004; Drost et al. 2011 and references therein). The peri-Gondwanan terranes, now dispersed and incorporated in the Appalachian, Variscan, and Alpine orogenic belts, share many similarities in their protracted tectonic history. First, they record the Cadomian subduction, accretion, island arc growth, and deposition of intra-arc and back-arc siliciclastic sedimentary successions. Second, the

diachronous Cambro–Ordovician opening of the Rheic Ocean lead to the break-up of the Avalonian–Cadomian belt, and this event was associated with transtensional lithospheric thinning and intra-plate igneous activity (e.g., Crowley et al. 2000, 2002; Floyd et al. 2000; Dostal et al. 2001; Dörr et al. 2002; Pin et al. 2007). Third, later involvement of these terranes in younger orogens caused their extensive structural and metamorphic reworking and thus unravelling their structural history is generally fraught with large uncertainties (e.g., Neubauer 2002; Stampfli and Kozur 2006; Winchester et al. 2006).

The north-central TBU stands out, as it exposes exceptionally well the shallow level of the Cadomian crust that experienced no or only low grade Variscan regional metamorphism, and is thus a unique `archive' that records more than 300 M.y. of tectonic history. For a long time, however, the separation of the Cadomian deformations from the Variscan overprint in the Neoproterozoic basement of the TBU has been controversial, largely due to the lack of modern structural data. While the generally higher grade periphery of the TBU was studied in the 1990s (Cháb and Žáček 1994; Cháb et al. 1995; Zulauf 1997, 2001; Dörr et al. 1998), its north-central part remained largely unexplored although it offers an excellent opportunity to examine Cadomian vs. Variscan regional deformation and metamorphism, bracketed by the Cadomian angular unconformity and by the emplacement of Cambrian–Ordovician and Late Devonian intrusions.

The goal of this paper is to describe the geology, structures, deformational microstructures, and anisotropy of magnetic susceptibility (AMS) in this part of the TBU, with a special emphasis on the newly defined Krakovec shear zone (KSZ; Fig. V.1a). This transpressional shear zone is a principal orogen-scale tectonic feature that separates two crustal segments with contrasting Cadomian and Variscan deformation and metamorphic histories and delimits the northwestern front of Variscan ductile reworking in the TBU.

Putting our structural data from the KSZ into a broader context, we then discuss the timing and kinematics of plate convergence and complex deformation partitioning in the Bohemian Massif during the Late Devonian to early Carboniferous stages of the Variscan orogeny.

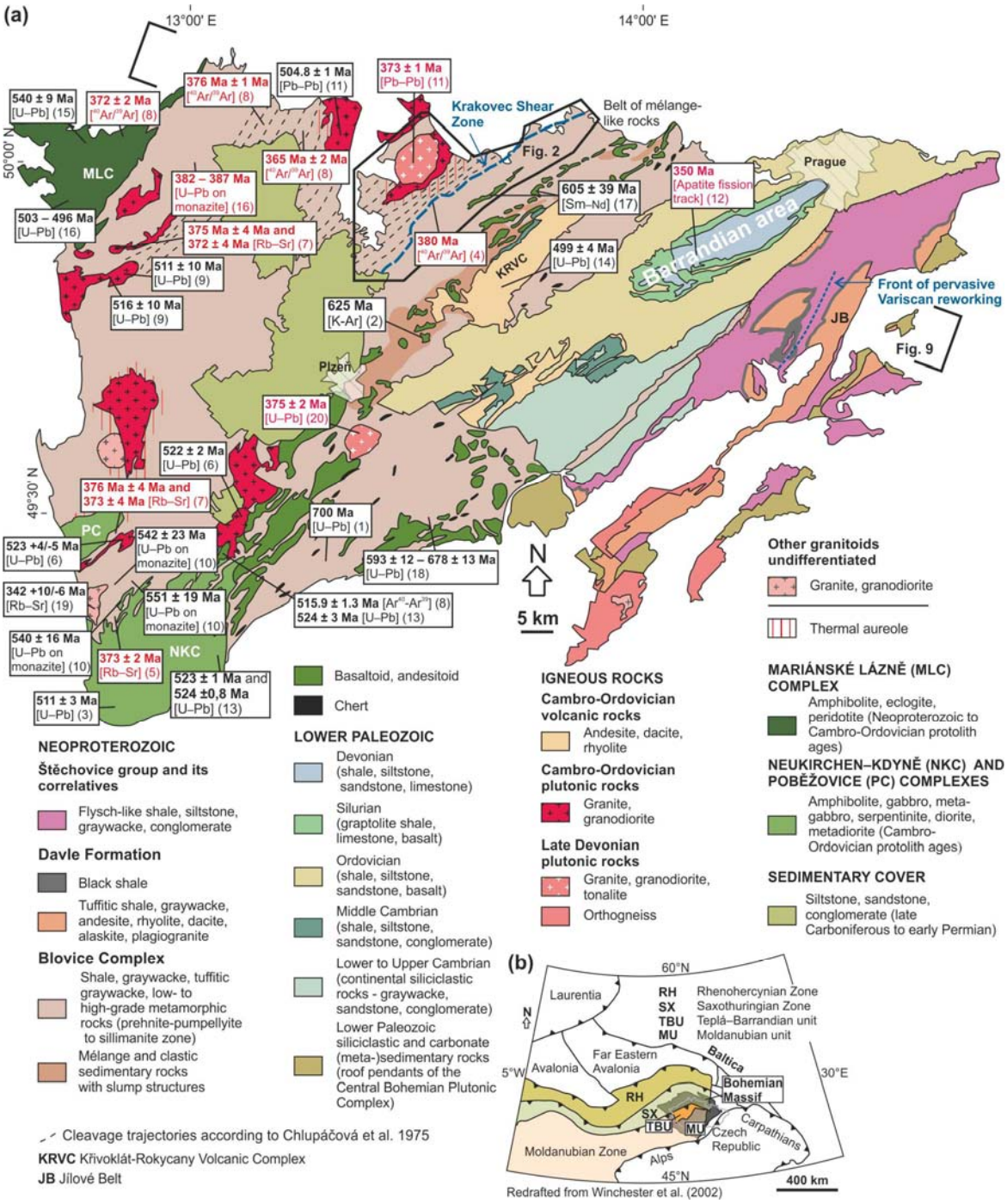

Fig. V.1. (a) Simplified geologic map of the Teplá–Barrandian unit (TBU) with geochronologic data mainly from its Neoproterozoic basement. The map was redrafted from 1:500,000 geologic map of the Czech Republic, published by the Czech Geological Survey in 2007. (b) Inset showing simplified lithotectonic zonation of the

Variscan orogenic belt in Western and Central Europe including main units and suture zones in the Bohemian Massif; modified after Winchester and PACE TMR Network Team (2002). Sources of geochronologic data: (1) Ordynec et al. (1984), (2) Dubanský (1984), (3) Gebauer (1993), (4) Dallmeyer and Urban (1994), (5) Košler et al. (1997), (6) Zulauf et al. (1997), (7) Glodny et al. (1998), (8) Dallmeyer and Urban (1998), (9) Dörr et al. (1998), (10) Zulauf et al. (1999), (11) Venera et al. (2000), (12) Filip and Suchý (2004), (13) Dörr et al. (2002), (14) Drost et al. (2004), (15) Timmerman et al. (2004), (16) Timmermann et al. (2006), (17) Pin and Waldhausrová (2007), (18) Drost et al. (2011), (19) Dörr and Zulauf (2010), (20) Žák et al. (2011a).

2. Geologic setting

The following geologic and lithologic units and principal tectonic features in the north-central TBU are relevant to the present study:

(1) To the northwest of the KSZ (Fig. V.2), the Neoproterozoic basement is dominated by chlorite–sericite and locally graphitic phyllites with minor intercalations of strongly deformed (`phyllitized') graywackes and several NE–SW-elongated bodies of mostly tholeiitic metabasalts (Fig. V.2). Mineral association chlorite + muscovite + albite + quartz ranks the phyllites to the chlorite zone whereas metamorphic grade increases up to the sillimanite zone in the western TBU (Cháb and Žáček 1994; Cháb et al. 1995). Although the age of this Barrovian metamorphism has been debated, the muscovite cooling ages of the whole-rock phyllite samples fall consistently between ~380–365 Ma in this part of the TBU (Dallmeyer and Urban 1994, 1998).

(2) The phyllites were intruded by the shallow-level mid-/late Cambrian Tis granite dated at 504.8 ± 1.1 Ma (Pb–Pb single zircon evaporation method, Venera et al. 2000; Fig. V.2). The pluton is exposed in three isolated outcrops at the present-day erosion level but is interpreted as a continuous tabular intrusion now largely concealed beneath the Permo–Carboniferous cover (Fig. V.1a; Chlupáčová et al. 1975; Kopecký et al. 1997; Venera et al. 2000; Klomínský et al. 2010). The Tis granite has been overprinted by widespread brittle deformation and alteration under lower greenschist facies conditions (Klomínský 1963; Chlupáčová et al. 1975; Kopecký et al. 1997). The age of this deformation is most likely Late

Devonian and is constrained at ~380 Ma by an Ar–Ar muscovite age from the host phyllites (Dallmeyer and Urban 1994).

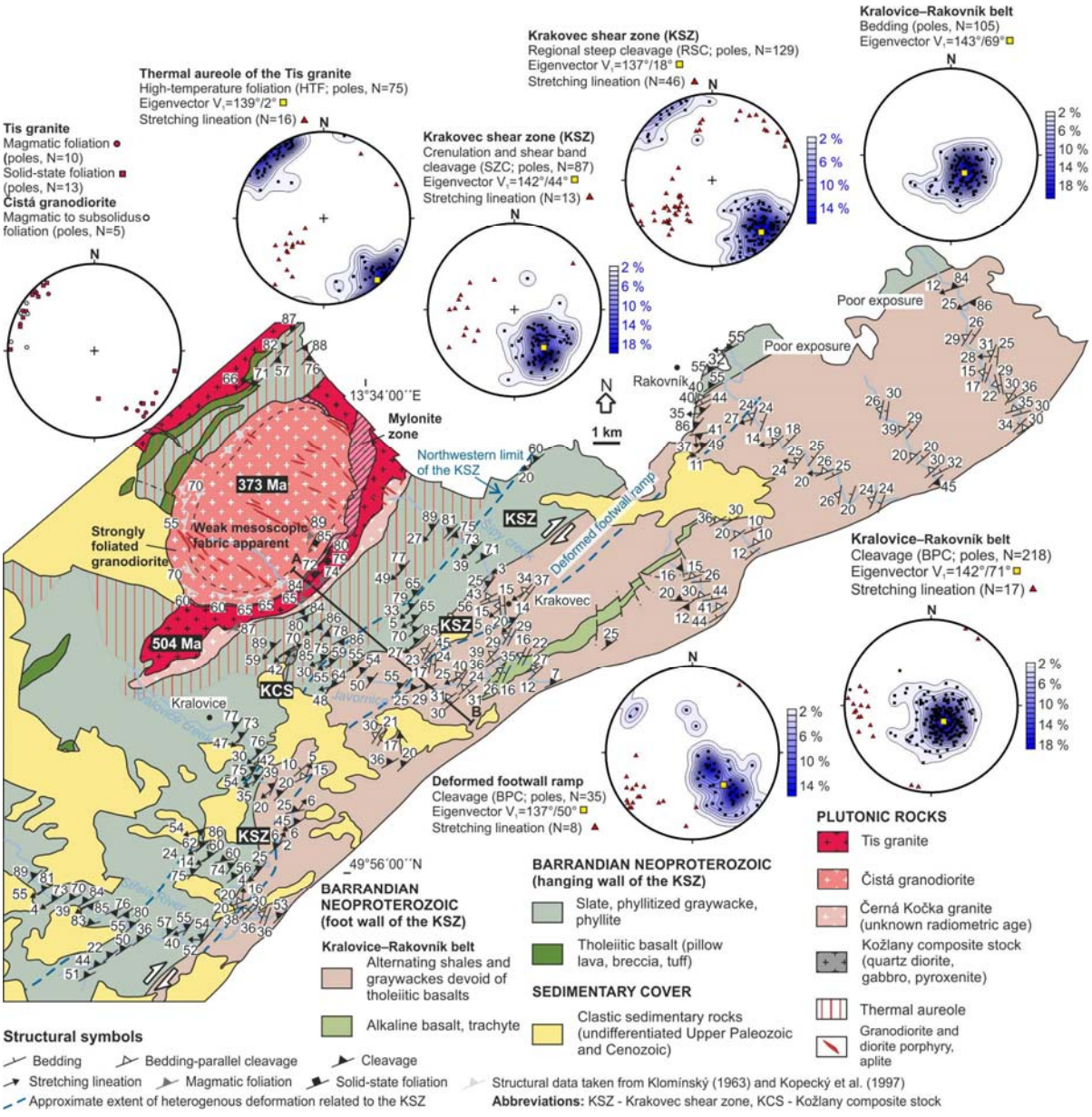

Fig. V.2. Structural map of the north-central Teplá–Barrandian unit. Stereonets (equal area projection, lower hemisphere) show orientation of bedding, cleavage, stretching lineation in the Neoproterozoic sedimentary and metasedimentary rocks, and magmatic, solid-state and subsolidus foliations in the Cambrian and Late Devonian granitoids (the Tis granite and the Čistá granodiorite, respectively). Geology based on the Czech Geological Survey maps 1:50,000, sheets 12-31 Plasy, 12-13 Jesenice, 12-14 Rakovník, and 12-32 Zdice.

(3) To the southeast, Devonian (373.1 ± 1.1 Ma, Pb–Pb single zircon evaporation method, Venera et al. 2000) Čistá granodiorite pluton intrudes across both the

Neoproterozoic phyllites and the southeastern irregularly shaped exposure of the Tis granite (Figs. V.1a, V.2). In plan view, the Čistá pluton has an elliptical shape with its long axis oriented NE–SW. Gravimetric data, verified by several boreholes, indicate that the shape of the pluton at depth is a steep-sided stock (Kopecký et al. 1997). The contact of the Čistá pluton with its wall-rock is generally steep and dips inwards or outwards in different parts of the pluton. The southwestern end of the pluton is concealed beneath the Carboniferous cover, while its northwestern margin is poorly exposed and is parallel to the NE–SW-trending lithologic contacts in the Neoproterozoic host rock. The Čistá granodiorite/Tis granite contact is delineated by a high-temperature mylonite to cataclasite and associated alkaline-metasomatic zone (Fig. V.2; Klomínský 1963; Kopecký et al. 1970; Kopecký et al. 1997; Venera et al. 2000).

(4) The southeastern margin of the Tis granite is rimmed by an up to ~800 m thick sheet-like body of the fine- to medium-grained leucocratic muscovite ± tourmaline granite (Fig. V.2; referred to as the Černá Kočka granite after Klomínský et al. 2010). The contact of the granite against the Neoproterozoic metapelites strikes NE–SW and dips steeply to the SE. Age of this granite remains unclear (Klomínský 1963; Kopecký 1987).

(5) Abundant dikes of aplite and granodiorite and diorite porphyry cut across all the granites, but are mostly confined to the Čistá granodiorite (Fig. V.2). The dikes are generally steep and strike NW–SE, thus are oriented at a high angle to the long axis of the Čistá pluton.

(6) The thermal aureole in the Neoproterozoic wall-rock around the granitoids is ~200–3000 m wide (Fig. V.2) and is defined mostly by hornfels and spotted schists. As the granitoids make up an intrusive complex consisting of multiple intrusions of different geometry and size and was assembled over a time span of >130 M.y., it is difficult to separate the thermal effect on wall-rock from each component intrusion. While the

northwestern segment of the aureole may reflect superimposed thermal effects from both the Tis granite and Čistá granodiorite, the southeastern areally extensive segment was predominantly affected by the Tis granite (Fig. V.2).

(7) The Krakovec shear zone (Fig. V.2) is a major tectonic feature to the southeast of the Tis pluton. This zone is about 2 km wide (in plan view), trends NE–SW, and is interpreted as a transpressional dextral shear zone that roughly coincides with the chlorite-in isograd of Cháb and Žáček (1994) and Cháb et al. (1995). To the northeast and southwest, the shear zone is concealed beneath Permo–Carboniferous cover (Figs. V.1a, V.2) so its true extent can not be determined. However, the along-strike length of its exposed part is about 35 km, suggesting that it is a first-order crustal-scale structure. The shear zone dips moderately to the northwest (beneath the Tis pluton and its host) and thrusts the phyllites over the southeasterly significantly less deformed graywackes. Sample from locality 9 in Dallmeyer and Urban (1994) dated using the $^{40}Ar/^{39}Ar$ method from within the KSZ constrains the age of thrusting to about 380 Ma.

(8) The NE–SW-trending Kralovice–Rakovník belt to the southeast of the KSZ (Fig. V.2) is an unmetamorphosed to very low grade bedded sequence that consists of up to 1–2 m thick graywacke beds alternating rhythmically with much thinner (cm to dm) slate and siltstone interbeds. Sedimentary structures (graded bedding, fine-scale lamination, subaquatic slumps and mélanges) are well preserved.

3. Mesoscopic structures

It has been shown that in areas of superposed heterogeneous deformations, the designation of foliations (e.g., S1, S2,..., Sn) to a particular succession of deformation phases (e.g., D1, D2,..., Dn) may be meaningless (e.g., Park 1969; Williams 1985; Tobisch and Paterson 1988; Lüneburg and Lebit 1998; Burg 1999; Potts and Reddy 1999; Miller et al.

2005; Passchier and Trouw 2005, p. 3–5; Forster and Lister 2008). As greatly exemplified by the north-central TBU, the foliations cannot be correlated in many cases, or even multiple foliations showing complex overprinting relationships occur in a single thin section. Therefore, we use acronyms to distinguish specific foliations dealt with in the text and our descriptions given below do not imply any regional temporal succession of the foliation development.

3.1. Structures in the granitoids and in their aureole

As detailed in several studies (Klomínský 1963; Kopecký et al. 1997; Chlupáčová et al. 1975; Žák et al. 2011a), the Čistá pluton exhibits a concentric (`onion-skin') internal structure (Fig. V.2). Its central, more felsic part shows weak or macroscopically not discernible magmatic fabric passing into the outer granodiorite with strong sub-vertical margin-parallel magmatic to solid-state foliation associated with variably oriented hornblende lineation. A thorough magnetic fabric analysis by Chlupáčová et al. (1975) revealed steep margin-parallel magnetic foliations and gently to steeply plunging magnetic lineations in the pluton.
The Tis granite southeast of the Čistá granodiorite shows a steep fabric gradient. In an up to 1000 m wide zone along the contact with the granodiorite (Fig. V.2), the Tis granite has been affected by pervasive solid-state deformation and transformed into mylonite with subvertical foliation that strikes NE–SW and dips to the NW or SE. Farther to the southeast, the ductile mylonitic fabric abruptly disappears and the Tis and Černá Kočka granites exhibit a well-preserved magmatic fabric.

The hornfelses and spotted schists in the thermal aureole southeast of the intrusive complex are dominated by a homogeneously oriented, steep to vertical pervasive high-temperature foliation (HTF) that strikes NE–SW (sub-parallel to the intrusive contact) and dips to the NW

or SE (Fig. V.2). A lineation is macroscopically not apparent, suggesting that the foliation is related to an oblate fabric ellipsoid. To the north of the intrusive complex, the foliation has a similar orientation to that along its southeastern margin, however, it exhibits a highly variable orientation in some places, and several generations of superposed crenulations are common.

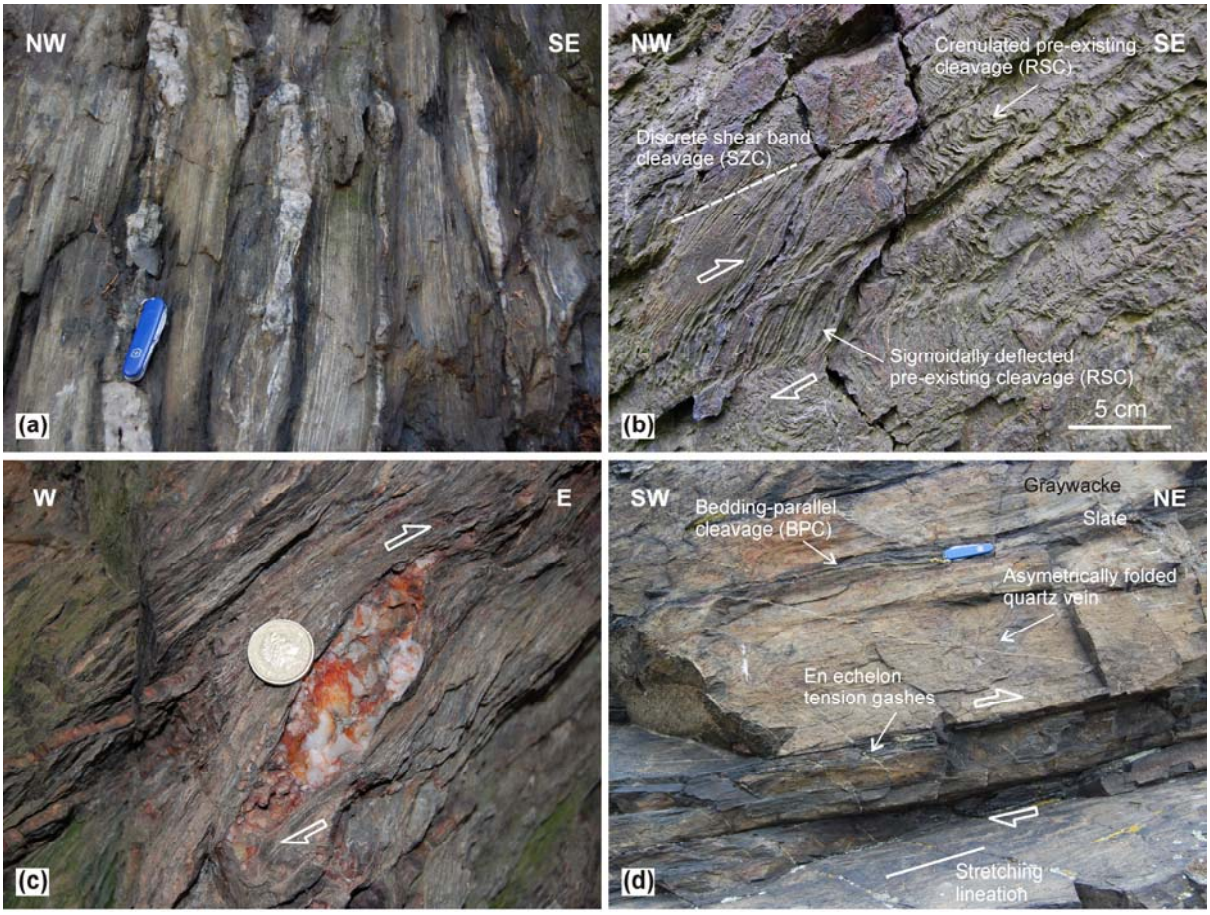

Fig. V.3. Characteristic structural features of the thermal aureole of the Tis pluton, phyllites outside the aureole, the Krakovec shear zone, and the footwall graywackes beneath the Krakovec shear zone. (a) Regional steep cleavage (RSC) in phyllite with cleavage-parallel veins and boundins of vein quartz, 1 km SSE of Plasy. Swiss Army knife is 9 cm long. (b) Sigmoidally deflected and intensely crenulated pre-existing cleavage (RSC) in the shear zone cleavage (SZC), phyllite of the Krakovec shear zone, 1.3 km SSE of Podšibenský Mlýn near Kralovice. (c) Asymmetric quartz lens in phyllite of the Krakovec shear zone indicating top-to-the-E kinematics, 1.3 km SSE of Podšibenský Mlýn near Kralovice. View is on cleavage-perpendicular and lineation-parallel section. Coin (23 mm in diameter) for scale. (d) Gently dipping graywacke beds rhythmically alternating with thin slate interbeds. En echelon tension gashes and asymmetrically folded quartz veins indicate of top-to-the-NE kinematics; 300 m NW of Krakovec. Swiss Army knife is 9 cm long.

3.2. Structures outside the aureole and in the Krakovec shear zone

The host rock outside the thermal aureole is characterized by a complex superposition of multiple cleavages. To the south and southeast, the phyllites and phyllitized graywackes are dominated by a regional steep cleavage (RSC) that is continuous on the macroscopic scale, largely obliterates bedding, and is developed in the chlorite zone. The cleavage is subvertical and strikes NE–SW (Figs. V.2, V.3a) and is associated with a mineral lineation that plunges moderately to the SW. This plane-strain fabric thus contrasts with the oblate fabric in the thermal aureole.

Approaching the shear zone, the RSC continuously reorients to shallower dip (to the NW), maintains the same strike (Fig. V.2), and bears the SW-plunging mineral lineation. Within the shear zone, this continuous RSC is overprinted by a discrete shear-band and crenulation cleavage (SZC; shear zone cleavage) that dips shallowly to moderately to the NW and strikes NE–SW, the associated lineation plunges moderately to the SW to WNW (Fig. V.2). The pre-existing RSC is either sigmoidally deflected or is intensely crenulated within the lithons between the adjacent shear planes (Fig. V.3b). Sigmoidal deflection of the pre-existing cleavage indicates regionally consistent top-to-the-E kinematics, in concert with other small-scale kinematic indicators (asymmetric minor folds, folded quartz veins, asymmetric quartz lenses; Fig. V.3c).

3.3. Structures in the footwall graywackes

In the Kralovice–Rakovník belt in the footwall of the KSZ, bedding dips gently to moderately to the W to NW (Figs. V.2, V.3d). This implies that any deformation (Cadomian or Variscan) was generally weak in the graywackes, resulting only in the tilt of bedding and formation of the bedding-parallel cleavage (BPC) preferentially in the thin slate interbeds. However, in a ~1 km wide (in plan view) zone below the KSZ (Fig. V.2), both the bedding and

cleavage steepen (dip increases to about 40°) and the graywackes exhibit a stretching lineation (Fig. V.3d) defined by elongated feldspar and biotite clasts. The lineation plunges gently to the SW and is thus roughly parallel to mineral lineation in the structurally higher phyllites of the KSZ. En echelon quartz veins and asymmetric minor folds in the graywackes (Fig. V.3d) are consistent with the dextral top-to-the-NE movement of the hanging-wall phyllites.

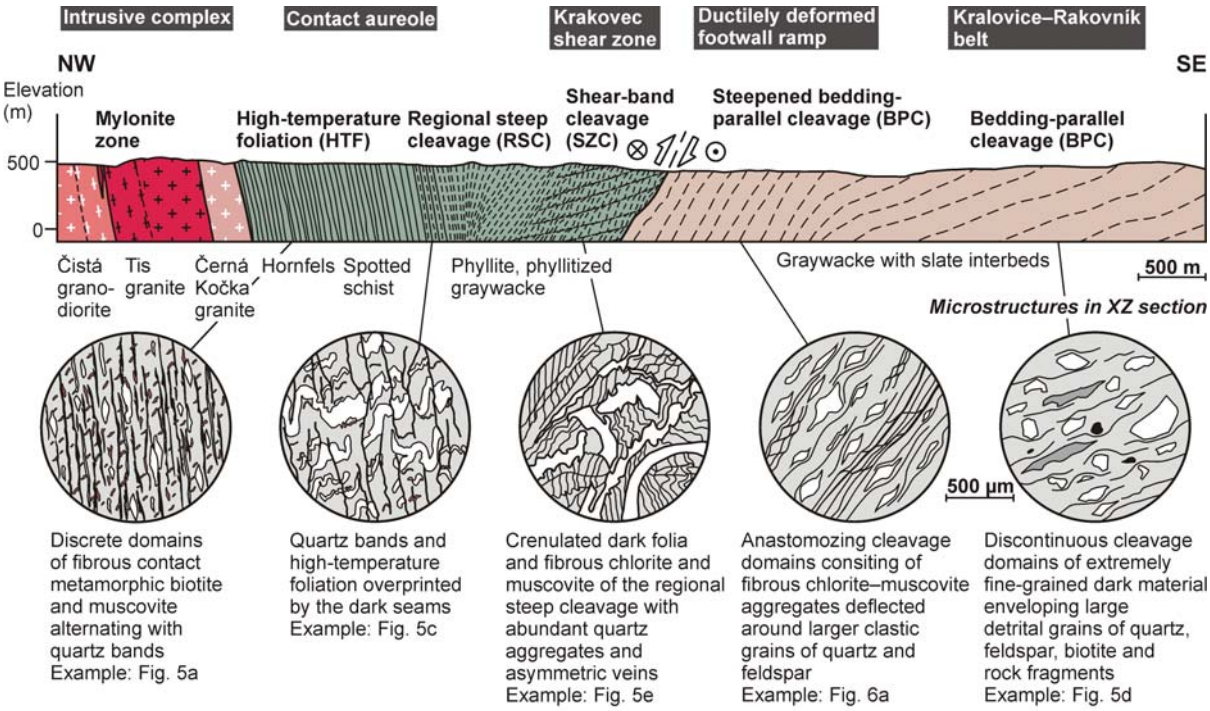

Fig. V.4. Idealized structural cross-section along line A–B (location shown in Fig. V.2) to show fabric and microstructural gradients across the Krakovec shear zone. Insets portray schematically the representative deformational microstructures (in the lineation-parallel and foliation-perpendicular section) in the individual rock units.

4. Deformational microstructures

Microstructures have been examined in 30 thin sections from samples taken along the NW–SE transects across the contact aureole, KSZ, and the footwall graywackes (Fig. V.4) in order to characterize foliation development, deformation mechanisms, and micro-scale kinematic indicators.

4.1. Microstructures in the thermal aureole

The hornfelses are dominated by disjunctive HTF (Fig. V.4; we use the terminology of Powell 1979, Passchier and Trouw 2005, and Vernon 2004 throughout this paper), which is defined by smooth, discrete domains of fibrous biotite and muscovite aggregates, typically of 50 μm in thickness, that alternate with microlithons (about 200 μm in thickness) composed of recrystallized irregular equant quartz grains (Figs. V.4, V.5a). In addition, the hornfelses contain abundant thicker (up to 500 μm) and widely spaced (>1000 μm) mica-poor quartz bands that are parallel to this foliation and exhibit asymmetric pinch-and-swell structures or microboudinage (Figs. V.4, V.5a). The quartz bands are recrystallized, resulting in irregularly-shaped and variously-sized grains (the grain size ranges from 10 to 200 μm). The grains commonly show undulose extinction, subgrains, but some also have sutured grain boundaries. This indicates recrystallization by both subgrain rotation and grain boundary migration under high-temperature conditions.

Farther away (~1 km) from the contact, the spotted schists exhibit continuous HTF defined by quartz ribbons (20 to 350 μm in length), aligned biotite grains and aggregates, and thin folia of very fine grained dark minerals. Scarce, probably cordierite porphyroblasts about 1 mm in size have been replaced by chlorite and muscovite and are parallel to this foliation (Fig. V.5b). Elsewhere, but at approximately the same distance from the contact, both the matrix and porphyroblasts are overgrown by fibrous aggregates of chlorite and muscovite present also in their strain shadows. Moreover, the contact metamorphic biotite grains in the matrix are merged and stretched into discrete thin folia that wrap around the quartz grains and ribbons. The chlorite and muscovite fibres and stretched contact-metamorphic biotite folia are attributed to the RSC. This indicates that the RSC developed in the chlorite zone and was associated with partial retrogression of the contact metamorphic

assemblage (most likely of late Cambrian age).

Approaching the KSZ, the banded hornfelsic rocks become heterogeneously overprinted by the RSC at various angles, developed here as a discrete crenulation cleavage (Figs. V.4, V.5c). This cleavage develops as smooth, subparallel dark seams cutting across the compositional banding and HTF (including the contact metamorphic biotite folia), which is intensely crenulated into tight to isoclinal symmetric microfolds with the dark seams parallel to their axial planes.

4.2. Microstructures in the Krakovec shear zone

On the microscale, the fine-grained phyllites in the KSZ are characterized by a complex superposition of multiple generations of cleavages and commonly contain disrupted and highly strained relics of graywacke laminae (Figs. V.4, V.5d). In the simplest cases, a smooth continuous (slaty) cleavage (assigned to RSC) defined by chlorite and muscovite fibres and elongate quartz grains is overprinted by a zonal gradational crenulation and shear band cleavage (SZC) with asymmetric microfolds (Fig. V.5d). The cleavage domains are defined by dark folia and fibrous chlorite and muscovite (Fig. V.5d). In more complex cases, the pre-existing continuous RSC is irregularly crenulated by the SZC and shows highly variable orientation even within a single thin section (Fig. V.5e–f). These rocks also contain abundant quartz aggregates and veins that have been folded and boudinaged or extensively disrupted as a result of heterogeneous deformation (Fig. V.5e–f). The veins are commonly heterogeneously recrystallized into a mosaic consisting of irregularly-shaped grains with bimodal grain size distribution. Larger grains (180 μm in size) with undulose extinction are surrounded by smaller (25 μm in size) strain-free grains, suggesting strain-induced grain boundary migration (bulging) recrystallization (Fig. V.5f). In line with the chlorite + muscovite mineral association, the quartz microstructures in the veins corroborate the greenschist

facies conditions for shearing along the KSZ.

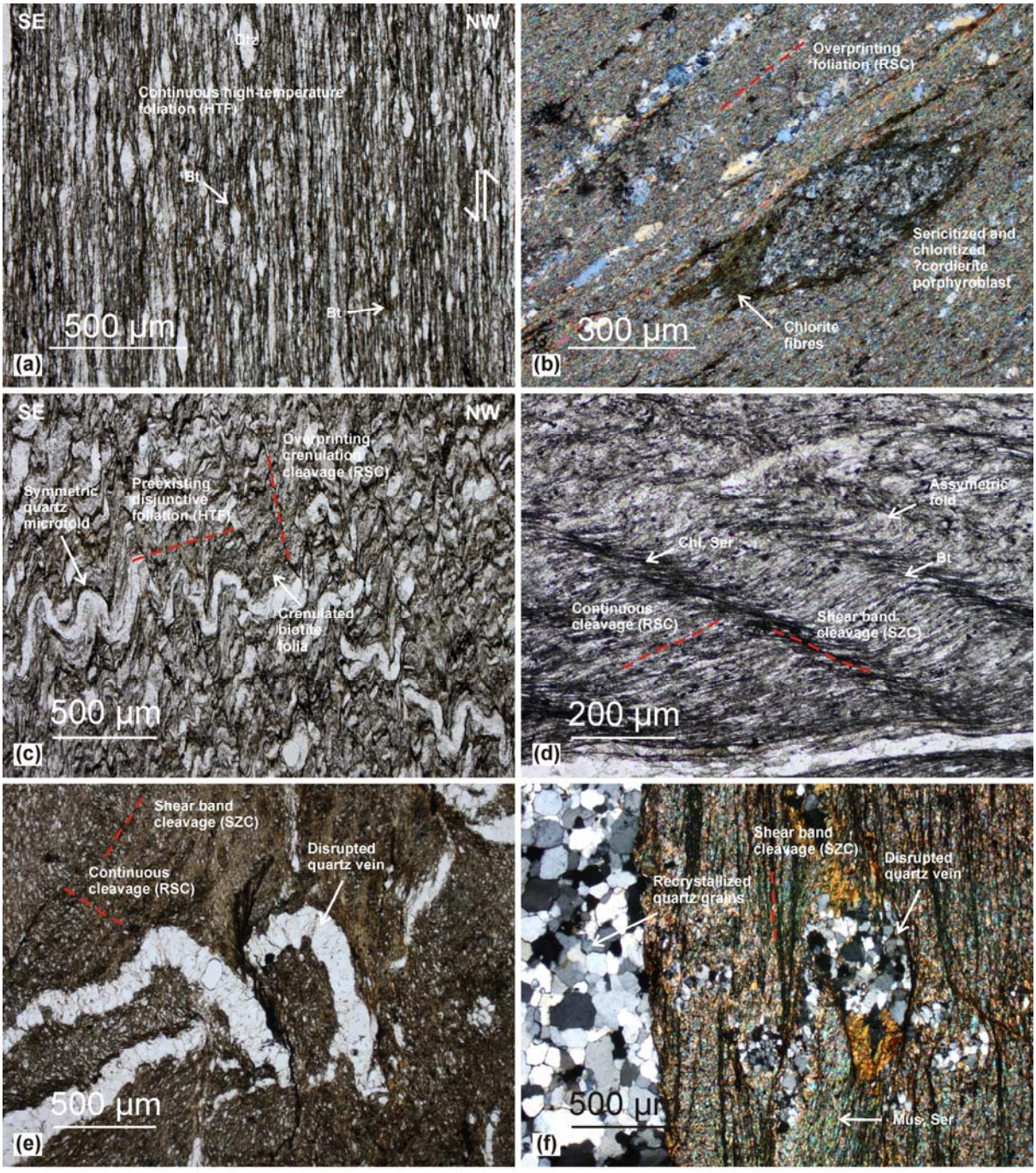

Fig. V.5. Deformational microstructures in the thermal aureole of the Tis pluton and in the Krakovec shear zone. (a) Spotted schists exhibiting continuous high-temperature foliation (HTF) defined by quartz ribbons, aligned biotite grains and aggregates, and thin folia of very fine grained dark minerals, 1.3 km SE of Hradecko. Plane-polarized light. (b) Cordierite porphyroblast replaced by chlorite and muscovite and stretched within the overprinting chlorite-zone cleavage (termed RSC in this paper, see text), locality V Tišině. Crossed polars. (c) Banded hornfelsic rock heterogeneously overprinted by a discrete crenulation cleavage (RSC), 1 km NNW of Kožlany. Plane-polarized light. (d) Smooth continuous cleavage (RSC) defined by chlorite and muscovite fibres and elongate quartz grains overprinted by zonal gradational crenulation and shear band cleavage (SZC) with asymmetric microfolds, locality Ožehák near Kožlany. Plane-polarized light. (e) Pre-existing continuous cleavage

(RSC) irregularly crenulated into SZC with abundant quartz aggregates and irregularly folded, boudinaged and disrupted veins, locality Ožehák near Kožlany. Plane-polarized light. (f) Sutured grain boundaries in the strongly disrupted quartz vein in phyllite indicating the strain-induced grain boundary migration (bulging) recrystallization, 800 m S of Podšibenský Mlýn near Kralovice. Crossed polars. Mineral abbreviations after Kretz (1983).

4.3. Microstructures in the footwall graywackes

The graywackes below the KSZ preserve bedding defined by alternating graywacke and siltstone laminae overgrown by chlorite and white mica (Fig. V.6a, b). Two types of cleavage are present in both lihologies but are more intensely developed in the finer-grained siltstone laminae. (1) A bedding-parallel disjunctive cleavage (BPC) is defined by anastomosing cleavage domains consisting of fibrous chlorite–muscovite aggregates deflected around the larger clastic grains of quartz and feldspar (Figs. V.4, V.6a, c). Quartz grains in the matrix (50 μm in size) have irregular boundaries, are elongated parallel to the cleavage domains, and show undulose extinction. The larger, angular to subangular quartz and feldspar clasts and their strain caps of intergrown chlorite and white mica are commonly asymmetric and show evidence of rotation indicating top-to-the-NE kinematics. (2) The BPC is cross-cut by widely spaced discrete C´-type SZC that is also defined by fibrous mica aggregates (Fig. V.6b, c). The SZC is apparent only on the microscale and is preferentially developed in the finer grained siltstone laminae (Fig. V.6b). The sigmoidal deflection of the BPC in microlithons and the obliquity between the two cleavages are consistent with top-to-the-NE kinematics.

In graywackes farther away from the KSZ (Fig. V.6d), the BPC is defined by fibrous muscovite aggregates that occupy much of the matrix and also by rough, discontinuous cleavage domains of extremely fine-grained dark material enveloping large detrital grains (spaced disjunctive cleavage). Single grains of detrital biotite in the matrix have irregular

shapes and frayed ends whereas in the cleavage domains the grains are thinned down, merge into folia (together with muscovite), and are also bent around the larger (rigid) clasts (Figs. V.4, V.6d).

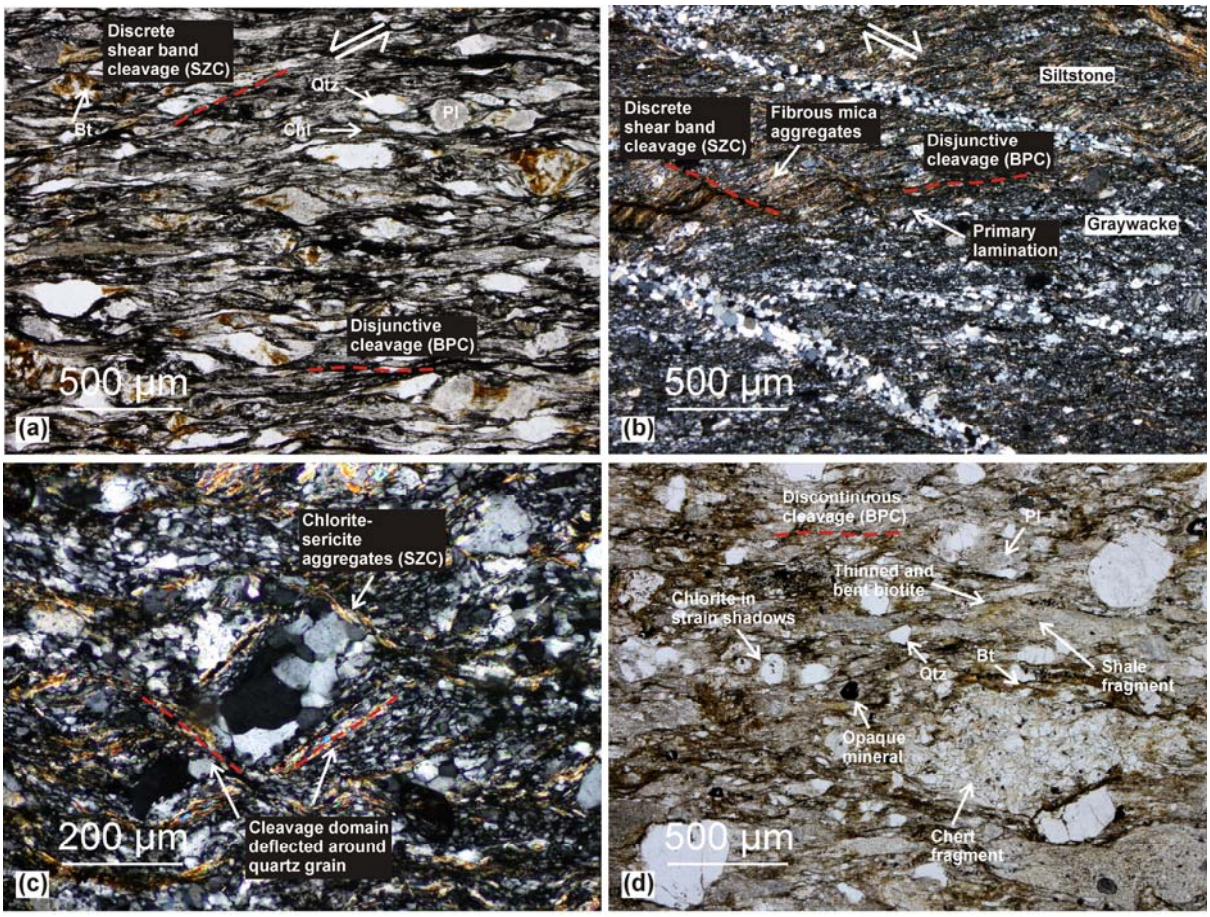

Fig. V.6. Deformational microstructures in the footwall graywackes. (a) Disjunctive cleavage (BPC) overprinted by discrete shear band cleavage (SZC) in the strongly deformed graywacke, 500 m NNW of Krakovec. Plane-polarized light. (b) Bedding defined by alternating graywacke and siltstone laminae overprinted by discrete shear band cleavage (SZC); arrows indicate kinematics, 1.25 km E of Hodyně. Crossed polars. (c) Cleavage domains (SZC) anastomozing around larger clastic grains of quartz and feldspar in graywacke, 1.25 km E of Hodyně. Crossed polars. (d) Rough, discontinuous cleavage domains (BPC) composed of extremely fine-grained dark material enveloping large porphyroclasts of quartz, feldspar, opaque minerals, felsic volcanic rocks, chert, and black shale; 200 m S of Uhrovic Mlýn. Plane-polarized light.

5. Anisotropy of magnetic susceptibility (AMS)

5. 1. Methodology

Anisotropy of magnetic susceptibility (see Hrouda 1982; Jackson and Tauxe 1991;

Rochette et al. 1992; Tarling and Hrouda 1993; Borradaile and Jackson 2010 for reviews) is used in this study to describe quantitatively gradients in fabric symmetry, intensity, and orientation across the principal lithotectonic units in the north-central TBU (Fig. V.7). The AMS is mathematically described as a symmetric second rank tensor, which can be visualized as an ellipsoid; its semi-axis lengths, $k1 \geq k2 \geq k3$, are termed the principal susceptibilities and their orientations, K1, K2, K3, are denoted as the principal directions. Such an ellipsoid defines a magnetic fabric where the maximum direction (K1) is denoted as magnetic lineation and the plane perpendicular to the minimum direction (K3) and containing the maximum and intermediate directions (K1, K2) is denoted as magnetic foliation. The AMS data are further described by the bulk susceptibility ($kb = (k1 + k2 + k3) / 3$), degree of anisotropy ($P = k1 / k3$), and anisotropy shape parameter ($T = 2\ln(k2 / k3) / \ln(k1 / k3) – 1$). If $1>T>0$ then the AMS ellipsoid is oblate, whereas for $0>T>–1$ the AMS ellipsoid is prolate.
In total, 143 oriented samples (cores 2.5 cm in diameter) were taken using a portable drill at 38 sampling sites along two NW–SE oriented transects (Fig. V.7). After laboratory cutting, these samples yielded 589 standard oriented specimens (ca. 2.2 cm in height). The AMS measurements were performed using an Agico MFK1-A Multi-function Kappabridge in the Laboratory of Rock Magnetism, Institute of Geology and Paleontology, Charles University in Prague. Statistical analysis of the AMS data was carried out using the ANISOFT 4.2 program (written by M. Chadima and V. Jelínek; www.agico.com).

5.2. Magnetic fabric

In the Tis and Černá Kočka granites, the AMS corroborates the fabric gradient along the NW–SE direction (Figs. V.2, V.7). The degree of anisotropy is high in the strongly deformed Tis granite at the Čistá granodiorite/ Tis granite contact (station JH290), ranging from 1.408 to 1.625 (average 1.525). The average P parameter then decreases considerably

with distance away from the contact down to P=1.111–1.297 (station JH243; average 1.135). Along with a decrease in the P parameter, the AMS ellipsoids exhibit only oblate (JH243; T=0.018–0.676) or weakly prolate to weakly oblate (neutral) shapes (station JH290). Further away from the contact, the P parameter is low (P=1.013–1.07) and the data points with P < 1.07 are symmetrically distributed about the T axis in the P–T plot, indicating both prolate (45 %) and oblate shapes of the AMS ellipsoid (T=– 0.64 to 0.817; Fig. V.7). The decreasing degree of anisotropy is also associated with the principal susceptibilities being more scattered about their respective mean directions (e.g., stations JH295, JH523). Regardless of the degree of anisotropy or shape parameter, magnetic foliations and lineations are relatively homogeneously oriented. Magnetic foliations strike NE–SW and dip moderately to steeply to the SE and NW, and are thus subparallel to the intrusive contacts and to the HTF and RSC in the host rocks (compare Figs. V.2 and V.7). Magnetic lineations plunge gently to moderately to the SW and are also subparallel to the stretching lineation in and outside the aureole (compare Figs. V.2 and V.7).

The contact metamorphic rocks in the thermal aureole exhibit a higher degree of anisotropy (ranging from 1.11 to 1.21) as compared to the granites and solely oblate shapes of the AMS ellipsoids (T ranges from 0.05 to 0.708; Fig. V.7). Magnetic foliations strike NE–SW and dip steeply to the SE or NW, magnetic lineations plunge moderately to steeply to the SW (Fig. V.7).

In the P–T plot (Fig. V.7), the data from phyllites of the KSZ reveal a clear trend from the prolate AMS ellipsoids and lower degree of anisotropy (P ranging from 1.054 to 1.128) towards the oblate AMS ellipsoids (82 % of the data) and higher degree of anisotropy (P ranging from 1.032 to 1.252). The prolate ellipsoids are scattered among several stations located close to the footwall graywackes. On a stereonet, the minimum principal

susceptibilities define two broad maxima corresponding to the `average' NE–SW-striking magnetic foliation dipping steeply to the NW or SE (Fig. V.7). Magnetic lineations plunge moderately to the SW (broad cluster in the stereonet in Fig. V.7) or to the NE. The exception from this overall trend is the southwesterly stations JH329, JH331, and JH332 where lineations plunge shallowly to the S (Fig. V.7) and are roughly parallel to the local N–S bend of the KSZ.

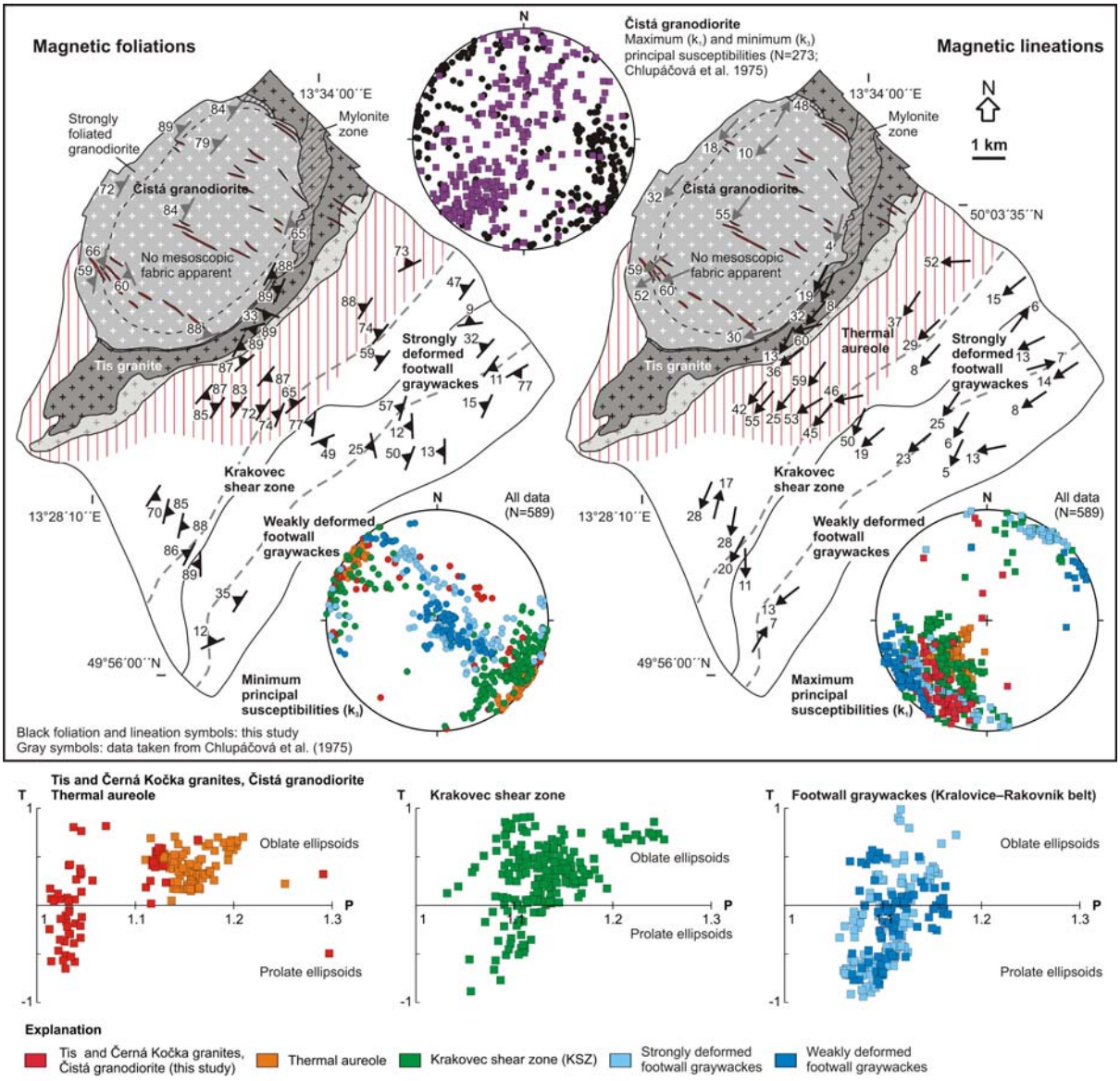

Fig. V.7. Map showing orientation of magnetic lineations and foliations along the Krakovec shear zone. Stereonets (equal area projection, lower hemisphere, geographic coordinate system) show the maximum and minimum principal susceptibilities, bottom panels are magnetic anisotropy P–T plots of all analyzed specimens.

Data from the Čistá pluton provided with the courtesy of F. Hrouda and M. Chlupáčová.

The footwall graywackes show a trend from the oblate AMS ellipsoids with higher degree of anisotropy (P from 1.067 to 1.174) towards the prolate AMS ellipsoids and lower degree of anisotropy (P ranges from 1.056 to 1.166). However, the prolate (63 %) AMS ellipsoids are more frequent in comparison to the phyllites (Fig. V.7). The shape of the AMS ellipsoid also seems to vary along strike of the belt, as stations located to the southwest (close to the N–S bend of the KSZ) yield oblate AMS ellipsoids whereas stations to the northeast yield prolate ellipsoids. In contrast, magnetic fabric does not show any significant along-strike variations. Regardless of the distance from the KSZ, magnetic lineations plunge gently to the SSW–WSW or to the NE–NNE. The exception from the overall fabric trend is station JH326 where lineations plunge to the S and foliations are steep and strike N–S, parallel to the N–S bend of the KSZ (Fig. V.7). The minimum principal susceptibilities tend to define a girdle about NE–SW horizontal axis on a stereonet, with a prominent maximum of data points close to its center. This girdle corresponds to flat-lying magnetic foliations in the weakly deformed graywackes to the SE that are reoriented to moderately dipping foliations as the KSZ is approached, which is in concert with the mesoscopic structural data.

5.3. Magnetic mineralogy

In order to analyze the carriers of magnetic fabric, magnetic susceptibility of representative samples was measured as a function of temperature (from the temperature of liquid nitrogen to 700 °C and back at a heating rate of 10 °C/min). Powdered samples were heated in argon atmosphere to minimize mineral changes due to oxidation of samples in increased temperature.

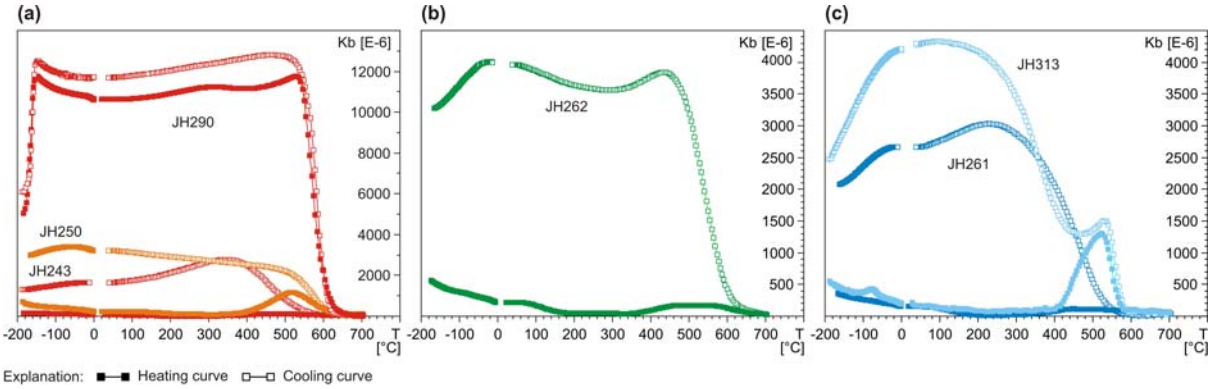

Fig. V.8. Thermomagnetic heating and cooling curves showing variations of the bulk susceptibility (Kb) with temperature for the following specimens: a JH290 – the Čistá granodiorite, JH243 – the Tis granite, JH250 – hornfelsic metapelite from the thermal aureole; b JH262 – phyllite near the outer boundary of the thermal aureole; c JH313 – strongly deformed footwall graywacke, JH261 – weakly deformed footwall graywacke.

The magnetic mineralogy of granodiorite sample JH290 is dominated by magnetite as is clearly demonstrated by a pronounced Verwey transition (rapid susceptibility increase at ca. –170 °C) and the Curie temperature corresponding to pure magnetite (abrupt susceptibility decrease at ca. 580 °C, Fig. V.8a). Furthermore, the magnetic susceptibility of JH290 sample is about two orders of magnitude higher compared to other analyzed samples, ca. 10,000 × 10–6 SI. The cooling curve follows more or less the trend of the heating curve implying that no mineral changes were induced during the experiment. The magnetic mineralogy of granite sample JH243 as well as sample JH250 from the contact aureole is dominated by paramagnetic minerals (Fig. V.8a). The room temperature magnetic susceptibility is lower than 250 × 10–6 SI. When the samples are heated from the temperature of liquid nitrogen, magnetic susceptibility decreases hyperbolically up to ca. 300 °C (Fig. V.8a). Gradual hyperbolic decrease is typical of paramagnetic minerals where magnetic susceptibility is inversely proportional to temperature. Further susceptibility increase observed above 300 °C and also on the cooling curve (Fig. V.8a) can be attributed to the growth of new magnetite as a result of phyllosilicate (and other iron minerals) decomposition and oxidation during increased temperature.

The magnetic mineralogy of rocks from the KSZ (JH262; Fig. V.8b) as well as of the footwall graywackes (JH261 and JH313; Fig. V.8c) is similar and is dominated by paramagnetic minerals, most probably phyllosilicates. The room temperature magnetic susceptibility is lower than 300 × 10–6 SI and susceptibility as a function of increased temperature follows a hyperbolic trend (Fig. V.8b, c). The susceptibility increase seen above 400 °C and on the cooling curve indicates magnetite growth during the experiment.

6. Discussion

6.1. Significance, kinematics, and timing of movements along the Krakovec shear zone

The Variscan age of deformations associated with the KSZ is evidenced by the widespread chlorite zone cleavage (RSC) that clearly overprints the late Cambrian HTF in the Tis granite aureole (Figs. V.2, V.4, V.5b–c). Similarly, Variscan overprint of low-pressure/high-temperature aureoles around Cambrian plutons was documented elsewhere in the TBU by Kachlík (1996), Zulauf (1997), Zulauf et al. (1997), and Glodny et al. (1998). In addition, the age is constrained by the Ar–Ar cooling ages on micas at around 380–365 Ma (Fig. V.1; Dallmeyer and Urban 1994, 1998) and by syntectonic emplacement of the ~373 Ma Čistá granodiorite as discussed later.

The earliest Variscan deformation recognized in the phyllites along the KSZ is represented by the RSC and the dominant SE-plunging mineral lineation (Figs. V.2, V.4). We interpret this penetrative fabric, which largely obliterates any pre-existing structures, in terms of dextral transpressional shearing that was localized between two rigid backstops. The northwesterly one is represented by the Tis pluton and a steep edge of its thermal aureole (composed of hornfelsic rocks) whereas the opposite, southeasterly one is represented by the footwall

graywackes inclined beneath the KSZ (Fig. V.4). These two rigid backstops imparted geometric boundary conditions for the transpressional deformation and governed the foliation and lineation pattern observed along the KSZ (Fig. V.2). We envisage that during the Late Devonian convergence of the Saxothuringian and Teplá–Barrandian microplates, the weaker phyllites were squeezed asymmetrically between the two backstops and were extruded northeastward along the footwall graywackes (Fig. V.9). This process was associated with dextral kinematics which is well documented and consistent throughout the KSZ (Figs. V.3c–d, V.4d, V.6b). Progressive transpressional deformation lead to the development of the SZC that overprinted the RSC (Figs. V.2, V.3b, V.4, V.5d–e) and further accommodated top-to-the-E(ENE) thrusting of the phyllites over the graywackes (Figs. V.2, V.4, V.9).

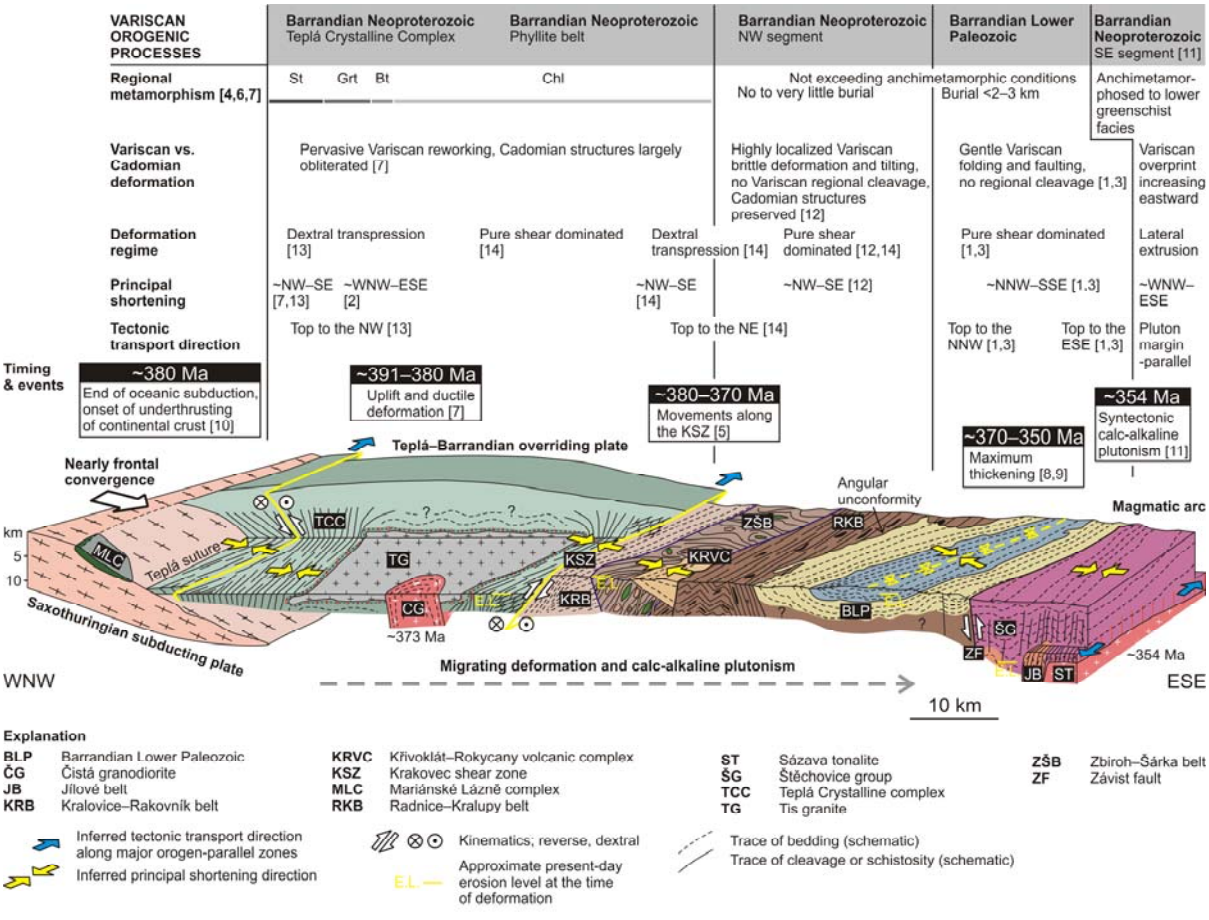

Fig. V.9. Idealized synthetic block diagram (see Fig. V.1 for location) showing our proposed plate-tectonic model for the TBU during Late Devonian to early Carboniferous (~380–346 Ma) Saxothuringian/Teplá–Barrandian convergence. Slight obliquity of the nearly frontal convergence was accommodated along several orogen-parallel dextral transpressive zones (including the KSZ). The table summarizes the relevant Variscan orogenic processes. See text for discussion. References: (1) Havlíček (1963), (2) Chlupáčová et al. (1975), (3) Havlíček (1981), (4) Cháb and Žáček (1994), (5) Dallmeyer and Urban (1994), (6) Cháb et al. (1995), (7) Zulauf (2001), (8) Suchý et al. (2002), (9) Filip and Suchý (2004), (10) Strnad and Mihajlevič (2005), (11) Žák et al. (2005a), (12) Hajná et al. (2011), (13) Kachlík, unpublished data, (14) this study.

The above inferences are soundly corroborated by the AMS data that reveal progressive reworking of the flat-lying magnetic foliation in the footwall graywackes into steep orientation dominant in all units to the northwest of the KSZ (Fig. V.7). Provided that the same magnetic carriers are compared (phyllosilicates in our case; see section Magnetic mineralogy, Fig. V.8), this reorientation, accompanied by steepening of the magnetic lineation and increasing degree of anisotropy and oblateness, is consistent with increasing transpressional strain along the KSZ.

The Čistá granodiorite intruded at ~373 Ma (Venera et al. 2000) and its Pb–Pb zircon age overlaps with the Ar–Ar cooling ages from the host phyllites (Fig. V.1a; Dallmeyer and Urban 1994, 1998). The radiometric ages thus suggest that the granodiorite emplacement was broadly synchronous with the regional deformation. Indeed, although the Čistá pluton crops out beyond the shear zone at the present-day erosion level, is largely discordant to the host rock structures (Figs. V.2, V.7, V.9), and exhibits an ˙onion-skin' concentric foliation pattern, magnetic lineations indicate its syntectonic emplacement. The pluton contains steep lineations interpreted to record diapiric ascent (Chlupáčová et al. 1975), but also prominent SE-plunging lineations that are concordant with those measured in the host rocks (Fig. V.7). Therefore, we conclude that the pluton intruded during transpressional deformation along the KSZ and that its internal fabric records diapiric ascent partially overprinted by tectonic strain. This inference is further supported by the presence of NW–SE trending granodiorite and aplite dikes in the Čistá granodiorite. The dikes are oriented at a

high angle to the SE-plunging lineations and thus may represent late-stage melts emplaced after solidification of the main portion of the pluton and recording the NE–SW principal extension along the KSZ (Figs. V.2, V.7).

6.2. Late Devonian to early Carboniferous syn-convergent strain partitioning in the TBU and its implications for the plate convergence and assembly of the Bohemian Massif

Structural features of the TBU allow the detailed reconstruction of Late Devonian to early Carboniferous (pre-380 to 346 Ma) convergent stages of the Variscan orogeny in Central Europe, from initial subduction and closure of the Saxothuringian Ocean to subsequent underthrusting of the continental lithosphere beneath the TBU (e.g., Franke 2000; Konopásek and Schulmann 2005; Schulmann et al. 2009; Babuška et al. 2010).

Previous studies interpreted the TBU mostly as a coherent block (`median massif') that acquired a simple doubly-vergent fan-like architecture during the Variscan convergence (e.g., Matte et al. 1990; Holubec 1995; Zulauf 1997; Dörr et al. 1998). This assertion is generally in agreement with our data, however, we suggest that to understand the complex tectonic evolution of the TBU in detail, it is crucial to consider it as a heterogeneous composite where the overall deformation resulting from the Saxothuringian/Teplá–Barrandian convergence was strongly partitioned. Our proposed tectonic model is depicted in Fig. V.9. In this model, the TBU is interpreted as consisting of pure shear-dominated domains that accommodated orogen-perpendicular shortening alternating with narrow, orogen-parallel, high-strain zones that accommodated dextral (northestward) transpression or bilateral extrusion (material flowed laterally in both directions; Fig. V.9). Localization of the orogen-parallel flow into narrow zones seems to have been controlled either by pre-

existing major lithologic boundaries acting as rigid ramps (note that the KSZ separates chlorite zone phyllites from graywacke-dominated belts with well preserved Cadomian structures and only weak Variscan overprint; Figs. V.1, V.9, see also Hajná et al. 2010, 2011 for details) or by thermal softening in the aureoles of arc-related calc-alkaline plutons (Fig. V.9; Žák et al. 2005a, 2009).

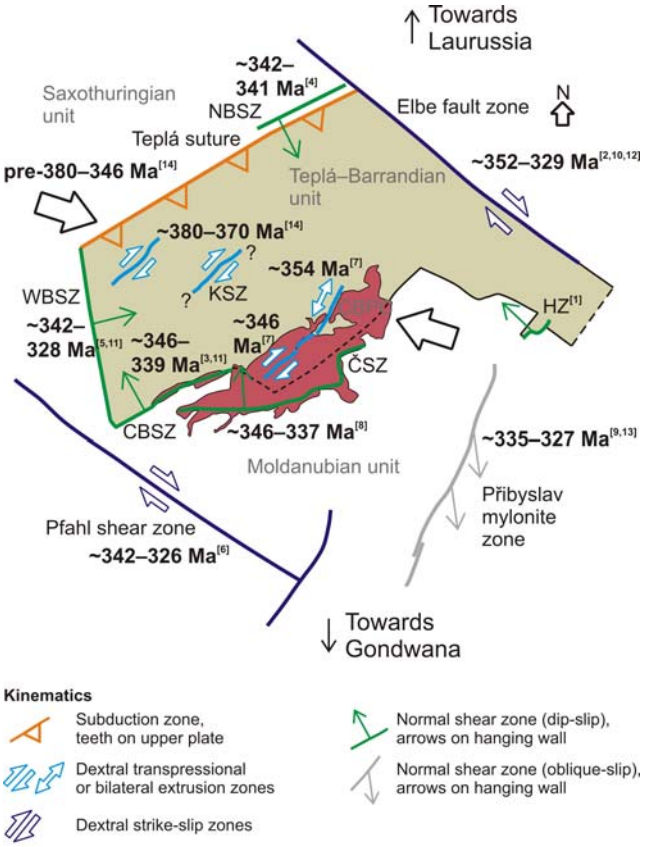

Fig. V.10. Schematic sketch emphasizing major Variscan suture and shear zones in the Teplá–Barrandian unit and vicinity. Importantly, these zones are associated with contrasting kinematics (indicated by arrows) and the movements were markedly diachronous; see text for discussion. Present-day outline of the TBU taken from 1:500,000 geologic map of the Czech Republic, published by the Czech Geological Survey in 2007. References: (1) Pitra et al. (1994), (2) Wenzel et al. (1997), (3) Scheuvens and Zulauf (2000), (4) Zulauf et al. (2002a), (5) Zulauf et al. (2002b), (6) Siebel et al. (2005), (7) Žák et al. (2005a), (8) Žák et al. (2005b), (9) Verner et al. (2006), (10) Hoffmann et al. (2009), (11) Dörr and Zulauf (2010), (12) Pertoldová et al. (2010), (13) Žák et al. (2011b), (14) this study. CBPC Central Bohemian Plutonic Complex, CBSZ Central Bohemian shear zone, ČSZ Červená shear zone, HZ Hlinsko zone, KSZ Krakovec shear zone, NBSZ North Bohemian shear zone, WBSZ West Bohemian shear zone.

The regional trends of Variscan foliations and stretching lineations (assumed to parallel the XY planes and X axes of finite strain ellipsoid, respectively) vary only by ~20–30° from one domain to another across the entire TBU (Fig. V.9) and are compatible with the NW–SE to WNW–ESE inferred principal shortening (Chlupáčová et al. 1975; Zulauf 2001; Hajná et al. 2011; this study). We argue that the far-field principal shortening direction must have been WNW–ESE to produce dextral displacement along the NW–SE-trending zones including the KSZ, a conclusion that is nearly the same as we reached for the

southeastern segment of the TBU (Žák et al. 2009). Assuming that this far-field shortening was close to the plate convergence vector, the Saxothuringian/Teplá–Barrandian convergence was nearly frontal in the WNE–ESE direction during the Late Devonian to early Carboniferous. This inference is also additionally supported by southeastward younging of deformation and arc-related plutonism in the TBU (Fig. V.9; this study; Žák et al. 2011a).

The above inferences, together with recent geochronologic and kinematic data from major lithotectonic boundaries in the vicinity of the TBU, provide the following refined view on timing and relative movements of the neighboring microplates during the assembly of the Bohemian Massif (see also Pharaoh 1999; Franke and Zelazniewicz 2002; Winchester et al. 2006 for further discussions). We have shown that the pre-380–346 Ma Saxothuringian/Teplá–Barrandian convergence was nearly frontal (this study; see also Zulauf 1997 and Žák et al. 2009) and that the presumed minor obliquity of the subduction vector with respect to the Teplá–Barrandian plate margin was accommodated by a few, narrow, orogen-parallel zones as shown in Fig. V.9. These findings are at variance with the still popular strike-slip models for Variscan plate movements in the Bohemian Massif (e.g., Badham 1982; Matte 1986; Rajlich 1987; Matte et al. 1990; Pitra et al. 1999) in addition to the fact that no throughgoing and kinematically and temporally compatible strike-slip shear zones or faults have been found to delineate the TBU's margins (Zulauf 1994; Scheuvens and Zulauf 2000; Zulauf et al. 2002a, b; Žák et al. 2009; Dörr and Zulauf 2010). Furthermore, minor variations in the inferred principal shortening directions over at least 30 M.y. (Fig. V.9) suggest that the TBU underwent no significant rotation as a rigid block about vertical axis during the Late Devonian to early Carboniferous. The prolonged time span of subduction-related shortening/transpression lasting till ~346 Ma (Fig. V.9; Žák et al. 2009) also casts doubt on the presumed Famennian upper age limit for ductile deformation of the TBU (~365

Ma according to Franke 2000) as inferred only from borehole data in the Bohemian Cretaceous basin far east of the present-day exposure of the TBU (Chlupáč and Zikmundová 1976; Čech et al. 1988).

The convergent stage was terminated by a rapid collapse of the thickened Teplá–Barrandian lithosphere and coeval exhumation of the middle and lower crust (Moldanubian unit) at ~346–337 Ma (Fig. V.10; Žák et al. 2005b, in press; Dörr and Zulauf 2010; Franěk et al. 2011). At approximately the same time, the northeastern margin of the amalgamated Saxothuringian/Teplá–Barrandian/Moldanubian block was truncated and dextrally displaced along the NW–SE-trending Elbe fault zone that parallels the southeastern margin of Baltica (Fig. V.10; Kachlík 1999; Franke and Zelazniewicz 2002), with movement starting from ~352 Ma (Pertoldová et al. 2010) or from ~342 Ma and lasting till at least ~329 Ma (Wenzel et al. 1997; Hofmann et al. 2009). In turn, this suggests that the orogenic processes governed by the prolonged frontal Saxothuringian subduction/underthrusting, including the internal deformation of the Teplá–Barrandian overriding plate as described in this contribution, were abruptly replaced by overall dextral strike-slip movements (Fig. V.10), perhaps driven by the westward motion of Gondwana with respect to Laurussia at around 345 Ma (e.g., Martínez Catalán 2011 and references therein).

7. Conclusions

(1) The Krakovec Shear Zone (KSZ) is an important crustal-scale dextral transpressional zone which splits the supracrustal Teplá–Barrandian unit into two segments of contrasting style and intensity of Variscan deformation. To the NW, the degree of Variscan metamorphism associated with steep regional cleavage increases from the chlorite up to the kyanite/sillimanite zone (in the Teplá Crystalline Complex), whereas to the SE the Variscan overprint is represented only by brittle deformation in the graywacke-dominated lithologies

with well preserved Cadomian structures.

(2) Structural features in the KSZ show that the Variscan deformation in the Teplá–Barrandian unit was partitioned into pure shear-dominated domains that accommodated orogen-perpendicular displacements alternating with narrow, orogen-parallel, high-strain zones that accommodated dextral (northestward) transpression or bilateral extrusion.

(3) Relatively uniform regional foliation trends and dextral kinematics along the localized shear zones accomodating the oblique component of the subduction vector indicate WNW–ESE far-field principal shortening during the nearly frontal Saxothuringian/Teplá–Barrandian convergence. This inference is supported by southeastward younging of deformation and arc-related plutonism in the TBU.

(4) The inferred nearly frontal pre-380–346 Ma Saxothuringian/Teplá–Barrandian convergence challenges the strike-slip models for the early Variscan plate movements in the Bohemian Massif. Furthermore, subtle variations in the inferred principal shortening directions over at least 30 M.y. rule out any significant rotation of the TBU about vertical axis as a rigid block during the Late Devonian to early Carboniferous.

(5) The subduction-related shortening was terminated by a rapid, gravity-driven collapse of the thickened Teplá–Barrandian lithosphere at ~346–337 Ma and was followed by dextral strike-slip movements along Baltica margin-parallel zones, driven by the westward movement of Gondwana from approximately 345 Ma onward.

References

Babuška V, Fiala J, Plomerová J (2010) Bottom to top lithosphere structure and evolution of western Eger Rift (Central Europe). Int J Earth Sci 99:891–907

Badham JP (1982) Strike slip orogens – an explanation for the Hercynides. J Geol Soc London 139:495–506

Borradaile GJ, Jackson M (2010) Structural geology, petrofabrics and magnetic fabrics (AMS, AARM, AIRM). J Struct Geol 32:1519–1551

Burg JP (1999) Ductile structures and instabilities: their implication for Variscan tectonics in the Ardennes. Tectonophysics 309:1–25

Čech S, Havlíček V, Zikmundová J (1988) Upper Devonian and Lower Carboniferous in north-eastern Bohemia (based on boreholes in the Hradec Králové area). Bull Central Geol Surv 64:65–75
Cháb J, Žáček V (1994) Metamorphism of the Teplá Crystalline Complex. KTB Report 94:33–37
Cháb J, Suchý V, Vejnar Z (1995) Teplá–Barrandian Zone (Bohemicum): metamorphic evolution. In: Dallmeyer RD, Franke W, Weber K (eds) Pre-Permian Geology of
Central and Eastern Europe. Springer, Berlin, pp 404–410
Chlupáč I, Zikmundová J (1976) The Devonian and Lower Carboniferous in the Nepasice bore in East Bohemia. Bull Central Geol Surv 51:269–278
Chlupáčová M, Hrouda F, Janák J, Rejl L (1975) The fabric, genesis and relative age relations of the granitic rocks of the Čistá–Jesenice massif. Gerlands Beitr Geophys 84:487–500
Crowley QG, Floyd PA, Winchester JA, Franke W, Holland JG (2000) Early Palaeozoic rift-related magmatism in Variscan Europe: fragmentation of the Armorican Terrane Assemblage. Terra Nova 12:171–180
Crowley QG, Timmermann H, Noble SR, Holland JG (2002) Palaeozoic terrane amalgamation in central Europe: a REE and Sm-Nd isotope study of the pre-Variscan basement, NE Bohemian Massif. In: Winchester JA, Pharaoh TC, Verniers J (eds) Palaeozoic amalgamation of central Europe. Geol Soc London Spec Publ 201:157–176
Dallmeyer RD, Urban M (1994) Variscan vs. Cadomian tectonothermal evolution within the Teplá–Barrandian zone, Bohemian Massif, Czech Republic: evidence from 40Ar/39Ar mineral and whole-rock slate/phyllite ages. J Czech Geol Soc 39:21–22
Dallmeyer RD, Urban M (1998) Variscan versus Cadomian tectonothermal activity in northwestern sectors of the Teplá–Barrandian zone, Czech Republic: constraints from 40Ar/39Ar ages. Geol Rundsch 87:94–106
Dörr W, Zulauf G (2010) Elevator tectonics and orogenic collapse of a Tibetan-style plateau
in the European Variscides: the role of the Bohemian shear zone. Int J Earth Sci 99: 299–
325
Dörr W, Fiala J, Vejnar Z, Zulauf G (1998) U–Pb zircon ages and structural development
of metagranitoids of the Teplá crystalline complex – evidence for pervasive
Cambrian plutonism within the Bohemian Massif (Czech Republic). Geol Rundsch
87:135–149
Dörr W, Zulauf G, Fiala J, Franke W, Vejnar Z (2002) Neoproterozoic to Early Cambrian history of an active plate margin in the Teplá–Barrandian unit – a correlation of U–Pb isotopic-dilution TIMS ages (Bohemia, Czech Republic). Tectonophysics 352:65–
85
Dostal J, Patočka F, Pin C (2001) Middle/Late Cambrian intracontinental rifting in the central west Sudetes, NE Bohemian Massif (Czech Republic): geochemistry and petrogenesis of the bimodal metavolcanic rocks. Geol J 36:1–17
Drost K, Linnemann U, McNaughton N, Fatka O, Kraft P, Gehmlich M, Tonk C,
Marek J (2004) New data on the Neoproterozoic–Cambrian geotectonic setting
of the Teplá–Barrandian volcano-sedimentary successions: geochemistry, U–Pb
zircon ages, and provenance (Bohemian Massif, Czech Republic). Int J Earth Sci
93:742–757
Drost K, Gerdes A, Jeffries T, Linnemann U, Storey C (2011) Provenance of Neoproterozoic and early Paleozoic siliciclastic rocks of the Teplá–Barrandian unit (Bohemian Massif): evidence from U–Pb detrital zircon ages. Gondwana Res 19:213–231
Dubanský A (1984) Determination of the radiogenic age by the K–Ar method
(geochronological data from the Bohemian Massif in the ČSR region). Collect Sci Works Tech Univ Ostrava
30:137–170
Filip J, Suchý V (2004) Thermal and tectonic history of the Barrandian Lower Paleozoic, Czech Republic: is there a fission-track evidence for Carboniferous–Permian overburden
and pre-Westphalian alpinotype thrusting? Bull Geosci 79:107–112
Floyd PA, Winchester JA, Seston R, Kryza R, Crowley QG (2000) Review of geochemical variation in Lower Palaeozoic metabasites from the NE Bohemian Massif: intracratonic rifting and plume-ridge interaction. In: Franke W, Haak V, Oncken O, Tanner D (eds) Orogenic processes: quantification and modelling in the Variscan Belt. Geol Soc London Spec Publ 179:155–174
Forster MA, Lister GS (2008) Tectonic sequence diagrams and the structural evolution of schists and gneisses in multiply deformed terranes. J Geol Soc London 165:923–939
Franěk J, Schulmann K, Lexa O, Tomek Č, Edel JB (2011) Model of syn-convergent extrusion of orogenic lower crust in the core of the Variscan belt: implications for exhumation of high-pressure rocks in large hot orogens. J Metamorph Geol 29:53–78

Franke W (2000) The mid-European segment of the Variscides: tectonostratigraphic units, terrane boundaries and plate tectonic evolution. In: Franke W, Haak V, Oncken O, Tanner D (eds) Orogenic Processes: quantification and modelling in the Variscan Belt. Geol Soc London Spec Publ 179:35–61
Franke W, Zelazniewicz A (2002) Structure and evolution of the Bohemian arc. In: Winchester JA, Pharaoh TC, Verniers J (eds) Palaeozoic amalgamation of Central Europe. Geol Soc London Spec Publ 201: 279–293
Gebauer D (1993) Geochronologische Übersicht. In: Bauberger W (ed) Geologische Karte von Bayern 1:25000, Erläuterungen zum Blatt Nr. 6439 Tännesberg Bayer. Geol L Amt, München, pp 10–22
Glodny J, Grauert B, Fiala J, Vejnar Z, Krohe A (1998) Metapegmatites in the western Bohemian massif: ages of crystallisation and metamorphic overprint, as constrained by U–Pb zircon, monazite, garnet, columbite and Rb–Sr muscovite data. Geol Rundsch 87:124–134
Hajná J, Žák J, Kachlík V, Chadima M (2010) Subduction-driven shortening and differential exhumation in a Cadomian accretionary wedge: the Teplá–Barrandian unit, Bohemian Massif. Precambrian Res 176:27–45
Hajná J, Žák J, Kachlík V (2011) Structure and stratigraphy of the Teplá–Barrandian Neoproterozoic: a new plate-tectonic reinterpretation. Gondwana Res 19:495–508
Havlíček V (1963) Tectogenetic disruption of the Barrandian Paleozoic. J Geol Sci 1:77–102
Havlíček V (1981) Development of a linear sedimentary depression exemplified by the Prague basin (Ordovician–Middle Devonian; Barrandian area – central Bohemia). J Geol Sci 35:7–48
Hofmann M, Linnemann U, Gerdes A, Ullrich B, Schauer M (2009) Timing of dextral strike-slip processes and basement exhumation in the Elbe Zone (Saxo-Thuringian Zone): the final pulse of the Variscan Orogeny in the Bohemian Massif constrained by LA-SF-ICP-MS U–Pb zircon data. Geol Soc London Spec Publ 327:197–214
Holubec J (1995) Structure (the Teplá–Barrandian Zone). In: Dallmeyer RD, Franke W, Weber K (eds) Pre-Permian Geology of Central and Eastern Europe. Springer, Berlin, Heidelberg, New York, pp 392–397
Hrouda F (1982) Magnetic anisotropy of rocks and its application in geology and geophysics. Geophys Surv 5:37–82
Jackson M, Tauxe L (1991) Anisotropy of magnetic susceptibility and remanence: developments in the characterization of tectonic, sedimentary, and igneous fabric. Rev Geophys 29:371–376
Kachlík V (1996) Contact metamorphic host rocks of the Lestkov massif and their significance for reconstruction of tectonometamorphic evolution of the Tepla´–Barrandian unit. Geoscience Research Reports for 1996, pp 81–82
Kachlík V (1999) Relationship between Moldanubicum, the Kutná Hora crystalline unit, and Bohemicum (Central Bohemia, Czech Republic): a result of the polyphase nappe tectonics. J Czech Geol Soc 44:201–289
Klomínský J (1963) Geology of the Čistá Massif. J Geol Sci 3:75–99
Klomínský J, Jarchovský T, Rajpoot GS (2010) The atlas of plutonic rocks and orthogneisses in the Bohemian Massif. Radioactive Waste Repository Authority of the Czech Republic, Technical Report No. TR-01-2010, Prague
Konopásek J, Schulmann K (2005) Contrasting Early Carboniferous field geotherms: evidence for accretion of a thickened orogenic root and subducted Saxothuringian crust (central European Variscides). J Geol Soc London 162:463–470
Kopecký L (1987) The Čistá ring structure, Czechoslovakia. In: Proceedings of the 1st Seminar on carbonatites and alkaline rocks of the Bohemian Massif and ambient regions. Czech Geological Survey, Prague, pp 23–58
Kopecký L, Dobeš M, Fiala J, Šťovíčková N (1970) Fenites of the Bohemian Massif and the relations between fenitization, alkaline volcanism and deep fault tectonics. J Geol Sci 16:51–107
Kopecký L, Chlupáčová M, Klomínský J, Sokol A (1997) The Čistá–Jesenice pluton in western Bohemia: geochemistry, geology, petrophysics and ore potential. J Geol Sci 31:97–127
Košler J, Bowes DR, Farrow CM, Hopgood AM, Rieder M, Rogers G (1997) Constraints on the timing of events in the multi-episodic of the Teplá–Barrandian complex, western Bohemia, from integration of deformational sequence and Rb–Sr isotopic data. N Jb Miner Mh 5:203–220
Kretz R (1983) Symbols for rock forming minerals. Am Miner 68:277–279
Lüneburg CM, Lebit HDW (1998) The development of a single cleavage in an area of repeated folding. J Struct Geol 20:1531–1548
Martínez Catalán JR (2011) Are the oroclines of the Variscan belt related to late Variscan strike-slip tectonics? Terra Nova 23:241–247
Matte P (1986) Tectonic and plate tectonic model for the Variscan belt of Europe. Tectonophysics 126:329–374
Matte P, Maluski H, Rajlich P, Franke W (1990) Terrane boundaries in the Bohemian Massif: result of large-scale Variscan shearing. Tectonophysics 177:151–170

Miller RB, Paterson SR, Lebit H, Alsleben H, Lüneburg C (2005) Significance of composite lineations in the mid- to deep crust: a case study from the North Cascades, Washington. J Struct Geol 28:302–322
Murphy JB, Pisarevsky SA, Nance RD, Keppie JD (2004) Neoproterozoic–Early Paleozoic evolution of peri-Gondwanan terranes: implications for Laurentia–Gondwana connections. Int J Earth Sci 93:659–682
Nance RD, Murphy JB, Strachan RA, D'Lemos RS, Taylor GK (1991) Late Proterozoic tectonostratigraphic evolution of the Avalonian and Cadomian terranes. Precambrian Res 53:41–78
Nance RD, Gutiérrez-Alonso G, Keppie JD, Linnemann U, Murphy JB, Quesada C, Strachan A, Woodcock NH (2010) Evolution of the Rheic Ocean. Gondwana Res 17:194–222
Neubauer F (2002) Evolution of late Neoproterozoic to early Paleozoic tectonic elements in Central and Southeast European Alpine mountain belts: review and synthesis. Tectonophysics 352:87–103
Ordynec GJ, Žukova VI, Habásko J (1984) Prevariscan uranium mineralisation in the Proterozoic of the Bohemian Massif. J Miner Geol 29:69–77
Park RG (1969) Structural correlation in metamorphic belts. Tectonophysics 7:323–338
Passchier CW, Trouw RAJ (2005) Microtectonics. Springer, Berlin
Pertoldová J, Verner K, Vrána S, Buriánek D, Štědrá V, Vondrovic L (2010) Comparison of lithology and tectonometamorphic evolution of units at the northern margin of the Moldanubian Zone: implications for geodynamic evolution in the northeastern part of the Bohemian Massif. J Geosci 55:299–319
Pharaoh TC (1999) Palaeozoic terranes and their lithospheric boundaries within the Trans-European Suture Zone (TESZ): a review. Tectonophysics 177:263–292
Pin C, Waldhausrová J (2007) Sm–Nd isotope and trace element study of Late Proterozoic metabasalts ("spilites") from the Central Barrandian domain (Bohemian Massif, Czech Republic). In: Linnemann U, Nance D, Kraft P, Zulauf G (eds) The evolution of the Rheic Ocean: from Avalonian–Cadomian active margin to Alleghenian–Variscan collision. Geol Soc Am Spec Paper 423:231–247
Pin C, Kryza R, Oberc-Dziedzic T, Mazur S, Turniak K, Waldhausrová J (2007) The diversity and geodynamic significance of Late Cambrian (ca. 500 Ma) felsic anorogenic magmatism in the northern part of Bohemian Massif: a review based on Sm–Nd isotope and geochemical data. In: Linnemann U, Nance D, Kraft P, Zulauf G (eds) The evolution of the Rheic Ocean: from Avalonian–Cadomian active margin to Alleghenian–Variscan collision. Geol Soc Am Spec Paper 423:209–229
Pitra P, Burg JP, Schulmann K, Ledru P (1994) Late orogenic extension in the Bohemian Massif: petrostructural evidence in the Hlinsko region. Geodyn Acta 7:15–30
Pitra P, Burg JP, Giraud M (1999) Late-Variscan strike-slip tectonics between the Teplá–Barrandian and Moldanubian terranes (Czech Bohemian Massif): petrostructural evidence. J Geol Soc London 156:1003–1020
Potts GJ, Reddy SM (1999) Construction and systematic assessment of relative deformation histories. J Struct Geol 21:1245–1253
Powell CM (1979) A morphological classification of rock cleavage. Tectonophysics 58:21–34
Rajlich P (1987) Variscan ductile tectonics in the Bohemian Massif. Geol Rundsch 76:755–786
Rochette P, Jackson M, Aubourg C (1992) Rock magnetism and the interpretation of anisotropy of magnetic susceptibility. Rev Geophys 30:209–226
Scheuvens D, Zulauf G (2000) Exhumation, strain localization, and emplacement of granitoids along the western part of the Central Bohemian shear zone (Bohemian Massif). Int J Earth Sci 89:617–630
Schulmann K, Konopásek J, Janoušek V, Lexa O, Lardeaux JM, Edel JB, Štípská P, Ulrich S (2009) An Andean type Palaeozoic convergence in the Bohemian Massif. CR Geosci 341:266–286
Siebel W, Blaha U, Chen F, Rohrmüller J (2005) Geochronology and geochemistry of a dyke–host rock association and implications for the formation of the Bavarian Pfahl shear zone, Bohemian Massif. Int J Earth Sci 94:8–23
Stampfli GM, Kozur HW (2006) Europe from the Variscan to the Alpine cycles. Geol Soc London Mem 32:57–82
Strnad L, Mihajlevič M (2005) Sedimentary provenance of Mid-Devonian clastic sediments in the Teplá–Barrandian Unit (Bohemian Massif): U–Pb and Pb–Pb geochronology of detrital zircons by laser ablation ICP-MS. Mineral Petrol 84:47–68
Suchý V, Dobeš P, Filip J, Stejskal M, Zeman A (2002) Conditions for veining in the Barrandian Basin (Lower Paleozoic), Czech Republic: evidence from fluid inclusion and apatite fission track analysis. Tectonophysics 348:25–50
Tarling DH, Hrouda F (1993) The magnetic anisotropy of rocks. Chapman and Hall,

London
Timmermann H, Štědrá V, Gerdes A, Noble SR, Parrish RR, Dörr W (2004) The problem of dating high-pressure metamorphism: a U–Pb isotope and geochemical study on eclogites and related rocks of the Mariánské Lázně Complex, Czech Republic. J Petrol 45:1311–1338
Timmermann H, Dörr W, Krenn E, Finger F, Zulauf G (2006) Conventional and in situ geochronology of the Teplá crystalline unit, Bohemian Massif: implications for the processes involving monazite formation. Int J Earth Sci 95:629–647
Tobisch OT, Paterson SR (1988) Analysis and interpretation of composite foliations in areas of progressive deformation. J Struct Geol 10:745–754
Venera Z, Schulmann K, Kröner A (2000) Intrusion within a transtensional tectonic domain: the Čistá granodiorite (Bohemian Massif) – structure and rheological modelling. J Struct Geol 22:1437–1454
Verner K, Žák J, Hrouda F, Holub FV (2006) Magma emplacement during exhumation of the lower- to mid-crustal orogenic root: the Jihlava syenitoid pluton, Moldanubian Unit, Bohemian Massif. J Struct Geol 28:1553–1567
Vernon RH (2004) A practical guide to rock microstructure. Cambridge University Press, Cambridge
Wenzel T, Mertz DF, Oberhänsli R, Becker T, Renne PR (1997) Age, geodynamic setting, and mantle enrichment processes of a K-rich intrusion from the Meissen massif (northern Bohemian massif) and implications for related occurrences from the mid-European Hercynian. Geol Rundsch 86:556–570
Williams PF (1985) Multiply deformed terrains – problems of correlation. J Struct Geol 7:269–280
Winchester JA, PACE TMR Network Team (2002) Paleozoic amalgamation of Central Europe: new results from recent geological and geophysical investigations. Tectonophysics 360:5–22
Winchester JA, Pharaoh TC, Verniers J, Ioane D, Seghedi A (2006) Palaeozoic accretion of Gondwana-derived terranes to the East European Craton: recognition of detached terrane fragments dispersed after collision with promontories. Geol Soc London Mem 32:323–332
Žák J, Schulmann K, Hrouda F (2005a) Multiple magmatic fabrics in the Sázava pluton (Bohemian Massif, Czech Republic): a result of superposition of wrench-dominated regional transpression on final emplacement. J Struct Geol 27:805–822
Žák J, Holub FV, Verner K (2005b) Tectonic evolution of a continental magmatic arc from transpression in the upper crust to exhumation of mid-crustal orogenic root recorded by episodically emplaced plutons: the Central Bohemian Plutonic Complex (Bohemian Massif). Int J Earth Sci 94:385–400
Žák J, Dragoun F, Verner K, Chlupáčová M, Holub FV, Kachlík V (2009) Forearc deformation and strain partitioning during growth of a continental magmatic arc: the northwestern margin of the Central Bohemian Plutonic Complex, Bohemian Massif. Tectonophysics 469:93–111
Žák J, Kratinová Z, Trubač J, Janoušek V, Sláma J, Mrlina J (2011a) Structure, emplacement, and tectonic setting of Late Devonian granitoid plutons in the Teplá–Barrandian unit, Bohemian Massif. Int J Earth Sci 100:1477–1495
Žák J, Verner K, Finger F, Faryad SW, Chlupáčová M, Veselovský F (2011b) The generation of voluminous S-type granites in the Moldanubian unit, Bohemian Massif, by rapid isothermal exhumation of the metapelitic middle crust. Lithos 121:25–40
Žák J, Verner K, Holub FV, Kabele P, Chlupáčová M, Halodová P (2012) Magmatic to solid state fabrics in syntectonic granitoids recording early Carboniferous orogenic collapse in the Bohemian Massif. J Struct Geol. 36:27–42
Zulauf G (1994) Ductile normal faulting along the West Bohemian Shear Zone (Moldanubian/Teplá–Barrandian boundary): evidence for late Variscan extensional collapse in the Variscan Internides. Geol Rundsch 83:276–292
Zulauf G (1997) From very low-grade to eclogite-facies metamorphism: tilted crustal sections as a consequence of Cadomian and Variscan orogeny in the Teplá–Barrandian unit (Bohemian Massif). Geotekt Forsch 89:1–302
Zulauf G (2001) Structural style, deformation mechanisms and paleostress along an exposed crustal section: constraints on the rheology of quartzofeldspathic rocks at supra- and infrastructural levels (Teplá–Barrandian unit, Bohemian Massif). Tectonophysics 332:211–237
Zulauf G, Dörr W, Fiala J, Vejnar Z (1997) Late Cadomian crustal tilting and Cambrian transtension in the Teplá–Barrandian unit (Bohemian Massif, Central European Variscides). Geol Rundsch 86:571–587
Zulauf G, Schitter F, Riegler G, Finger F, Fiala J, Vejnar Z (1999) Age constraints on the Cadomian evolution of the Teplá–Barrandian unit (Bohemian Massif) through electron microprobe dating of metamorphic monazite. Z

Dtsch Geol Ges 150:627–640
Zulauf G, Dörr W, Fiala J, Kotková J, Maluski H, Valverde-Vaquero P (2002a) Evidence for high-temperature diffusional creep preserved by rapid cooling of lower crust (North Bohemian shear zone, Czech Republic). Terra Nova 14:343–354
Zulauf G, Bues C, Dörr W, Vejnar Z (2002b) 10 km minimum throw along the West Bohemian shear zone: evidence for dramatic crustal thickening and high topography in the Bohemian Massif (European Variscides). International Journal of Earth Sciences 91:850–864

SUMMARY

1. Cadomian active margin processes (Parts 1–3)

(i) The Neoproterozoic (Cadomian) basement of the Teplá–Barrandian unit reveals a complex structure and mostly unclear stratigraphic relations of its components. This unit exposes perhaps the best preserved fragment of an accretionary wedge in the Avalonian–Cadomian belt, represented by the newly defined Blovice Complex. Volcanic arc is represented by the Davle Group, overlain by flysch-like successions of the Štěchovice Group, and the Svrchnice Formation is interpreted as deposits of a retro-arc basin.

(ii) The accretionary wedge fragment is made up of three units differing in lithology, style and intensity of deformation, magnetic fabric, and degree of Cadomian regional metamorphism, which increase to the SE, i.e., towards the volcanic arc:

The flysch-like Kralovice–Rakovník belt to the NW is the most outboard (trenchward) unit which has never been significantly buried and experienced only weak deformation and folding.

The central, mélange-like Radnice–Kralupy belt is interpreted as a complex of Franciscan-type mélanges of dual, sedimentary and tectonic origin. The olistostromal successions of graywackes that exhibit chaotic texture and slates containing graywacke and chert olistoliths are interpreted to represent gravity flow deposits (submarine slides) presumably along the trench slope. Their compositions indicate multiple episodes of mixing of arc-derived and deepwater material. Moreover, abundant bodies of (meta-)basalts, interpreted as dismembered seamount chains, were emplaced tectonically into various structural levels of this sedimentary mélange by either offscraping or by horizontal ductile flow, presumably in a subduction channel during flat-slab oceanic subduction.

To the SE of the mélange belt, the inboard (arcward) Zbiroh–Šárka belt is

lithologically monotonous (dominated by graywackes and slates), was buried to depths corresponding up to the lower greenschist facies conditions, where it was overprinted by a pervasive cleavage.

Juxtaposition and exhumation of these three belt, separated by brittle faults, and tilting of at least the mélange unit, indicated by presence of the lower and upper structural level in the same erosion level must have occured before sedimentation of the undeformed Middle Cambrian marine sediments in the Skryje–Týřovice basin.

(iii) The structural and stratigraphic relations are consistent with the S to SE-directed Cadomian subduction beneath the TBU that have lead to the involvement of trench-fill turbidites, chaotic deposits, and diverse ocean floor (meta-)basalts into the accretionary wedge. The wedge formation temporally overlapped with the growth and coeval erosion of the volcanic arc (the Davle Group) around *ca.* 620–560 Ma. During *ca.* 560 to 544 Ma, the rear of the wedge and some elevated portions of the arc were eroded to supply the deep-water flysch sequences of the Štěchovice Group (*ca.* 560 to 544 Ma), whereas the comparable Svrchnice Formation was deposited in a southeasterly retro-arc basin largely sourced from the nearby continental margin. Our new U–Pb ages also revealed an extended duration of the mélange-forming processes till the early Cambrian (*ca.* 527 Ma). The Cadomian orogeny in the TBU was terminated around *ca.* 550– 540 Ma by slab breakoff, by final attachment of the most outboard *ca.* 540 Ma oceanic crust of the Mariánské Lázně Complex, and by intrusion of *ca.* 544–524 Ma boninite dikes marking the transition from a destructive to transform margin during the early/middle Cambrian.

2. Cambro–Ordovician rifting and extension of the TBU from Gondwana (Part 4)

(i) Cambro–Ordovician rifting is an important global geodynamic event following the

cessation of the Cadomian subduction and causing the break-up of the northern margin of Gondwana. In the TBU, sedimentation of marine Middle Cambrian shales in the Příbram–Jince Basin and Skryje–Týřovice area was followed by rift-related subaerial volcanism in the Křivoklát–Rokycany volcanic complex (KRVC; *ca.* 504–495 Ma) and by deposition of Ordovician siliciclastic sedimentary successions.

(ii) Directions of the principal crustal extension can be reconstructed from orientations of dikes, interpreted as being feeders to the associated extrusive rocks of the Křivoklát–Rokycany Volcanic Complex. Two types of dikes have been recognized: (1) Andesitic dikes, correlated with the earliest volcanic rocks of the KRVC (younger than *ca.* 504 Ma), and (2) a group of younger basalt dikes that intrude the Lower to Middle Ordovician rocks of the Klabava Formation. Orientation of the principal extension is recorded also by the depocenters and facies distribution in the Lower Ordovician of the Prague Basin which developed on eroded Cadomian accretionary wedge presumably through reactivation of inherited NE–SW-trending Cadomian faults.

(iii) The Upper Cambrian dikes and Lower Ordovician rocks of the Prague Basin record a major kinematic change in the amount and directions of regional extension. Andesitic dikes supplying the KRVC indicate minor E–W crustal extension in the late Cambrian whereas the Tremadocian to Darriwilian lithofacies distribution and linear array of depocentres suggest opening of this Rheic Ocean rift-related basin during the NW–SE pure shear-dominated extension. This kinematic change was accompanied by the onset of basic submarine volcanism, presumably resulting from decompression mantle melting as the amount of extension increased. The triggering mechanism of this extension may have been the onset of subduction of the Iapetus Ocean at around 510 Ma, whereas the advanced extension was broadly coeval along the Avalonian–Cadomian belt. Unequal extension resulted in the break-

up and drift of some terranes while other portions of the belt remained adjacent to Gondwana.

3. Variscan subduction to terrane collisions (Part 5)

(i) Variscan orogenic processes in the TBU are well recorded by its strongly deformed and metamorphosed margins, whereas its central part was only weakly deformed and tilted. However, previous studies interpreted the TBU mostly as a coherent block that acquired a simple doubly vergent fan-like architecture during the Variscan convergence. In this thesis, it is suggested that the overall deformation resulting from the Saxothuringian/Teplá–Barrandian convergence was strongly partitioned. First, the most intriguing new finding was mapping and detailed structural analyzing of the NE–SW-trending dextral transpressional Krakovec Shear Zone (KSZ) which represent a principal orogen-scale tectonic feature that separates two crustal segments with contrasting Cadomian and Variscan deformation and metamorphic histories and delimits the northwestern front of Variscan ductile reworking in the TBU.

(ii) On the basis of the new and previously published structural data, a synthetic model for the deformation partitioning in the Teplá–Barrandian upper crust in response to the Late Devonian to early Carboniferous subduction and underthrusting of the Saxothuringan lithosphere was proposed. In this model, the TBU is interpreted as consisting of pure shear-dominated domains that accommodated orogen-perpendicular shortening alternating with narrow, orogen-parallel, high-strain zones that accommodated dextral (northestward) transpression or bilateral extrusion.

(iii) Together with the recently published geochronologic and kinematic data from major lithotectonic boundaries in the vicinity of the TBU, a refined view on timing and

relative movements of the neighboring microplates during the assembly of the Bohemian Massif was compiled. In summary, the Saxothuringian/Teplá–Barrandian convergence was nearly frontal during *ca.* 380–346 Ma. The convergent stage was terminated by a rapid collapse of the thickened Teplá–Barrandian lithosphere and coeval exhumation of the middle and lower crust (Moldanubian unit) at *ca.* 346–337 Ma followed by, or partly simultaneous with, dextral strike-slip along the Baltica margin-parallel zones, driven by the westward movement of Gondwana from approximately 345 Ma onwards.